An experimental investigation of the collapse behaviour of an unsaturated compacted soil along the static compaction curves

Sahar Satar Al-Khyat

Geoenvironmental Research Centre

School of Engineering

Cardiff University

UK

Thesis submitted in candidature for the degree of Doctor of Philosophy at Cardiff University

2018

This work is dedicated to the memory of my father-in-law

Acknowledgements

In the name of Allah, the Most Gracious, the Most Merciful

I would like to express sincere gratitude and appreciation to my academic supervisors Dr Snehasis Tripathy and Dr Peter Cleall for their expert guidance and valuable feedback. It has been a real privilege working under their supervision that provides me with an invaluable experience and encouragement to successfully complete this thesis.

I am deeply indebted to my sponsor, the Higher Committee for Education Development in Iraq (HCED) for their financial support and immediate response in solving problems I encountered during my PhD study. I wish to extend my appreciation to the Ministry of Higher Education and Scientific Research / AL-Mustansiriyah University and to the Iraqi Cultural Attaché in London for the help and support during the study period.

Further gratitude and appreciation are expressed to various people at Cardiff University including all the technical staff at ENGIN, particularly Mr Steffan Jones, for their help in overcoming the challenges of my experiments and all the staff of ENGIN Research Office for always keeping their door open for my inquiries. 1 would like particularly to thank Dr Stephen Rees for accepting to be the annual reviewer of my research and for his valuable comments.

I am extremely grateful to all my friends with whom I have shared the office together with all those who I have met at Cardiff University, particularly those in the GRC for their enjoyable discussion and cooperation.

Special thanks are given to my husband, Mahdi, for his persistent love, tremendous support and so much else. My daughter and son, who have inspired me with their understanding, patience and love, many thanks Zahraa and Ali.

I thank also my parents, sisters, relatives, colleagues and friends, in Iraq, who have endured me for my passion in research. They have shown both patience and good cheers throughout this challenging but exciting period of my life.

Sahar Al-Khyat

2018

Abstract

Unsaturated compacted soils are used in many civil engineering works, such as earth dams, embankments, soils beneath foundations and pavements. A major problem encountered with these soils is the tendency to collapse upon wetting under certain conditions. There has been extensive research into the collapsibility of compacted soils. However, comprehensive investigation into the hydro-mechanical behaviour of unsaturated compacted soils under various loading, wetting and compaction conditions is needed for the engineers to devise safe and cost-effective solutions to such problem. The outcomes of such a study also provides a wider perspective on soil collapsibility and generate geotechnical data and parameters useful for establishing and validating constitutive models.

This thesis presents a laboratory-based experimental study of the collapse behaviour of compacted soil mixtures of 40% silt, 40% sand and 20% clay. Series of laboratory tests were conducted including basic characterisation, static compaction behaviour, suction measurements, single and double-oedometer tests, and suction-controlled oedometer tests under wetting. In this context, a new static compaction testing procedure is developed for establishing static compaction curves of the soil both in terms of applied compaction pressure and compaction energy. One-dimensional volume change behaviour of compacted samples along the established static compaction curves was explored. Statically compacted specimens with various compaction conditions were subjected to a wide range of vertical stresses. The compatibility of various controlled-suction wetting tests was also explored. The experimental data obtained were analysed in terms of collapse strain and soil-water characteristic curves (SWCC) based on theories of unsaturated soil mechanics.

The proposed procedure of the static compaction tests showed the potential effectiveness in establishing static compaction curves at various levels of compaction energy and pressure. The static compaction pressure required to transmit constant compaction energy was found to decrease with increasing the water content of specimens, whereas increased compaction energy was observed along the compaction pressure curves. The static compaction was also found to induce suction changes of specimens. The study generated new knowledge in the form of linking the compaction effort with the collapse behaviour at a various range of applied vertical stresses and suction. The collapse behaviour of compacted specimens along the static compaction curves was found to be predominantly controlled by the applied compaction pressure during specimen preparation. Similarly, the wetting SWCCs of compacted specimens along the static compaction curve were found to be strongly influenced by the static pressure of compaction at low suctions.

Table of contents

List of Figures

List of Tables

Chapter 1

Introduction

1.1 Background

Many soils considered problematic in geotechnical engineering because of their potential to exhibit complex volumetric behaviour under changing environmental conditions, such as swelling and collapse following wet climatic periods (Evans et al. 2004). This characteristic is attributed to their composition, mineralogy, fabric or the nature of pore fluids (Bell and Culshaw 2001). Different types of problematic soils have been recognised, however, one of the most significant ground related hazards to the built environment is collapsible soils.

Collapsible soils can be defined as any unsaturated soils with a metastable structure that are capable of sustaining a relatively large overburden pressure but at risk to experience a significant reduction in volume in response to wetting (Ng and Menzies 2007).

The collapse behaviour is associated with the wetting-induced volume change of unsaturated soils (Tadepalli and Fredlund 1991). Such volume change can cause damage to the lightly loaded structure including houses, buildings, roads and pipelines; failure in earth dams and slope failure. The expected future variations in climate could potentially cause significant changes in the soil moisture regime and exacerbate problems associated with expanding the occurrence of the unsaturated soils (Barden et al. 1973). Consequently, enormous damage can occur due to collapse in terms of both economic and human loss (Fredlund 1979; Lawton et al. 1992; Sun et al. 2013). Therefore, structures founded on collapsible soils require special considerations for

their design. Thus, a thorough and comprehensive study on the hydro-mechanical behaviour of such soil will lead to a better understanding of its response to various loading, wetting and compaction conditions.

Collapsible soils are found in many parts of the world (Figure 1.1), typically in arid and semi-arid climate areas. The well-known examples being the extensive deposits of loess (aeolian deposit) in Europe, Russia, North and South America, China and Iran (Rogers 1995; Houston et al. 2001; Northmore et al. 2008; Al-Janabi 2014). Further to the natural collapsible soils, compacted soils that used in many civil engineering works, such as earth dams, embankments, soils beneath foundations and pavements tend to collapse upon wetting under certain conditions (Houston and Houston 1997; Lawton et al. 1992; Pereira et al. 2005). In Iraq, while collapsible soils in the form of thin loess deposit (Yahia 1971) and gypseous soils cover about 20% to 30 % of its total area (Al-Saoudi et al. 2013; Fattah and Dawood 2016), the classical framework of soil mechanics are merely used in analysing the collapse behaviour.

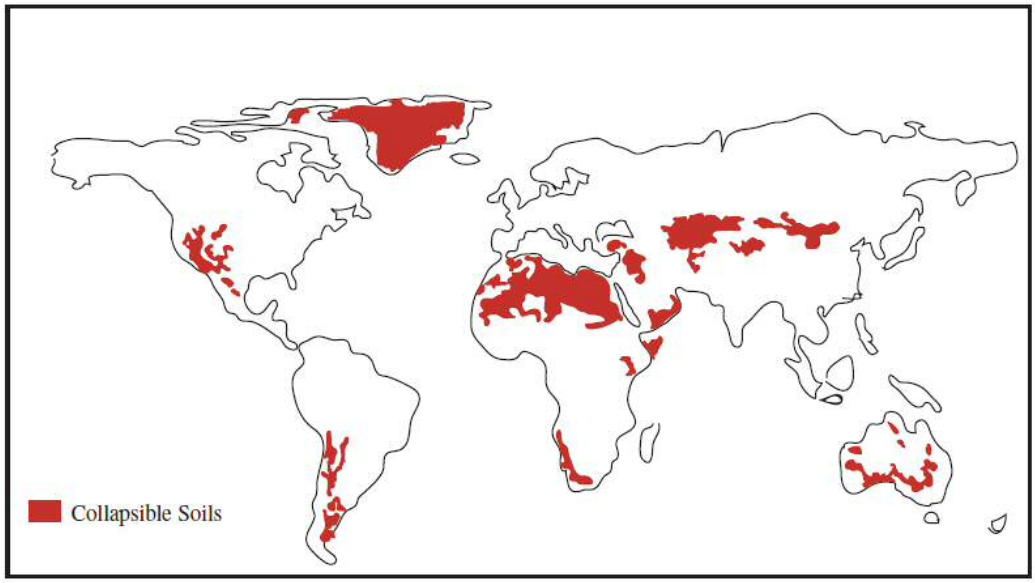

Figure 1.1 Distribution of collapsible soils around the world (after Al-Janabi 2014)

Types of wetting ranging from local, slow, gradual to intense driven by the environmental conditions are identified to triggering the mechanism of collapse in unsaturated soils (Xanthakos et al. 1994; Houston et al. 1995). Intense wetting, for example, is possible during heavy rainfall and extensive irrigation.

Wetting-induced collapse strain is often quantified by conducting single or double oedometer tests (Houston et al. 1988). The literature review suggested that the initial water content, compaction effort and applied pressure are the main factors in controlling the amount of collapse strain of compacted soils (Lawton et al. 1989; Basma and Tuncer 1992; Pereira and Fredlund 2000; Houston et al. 2001; Delage et al. 2005; Aziz et al. 2006; Sharma and Singhal 2006; Jiang et al. 2012; Okonta 2012; Singhal et al. 2015; Fattah and Dawood 2016). However, the collapse behaviour of compacted soil samples along the compaction curve (i.e., water content – dry density relationship for a given compaction effort) has yet to be explored.

Collapsible soils are unsaturated at the time of placement. Such soils possess a negative pore-water pressure or suction (Lu and Likos 2004). Suction of unsaturated soils reduces significantly by wetting as indicated by the typical wetting curve of the soil-water characteristic curve (SWCC). The SWCC is a crucial function used to predict and interpret the behaviour and response of unsaturated soils (Fredlund et al., 2012). Prediction of collapse settlement based on the SWCC has been recently proposed and validated by Xie et al. (2018). As influenced by suction changes, the collapse behaviour of unsaturated soils has been extensively studied by conducting wetting tests that allowed suction to be controlled (e.g., Chen et al. 1999; Sivakumar and Wheeler 2000; Sun et al. 2004; Jotisankasa et al. 2007; Muñoz-Castelblanco et al. 2011; Haeri et al. 2014; Karami et al. 2015). Various methods can be utilised to control suction for testing unsaturated soils. The most commonly used technique for controlling suction is the axis

translation technique (Fredlund and Rahardjo 1993). Suction-controlled wetting tests using the axis translation technique have been performed under the oedometer (Airò Farulla et al. 2010; S Mohsen Haeri et al. 2016) and triaxial conditions (Pereira and Fredlund 2000; Sun et al. 2007; Haeri et al. 2014; Liang et al. 2016). In these types of tests, both single and multiple specimens can be tested. A single soil sample is commonly used for all the suction reduction steps. Measurement of water content corresponded to the applied suction reduction steps cannot be made until the end of the tests. The corresponding water contents, therefore, are computed based on the final measured one. Several studies, however, have acknowledged the dissimilarity between the measured and calculated final water contents (e.g., Perez-Garcia et al. 2008). On the other hand, while testing multiple specimens allowed for water content to be measured at each applied suction, variability in the soil fabric, density and water content are issues introduced by such testing procedure. Therefore, a detailed investigation by exploring various types of testing procedure and studying the influence of test results in terms of water retention and volume change is required.

The volume change behaviour of soils is fundamentally interrelated to the hydraulic characteristics. Thus, the collapse behaviour is directly affected by the variations in matric suction associated with wetting. Three distinct phases of collapse deformation as influenced by suction changes have been identified (Kato and Kawai 2000; Pereira and Fredlund 2000; Futai and Almeida 2005; Zhou and Sheng 2009; Garakani et al. 2015). Further to the effect of matric suction, the level of the applied stress also influences the collapse. While the increase in the applied net stress leads to higher soil collapsibility (Pereira and Fredlund 2000), it was also noted that the collapse potential (i.e., the magnitude of one-dimensional collapse up on wetting at a given applied stress) reaches a maximum and then reduces with increasing stress (Dudley 1970; Wheeler and

Sivakumar 1995; Sun et al. 2004; Vilar and Rodrigues 2011). The uniqueness of SWCCs of collapsible soils under different applied net stresses is still debated (Pereira and Fredlund 2000; Pereira et al. 2005; Sun et al. 2007; Garakani et al. 2015; Haeri et al. 2016; Liang et al. 2016). Although several studies explored the collapse behaviour under different stress states, the focus is only given to an initial state of the compacted soil. Therefore, further work is needed to provide an integrated study of the effects of stress and compaction states on the volume change and SWCCs of collapsible soils.

The concepts of unsaturated soil mechanics are more applicable for interpreting the collapse behaviour of unsaturated compacted soils (Alonso et al. 1990; Pereira and Fredlund 2000; Loret and Khalili 2000; Khalili et al. 2004; Lu 2011). The single-valued effective stress equation (Bishop 1959) has resulted in limited success (Jennings and Burland 1962). Khalili et al. (2004) investigated the validity of the effective stress concept in unsaturated collapsible soils. The results suggested that incorporating an appropriate plasticity model is needed for capturing the collapse by the single effective stress approach. The collapse behaviour is better described by the two independent stress variables approach (Fredlund and Morgenstern 1977). Nonetheless, this type of framework cannot be reconciled with classical saturated soil mechanics (Nuth and Laloui 2008). Recently, Lu and Likos (2006) and Lu et al. (2010) proposed the suction stress approach to determine the effective stress of unsaturated soil. In its simplest form, the suction stress concept avoids many challenging difficulties in experimental determination and theoretical development of the previous approaches. In this research, the experimental results were analysed according to the above-mentioned approaches.

Unsaturated compacted soil samples were considered in this research to study the collapse behaviour in response to various loading, wetting and compaction conditions. The compacted soil was a mixture of 40% silt, 40% sand and 20% clay.

1.2 Research objectives

The overall aim of this research was to study in detail the collapse behaviour of unsaturated compacted soil during wetting-induced collapse tests.

The following objectives are set to fulfil the research aim.

1. To investigate methods of preparing compacted soil samples that have a tendency to collapse upon wetting and to develop a simple and effective compaction method, by which the initial placement conditions can be better defined.
2. To identify the role of the compaction state (i.e., applied static compaction efforts) and stress state (i.e., applied vertical stress) in the collapse of statically compacted samples.
3. To explore the effect of various testing procedures on the collapse behaviour both in terms of deformation and water absorption characteristics during suction-controlled oedometer tests.
4. To study changes in collapse and SWCCs of compacted soil samples under various stress states (i.e., vertical net stress and matric suction) and various compaction conditions.
5. To examine the applicability and evaluate the validity of different effective stress approaches for unsaturated soils in describing the collapse behaviour, in particular, the suction stress characteristics curve approach.

1.3 Thesis overview

The structure of the thesis is organised into nine consecutive chapters. After the background introduction to the research in Chapter 1, a brief and critical review of essential previous theoretical and experimental works relevant to the topic of this study is given in Chapter 2. Characterisation of the soil used, the experimental programme and details of the experimental setup and procedure used for studying the collapse behaviour are provided in Chapter 3. Static compaction behaviour of the soil used was studied in Chapter 4 by proposing a simple testing procedure to establish static compaction curves both in terms of compaction energy and compaction pressure. Factors influencing the established static compaction curves as well as suction measurements along compaction curves are all discussed in Chapter 4. From the results of chapter 4, specimen conditions were selected for the main testing programme in the following chapters. Chapter 5 explores the collapse behaviour of soil samples along the established static compaction curves by carrying out a series of single and double oedometer tests. Suction-controlled oedometer tests were performed on single and multiple specimens by adopting various testing procedures as presented in Chapter 6. Based on the results of Chapter 6, the appropriate procedure of suction-controlled oedometer tests for the work carried out in Chapter 7 was selected. By which, the effect of different stress states and compaction conditions are discussed in Chapter 7. The results of chapters 7 were replotted based on the effective stress approaches in unsaturated soils as presented in Chapter 8. Finally, the key findings concluded from various parts of the thesis and the recommendations for future work are presented in chapter 9. The overall structure of the thesis and the contents of each chapter are provided in Figure (1.2).

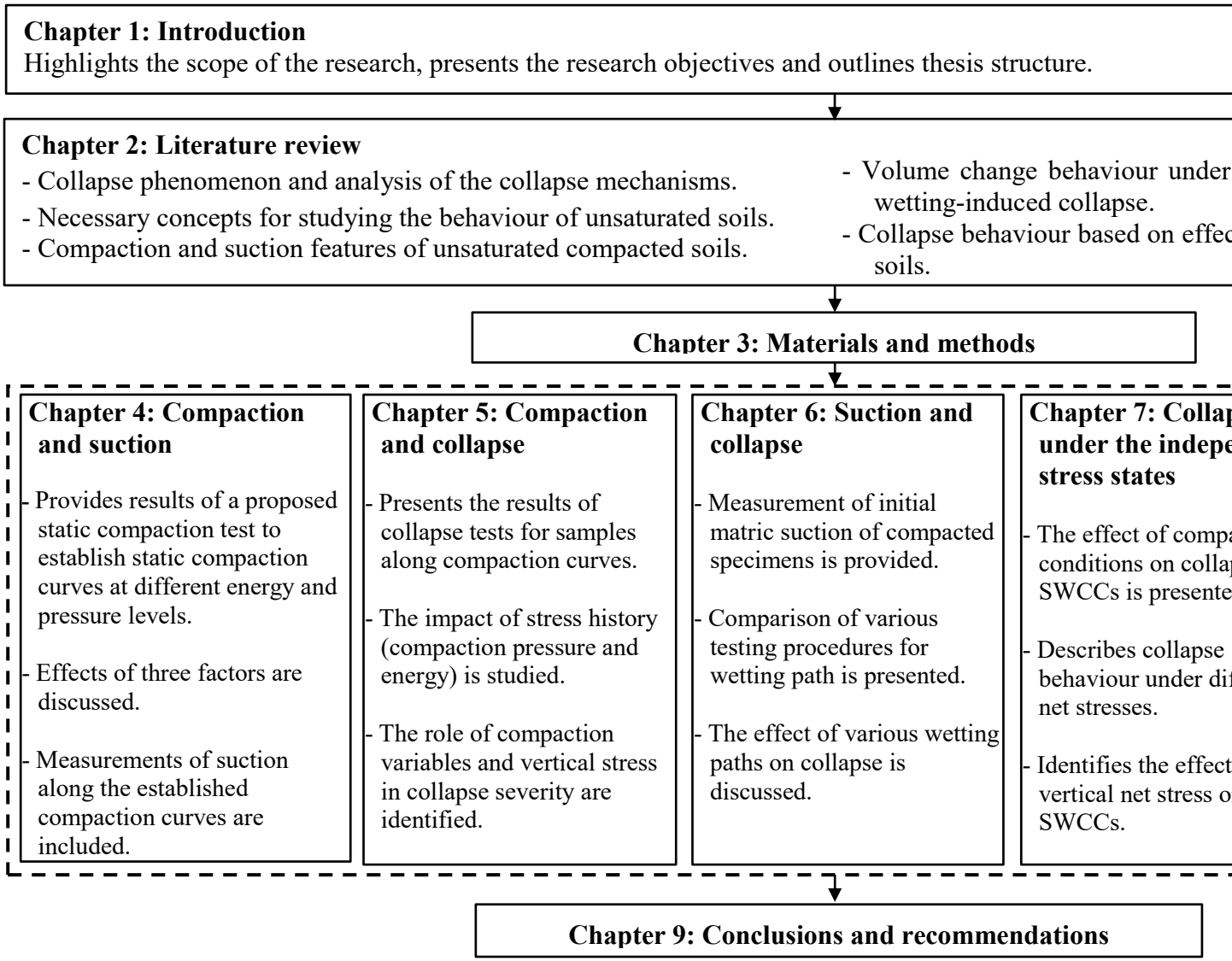

Figure 1.2 Outlines of the thesis chapters

Chapter 2

Literature Review

2.1 Introduction

In recognition of the problems associated with collapsible soils, this review aims to provide an appraisal of the collapse behaviour both in terms of volume change and water-retention characteristics of unsaturated compacted soils. The collapse phenomenon and mechanisms of collapse are introduced. Necessary concepts for studying the behaviour of unsaturated soils, such as suction and measurement and control methods of suction are discussed. The review also focused on the compaction and suction features of unsaturated compacted soils. A critical review of the collapse behaviour of compacted soils during single and double oedometer tests along with suction-controlled oedometer is presented. The last section of this review deals with the effective stress approaches of unsaturated soils and their effectiveness in describing the collapse behaviour.

The overall aim of this research was to study in detail the collapse behaviour of unsaturated compacted soil during wetting-induced collapse tests and the objectives of this review are to, (*i*) provide a concise review of the development of theories and experimental works regarding the collapse behaviour, (*ii*) collate information on the volume change behaviour during wetting tests both under and without suction control and (*iii*) identify gaps in knowledge that will be covered in this study.

2.2 Collapsibility of unsaturated soils

Unsaturated soils cover almost 40% of natural soils on the earth surface (Uchaipichat 2011). Unsaturated soils have been commonly encountered in both geotechnical and geoenvironmental engineering practice (Fredlund 2000). One of the most common problems associated with unsaturated soils is the susceptibility to collapse upon wetting. In the following sections, the collapsibility of unsaturated soils is discussed.

2.2.1 Collapse phenomenon

The term "collapse" means any marked, sudden change of stability (Feda 1995). Collapsibility of soils refers to a considerable reduction in the total volume due to wetting. Collapsible soils are unsaturated soils that deposited into a loose honeycomb-type structure and have a relatively high apparent strength at its natural water content. Ideally, four requirements initiate collapse of unsaturated soils: (i) an open and metastable structure, (ii) a relatively high applied stress, (iii) sufficient inter-particle bonds (e.g., capillary forces) and (iv) water inundation to trigger the collapse (Dudley 1970; Barden et al. 1973; Mitchell 2005).

Collapse as a generally occurring phenomenon can be encountered in arid and semi-arid regions. In these areas, unsaturated conditions are relevant due to the deeply positioned groundwater table. Upon wetting, changes occur in the volume and shear strength of the soil. Different types of collapsible soils have been identified in the literature (Dudley 1970; Rogers 1995; Houston et al. 2001). The classical ones are naturally deposited, such as loess that covers over 10% of the earth's surface (Evans et al. 2004), gypseous deposits and some residual soils. Man-made fills, such as compacted soils may also produce collapse behaviour under certain conditions.

2.2.2 Composition of collapsible soils

The collapsible soils are often a mixture of silt, sand and clay with a wide range of proportion as given in Table (2.1). In Britain, the existence of collapsible soils is very modest (Assallay et al. 1997). However, loess deposited are encountered in Pegwell Bay in Kent, in the south-east of England (Northmore et al. 2008). The metastable structure of the Pegwell Bay loess deposits formed the main feature of the collapsible soils. The thickest loess deposits of Pegwell Bay soil are generally < 5 m and the field densities ranged from 14.5 to 16 kN/m^3 (Fookes and Best 1969).

Table 2.1 Summary of the particle size distribution for reported collapsible soils

Reference	Soil type	Silt (%)	Clay (%)	Sand (%)
Habibagahi and Mokhberi (1998)	Compacted loess	66	25	9
Rao and Revanasiddappa (2000)	Compacted residual	26	32	42
Aziz et al. (2006)	Compacted residual	15	40	45
Jotisankasa et al. (2007)	Prepared	52	26	22
Muñoz-Castelblanco et al. (2011)	Natural loess	82	16	2
Leong et al. (2013)	Compacted residual	39	11	50
Karami et al. (2015)	Prepared	20	29	51
Liang et al. (2016)	Natural loess	74	20	6

2.2.3 Collapse mechanism

The basic mechanism of collapse involves particle re-arrangement from a metastable open structure to a denser hydrocollapsed structure (Miller et al. 1998). For the study of collapse mechanism, where the state changes from metastable to unstable, several approaches have been differentiated. Two collapse mechanisms of soil structure were suggested by Feda (1995); micromechanical and macromechanical. Recently, the mechanism of loess collapsibility discussed based on microstructure, soil mechanics-based approaches and traditional approaches (Li et al. 2016).

The micromechanical analysis means a study of the role of structural components, fabric, bonding and pore distribution. Based on this approach, collapse behaviour is analysed in terms of three aspects: collapse by de-ponding, fabric transition and particle breakage. Similar factors called particle pattern, pore form, and bonding material are identified for loess (Li et al. 2016). The investigation of the microscopic soil behaviour requires either an electron-scanning microscope or indirect tests, such as mercury intrusion porosimetry. The microstructural analysis is physically good at explaining the collapse mechanism, but collapse is subjectively analysed and qualitatively expressed (Alonso et al. 1993; Chen et al. 2006).

The macromechanical analysis is confined to the behaviour observed where the soil is treated as a continuum. Phenomenological quantities, such as stress and strain are often considered for the analysis. The parallel approach is the soil mechanics-based approach, in which concepts of soil mechanics are used for interpreting the collapse (Li et al. 2016). Since collapsible soils are characteristically formed under unsaturated conditions, the principles of unsaturated soils mechanics are more rational to be embraced (Fredlund and Rahardjo 1993).

The traditional analysis concerns the role of a sole parameter in explaining the collapse mechanism, such as loss of capillary tension or shortage of clays. It also based on correlating collapse to conventional soil properties including void ratio, density, water content, Atterberg limits and grain size distribution etc. The validity of this approach has been questioned since the collapse behaviour cannot be universally explained based on one parameter and neglecting other intimately related factors (Li et al. 2016).

A combination of microstructural and macromechanical approaches would be the optimum method of interpretation the collapse mechanism (Feda 1995). However, this study is limited to analysing the collapse behaviour of compacted soils based on the soil mechanics-based approach and exclusively under wetting-induced collapse.

2.3 Soil suction

Soil suction is a measure indicating the free energy state of soil water (Fredlund and Rahardjo 1993) or the relative humidity of the pore-water vapour in the soil. It is also referred to the ability of soils to attract and retain water and therefore, considered a critical variable that governs the mechanical behaviour as well as the flow regime of partly saturated soils. Thermodynamic considerations indicated that soil suction corresponding to zero water content is approximately 10^6 kPa (Fredlund 1991).

Soil suction (also termed total suction,) consists of two components: matric suction ( ) and osmotic suction ((Richards 1974) as given in Equation (2.1). The matric suction is generated by two energy components (per unit volume): capillary potential and adsorption potential and is commonly defined as the excess of pore air pressure, , over pore water pressure, , as expressed by Equation (2.2). The osmotic suction originates from the dissolved salts contained in the pore water.

(2.1)

(2.2)

Based on the assumption that solutes present in the soil water are dilute enough, the osmotic suction is often considered insensitive to changes in water content (Blatz et al. 2008). Matric suction is generally approximated equal to the total suction in unsaturated soils (Fredlund and Rahardjo 1993)

In experiments, suction can be either measured or controlled. Several techniques are introduced for measuring and controlling suction and detailed discussions of these techniques are available throughout the literature (Lee and Wray 1995; Rahardjo and Leong 2006; Ng and Menzies 2007; Bulut and Leong 2008; Delage et al. 2008; Murray and Sivakumar 2010; Fredlund et al. 2012). Selection of the appropriate technique depends on the suction to be measured (i.e., total, matric or osmotic) and suction range of interest. Since comprehensive reviews of suction measurement and control techniques are already exist, only techniques used in this research are reviewed.

2.3.1 Suction control techniques

The commonly used methods for inducing matric suction in unsaturated soils are the axis translation and osmotic techniques, and for controlling total suction is the vapour equilibrium technique. For suction up to 1.5 MPa, the axis translation method is often used, whereas for a higher range of suction the vapour equilibrium technique can be utilized to apply total suction up to 250 MPa (Fredlund et al. 2012). Since the desired matric suction to be studied in this research is below 1500 kPa, the axis translation technique will be used. The principles of this technique along with its limitation are critically reviewed in the following sections.

2.3.1.1 Axis-translation technique

The axis-translation technique is a frequently used laboratory technique for imposing matric suction. It is based on the hypothesis that any change in air pressure is directly translated into an equal change in pore water pressure as long as both soil particles and fluid are incompressible. The pressures differential (i.e., matric suction) therefore, remains constant (Hilf 1956). Such translation will allow measuring and controlling the pore water pressure.

The axis-translation technique is often accomplished by separating air and water phases in soil through a saturated high air-entry ceramic disk. The disk allows water passage but prevents the flow of free air when the applied matric suction does not exceed the air-entry value of the ceramic disk. The maximum matric suction that can be applied or measured is 1500 kPa (i.e., the highest air entry value of currently available ceramic disks in the market). For reliable measurements of matric suction, the axis-translation technique requires continuity in both the air and water phases (Murray and Sivakumar 2010).

Under undrained condition, matric suction can be measured by translating the origin of the reference air pressure. When controlling suction, two procedures are possible to be followed; air-overpressure and water-sub pressure techniques (Romero 2001). The air-overpressure method involved changing the water pressure while keeping the air pressure at a constant value. In contrast, modifying the air pressure while maintaining a constant water pressure describes the water-sub pressure technique.

The axis-translation technique has also been successfully applied to different types of equipment for the volume change and shear strength testing of unsaturated soils, including oedometer (Romero et al. 2003; Airò Farulla et al. 2010; S Mohsen Haeri et

al. 2016), direct shear apparatus (Gan et al. 1988) and triaxial apparatus (Wheeler and Sivakumar 1995; Pereira and Fredlund 2000; Sun et al. 2007; Haeri et al. 2014; Karami et al. 2015; Liang et al. 2016).

2.3.1.2 Challenges of utilising the axis-translation technique

Despite the effectiveness of using the axis-translation technique in measuring and controlling matric suction, its application involves difficulties and limitations. The challenges include the air diffusion, soil-water evaporation and compressibility of occluded air at high degrees of saturation (Bocking and Fredlund 1980; Delage et al. 2008; Vanapalli et al. 2008; Marinho et al. 2008).

Air diffusion through the saturated ceramic disk is one of the leading problems (Fredlund 1975; Bocking and Fredlund 1980). The air dissolves in the water of the disk and diffuses as air bubbles underneath the disk (Figure 2.1). The diffused air prevents the water phase continuity between the water in the ceramic disk and the water in the compartment (Tripathy et al. 2011). The diffused air also introduces inaccuracy to the measurement of water volume exchange or pore-water pressure and tends to underestimate the actual matric suction of the soil.

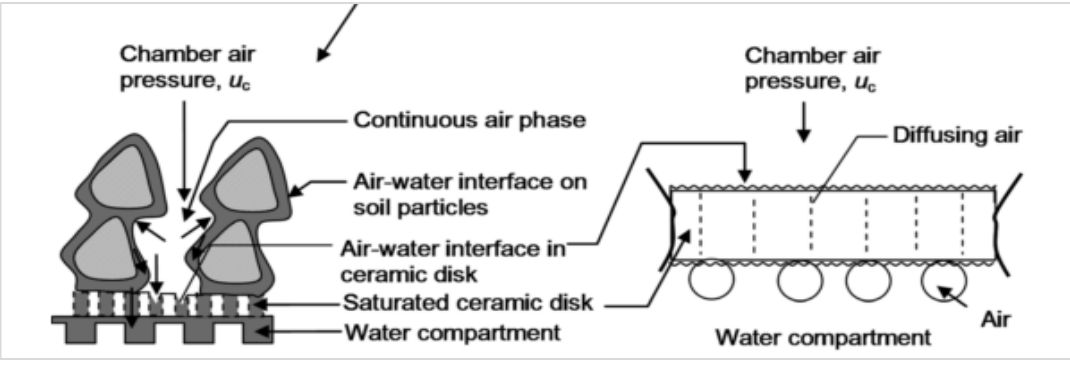

Figure 2.1 Water phase continuity requirement and diffusion of air into the saturated ceramic disk (after Tripathy et al. 2011)

Fredlund and Rahardjo (1993) stated that tests lasting more than a day would experience air diffusion. The rate of air diffusion, however, varied fairly with the applied matric suction. Padilla et al. (2006) measured the diffusion rate at different pressures for 1, 3, 5, and 15 bar ceramic disks. The 1 and 3 bar disks did not generate a measurable amount of diffused air, whereas the 5-bar disk generated diffused air relatively less than the 15-bar disk. For reliable application or measurement of matric suction, periodic flushing of the diffused air has been suggested (Padilla et al. 2006; Vanapalli et al. 2008).

Another challenge of utilising the axis-translation technique is the evaporation of soil-water through the top coarse porous stone in contact with the compressed air lines (Romero 1999; Oliveira and Fernando 2006). Such water loss is originated by the difference in the relative humidity of the air above the soil surface and the pore water of the soil specimen. This difference will affect matric suction and the real exchange of water volume. Depending on the applied suction value, the opposite effects of diffused air and evaporated water may either cancel each other out or one may prevail (Airò Farulla and Ferrari 2005).

2.3.2 Suction measurement techniques

Suction measurement techniques can be categorised as either a direct or indirect measurement. The direct measurement of soil suction relies on direct observation of the pore water pressure, whereas indirect methods involve the measurement of a physical property that is directly related to suction, such as relative humidity, electrical resistance, and water content (Ridley and Wray 1996). Techniques used to produce this research including null-type axis-translation technique, chilled-mirror dew-point technique, and water potential sensor are briefly reviewed in the following sections.

2.3.2.1 Null-type axis-translation technique

Based on the axis-translation technique, matric suction of unsaturated soils can be directly measured using null pressure plate apparatus (Olson and Langfelder 1965; Fredlund and Rahardjo 1993; Leong et al. 2003; Tripathy et al. 2004). Generally, any system provides separation between water and air phase, usually by using a ceramic disk with high air-entry value can be used to conduct this type of tests (e.g., Leong et al. 2009; Power and Vanapalli 2010; Tripathy et al. 2011). This technique is called a null-type because the water pressure is maintained at zero throughout the test. It can be used to measure matric suction up to 1500 kPa as limited by the available air-entry value of the ceramic disk.

The equilibration time required for measuring matric suction is dominated by the type of the soil, size of specimens, and permeability characteristic of the ceramic disk used. Equilibration may occur within 30 minutes up to several hours (Fredlund and Rahardjo 1993; Tripathy et al. 2005; Rahardjo and Leong 2006). In general, drier specimens would take a longer time to equilibrate in null-type tests as the increase in suction level was found to increase the equilibration time (Oliveira and Marinho 2008).

Two distinct factors were noted to affect the equilibration time and reliability of suction measurements using the null-type tests; the flexibility of the measuring system and the compaction conditions of soils (Tripathy et al. 2011).

2.3.2.2 Chilled-mirror dew-point technique

Several models of hygrometers are commercially available, such as WP4 (Decagon Devices 2007) and WP4C dew-point potentiometer (Decagon Devices 2010). These

devices implement the chilled-mirror dew-point technique to indirectly determine the total suction of soils.

The working principle of this technique (using WP4C dew-point potentiometer) involves measuring the dew-point of ambient water vapour in a sealed chamber at equilibrium with water in the soil specimen by a chilled mirror. A fan included in the sealed chamber facilitates the equilibrium process. The mirror is cooled to a dew-point of the equilibrated water vapour by an attached Peltier thermoelectric. By reaching the dew-point temperature cell, condensation will begin to form on the mirror surface. Detection of the dew point at which condensation first occurs on the mirror is observed by a beam of light directed onto the mirror and reflected into a photodetector cell. A thermocouple attached to the mirror records the dew point temperature. The device is also equipped with a temperature controller to set the temperature of the soil specimen at which relative humidity measurement has to be made. The dew-point with the set specimen temperature is then used to determine the relative humidity by using Equation (2.3). Total suction corresponding to the determined relative humidity can be calculated based on Kelvin's law (Equation 2.4). The calculations are performed by software within the device and displayed on an LCD panel in MPa along with the specimen temperature.

(2.3)

(2.4)

where is the relative humidity, and are the dew point and the absolute temperature, respectively (i.e. T = (273.15 + t) K), t is the temperature in ˚C, is the total suction (kPa), R is the universal (molar) gas constant (8.31432 J. mol^{-1}. K^{-1}), is the specific volume of water or the inverse of the density of water (i.e. 1/ m^3/kg), is the density of pure water (i.e. 998 kg/m^3 at t = 20 ˚C), is the molecular mass of water vapour (i.e. 18.016 kg/kmol).

The chilled-mirror technique has been used as a reference method for comparison with other suction measurement techniques (Leong et al. 2003; Agus and Schanz 2005; Cardoso et al. 2007; Petry and Jiang 2007; Tripathy et al. 2014; Rorke et al. 2015). Petry and Jiang (2007) results indicated less variance and more conservative values of suction obtained using the chilled-mirror dew-point technique as compared to the filter paper method. In contrast, Leong et al. (2003) observed that total suctions obtained by the chilled-mirror dew-point technique were always greater than the sum of matric and osmotic suctions independently measured using the null-type tests and the pore fluid squeezer, respectively.

The advantages of this technique are its simplicity in providing measurements that are consistent and repeatable along with reducing the time of determining the total suction of unsaturated soils (Petry and Jiang 2007). However, the main limitations are the decreasing accuracy at low suction values (Leong et al. 2003), and a possible lack of thermodynamic equilibrium between the soil sample and the sample chamber (Campbell et al. 2007).

2.3.2.3 Water potential sensor

Calibrated water potential sensors, such as MPS-2 and MPS-6 (Decagon Devices 2014) allow indirect measurement of matric suction of soils. The working principle of the MPS-6 includes measuring water potential of soils by a solid matrix equilibration technique. The technique based on introducing a known material with a static matrix of pores (porous ceramic disk) into a soil until attaining a hydraulic equilibrium. At equilibrium, the measured water potential of the solid matrix is equal to the water potential of the soil. The ceramic disk of the sensor is calibrated to a unique pre-established water characteristic curve. Any change in the water content of the ceramic disk due to introducing the soil can be detected. The water content can be then related to the corresponding suction value using the water characteristic curve of the ceramic disk shown in Figure (2.2). The water retention characteristic of the ceramic disks is established based on the mercury intrusion porosimetry data (Decagon Devices 2014).

Performance of these sensors has been evaluated by Tripathy et al. (2016) and Nolz and Kammerer (2017). The results revealed that the MPS-2 and MPS-6 sensors offer suitability in measuring a wide range of suction values.

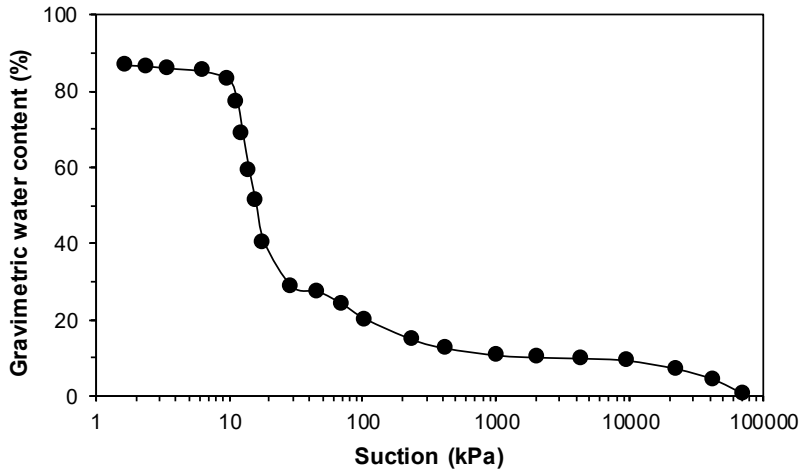

Figure 2.2 Water retention curve of the ceramic disc of the MPS-6 sensor (modified after Decagon Devices 2014)

2.4 Soil-water characteristic curve (SWCC)

A soil-water characteristic curve (SWCC) is a function describing the relationship between soil suction (matric or total) and the amount of water (gravimetric, volumetric or degree of saturation). The SWCC is the most crucial soil property function that used for application of unsaturated soil mechanics into engineering practice and for estimating other unsaturated soil properties, such as shear strength and the coefficient of permeability (Fredlund 2002).

In the following sections, a brief review concerning the features of SWCCs and of measurement methods are presented. Since the SWCC of a soil is not unique, influencing factors are also discussed. Emphasis will be given to SWCCs of collapsible soils. The mathematical expressions proposed to best fit the SWCCs are also reviewed.

2.4.1 Features of SWCCs

The SWCCs are typically plotted from a low suction value (e.g. 0.1 kPa) to the maximum value of 10^6 kPa. A complete SWCC consists of drying (desorption) and wetting (sorption) curves. The drying curve represents the water desorption of soil when the matric suction increases while the reverse process represents the wetting curve. However, the drying and wetting SWCCs of a given soil are not unique. The difference in the drying and wetting curves is related to a hydraulic hysteresis, in which higher suction is in the drying curve at a given water content. Hysteresis can be attributed to several phenomena including the ink-bottle effect resulting from irregular shapes of pores, different contact angles for advancing and receding water menisci and entrapped air in newly wetted soil (Lu and Likos 2004). Figure (2.3) illustrates typical drying and wetting curves of the SWCC showing some of the key features.

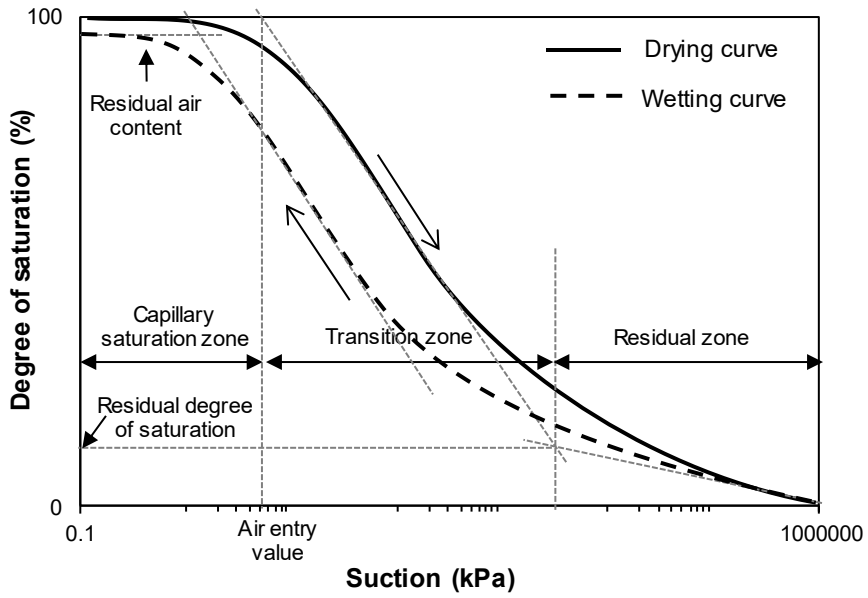

Figure 2.3 Typical drying and wetting SWCC curves (modified after Vanapalli et al. 1996)

A noticeable feature of the wetting SWCC behaviour is that soil specimens may not reach full saturation when reducing the suction to zero. This behaviour is primarily related to the occluded air during the wetting process. Since the drying curve is easier to measure, most of the existing SWCC data are for soils under the drying process (Fredlund 2006).

The SWCC, for drying and wetting curve, typically a sigmoidal function having an inflection point when plotted on a semi-logarithmic scale. The S-shaped curve is for soils with a normal pore size distribution. However, SWCCs can also have more complex shapes, mainly because of both structure and composition of a soil. For example, a bimodal SWCC is usually associated with a bimodal pore size distribution (Burger and Shackelford 2001). The bimodal SWCC has been observed in some structured soils such as aggregated loams, loess deposits, residual soils and collapsible clays (Othmer et al. 1991; Rahardjo et al. 2004). The shapes of SWCCs can, therefore, be used as an indication of the pore size distribution of the soil.

Any SWCC can consist of three different saturation stages: capillary saturation where soil remains fully saturated, transition stage and residual stage.

The border between saturated and unsaturated condition is known as the air entry or expulsion value for the drying and wetting curve respectively. The air entry value can be defined as the suction value at which the air starts to enter the largest pores in the soil for initially saturated soil, whereas the air expulsion value is the suction required for air to expel from the largest pores in the soil during the main wetting curve.

The residual condition, defining both the residual degree of saturation and the corresponding value of soil suction, indicates a discontinuous liquid phase that forms a thin film of water surrounding the soil particles (Vanapalli et al. 1998). The residual degree of saturation is irreducible saturation at which water can only be transferred through the soil as water vapour.

2.4.2 Measurement of SWCCs

The suction-water content SWCC of a soil can be established either by imposing suction and determining the corresponding water content or by measuring suction at various water contents. In general, a combination of methods is often utilised to establish the SWCC because there is no unique technique or device that can cover the entire range of suction. Various devices and techniques are currently available for measuring the SWCC of a soil (Fredlund et al. 2012), such as pressure plate, filter paper, thermal and electrical conductivity sensors and null-type axis translation. These techniques vary widely in terms of the measurement range, working principle, equilibrium time and complexity.

The SWCC is conventionally measured assuming no major changes in the total volume of a soil specimen. However, this assumption is not valid for testing highly deformable soils, such as collapsible and expansive soils. For this reason, the volume change measurement must be considered while measuring the SWCC to provide reliable information. Further, it is often measured under zero applied net stress. Ignoring the effect of both volume change and applied stress may lead to erroneous results in the established SWCC and therefore it would not be realistic for estimating properties of unsaturated soils. To this end, modified pressure plate, oedometer and triaxial apparatus have been used to properly establish the SWCC that is closer to the real condition of the soil (Aversa and Nicotera 2002; Leong et al. 2004; Miller et al. 2008).

Although measuring the SWCC of deformable soils require measurements of volume change, researchers dealting with collapsible soils have used conventional methods. Pereira and Fredlund (2000) measured the drying SWCC of compacted collapsible soil using Tempe cell and pressure plate apparatus to predict the range of matric suction needed to be considered in their laboratory programme. Similarly, a drying test of the SWCC conducted on compacted Pearl clay by using both the pressure plate method and vapour equilibrium technique (Gao and Sun 2017). Munoz-Castelblanco et al. (2012) and Haeri et al. (2014) determined the drying and wetting SWCCs of loess collapsible soil using filter paper, high capacity tensiometer and pressure plate techniques. On the other side, wetting SWCCs of collapsible soils that have been established under external stress and with measurements of volume change are limited by the low suction range (< 1500 kPa) of the used oedometer or triaxial apparatus (e.g., Sun et al. 2007).

2.4.3 Factors influencing the SWCCs

The shape and salient features of the SWCC are influenced by several factors including soil type, structure and mineralogy, applied stress, stress history, initial compaction condition and testing method. A critical review of these factors is made by Malaya and Sreedeep (2012). It is essential to study and understand these factors before using the SWCC data. Among these factors, the applied stress and compaction state have the greatest effect (Zhou and Yu 2005).

2.4.3.1 Influence of applied stress

The SWCC of various types of soils under different net stresses has been determined in several studies (Vanapalli et al. 1996; Ng and Pang 2000; Lee et al. 2005; Miller et al. 2008). Results of these studies indicated that SWCCs are stress dependent, such that a higher AEV was observed at a higher net stress. This behaviour is generally due to the presence of a lower void ratio of smaller average pore sizes for soils under a higher net stress, caused the soil to have higher ability to retain water at a given matric suction.

For collapsible soils, however, there are some contradictions reported in the literature regarding the effect of net stress on the wetting SWCCs. While uniqueness in the measured SWCCs under different loading levels has been obtained (Pereira and Fredlund 2000; Pereira et al. 2005; Garakani et al. 2015; Haeri et al. 2016), the effect of externally applied stress was considerable on the SWCCs (Sun et al. 2007; Liang et al. 2016). The reported contradictory features of the wetting SWCCs is caused by the differences in the soil structure (e.g., undisturbed and reconstituted specimens), type of the tests (e.g., constant stress with varying suction test or constant suction with

varying stress test) and the loading condition (e.g., Ko and triaxial) (Haeri et al. 2012; Haeri et al. 2016).

The SWCCs were also observed to be affected by the stress history, particularly at low suction (Vanapalli et al. 1999). The air entry value increased with the increase in the pre-consolidation pressure as indicated by mercury intrusion porosimetry (Delage and Lefebvre 1984).

2.4.3.2 Influence of initial compaction conditions

Several studies have investigated the effect of initial compaction conditions (i.e., water content, dry density and compaction effort) on the SWCC of soils. A soil with different initial dry densities (subjected to different compaction efforts) exhibited distinctive characteristics of wetting and drying SWCCs (Gallipoli et al. 2003; Yang et al. 2004; Gallage and Uchimura 2010; Gao and Sun 2017). All these studies revealed that soil specimens with a higher initial dry density have higher AEV and residual suction at a given matric suction. This kind of right shifting in the SWCCs to a higher suction range has been interpreted by the alteration in the pore size distribution associated with the reduction in the voids of denser specimens that would require a higher suction to empty or fill the voids with water. At higher suctions, the effect of compaction effort tends to diminish (Marinho and Stuermer 2000).

Vanapalli et al. (1999) and Zhou and Yu (2005) examined the effect of initial water-content on the soil water retention behaviour. The SWCCs are affected by the initial water content at saturation, whereas SWCCs with different initial water contents tend to converge at high suction. The study indicated that an increase in the initial water content causes an increase in the AEV and a steeper slope of the SWCCs.

2.4.4 Equations for describing SWCCs

Various forms of equations for determining the SWCC variables (i.e., air-entry value, residual water content and residual suction) using computational analyses have been proposed by many researchers. All the proposed mathematical expressions have one variable that is related to the AEV and a second variable related to the desaturation rate of the soil. A third variable, if needed, can provide information about the asymmetry of SWCCs (Fredlund 2006). Generally, these empirical equations can fit the measured SWCCs data using optimization procedures with the error minimized by iterating the parameters.

Several fitting approaches can be used for the analysis, such as Solver subroutine included in Microsoft Excel, SWRC-fit software by Seki (2007) and RETC programme by van Genuchten et al. (1991). The derived fitting parameters may vary depending on the convergence procedure, number of iterations, and the assumed initial values.

A detailed review of SWCC parametric models is provided by Leong and Rahardjo (1997) and Sillers et al. (2001). A summary of the most widely used equations are given in Table (2.2). Some models of the SWCC include a normalized variable for saturation or water content to isolate the physical behaviour of a soil from the saturated condition to the residual condition. According to Fredlund (2002), the normalized form can be used when studying the soil behaviour in the transition zone.

Table 2.2 Summary of the most frequently used models for describing the SWCCs

Model	Equation	Parameters
Brooks and Corey (1964)		= air entry value (kPa) = pore size distribution index = soil suction (kPa)
van Genuchten (1980)		= inverse of the air entry value (1/kPa) = indicator of pore size distribution =
Fredlund and Xing (1994)		= air entry value of the soil (kPa) = a function of water extraction rate = a function of residual water content = correction factor

and are the residual and saturated volumetric water content respectively.

2.5 Soil compaction

2.5.1 Compaction characteristics

Compaction is defined as a method of mechanically increasing the dry density of soils by rearranging the soil particles into a closer state (Head 1980). However, complete elimination of air voids is unachievable causing the compacted soils to be unsaturated. Compaction is widely utilized in the construction of earth structures, such as embankments, earth dams, retaining walls, landfills and foundations to improve the engineering properties (e.g., strength, compressibility, and permeability).

Compaction often leads to a distinct type of soil fabric (i.e., the arrangement of particles, pores and particle groups) (Lambe 1958). The fabric of compacted soils is dominated by the compaction water content, compaction efforts and compaction methods. The corresponding effect of the compaction water content on the soil fabrics has been reported by several studies (Lambe 1958; Lambe and Whitman 1969; Delage et al. 1996; Cetin et al. 2007). These studies showed that soils compacted dry of optimum and wet of optimum produce different fabrics and hence behave differently despite having a same dry density. Generally, a flocculated structure develops when fine materials are compacted at water contents dry of optimum. As the compaction water content increased from the dry side to the wet side, the soil structure changed gradually and monotonically from the more flocculated to the deflocculated or dispersed. At a constant compaction water content but increased compaction efforts, the fabric of the dry side changes from more flocculated to less flocculated and for the wet side from a dispersed to a more dispersed.

The structure of compacted soils could be either of bimodal or unimodal pore size distribution depending mainly on water contents and soil type. Soils having two main peaks in their pore size distribution are bimodal, whereas one peak represents the unimodal structure. The smaller pore radii represent intra-aggregate pores within the particle aggregates while much larger pore radii represent inter-aggregate pores between the aggregates. The boundary radius between the macro and micro pores is approximately 2 m (Li and Zhang 2009). The bimodal distribution of pore corresponds to two distinct structural levels: a microstructural and a macrostructural. Generally, soils compacted at the dry side of optimum possess a bimodal mode (also termed double structure or double porosity system), whereas those compacted at the wet side of optimum exhibit unimodal pore size distribution (Sridharan et al. 1971;

Garcia-Bengochea 1979; Delage et al. 1996; Lloret et al. 2003; Thom et al. 2007; Monroy et al. 2010; Alonso et al. 2013). Similarly, different compaction methods produce different forms of soil fabric and thereby significantly influence the subsequent hydro-mechanical behaviour of unsaturated soils (Sivakumar and Wheeler 2000; Estabragh et al. 2004; Crispim et al. 2011).

Compaction-induced state of a soil is another feature of the compaction process. As such soils can be characterised by a stress history, yield stress and phase variables (Prakash et al. 2014). The effect of compaction process manifests itself in the form of inducing yield stress.

2.5.2 Laboratory compaction methods

The basic theoretical background of the compaction concept along with introducing a compaction curve of soils was developed by Proctor (1933). Different methods of compaction can be carried out in the laboratory, including dynamic, static, kneading and vibratory. Results of these methods typically show the change in dry density for a range of water contents at a desired compaction effort. The objective of the compaction test is to establish the compaction curve and thereafter to determine the optimum water content and maximum dry density. Typically, the determined compaction curve is used as a guide for control of the field compaction specifications.

Among other methods, dynamic (Proctor) is the most common and standard laboratory compaction tests (ASTM D698-00; ASTM D1557-07; BS 1377-4 1990). It has, however, some shortcoming in application to correlate with field data since the compaction procedures used in the field (e.g., commonly using rollers) might differ from the Proctor standard and it applies a defined energy input that may be different

from the compaction energy applied in the field (Venkatarama-Reddy and Jagadish 1993; Yaghoubi et al. 2017). A typical shape of Proctor compaction curves is inverted parabolic. The occurrence of a maximum dry density at given optimum water content has been interpreted by various theories as reviewed by Fredlund et al. (2012). Irregularly shaped compaction curves (i.e., double peak, 1 1/2 peak and straight line) were also recognised in the literature (Lee and Suedkamp 1972), in which mineralogy and the index properties of a soil are believed to affect the shape of the compaction curve.

The static compaction method has been categorised as more practical, easier and faster than dynamic compaction (Asmani et al. 2013). It may be due to the difference in the applied compaction effort to obtain the same compaction condition (Venkatarama-Reddy and Jagadish 1993). A greater maximum dry unit weight by about 0.69 kN/m^3 produced using the static test compared to the Proctor test at the same compaction energy and water content (Venkatarama-Reddy and Jagadish 1993). A similar observation has been made by Hafez et al. (2010) and it can be related to the conceivable energy losses during the dynamic compaction process due to the impact of the falling weight. In this context, Sridharan and Sivapullaiah (2005) designed a mini compaction apparatus to establish dry unit weight-water content relationships of fine-grained soils. They identified energy losses in their proposed compaction apparatus mainly in the impact between the hammer and the energy transferring foot of the frame. The kinetic energy losses are the energy dissipated into heat, sound and high-frequency elastic vibrations (Beer and Johnston 1990). Local deformations at the plane of contact of energy transferring foot and hammer during the time of impact also contribute to energy losses (Goldsmith 1960).

2.5.3 Static compaction

A typical form of one-dimensional static compaction test is accommodating soil into a compaction mould and a static load is gradually applied to the whole area of the sample. During the compaction process, the height of the soil sample decreases continually until the requisite level of compaction is achieved. Results of the test at a range of water contents can then be analysed to establish the compaction curves under various compaction energy or compaction pressures levels.

Two types of static compaction procedures are identified in the literature; constant peak stress-variable stroke compaction (Turnbull 1950; Olivier and Mesbah 1987) and variable peak stress-constant stroke compaction (Venkatarama-Reddy and Jagadish 1993). In the former procedure, statically compacted samples are prepared by applying a specific peak stress in a gradual manner leading to produce samples of different thicknesses depending on the water contents; further details about this test process can be found in Venkatarama Reddy and Jagadish (1995). In the latter test procedure, a desired final thickness of samples is achieved by applying a static force progressively such that the peak stress can vary according to the water contents of soil samples. Nevertheless, there is a lack of knowledge concerning samples preparation and factors influencing the results of static compaction tests. Additionally, both procedures have some limitations in which a static compaction curve plotted for constant peak stress having varied energy values and therefore interpretation cannot be based on a specific energy level. On the other hand, establishing static compaction curves at different energy levels is described as a cumbersome process (Venkatarama-Reddy and Jagadish 1993). Therefore, developing a simple, effective and fast testing procedure along with exploring the influencing factors is needed.

Unlike dynamically compacted soils, various shapes of compaction curves have been reported in the literature for statically compacted soils, such as Convex and concave curves (Romero et al. 1999; Tarantino et al. 2005; Tarantino and De Col 2008; Zhemchuzhnikov et al. 2016) and relatively straight lines (Venkatarama-Reddy and Jagadish 1993). Many factors could affect the mechanism responsible for the shape of compaction curves including compaction procedure, strain rate, compaction mould, boundary condition (drained or undrained test), soil composition and index properties.

2.5.3.1 Factors influencing the static compaction curves

Factors affect the results of the static compaction test, for instance, information on the displacement rate and size of the compaction mould are still scarce in the literature. Static compaction test can be performed at a constant rate of strain or stress. During the test, the compaction speed is an important factor. High compaction speed can immediately lead to an increase in the pore pressure of fine-grained soils (Zhemchuzhnikov et al. 2016). A fixed displacement rate (0.2 to 2 mm/min) is usually used. However, the effect of varying compaction rate on the static compaction test has yet to be explored.

The dependability of compaction curves on the size of compaction mould has been investigated. Venkatarama-Reddy and Jagadish (1993) carried out static compaction tests on three different sample sizes. The results clearly showed that a larger sample requires less energy per unit volume to achieve the same dry density. This can be attributed to the higher ratio of sample surface area in contact with the mould to volume of a smaller specimen. Similar results were reported by Lawton et al. (1989), but for dynamically compacted samples using the standard compaction moulds and odometer rings.

2.5.4 Compaction-induced suction

Several studies have linked compaction variables, such as compaction water content and dry density with suction (e.g., Croney and Coleman 1961; Krahn and Fredlund 1972; Vanapalli et al. 1999; Tripathy et al. 2005; Yang et al. 2012). Together, these studies outlined that suction is dependent on the water content and of secondary influence on the dry density of a compacted soil.

Under the effect of compaction water content on suction, a unique relationship was identified. Higher the compaction water content, less the soil suction due to the formation of a relatively flat air-water interface since the pores between the soil particles are nearly filled with water.

Contradictory results about the effect of compaction dry density on the soil suction at a constant compaction water content have been reported in the literature as discussed in the following section.

2.5.4.1 Suction contours along compaction plane

The relationship of dry density-water content and suction plotted along the compaction plane has been translated into suction contours. The suction contours can be established by measuring suction of compacted samples and plotting the results along the domains of compaction curves. By considering suction contours, the effect of increasing dry density (or compaction effort) at a constant water content, during or after compaction, on suction behaviour can be clarified. Compaction-induced suction change and establishing contours of equal suction have been the interest of a number of researchers as summarised in Table (2.3). Noting that, suction in most of these studies was measured for unloaded compacted soils (Kodikara 2012).

Table 2.3 Summary of typical types of suction contours on compaction curves

Reference	Soil type	Compaction method	Suction component	Suction measurement method	S at lov
Romero et al. (1999)	Boom clay	static	total and matric	vapour equilibrium and air overpressure techniques	Slightly positi vertical at
Dineen et al. (1999)	bentonite enriched sand	dynamic and static	matric	filter paper and/or Imperial Collage Suction probe	Linear and ve high incl equal
Leong et al. (2003)	Mudstone and sandstone	dynamic	total and matric	null-type axis-translation and chilled mirror dew-point	Either verti
Gonzalez and Colmenares (2006)	Kaolin	dynamic and static	matric	filter paper technique	Nearly vert inclined t
Tarantino and De Col (2008)	Speswhite kaolin	static	total and matric	Trento high-capacity tensiometer and psychrometer probe	Negative slope at (12
Nowamooz and Masrouri (2008)	40% silt and 60% bentonite	static	total	filter paper technique	Verti

NB: is water content and is the degree of saturation.

Based on the summary provided in Table (2.3), three types of suction contours (i.e., vertical line, positive slope and negative slope) have been differentiated along the compaction plane. A characteristic feature of these studies is that at low water contents and for increased compaction efforts suction either remains constant or changes slightly as shown in Figures (2.4a and b).

(a)

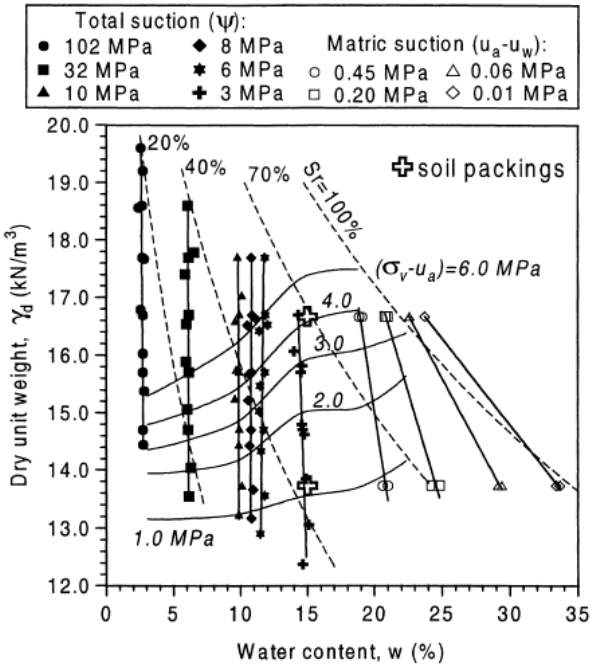

(b)

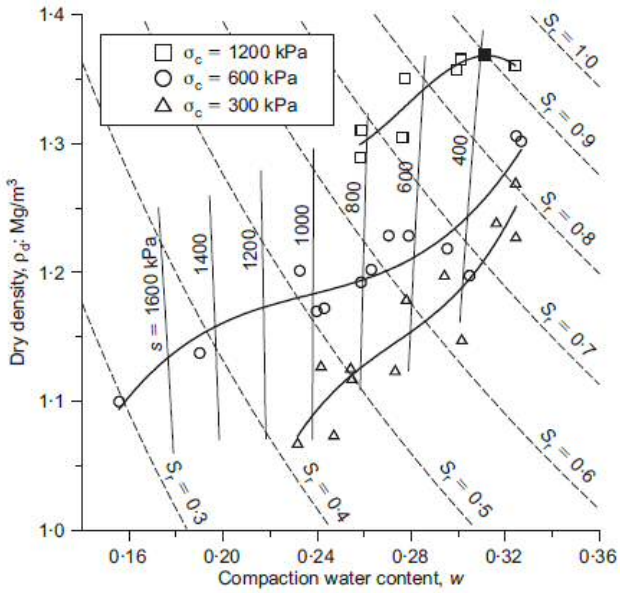

Figure 2.4 Types of suction contours on compaction curves, (a) after Romero et al. (1999) and (b) after Tarantino and De Col (2008)

Kurucuk et al. (2009) studied the effect of suction on the overall compaction process. The results indicated that the change in suction with loading is very small in the first loading step and suction stays constant during the following loading steps. Therefore, it appears to be acceptable to assume that suction remains constant with loading. This kind of behaviour was interpreted based on double porosity effects. As such, the low water content is mainly occupied in the intra-aggregate pores and since compaction primarily affects the inter-aggregate pores which contain no or few water, a small or potentially unchanged value of suction is measured.

In the range of high water content, however, two opposite trends of suction changes for increased dry density were reported; a decreasing in suction values that indicating a negative slope of suction contours and a positive slope with increased values of suction. The former behaviour introducing the effect of loading mechanism on the inter-aggregate water that leads to increasing the degree of saturation and thereby decreasing suction. The latter striking behaviour was first observed by Tombolato et al. (2005) indicating suction increased as the degree of saturation increased. They explained this behaviour by the dependency of the main wetting curve upon void ratio. Della Vecchia et al. (2015) also observed that the changes in the pore size distribution during compaction affect the wetting water retention curves.

Tarantino and Tombolato (2005) provided a further explanation of the increased suction with the increase in the degree of saturation during the compaction process as shown in Figure (2.5). Under the static compaction to a certain compaction pressure, the soil specimen experienced main wetting with increasing the degree of saturation (point A1 in Figure 2.5). Upon unloading, the soil moved to point A2. If the water retention curve was independent of void ratio, suction would be expected to decrease significantly during loading and slightly increase upon the subsequent unloading (path

C1-C2). However, due to the dependency of the water retention curve on the void ratio, further loading to a higher compaction pressure produced a decrease in void ratio and an increase in the degree of saturation. At the same time, the main wetting curve moved rightward. As a result, the main wetting curve dragged the soil to point B1. The subsequent unloading moved the soil to B2. The position of point B2 on the left side of point A1 indicated increasing suction with the increase in the degree of saturation. This could explain the positive slope of the contours of equal suction observed in the specimens at higher water contents.

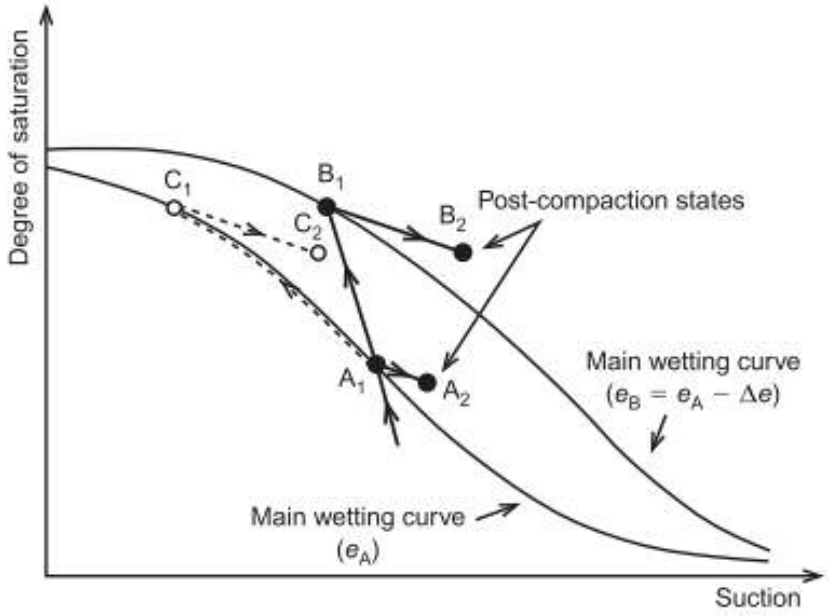

Figure 2.5 Effect of void-dependent retention curve on suction of compacted soil (after Tarantino and Tombolato, 2005)

2.6 Wetting-induced volume change in unsaturated soils

Rainfall, irrigation and rising of water tables are common sources of wetting that cause water to infiltrate into soil strata. Upon wetting and the decrease in suction associated with it, unsaturated soils are most likely to collapse and/or to swell under constant vertical stress depending on the type of soil, compaction water content and the level of vertical stress at wetting (Alonso et al. 1987; Lawton et al. 1992; Houston et al. 2001; Sivakumar et al. 2015). In general, compacted soils are expected to swell when wetted under low loads and collapse when wetted at higher loads (Leong et al. 2013).

The wetting-induced collapse of metastable structured soils, such as loess and some compacted soils has been studied by a number of researchers (e.g., Barden et al. 1973; Lawton et al. 1989; Wheeler and Sivakumar 1995; Pereira and Fredlund 2000; Sun et al. 2004; Nouaouria et al. 2008). A decrease in volume at constant vertical stress due to wetting is an indication of the soil collapse. The amount of such volume change is expressed as a collapse strain or collapse potential. It is usually determined using a conventional oedometer apparatus (Houston et al. 2001). However, knowing that matric suction is the only stress state variable that changes during wetting (Tadepalli and Fredlund 1991), and that collapse is attributed to the loss of strength associated with suction decrease resulted from wetting (Fredlund and Gan 1995), collapse behaviour has been rationally analysed by incorporating suction controlled wetting tests. In experimental studies, therefore, wetting of unsaturated soil tests have been performed by either inundation using conventional oedometer or by finite reduction of matric suction during wetting tests using, for example, suction-controlled oedometer. In the following sections, both approaches are reviewed.

2.6.1 Volume change during wetting without suction control

The one-dimensional volume change response to wetting is often investigated in the laboratory using a conventional oedometer cell. The frequently used wetting-induced collapse tests are single oedometer and double oedometer. Typical results of both types of tests are represented in Figure (2.6).

In the single oedometer tests (ASTM D5333-03; ASTM D4546-14), a compacted specimen is incrementally loaded to a particular stress and then inundated with water. By repeating the procedure for a range of stresses, the saturated compression curve can be traced. Whereas, in the double oedometer tests (Jennings and Knight 1957) two identical specimens are tested in the oedometer. One specimen is loaded at the as compacted condition giving the unsaturated compression curve while the other specimen is inundated with water and loaded to obtain the saturated compression curve. The loading sequence should be identical for both specimens. To obtain the same information, the single oedometer test requires several specimens and correspondingly longer testing duration compared to the double oedometer tests. Despite these factors, the single oedometer test resembles the in-situ condition and the collapse deformation with the inundation time can be monitored.

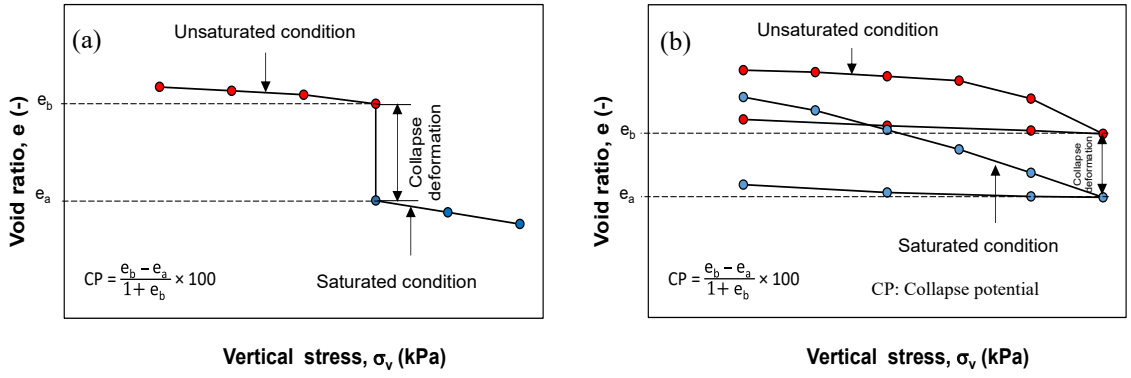

Figure 2.6 Typical results of (a) single and (b) double oedometer tests

For both tests (single and double oedometer), the collapse/swell strain for any stress level can be determined by using either Equation (2.5) or (2.6).

— (2.5)

——— (2.6)

where is the collapse/swell strain (%) presented in negative for collapse, and are the change in specimen height and void ratio caused by wetting under the desired pressure, respectively or the difference between the samples and and are the specimen height and void ratio immediately before wetting.

Since wetting-induced collapse is essentially independent of the loading-wetting sequence (Jennings and Knight 1957; Lawton et al. 1989), relatively similar values in the estimated collapse potential from both testing procedures (single and double oedometer tests) were obtained (Lawton et al. 1992; Fredlund and Gan 1995; Lim and Miller 2004; Leong et al. 2013). However, the double oedometer tests was seen to overpredict the amount of collapse (Booth 1977), whereas it was observed to underestimate the collapse potential (Medero et al. 2009) as a comparison to the single oedometer tests. Therefore, it is recommended to use the double oedometer only after verification with the single oedometer tests (Lawton et al. 1992).

Several factors have been identified to influence the amount of collapse strain exhibited by compacted soils including the inundation vertical stress and the initial soil conditions (e.g., water content, dry density, degree of saturation) as will discussed briefly in the following sections.

2.6.1.1 Effect of inundation vertical stress

Inundation stress, also known as wetting stress, is the overburden pressure at which the soil is inundated. It has been noticed to be one of the key factors that control wetting-induced collapse behaviour of soils. Previous studies suggested that the amount of collapse is dependent on the inundation stress level. Generally, collapse strain increases with increasing the inundation vertical stress up to a certain level of stress and decreases thereafter (Sharma and Singhal 2006; Muñoz-Castelblanco et al. 2011; Okonta 2012; Rabbi et al. 2014; Singhal et al. 2015). Therefore, the maximum collapse strain occurs at some critical value of stress (i.e., threshold wetting pressure) beyond which it begins to decrease. Such critical stress was found to be equivalent to the yield stress (Lawton et al. 1989, 1992; Jiang et al. 2012; Elgabu 2013; Al-Obaidi 2014). The explanation of this behaviour is based on the fact that higher the applied load greater the soil compression that resulted in increasing the collapse potential. However, beyond the yield stress, reduction in collapse strain is caused by the densification and increasing the degree of saturation resulting from the virgin compression of the samples.

The yield stress is also called the pre-consolidation pressure and is usually estimated from compression curves using the graphical procedure proposed by Casagrande (1936). Other methods of determining the pre-consolidation pressure are outlined in Prakash et al. (2014). For unsaturated soil, the yield stress can also be determined from compression curves under constant suction (Zhou and Sheng 2009).

2.6.1.2 Effect of initial compaction conditions

Numerous studies have attempted to identify critical compaction parameters for minimizing the potential of wetting-induced collapse. Compaction water content and dry density have been recognised as major contributing factors for the severity of collapse. Compacted soils at the dry side of the optimum and at a low dry density are essentially collapsible soils (Barden et al. 1973; Pereira and Fredlund 2000).

A low collapse potential has been observed in compacted samples tested at high initial water content and high dry density (Lawton et al. 1989; Basma and Tuncer 1992; Houston et al. 2001; Delage et al. 2005; Aziz et al. 2006; Sharma and Singhal 2006; Jiang et al. 2012; Okonta 2012; Fattah and Dawood 2016). The decrease in collapse potential with water content is because compacted soils of high water content have already experienced bond weakening, compression and reduction in the metastable forces, and accordingly a lower tendency to collapse upon wetting. While at high initial densities the decrease in collapse is believed to be related to the low void ratio that reduces the compression response.

The collapse potential decreases linearly with increasing initial water content at a constant dry density and increasing initial dry density at a constant water content (Fredlund and Gan 1995; Lim and Miller 2004).

The initial compaction condition along with some other physical properties, such as grain size distribution and Atterberg limits have been related to collapsibility by empirical equations (Feda 1995; Ayadat and Hanna 2007; Zorlu and Kasapoglu 2009). However, the validity of using such proposed equations for universal purposes has been questioned (Sun 1957; Yang 1988).

2.6.2 Volume change during wetting under suction control

Although the collapse strain of soils can be successfully determined from the results of both single and double oedometer tests, field evidence indicates that collapse may occur due to a gradual increase in water content (i.e., decrease in suction) and that collapse may complete before even approaching full saturation (Tadepalli et al. 1992; Houston et al. 2001). Due to the reduction in matric suction resulted from wetting, large collapse deformation and volume changes occur. The collapse behaviour as affected by suction changes has been investigated using suction-controlled wetting tests (e.g., Chen et al. 1999; Sivakumar and Wheeler 2000; Sun et al. 2004; Jotisankasa et al. 2007; Muñoz-Castelblanco et al. 2011; Haeri et al. 2014; Karami et al. 2015).

Suction-controlled wetting tests can be adopted at a constant net stress using suction-controlled oedometer or triaxial apparatus. After loading a soil sample to a desired net stress value, the wetting path can be commenced by decreasing the suction value in a stepwise manner from the initial value up zero suction. Both single and multiple specimens can be tested, however, the compatibility of such test results are not known.

Results obtained from a controlled-suction test conducted on collapsible soils provide information about the effect of matric suction on soil collapsibility. The test data enable establishing soil-water characteristic curve under a given applied stress. The tests can also be performed under increasing applied net stress. Thus, the influence of stress state variables (e.g., net stress and matric suction) and the loading conditions (e.g., stress path) on the hydro-mechanical behaviour of collapsible soils can be investigated as reviewed in the subsequent sections.

2.6.2.1 Effect of matric suction and net stress

Matric suction has been observed to affect the collapse, as such the increase in the initial matric suction invariably leads to increase the collapse potential of soils (e.g., Rabbi et al. 2014) and the rate of changes in collapse deformation depends on the level of suction. Three distinct phases of collapse deformation as influenced by suction changes have been defined by Pereira and Fredlund (2000), namely pre-collapse, collapse and post-collapse phases. The pre-collapse phase occurs at high matric suction and is typically associated with low volumetric elastic deformation. Similarly, negligible volumetric deformation attributed to secondary compression occurs during the post-collapse phase at low matric suctions. However, a considerable non-recoverable deformation occurred at intermediate matric suction ranges. This collapse phase results from the combination of the rearrangement of soil particles and the local shear behaviour between soil particles and soft cementing bonds. A similar observation in the collapse behaviour during controlled wetting on both compacted and natural soils has been made by (Chen et al. 1999; Kato and Kawai 2000; Futai and Almeida 2005; Zhou and Sheng 2009; Garakani et al. 2015).

It has been widely recognised that, at a given value of matric suction and for natural and compacted samples, the increase in the applied net stress leads to higher collapse (Pereira and Fredlund 2000). This is due to the changes in the pore size distribution and the rate of water adsorption accompanied by increasing the load. However, it was also noted that the collapse potential reaches a maximum and then reduces with increasing stress (Dudley 1970; Wheeler and Sivakumar 1995; Sun et al. 2004; Vilar and Rodrigues 2011).

2.6.2.2 Effect of initial compaction conditions

For a given net stress under which the wetting process occurs, there is a tendency for specimens compacted at low dry densities to experience a greater collapse strain. Sun et al. (2007) studied the changes in volume and hydraulic characteristics of unsaturated collapsible soil called Pearl clay using controlled-suction triaxial tests with varying initial dry densities. The results showed that the volumetric collapse strain depended largely on the initial density. Limited studies have been done, however, on the effect of changing both the initial dry density and water content at a constant compaction energy on collapse behaviour, during controlled-suction wetting tests, because of the technical difficulties and time-consuming nature of such tests.

2.7 Collapse behaviour in unsaturated soil frameworks

Collapsible soils are essentially unsaturated since a full collapse often occurs prior to reaching fully saturated condition, and thereby the concepts of unsaturated soil mechanics are more applicable for interpreting their behaviour (Fredlund and Rahardjo 1993). In unsaturated soil mechanics, a number of theoretical frameworks have been developed for identifying appropriate stress state variables, such as the single effective stress approach (Bishop 1959), the two independent state variables approach (Fredlund and Morgenstern 1977) and the suction stress approach (Lu and Likos 2006; Lu et al. 2010). The stress state variables as defined by Fredlund and Rahardjo (1993) are "the non-material variables required for the characterisation of the stress condition". Nuth and Laloui (2008) provided an extensive analysis and discussion of effective stress concepts in partially saturated soils. The validity of the unsaturated soil mechanics theories is still a matter of intense discussion.

2.7.1 Single effective stress approach

For saturated soils, effective stress is the unique stress state variable as all the measurable effects, such as compression and dilation, can be controlled solely by such term (Terzaghi 1936). However, developing a similar concept for unsaturated soils needs to consider the presence of air phase and the corresponding air-water interphase. Analysis of unsaturated soils would be extremely simplified if the effective stress principle is applicable for such soils.

The single unsaturated effective stress is the difference between the externally applied stress and a scaled value of matric suction. A general form to represent the effective stress σ' in unsaturated soils was first developed by Bishop (1959) as given in Equation (2.7).

(2.7)

where is the effective stress, is the total stress, is the pore air pressure, is the pore water pressure, and define the net stress and matric suction respectively and is an effective stress parameter which describes the contribution of matric suction to effective stress. The effective stress parameter was basically introduced as a scaling factor averaging matric suction from the pore-scale level to a macroscopic level over the representative elementary volume.

The Bishop (1959) proposal received criticism because the role of matric suction in the effective stress varies with the degree of saturation, in which the experimental evidence identified no unique relationship between and the degree of saturation (Bishop and Donald 1961). Nonetheless, several investigators have advocated the use of the degree of saturation as the effective stress parameter in their constitutive models

(Loret and Khalili 2000; Gallipoli et al. 2003; Wheeler et al. 2003). The compatibility of the collapse phenomenon with the Bishop approach was questioned (Jennings and Burland 1962) since wetting leads to increase pore water pressure and correspondingly decrease the effective stress which would cause swell rather than collapse. However, it was evident that the collapse is due to a local shear failure between soil particles and thereby effective stress concept can be still applicable (Barden et al. 1973; Lu 2011).

It was outlined that the effective stress parameter is not only a function of the degree of saturation but also is strongly related to type of soil, soil structure, degree of saturation, stress and suction paths to which the soil was subjected (Fredlund and Rahardjo 1993; Khalili et al. 2004). Therefore, different equations have been introduced to define the effective stress parameter as summarized in Table (2.4).

Table 2.4 Summary of the effective stress parameter formula

Reference	Equation	Description
Bishop (1959)		= degree of saturation
Khalili & Khabbaz (1998)	—	= matric suction (kPa) = air entry value (kPa) — = the suction ratio
Vanapalli and Fredlund (2000)		= fitting parameter related to the soil type
Lu and Likos (2006); Alonso et al. (2010)		= effective degree of saturation

Khalili and Khabbaz (1998) showed that by plotting the values of against the suction ratio, a unique relationship is obtained for most soils. Based on shear strength data of various soils, Khalili and Khabbaz (1998) proposed a formula for quantifying the

effective stress parameter (χ), which was verified a general volume change data (Khalili et al. 2004). Khalili et al. (2004) investigated the validity of the effective stress concept in collapsible soil. They suggested that implementing this concept to capture the collapse can only be adopted if an appropriate plasticity model is incorporated.

While the above approaches have been derived from a macroscopic point of view, Vanapalli et al. (1996), Lu and Likos (2006) and Alonso et al. (2010), presented a micromechanically based concept for describing effective stresses. They defined in terms of the effective degree of saturation. A comparative study of the applicability of the different effective stress approaches for analysing the behaviour of loess soils was made by Garakani et al. (2015). The results indicated a good agreement between the measured χ values and those predicted using χ equals to or among others and the effective stress during collapse decreases with the volume decrease of specimens.

Vanapalli and Fredlund (2000) conducted comparative studies on the proposed equations of the effective stress parameter as shown in Figure (2.7). The results indicated that χ equals to show the closest fit to the experimental data.

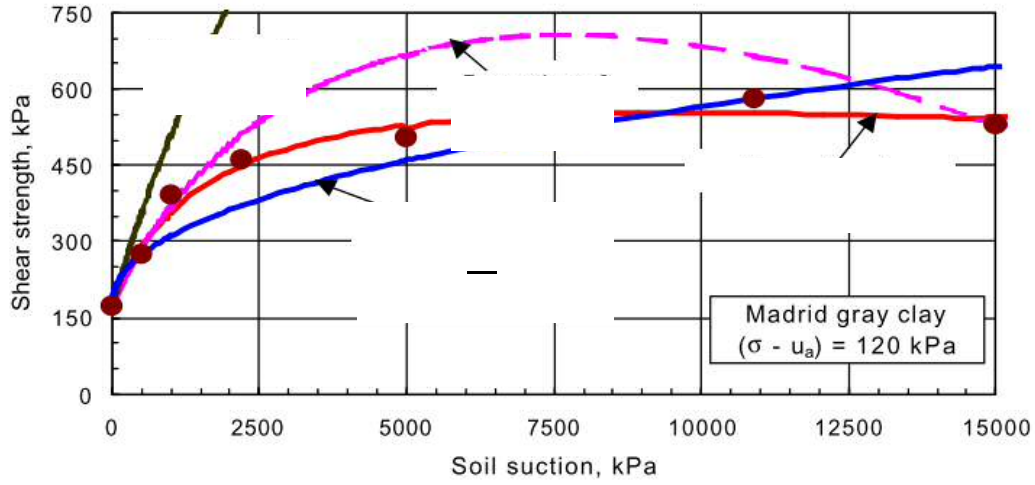

Figure 2.7 Comparison of predicted and measured shear strength values using different equations of the effective stress parameters (after Vanapalli and Fredlund, 2000)

2.7.2 Two-independent stress state variable approach

The theoretical and experimental challenges associated with determining the effective stress parameter identified in various research studies of (Bishop and Donald 1961; Jennings and Burland 1962; Bishop and Blight 1963; Burland 1965) has led to the favour of the two independent stress state variables approach. Coleman (1962) and Matyas and Radhakrishna (1968) were amongst the first to use the two-independent stress state variable approach for unsaturated soils. Progressively, based on multi-phase continuum mechanics, Fredlund and Morgenstern (1977) proposed a theoretical analysis of stress state variables for unsaturated soils by taking the contractile skin (air-water interphase) as the fourth phase of the soil. The typical stress state variables are the net stress and suction that have been used more frequently in the interpretation of experimental results and constitutive modelling.

While the use of two independent stress-state variables proposed by Fredlund and Morgenstern (1977) gains greater acceptance in constitutive modelling, it has also received criticism because it cannot be reconciled with classical saturated soil mechanics and additional parameters were required to represent changes in strength (Khalili et al. 2004; Nuth and Laloui 2008; Vanapalli 2009).

Analysis of collapse behaviour based on the two separate components of effective stress, the applied stress and the suction has been considered by many authors including (Barden et al. 1973; Pereira and Fredlund 2000; Sun et al. 2004; Liang et al. 2016). In this context, the reduction in matric suction accompanied by wetting reduces the strength and the capillary effects which caused the collapse of the soil structure, while the net stress controls the severity of the collapse.

2.7.3 Suction stress characteristic curve (SSCC) approach

Although Terzaghi's effective stress equation (2.8) has been proved to be suitable for most geotechnical engineering practice, it ignores the representation of physio-chemical forces which could have a considerable effect on the hydro-mechanical behaviour of soils.

(2.8)

For unsaturated soils, capillary forces should also be included along with the physio-chemical forces. The resultant of adapting all these forces (i.e., van der Waals attractive force, double-layer repulsive force, surface tension, and solid-liquid interface forces due to pore water pressure) in the effective stress concept represents suction stress (. Therefore, suction stress will represent the effective stress in the absence of any external applied stress. Based on the correspondence between suction stress and effective stress, Lu and Likos (2006) propose the suction stress characteristic curve (SSCC). The SSCC is the relationship between the suction stress and volumetric water content or matric suction. The effective stress of unsaturated soils based on the SSCC can be determined from Equation (2.9).

(2.9)

Lu and Likos (2004; 2006) explained that the SSCC can be experimentally determined from tensile strength tests or can be calculated based on the shear strength tests, or even can be estimated based on the soil-water characteristic curve (SWCC). Depending on the SWCC, Lu et al. (2010) showed that the van Genuchten (1980) model can be used to define the SSCC and correspondingly the effective stress.

The applicability of establishing the SSCC based on the SWCC has been experimentally validated (Lu et al. 2010; Oh et al. 2012; Lu et al. 2014) and the prediction of suction stress based on the SWCCs for various types of soil has been adopted in several studies (Chae et al. 2010; Lu 2011; Song et al. 2012; Haeri et al. 2014; Baille et al. 2016). A comparative study of the measured and predicted suction stress using compacted mixtures of sand and clay made by Pourzargar et al. (2014) showed that the drying, wetting and scanning SWCCs overestimated the suction stress for samples with saturation < 0.75. A similar observation was also made by Alsherif and McCartney (2014), but small adjustments were suggested in the fitting of the SWCC to provide a better fit between the SSCC and experimental suction stress.

The dependence of SSCCs on the soil type (Baille et al. 2014) and on the confining stresses for a silty sand soil were also examined in the study of Oh and Lu (2014). Under both drying and wetting conditions, a unique SWCCs and SSCCs were defined in terms of effective saturation. The results also indicated a good agreement between the measured and predicted SSCCs.

2.8 Concluding remarks

In this chapter, a brief review of the collapse phenomena and methods for analysing the collapse mechanism were presented. The concept of soil suction along with methods for measuring and controlling suction, general information on the soil-water characteristic curve (SWCC) and its features and factors affecting the SWCC were also covered. In addition, compaction characteristics and suction of compacted soils were also reviewed. Soil volume change during wetting-induced collapse under uncontrolled and controlled suction tests were discussed. A critical review of the effective stress approaches of unsaturated soils and their effectiveness in analysing the collapse behaviour was included.

The literature review presented in this chapter highlights some specific aspects related to the collapse behaviour of unsaturated compacted soils. These include:

1. The magnitude of collapse strain resulting from wetting affects by the level of the applied stress, initial compaction conditions and matric suction.
2. The procedure of static compaction tests and factors influencing the results has not been fully investigated. In this thesis, a detailed testing procedure along with exploring the effect of several factors are presented in Chapter 4.
3. Most of the studies focused on the effect of initial water content or initial dry density on collapse behaviour rather than to the effect of changing both parameters at a constant compaction effort. The collapse behaviour of specimens subjected to constant compaction energy and compaction pressure are investigated in Chapter 5.

4. The stepwise wetting by testing a single specimen during controlled-suction tests is the procedure that often used. In this study, various testing procedures are introduced and compared in Chapter 6.
5. Collapse behaviour is often analysed based on the two independent variables approach (covered in Chapter 7). However, analysing the behaviour based on the single effective stress and suction stress approaches needs further verification as will be examined in Chapter 8.

Chapter 3

Materials and Methods

3.1 Introduction

In this chapter, materials and methods used are presented. The properties of the selected material including specific gravity, Atterberg limits and particle size distribution along with compaction characteristics are also presented. Description of various devices and techniques used, as well as working principles, are detailed. The experimental programme planned to fulfil the objectives of the research, testing procedures for various laboratory tests are also described. A summary of the work presented is provided towards the end of the chapter.

3.2 Selection of material

Since the overall aim of this research was to study in detail the collapse behaviour of unsaturated compacted soil, the investigation was performed on materials with a tendency to collapse. Two types of materials were tested; natural and prepared. The material that exhibited the highest potential to collapse was selected for this study.

The natural soil was extracted from Pegwell Bay in south-east England. The Pegwell Bay loess was a silt-rich deposit (Table 3.1). The reported field densities of the soil were in the range of 14.5 to 16 kN/m^3 (Fookes and Best 1969), whereas the estimated maximum dry densities were between 17 and 17.5 kN/m^3. This type of soil was selected because of its metastable structure (Northmore et al. 2008).

The prepared soil was of similar composition as for collapsible soils reported in the literature (see Section 2.2.2). The water content and dry density of the prepared soil were also at a similar range with the reported collapsible soils (Basma and Tuncer 1992; Pereira and Fredlund 2000). Three types of commercially available materials, namely M400 silt, Leighton Buzzard sand and Speswhite kaolin were mixed to prepare the soil. The M400 silt was obtained from Sibleco UK Ltd, while Leighton Buzzard sand and Speswhite kaolin were supplied from Aggregate Industries.

Four mixtures were prepared by dry mixing the three materials at different proportions as given in Table (3.1). A predetermined amount of distilled water was added to the prepared powder mixture and mixed thoroughly. The mixtures were stored for one day to allow moisture equalisation. Specimens (100 mm dia. and 16 mm height) of both the natural and prepared soils were statically compacted inside oedometer rings. The compaction conditions of the specimens are given in Table (3.1).

Table 3.1 Composition and initial condition of specimens for the preliminary tests

Soil type	Specimens no.	Silt (%)	Sand (%)	Clay (%)	Initial compaction condition	
					water content (%)	dry unit weight (kN/m^3)
Natural	N1	84	7	9	8.3	14.5
	N2					16
	N3					17
	N4					17.5
Prepared	P1	50	30	20	10	14
	P2	45	30	25		
	P3	45	35	20		
	P4	40	40	20		

A series of preliminary wetting-after loading tests were conducted on the compacted specimens following ASTM D4546-14. The specimens were incrementally loaded to a pre-determined vertical stress and then inundated with water. The one-dimensional wetting-induced collapse or swell deformation was measured at suitable intervals and further used to determine the collapse/swell strain using Equation (2.5).

Figure (3.1) shows the variation of collapse/swell strain with the inundation time for all the tested specimens. As it can be seen, the natural soil exhibited collapse strains of 4% and 2%, and swelling strain of about 1% with the increased dry density of the specimens. Whereas, a much higher collapse strains varied from 10% to 16% were exhibited by the prepared soil of different composition. Therefore, under the chosen applied stress, initial compaction condition and soil composition, the prepared soil named P4 exhibited the greatest collapse strain and hence was selected for the remaining work of this study. The properties of the selected material (40% silt, 40% sand and 20% clay) are presented in the subsequent sections.

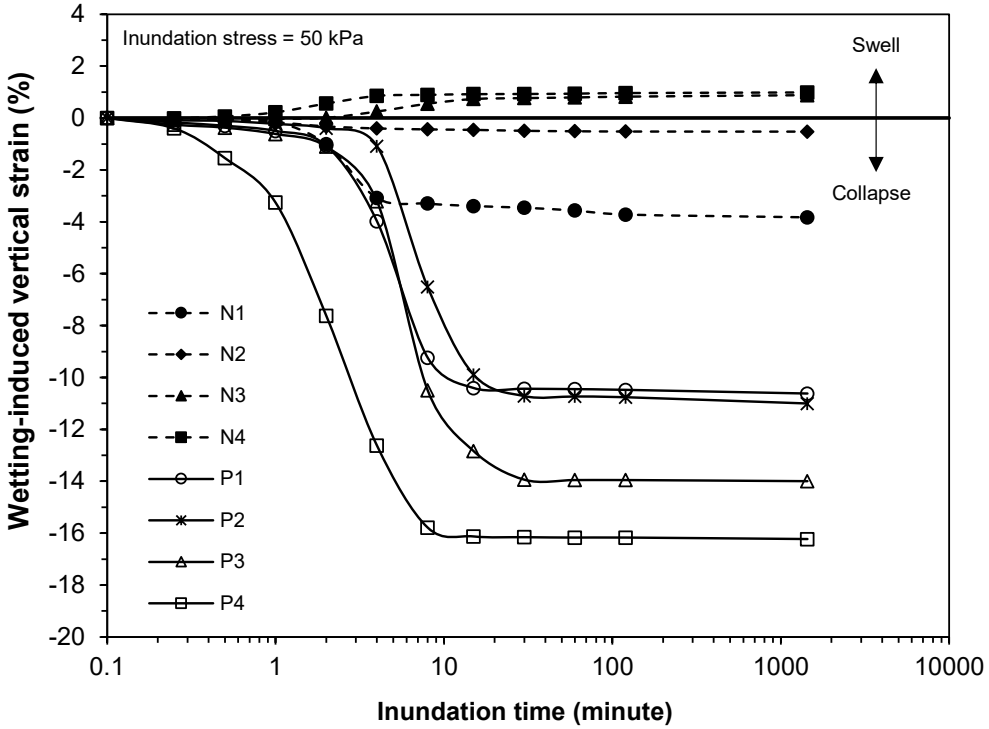

Figure 3.1 Time versus wetting-induced swell/collapse strain for all tested specimens

3.3 Properties of the material used

3.3.1 Specific gravity of soil solids

The specific gravity of soil particles was performed according to the BS 1377-2 (1990) procedure by small density bottle (pycnometer) method. Three specimens were prepared and tested in a controlled temperature laboratory (21.5 ± 2 °C). The average specific gravity value was calculated to be 2.65.

3.3.2 Atterberg limits

The Atterberg limits (i.e. liquid limit, plastic limit and shrinkage limit) were determined following methods described in BS 1377-2 (1990). The liquid limit of the material used was determined by the cone penetrometer method. The plastic limit was determined by the thread rolling method. The liquid and plastic limits were found to be 24% and 16%, respectively. The shrinkage limit was determined by the molten wax method (ASTM D4943-10). The shrinkage limit of the material used was found to be 10.7%.

3.3.3 Particle size distribution

The particle size distribution curve of the material used was established using the sieve and hydrometer methods (BS 1377-2 1990). Sieving combined with hydrometer method is the standard method to determine quantitatively the particle size distribution of soils. The hydrometer analysis is used for the sizing of fine-grained soils based on the assumption that all particles are spheres. Such assumption was noted to underestimate the maximum particle dimension by up to two orders of magnitude (Lu et al. 2000). Figure (3.2) shows the particle size distribution curve of the material used.

The results indicated a presence of a gap in the particle sizes ranging from 0.06 mm to 0.2 mm. Therefore, the soil was a gap-graded soil.

The particle size distribution curve together with the Atterberg limits result were used for classifying the soil. According to the British Soil Classification System for engineering purposes, the soil can be classified as Sandy CLAY of low plasticity (CLS).

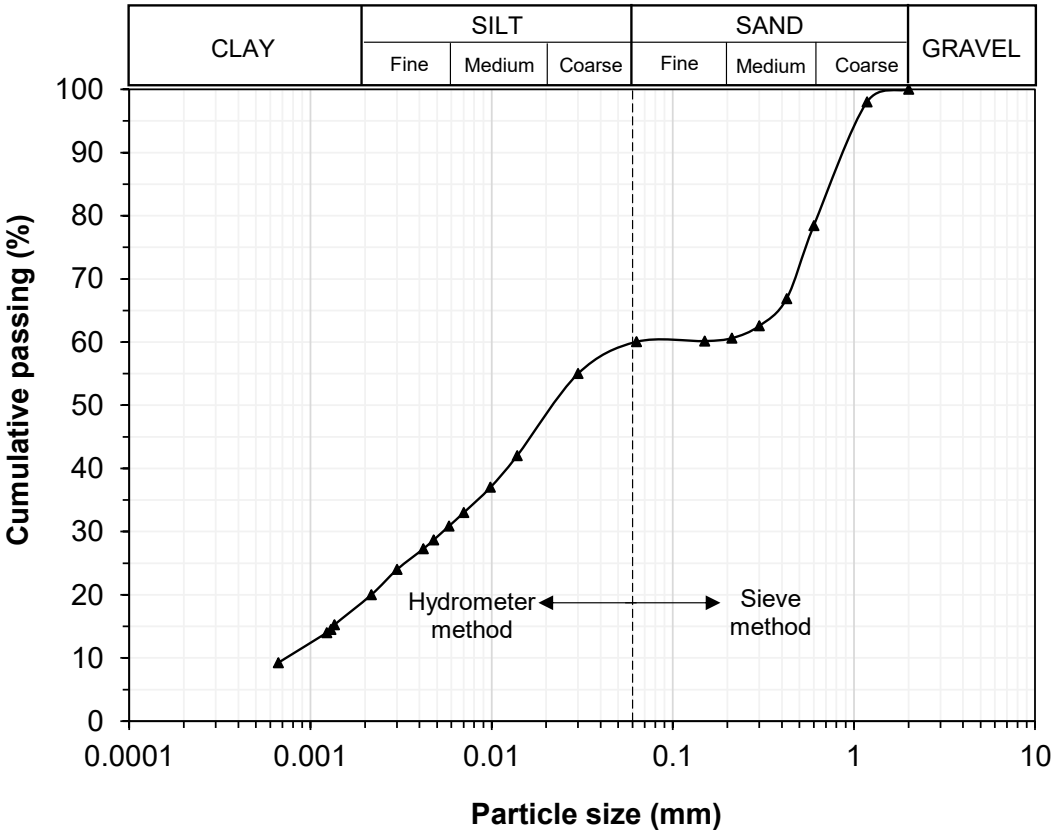

Figure 3.2 Particle size distribution curve of the soil used

3.3.4 Mineral composition

The mineralogy of the material used was determined by the X-ray diffraction method. A Philips automated powder diffractometer, PW 1710, was used for the analysis. The use of X-ray diffraction allows for the determination of specific minerals through measurement of the intercept angle and the c-axis spacing. The soil particles were ground to minimise the orientation preference and to maximise the specimen representativeness. The soil in powder form and at the initial water content was tested. Figure (3.3) shows the X-ray diffraction chart of the soil. Semi-quantitative analysis was conducted to assign the minerals to the corresponding peaks. The analysis indicated that the dominant mineral in the soil was quartz of 86% with kaolinite of 14%.

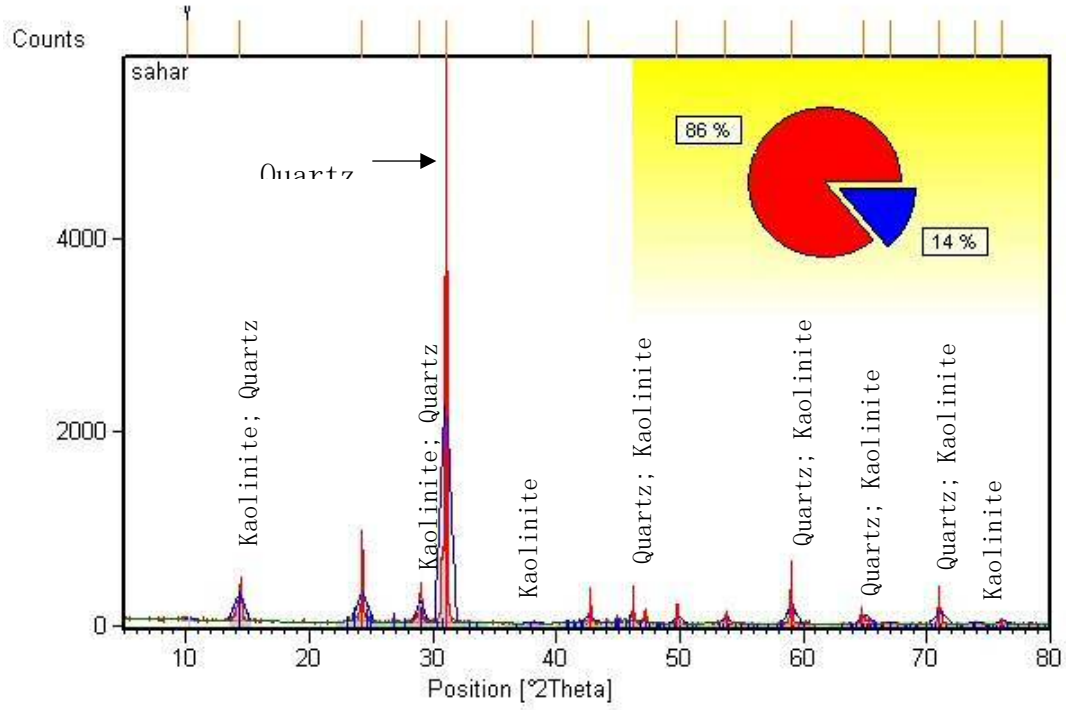

Figure 3.3 X-ray diffraction chart of the soil used

3.3.5 Compaction characteristics

Standard Proctor compaction tests were conducted according to BS 1377-4 (1990) with a light compaction effort. The soil was compacted in three layers in a standard 1000 cm^3 mould, using 27 blows per layer with a 2.5 kg rammer falling through a height of 300 mm, which yielded a standard compaction energy per unit volume on the soil of 596 kJ/m^3. Figure (3.4) shows the compaction curve of the soil used and the optimum condition. The maximum dry density of 18.5 kN/m^3 corresponds to the optimum water content of 13.3%.

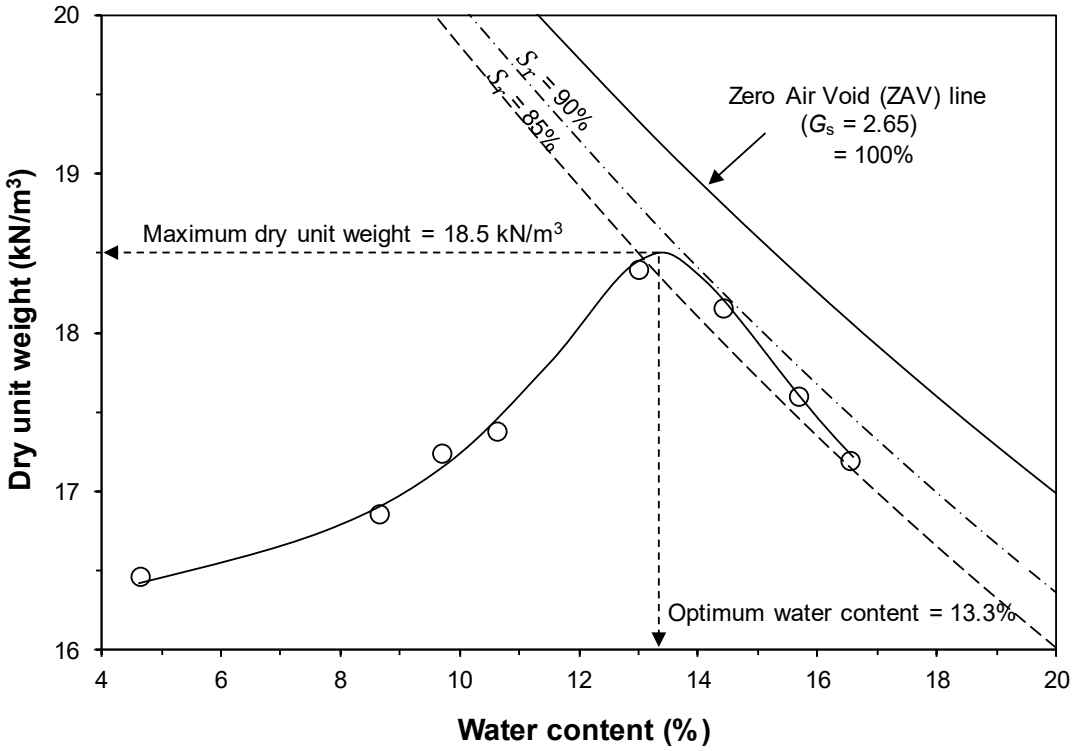

Figure 3.4 Standard Proctor compaction curve of the soil used

The properties of the soil used are summarised in Table (3.2).

Table 3.2 Properties of the soil used

Properties	Values
Specific gravity of soil solids, G_s	2.65
Atterberg Limits	
Liquid limit, LL (%)	24.0
Plastic limit, PL (%)	16.0
Shrinkage limit, SL (%)	10.7
Particle size distribution	
Sand (%)	40
Silt (%)	40
Clay (%)	20
BS light compaction characteristics	
Maximum dry unit weight, (kN/m^3)	18.5
Optimum water content, (%)	13.3
Soil classification	CLS

3.4 Experimental methods and programme

To fulfil the objectives of this research, several laboratory tests were carried out on the selected soil. The laboratory experiments were carried out in four series of tests. In test series I, static compaction behaviour and suction characteristic were studied. Static compaction tests were performed to establish the compaction curves of the soil both in terms of applied compaction pressure and compaction energy. The suction of the soil at various predetermined compaction conditions was measured using a chilled-mirror potentiameter. Further, suction measurement was also conducted on several soil-water mixtures using a calibrated water potential sensor. In test series II, collapse behaviour of statically compacted specimens along compaction curves of constant compaction energy and constant compaction pressure was studied. The collapse behaviour was studied by single and double oedometer tests. In test series III, soil specimens were taken through various wetting-induced collapse tests under a constant applied stress. A suction controlled oedometer was used for carrying out the tests. Both single and multiple specimens were considered. In test series IV, suction control wetting tests were conducted to studying the effects of applied stress and compaction states during the stepwise wetting process. An overview of the experimental programme is presented in Figure (3.5).

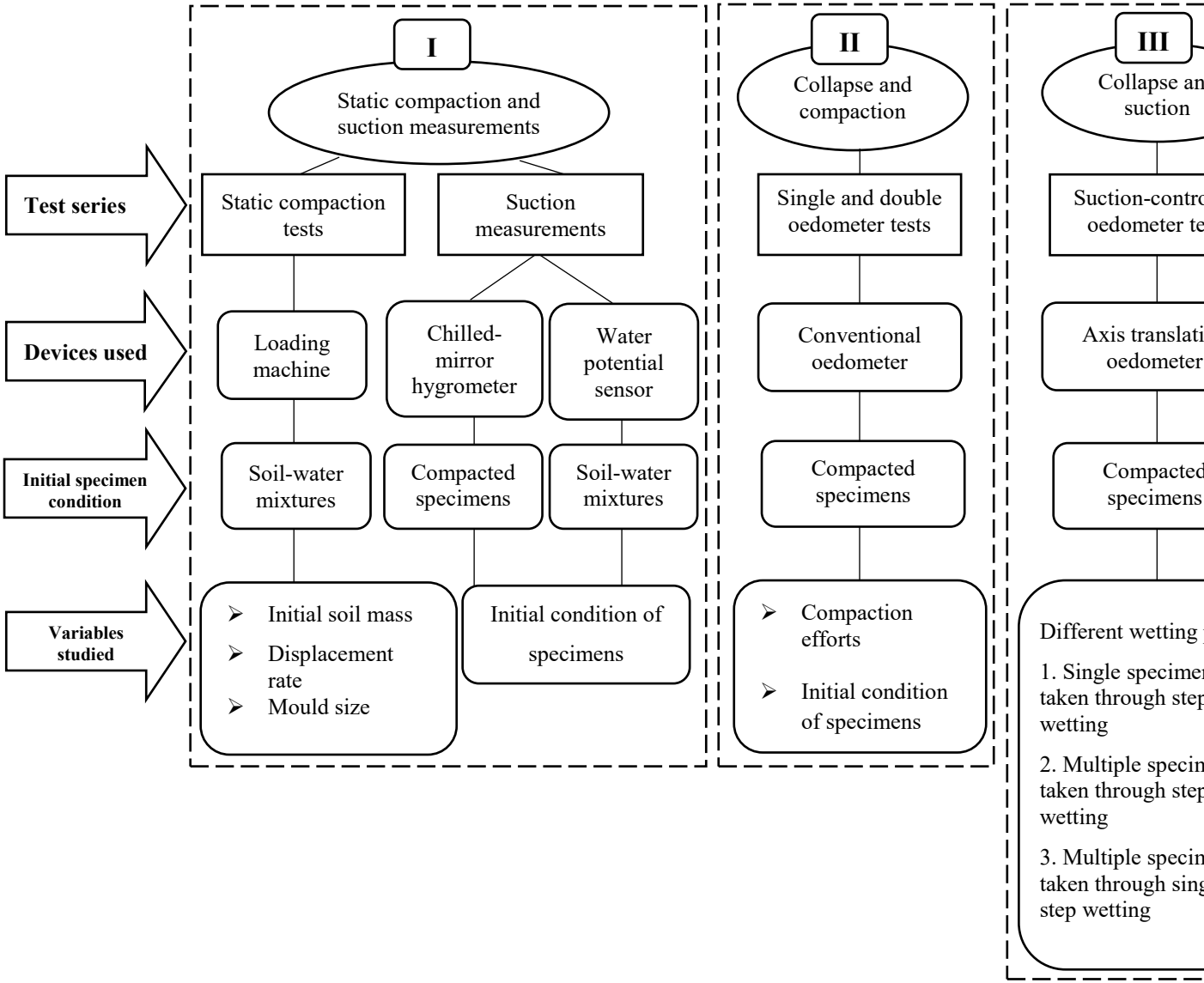

Figure 3.5 Overview of the experimental programme

3.5 Static compaction tests (Test series I)

3.5.1 Specimen preparation for the static compaction tests

Soil-water mixtures were prepared by mixing the soil used with a predetermined quantity of distilled water for about 15-30 minutes. The mixture was passed through a 2 mm sieve to eliminate lumps. The moist soil was wrapped in double plastic bags and stored in sealed plastic containers for at least 24 h to achieve a uniform distribution of water. In total, seven mixtures at water contents of 7.5, 8.6, 9.6, 10.5, 11.6, 12.9 and 14% were prepared.

A stainless steel oedometer ring (100 mm in diameter and 19 mm in height) was placed over a plate and used as a compaction mould. The inner surface of the oedometer ring was lubricated with silicon grease to reduce friction effects. Specimens were prepared by loosely placing the moist soil in the ring and levelling off any excess soil. The amount of the soil required to fill the ring was carefully considered. The soil mass was then recorded and further used for analysing the test results.

It is worth mentioning that, specimens at high water contents (i.e., approaching the plastic limit) could not be prepared following this procedure. This is because the moist soil at higher water contents formed a thin paste, and therefore, placing the soil in the ring could not be achieved.

3.5.2 Experimental setup for the static compaction tests

A loading machine shown in Figures (3.6a and b) was used for the static compaction tests. The machine has a maximum loading capacity of 40 kN. The main components of the machine are a loading frame, a load cell and a data acquisition system. It allows for the control of displacement rate and data transmission rate. The load cell is fitted in the loading frame that can manually and electrically move. A specially designed cylindrical piston was attached to the load cell and used as a compactor. The static load with the displacement data was configured via testXpert® software.

3.5.3 Testing procedure for the static compaction tests

The one-dimensional static compaction test was started by positioning the loading piston in direct contact with the top surface of the prepared specimen. The compaction stroke (displacement) was set at a displacement rate of 1.25 mm/min. The static load corresponded to the compaction stroke was collected at a data transmission rate of 10 Hz (i.e., 10 readings in 1 second). The tests were terminated when the degree of saturation approached ≥ 95% or when reaching the maximum loading capacity of the machine (40 kN), whichever occurred first.

(a)

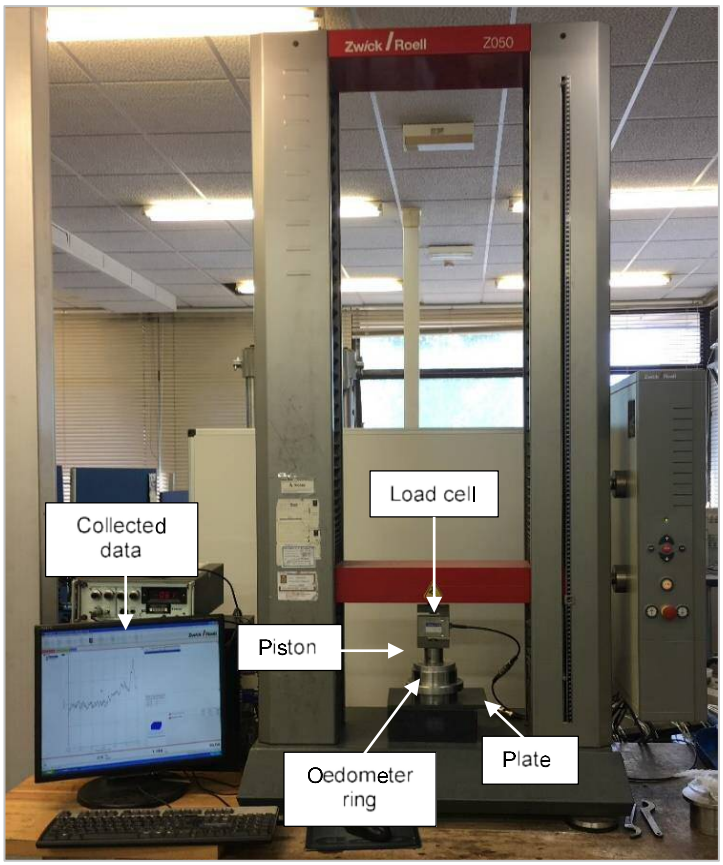

(b)

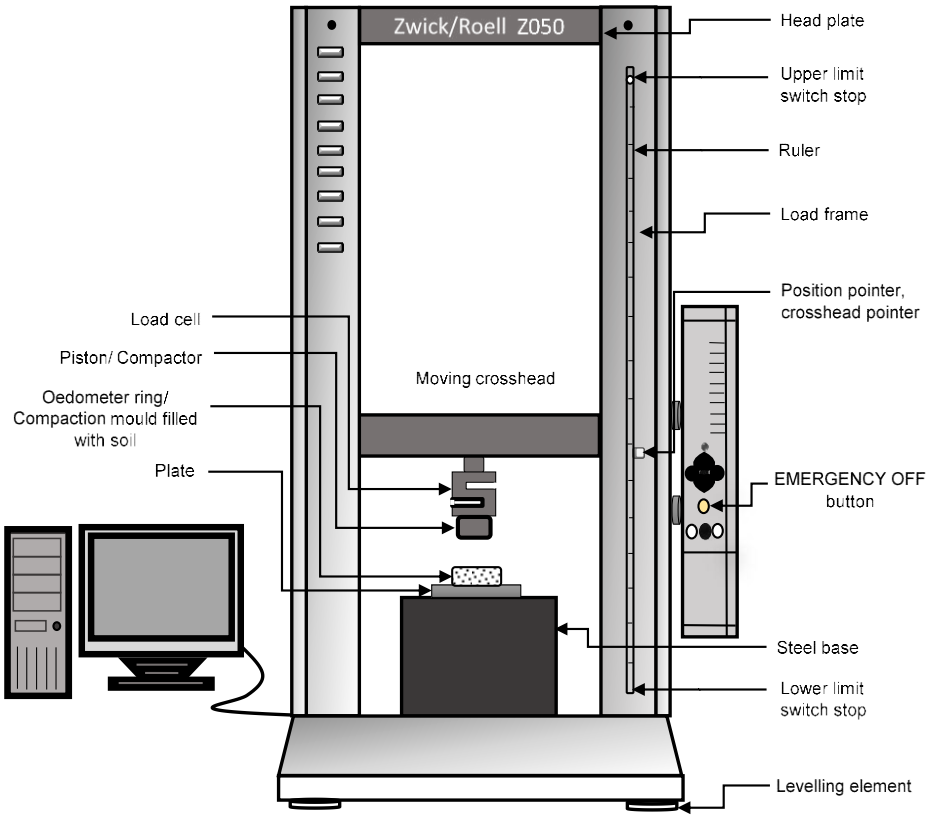

Figure 3.6 Static compaction test setup, (a) Photograph and (b) schematic drawing

3.6 Suction measurements (Test series I)

Two methods were used to measure the suction of the soil. The total suction of compacted specimens was measured by a chilled-mirror dew-point device. Matric suction of soil-water mixtures was measured by a water potential sensor. Both devices, specimen preparation and testing procedure are presented in the subsequent sections.

3.6.1 Chilled-mirror dew-point device

This device uses the chilled-mirror dew-point technique to indirectly determine the total suction of soil specimens, commercially known as the WP4C Dewpoint PotentiaMeter. The WP4C device (Figure 3.7) consists of a sealed chamber with a fan, a mirror, a photodetector cell, and an infrared thermometer (Decagon Devices 2010). It is also equipped with a drawer to place the specimen's cup. The device can measure suction from 0 to 300 MPa to an accuracy of ± 0.05 MPa from 0 to 5 MPa and 1% from 5 to 300 MPa. Typical measuring time is from 10 to 15 minutes for most soil specimens in a precise mode. A thermal equilibration plate can also be used to bring the temperature of the specimen cup to the set-point temperature of the device (Figure 3.9).

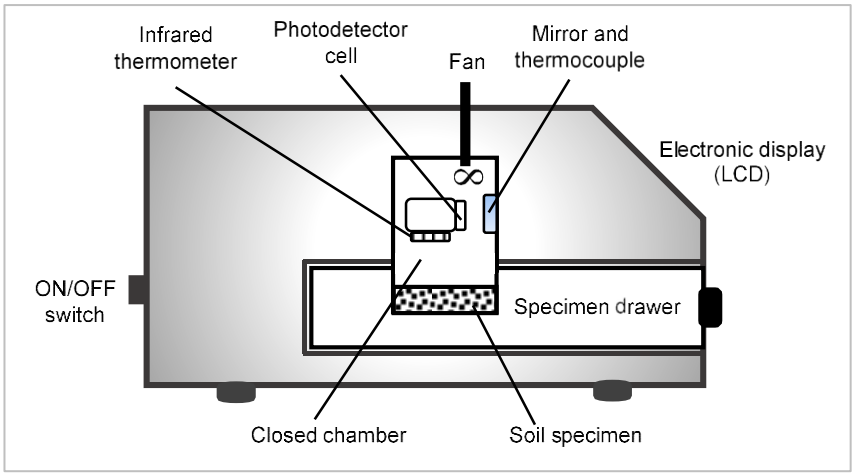

Figure 3.7 Schematic diagram of WP4C model of chilled-mirror dew point device

3.6.1.1 Specimen preparation for suction measurement using the chilled-mirror device

Compacted samples were prepared at pre-selected compaction conditions. A predetermined amount of distilled water was added to the soil and mixed thoroughly. The moist soil was then sieved through a 2 mm sieve, packed in double bags and stored in sealed plastic containers for at least one day. A stainless steel oedometer ring (100 mm in diameter and 19 mm in height) was internally lubricated with silicon grease and placed over a plate. Samples were prepared inside the oedometer ring by static compaction to a specified thickness of 4.5 mm. A loading machine was used to apply the required static load with a constant displacement rate of 1.25 mm/min. Two specimens were obtained by trimming the initially prepared compacted sample to the recommended size (half the capacity of the specimen cup). The procedure followed in preparing the compacted specimens is presented in Figure (3.8).

Figure 3.8 Specimens preparation steps for the suction measurement tests

3.6.1.2 Testing procedure

The WP4C device is calibrated before each test by using potassium chloride (KCl) solution. The cup containing the specimen was first placed on the temperature equilibration plate set at 25 ºC for about 10 minutes. The specimen was then

transferred to the device drawer as shown in Figure (3.9). The LED indicator light blinks to indicate the measurement. Total suction was measured for the two trimmed specimens, and the average value was considered. The testing duration varied between 10 to 30 minutes. The water contents of soil specimens after completion of total suction measurements were determined by the oven drying method. In total, suction of 49 compacted samples at different conditions along the compaction curves was measured and further used to construct suction contours as will be explained in the relevant chapter (Chapter 4).

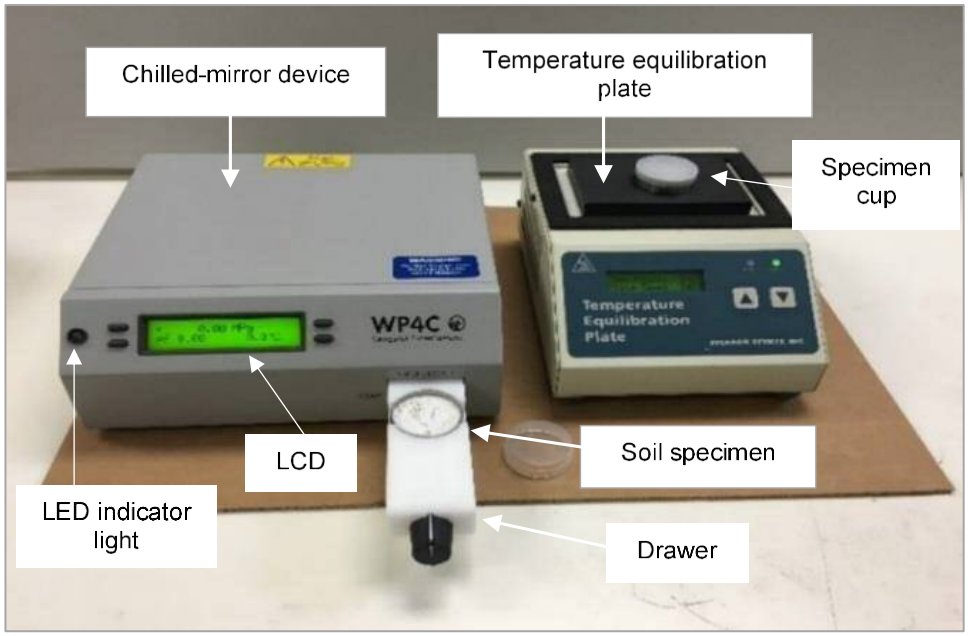

Figure 3.9 Suction measurement tests setup using the WP4C dew point potentiameter

3.6.2 Water potential sensor

A calibrated water potential sensor commercially named MPS-6 (Figure 3.10) was used to establish the matric suction-water content relationship of the soil used. It consists of two ceramic disks, a printed circuit board, and two grounded stainless-steel screens attached to the exteriors of the ceramic disks. The sensor is able to measure

suction from 9 to 100,000 kPa with an accuracy of ± (10% of reading + 2 kPa) for a suction range of 9 – 100 kPa. Whereas the accuracy of the sensor at high suctions depends upon the water retention characteristic of the ceramic disk (Figure 2.2). A thermistor located underneath the sensor enables monitoring of the temperature. The range, resolution, and accuracy of the thermistor are -40 to 60, 0.1, ±1 °C, respectively.

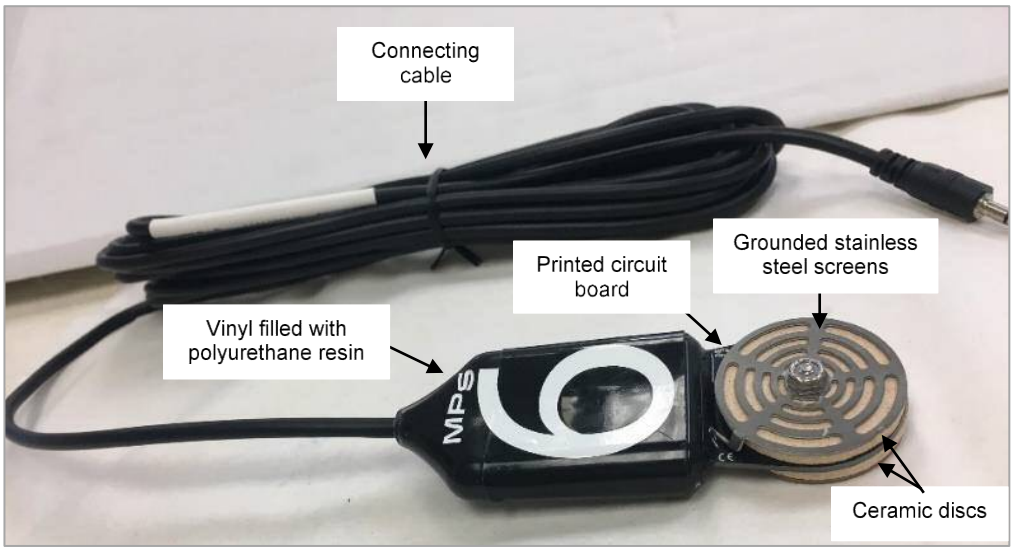

Figure 3.10 The water potential sensor used for suction measurement

3.6.2.1 Specimen preparation for suction measurement using the water potential sensor

Several soil-water mixtures were prepared by thoroughly mixing the soil with a predetermined amount of distilled water to achieve selected water contents. The moistened soil was then passed through a 2 mm sieve. The mixtures were packed in double bags and stored in sealed plastic containers for at least one day to allow moisture equilibration. In total, seven soil-water mixtures were prepared.

3.6.2.2 Testing procedure for the water potential sensor

Since the sensor allows measuring the matric suction of soils, hydraulic contact between the soil and the sensor is a prerequisite for the efficient operation of the sensor (Decagon Devices 2014). The test was started by inserting the MPS-6 sensor carefully in the prepared soil-water mixtures. The moist soil was packed in a ball around the entire ceramic disk and in loose manner surrounding the sensor. The soil specimens were wrapped in two sealed plastic bags and placed in a thermocol box as shown in the test setup in Figure (3.11). A data logger then recorded the variation of the suction and temperature at an interval of 60 minutes (recommended by the manufacturer). The tests were performed in a temperature-controlled laboratory (21.5 ± 2 °C).

A series of suction measurement tests were performed on the prepared mixtures by using initially dry sensors. Prior to all tests, sensors were air dried (i.e., initially dry sensor).

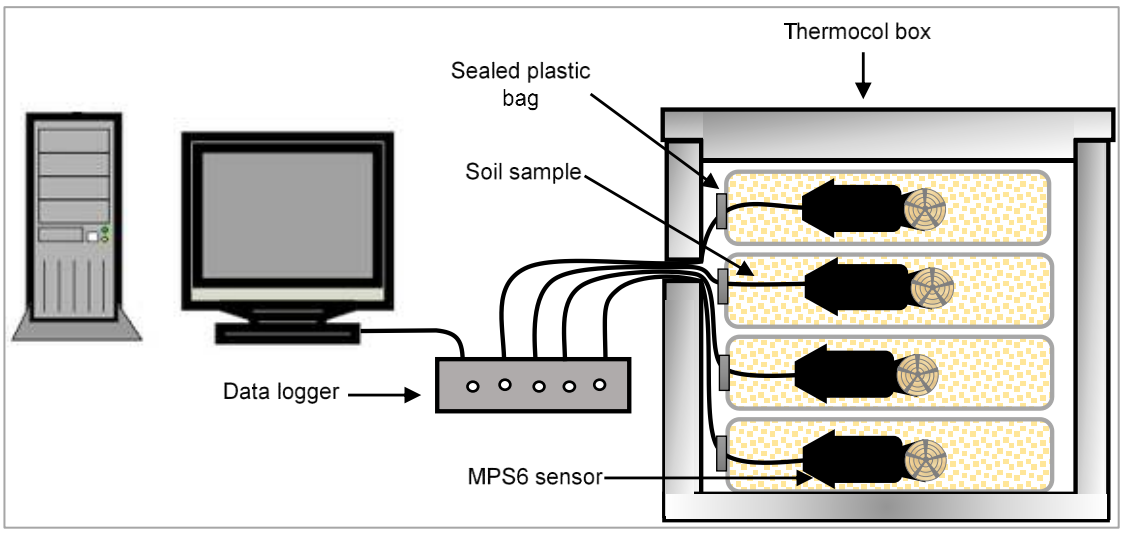

Figure 3.11 Test setup of suction measurements using MPS-6 sensors

3.7 One-dimensional collapse tests (Test series II)

3.7.1 Specimen preparation for collapse tests

Statically compacted specimens were prepared at pre-selected compaction conditions. The compaction conditions of the specimens were chosen to be located on the pre-established static compaction curves. A predetermined amount of distilled water was added to the soil and mixed thoroughly. The moistened soil was then passed through a sieve size of 2 mm to obtain compacted samples of a standard size for oedometer tests, the maximum size of particles < H/5, where H is the sample height (BS 1377-5 1990). The mixtures were packed in double bags and stored in sealed plastic containers for at least 24 hr. A stainless steel oedometer ring attached to a collar was greased and placed on a plate. Compacted specimens (100 mm dia. and 16 mm height) were prepared by statically compacting the moist soil inside the oedometer rings. A loading machine was used to apply the required static load with a constant displacement rate of 1.25 mm/min.

3.7.2 Testing procedure for collapse tests

The two procedures commonly used in the one-dimensional wetting-induced collapse are the single and double oedometer tests using the conventional oedometer. Both test procedures are presented in the following sections.

3.7.2.1 Single oedometer tests

Single oedometer tests were carried out on compacted specimens following the procedure specified in ASTM D4546-14. Multiple specimens were incrementally

loaded to pre-selected vertical stresses following a standard incremental loading procedure. Specimens were allowed to come to equilibrium under each load increment. A loading pressure range from 50 kPa to 800 kPa was applied. Under the desired vertical pressures, specimens were inundated with water. During the wetting process, the deformation was monitored at suitable intervals. The final one-dimensional wetting-induced deformation after 24 h was noted and further used to determine the collapse strain using Equation (2.5).

3.7.2.2 Double oedometer tests

Soil specimens in the double oedometer test were tested according to the procedure proposed by Jennings and Knight (1957). Two identical compacted specimens, at predetermined compaction conditions, were tested. In one test, the specimen was incrementally loaded to 800 kPa following a standard loading procedure (i.e., 12.5, 25, 50, 100, 200, 400, and 800 kPa). The unsaturated specimen was permitted to achieve equilibrium at each level of vertical stress and the final deformation was recorded. The load was released from the specimen through a successive decrement. The entire oedometer cell was covered with a plastic layer to maintain a constant water content throughout the test. In the other test, the specimen under a small seating pressure was inundated with water and allowed to come to equilibrium. The saturated specimen was consolidated using the same loading sequence used for the unsaturated specimen. Each load increment remained constant for 24 hours or until no further deformation occurred. The specimen was unloaded in a stepwise manner. The deformation was monitored at suitable intervals. Under any stress level, the difference in the height between the saturated and unsaturated specimens used to calculate the collapse strain using Equation (2.5).

3.8 Suction-controlled oedometer tests (Test series III and IV)

Suction-controlled oedometer tests were performed on compacted specimens by using an axis-translation oedometer. Compacted specimens (dia. = 100 mm height = 25 mm) were prepared by following the procedure presented in Section (3.7.1). Two series of tests were performed. In Test series III, soil specimens were taken through various suction control wetting tests under a constant applied stress. In test series IV, the suction control wetting tests were conducted on soil specimens under different applied stresses. All the tests were carried out in a temperature-controlled laboratory.

3.8.1 Experimental setup for the suction-controlled oedometer tests

A commercially available axis-translation oedometer cell (Figures 3.12a and b) was used in this study (CONTROLS Group Ltd). The oedometer cell with auxiliary devices (Figure 3.13) enable one-dimensional wetting tests by controlling suction using the axis translation technique (Hilf 1956). The water sub-pressure method (Romero 2001) was used for controlling the matric suction by decreasing the applied pore-air pressure while maintaining a constant pore-water pressure.

The bottom base of the oedometer cell fitted with a 500 kPa high air-entry (HAE) ceramic disk, a grooved water compartment and a flushing system comprised of inlet and outlet valves. The water compartment under the ceramic disk serves to keep the disk saturated and to facilitate the flushing of diffused air. A GDS pressure/volume controller is connected to the outlet valve for tracking water content changes and controlling the pore-water pressure. A stainless-steel specimen ring (100 mm diameter and height of 32 mm) can be assembled on the top of the ceramic disk.

The top part of the cell is designed to facilitate application of the desired pressures. It consists of two external ports, flexible diaphragm and loading ram. The pore air pressure was supplied by regulated compressed air to the top of the sample. This pressure is uniformly transmitted to the sample via the loading ram that ends in the upper porous stone in contact with the top surface of the sample. The application of the vertical net stress was accomplished with a pressure uniformly applied on the soil specimen via a flexible diaphragm filled with water.

Two pressure transducers, manufactured by Controls Ltd with a maximum capacity of 1000 kPa, were also used. One transducer was fitted to the top port to measure the air pressure. The other transducer was fitted to the port on the water compartment to measure the water pressure beneath the ceramic disk. The water pressure transducer was connected to a de-airing block that carried a bleed valve. This transducer was calibrated at the interface of the specimen-ceramic disk by clamping it to the exterior of the cell.

A linear vertical displacement transducer (LVDT) was fitted to a rod fixed in the bottom base of the cell. The lid of the LVDT was placed in contact with the loading ram to measure the vertical displacement. A data acquisition system continually stored data of the applied pressures, the vertical displacement and the water exchange.

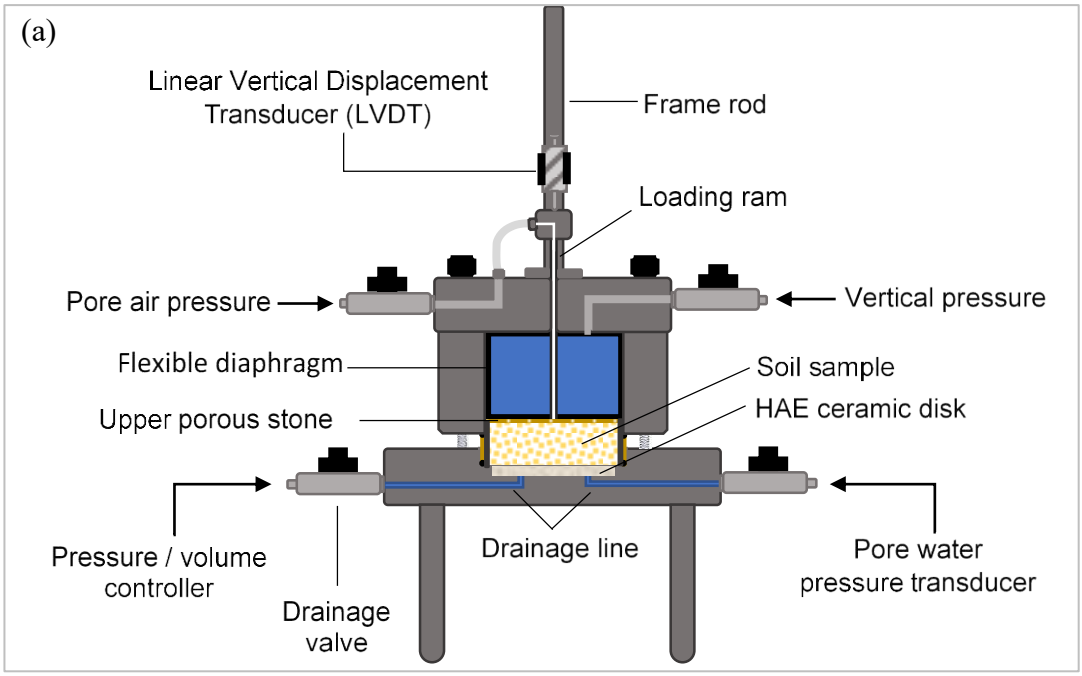

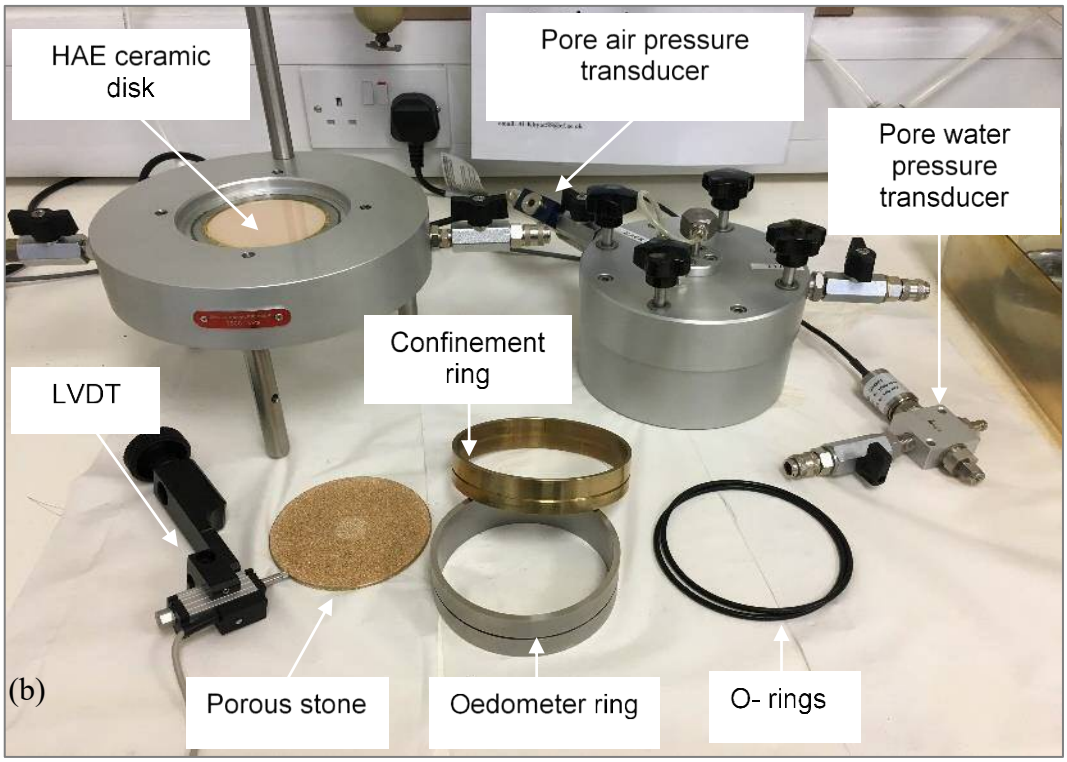

Figure 3.12 Suction-controlled oedometer cell, (a) Schematic diagram and (b) components

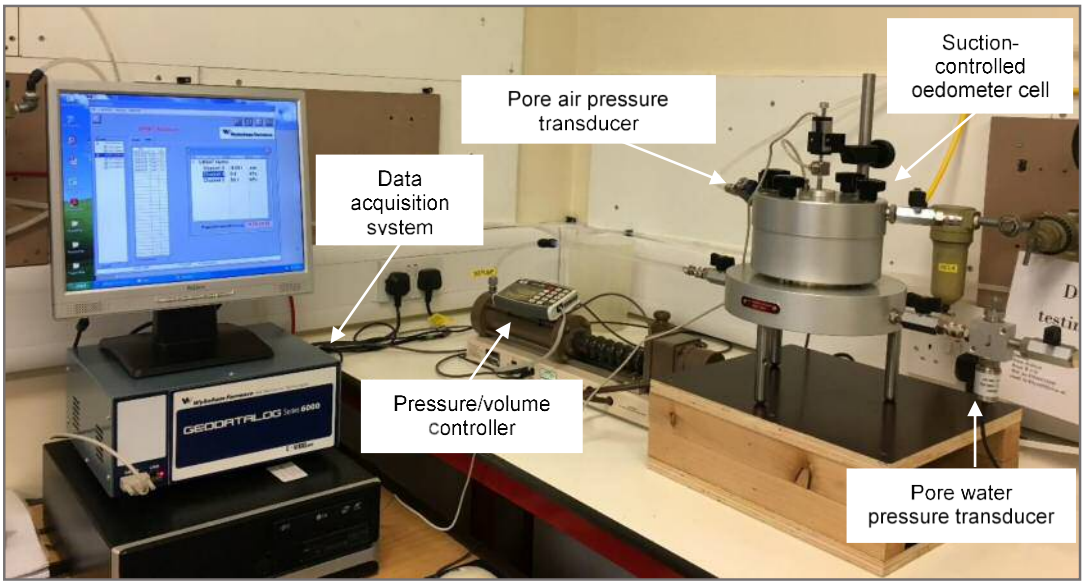

Figure 3.13 Test setup for the suction controlled-oedometer tests

3.8.2 Permeability of the high air entry (HAE) ceramic disk

Different procedures were suggested in the literature for saturating HAE disks (Fredlund and Rahardjo 1993; Leong et al. 2004; Tripathy et al. 2011; Sivakumar 2014). To ensure saturation of ceramic disks, the measured coefficient of permeability should attain a constant value and compare with the manufacturer value (Tripathy et al. 2011; Tarantino et al. 2011).

In this study, a HAE ceramic disk (98.7 mm thick) with a 5-bar entry value was saturated by forcing water to flow through the disk. The oedometer ring above the ceramic disk was filled with distilled de-aired water. An air pressure of 50 kPa was applied over a period of several days while continuously flushing the water compartment underneath the ceramic disk.

After the saturation process, the coefficient of permeability of the ceramic disk was measured. The oedometer ring above the ceramic disk was filled with distilled de-aired water. Different values of air pressures were applied, and the outflow water was

collected in a beaker. The mass of the water flowing out was determined by a weighing balance. Table (3.3) shows the applied pressures, the corresponding applied hydraulic gradients and the obtained outflow rates. The saturated coefficients of permeability of the ceramic disc were determined using Darcy's law (Figure 3.14). The average saturated coefficient of permeability of the disk used was found to be 3.53 10^{-10} .

Table 3.3 Data for determining coefficient of permeability of the ceramic disk used

Applied air pressure (kPa)	Hydraulic gradient (-)	Flow rate 10^{-6} (m^3/s)
50	517	0.0009
100	1033	0.0018
200	2066	0.0035
300	3099	0.0054
400	4133	0.0072

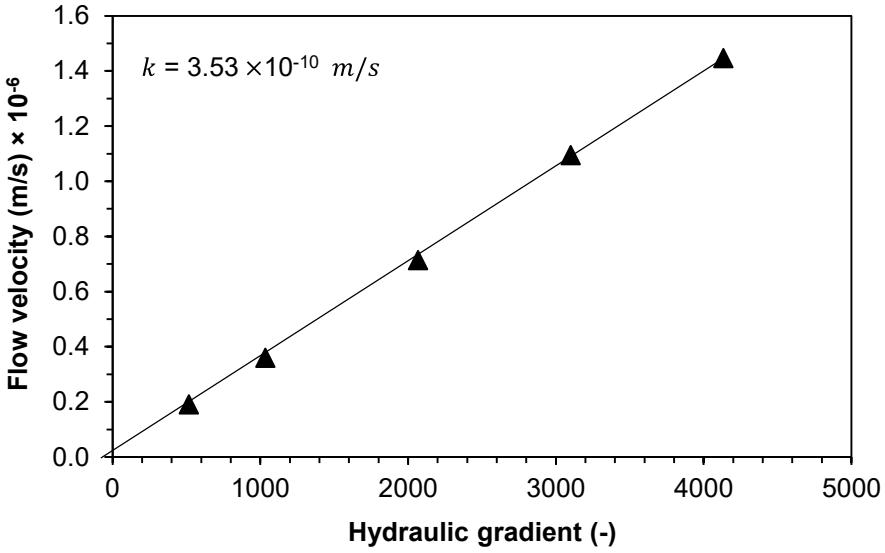

Figure 3.14 Coefficient of permeability of the ceramic disk used

3.8.3 Initial suction of specimens

In both test series III and IV, the initial suction of the compacted specimens was measured by the null-type axis translation technique. The suction measurements were carried out prior to the wetting-induced collapse tests using the suction control oedometer.

The ceramic disk was first wiped by a wet towel to provide water phase continuity. The compacted specimen was placed on the saturated ceramic disk. To ensure a good hydraulic connection between the specimen and the ceramic disk, a 1 kg mass was placed on the specimen via the loading ram (Olson and Langfelder 1965). This applied mass resulted in a vertical pressure of 1.25 kPa on the soil specimen. The drainage valves were kept closed (Figure 3.12a) during the test in order to measure the pore water pressure. Once the pore-water pressure transducer started recording a negative value, this value was countered by manually increasing the pore air pressure such that it always maintained at zero. At equilibrium, the matric suction is equal to the applied pore air pressure since the pore water pressure is null throughout the tests. The rationale behind measuring the initial matric suction using the same suction-controlled oedometer device was to eliminate changes in the water content of the compacted specimens.

3.8.4 Suction-controlled oedometer at various wetting tests (Test series III)

Wetting-induced collapse tests under suction control were carried out by independently regulating both vertical net stress (and matric suction (

to impose a desired state of stress within specimens.

Specimens were incrementally loaded to a predetermined vertical net stress. The specimens were permitted to achieve equilibrium at each stress increment. Deformation caused by loading was collected at suitable intervals. During the loading stage, the drainage valve was open.

Under a constant vertical net stress, the wetting process was accomplished by decreasing the pore air pressure to a targeted value of suction while the pore water pressure was kept at zero. Simultaneously, the vertical stress was reduced by the same amount of the reduced pore air pressure to maintain the constant vertical net stress throughout the tests.

Under each applied suction, water volume change was monitored by the pressure/volume controller. Water equalisation was assumed to be attained when the change in the water content was less than 0.04% per day (Sivakumar 1993), which is equivalent to a water volume change of about 0.14 cm^3/day (Haeri et al. 2014; Garakani et al. 2015). Saturation of the water compartment was ensured by flushing the possibly diffused air after the equalisation step.

During the wetting process, deformation, water volume change, pore air pressure and pore water pressure were collected every minute by Datacomm and GDSLab software.

Three wetting tests were followed by changing the applied matric suction between the initial measured value and zero suction as detailed in the subsequent sections. On completion of wetting-induced collapse tests under suction control, specimens were removed from the device and oven dried to measure the final water content.

3.8.4.1 Single specimen taken through stepwise wetting (Test 1)

The initially measured matric suction was reduced to zero by finite decreases of suction. A single specimen was used for the entire stepwise wetting process. The water content achieved at the intermediate suction reduction steps was calculated based on the water volume change reading collected by the pressure/volume controller.

3.8.4.2 Multiple specimens taken through stepwise wetting (Test 2)

The initially measured matric suction was reduced to a targeted suction value in a stepwise manner. Multiple specimens were required to cover the range of matric suction under study. The tests were terminated at different suction values after passing through the intermediate suction steps.

3.8.4.3 Multiple specimens taken through single-step wetting (Test 3)

The initial matric suction was reduced directly to a targeted suction level in a single step (by skipping the intermediate steps). Multiple specimens were required for covering the range of matric suction under study. Each test was terminated at the targeted suction value.

3.8.5 Suction-controlled oedometer tests at various applied stresses (Test series IV)

Stepwise wetting tests (Test 1 in Section 3.8.4.1) were carried out at various predetermined applied stresses (Figure 3.15). Several specimens at different compaction conditions were tested. The initial suction of the specimens was measured following the null-type axis translation procedure (Section 3.8.3). Further, the specimens were loaded to different vertical net stresses. At any given applied stress, the specimen was taken through stepwise suction reduction up to saturation. During the tests, deformation, water volume change, pore air pressure and pore water pressure were collected every minute. The final water content corresponding to zero suction was measured at the end of the tests by the oven drying method.

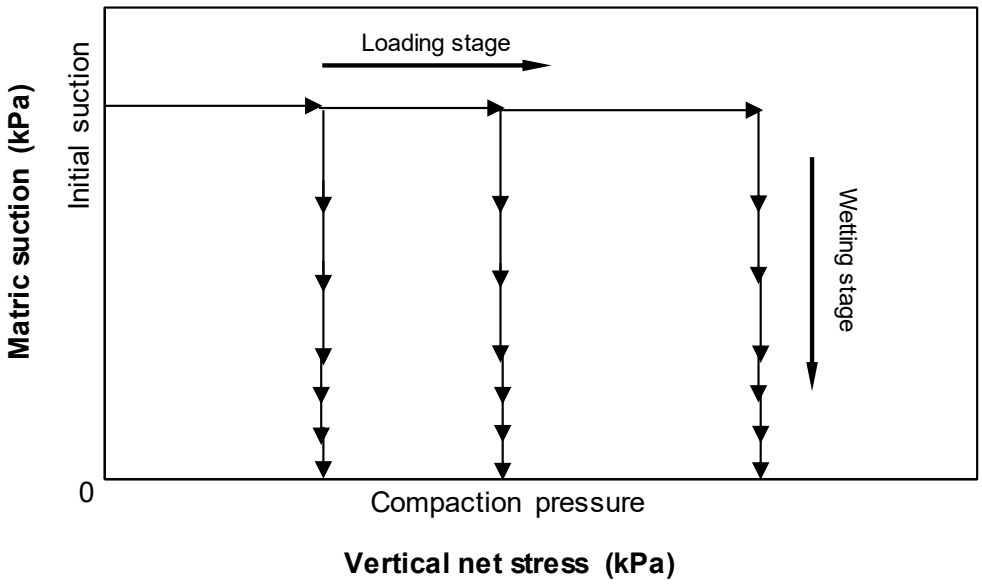

Figure 3.15 General stress paths for the suction-controlled oedometer tests (Test series IV)

3.9 Concluding remarks

In this chapter, a detailed description of selection of the material used in this study was presented. A summary of the properties of the material used determined was given in Table (3.2). An overview of the experimental methods and programme (Figure 3.5) were also included. Details of the samples preparation, the experimental setup and testing procedure for each test series were presented.

Wetting-induced collapse behaviour is studied in this thesis under both uncontrolled and controlled-suction conditions. Specimens are chosen to be subjected to either constant compaction pressure or constant compaction energy. Under suction control wetting tests, three wetting tests will be introduced and compared. The combined effects of various stress states and compaction conditions on the hydro-mechanical behaviour of the soil used is considered. It is therefore believed that this comprehensive study will enhance the fundamental understanding of the volume change behaviour of collapsible soils when subjected to various loading, wetting and compaction conditions.

Chapter 4

Static compaction behaviour and suction measurements

4.1 Introduction

Soil compaction is a pivotal activity in engineering practice because of its marked effect on improving the soil properties. It is believed that compaction is a soil fabric creation process (Lambe and Whitman 1969; Delage et al. 1996). Compaction parameters, such as compaction water content, dry density and compaction efforts have been noticed to have considerable effects on the hydro-mechanical behaviour of unsaturated soils (Lawton et al. 1989; Basma and Tuncer 1992; Sivakumar and Wheeler 2000; Aziz et al. 2006). To study the behaviour of compacted soils, researchers tend to prepare compacted specimens in laboratories. Among the available laboratory compaction methods, the static method seems a convenient method and promoting specimen homogeneity and test repeatability (Hafez et al. 2010; Asmani et al. 2013). However, reviewing the literature suggests that developing a simple, effective and fast static compaction test procedure is needed (Venkatarama-Reddy and Jagadish 1993). In this study, the developed procedure of the static compaction tests differs from the existing methods by (i) the initial soil mass is better defined, (ii) the test is not restricted to any specified value of peak stress or final thickness and the termination criteria of the tests is rather identified, (iii) a few tests are sufficient for establishing the compaction curves, (v) the generated data enabled establishing the

static compaction curves both in terms of compaction pressure and compaction energy at various levels, and (vi) factors influencing results of the proposed static compaction tests are identified.

Compaction-induced suction changes is another feature of the compaction process. Considerable research works have linked compaction variables, such as compaction water content and dry density with suction (e.g., Krahn and Fredlund 1972; Vanapalli et al. 1999; Tripathy et al. 2005; Yang et al. 2012). These studies outlined that suction is mainly affected by the water content and the dry density is of secondary influence. Contradictory results, however, about the effect of dry density on the soil suction at a constant compaction water content have been reported (Dineen et al. 1999; Leong et al. 2003; Gonzalez and Colmenares 2006; Tarantino and De Col 2008). In these studies, suction was observed to increase, remain constant or decrease with the increase in dry density. Therefore, it is necessary to understand the effect of compaction parameters on the suction of the soil used in this study.

The objectives of this chapter are to (*i*) examine the applicability of the proposed procedure for static compaction tests in establishing static compaction curves, (*ii*) identify the effects of initial soil mass, displacement rate and compaction mould size on the test results, (*iii*) investigate the changes in suction with increasing dry density and with increasing water content of specimens along the compaction plane.

In this chapter, results of the static compaction tests and suction measurements are presented. The experimental programme (Test series I; Section 3.5 and Section 3.6) is recalled in Section (4.2). The effects of initial soil mass, displacement rate and compaction mould size on the static compaction curves are explained in Section (4.3.2). Results of the suction measurements are presented in Section (4.3.3). The main findings from this chapter are summarised in Section (4.4).

4.2 Experimental programme

Under test series I (Section 3.5), a detailed description of the developed procedure is presented. Seven specimens (dia. = 100 mm and height = 19 mm) at various water contents were prepared following the procedure specified in Section (3.5.1). The quantity of moist soil required to fill in the compaction mould (100 mm in diameter and 19 mm in height) by several trials is given in Table (4.1). The condition of specimens prior to the compaction tests is listed in Table (4.2). Static compaction tests were carried out using the test set up shown in Figure (3.6). The tests were performed on the prepared specimens as detailed in Section (3.5.3).

In Section (3.6), two methods were used to measure suction of soil specimens. The total suction of compacted specimens along the static compaction curves was measured by the chilled mirror dew point device (WP4C). Preparation of the compacted specimens is detailed in Section (3.6.1.1) for measuring the total suction using the test set up shown in Figure (3.9). The tests were performed on specimens as detailed in Section (3.6.1.2). In total, suction measurements were carried out on 21 specimens along the static compaction energy curves and 28 specimens along the static compaction pressure curves. Matric suction of specimens with no stress history was measured by the water potential sensor (MPS-6). Specimens as soil-water mixtures were prepared for suction measurements as detailed in Section (3.6.2.1). Suction was measured using the test set up shown in Figure (3.11). The tests were performed on specimens as detailed in Section (3.6.2.2).

Table 4.1 Variation in the initial soil mass of specimens

Compaction water content (%)	Soil mass (g)		
	Trial 1	Trial 2	Trial 3
7.5	121.56	123.14	122.84
8.6	125.28	126.97	127.57
9.6	128.09	128.93	128.23
10.5	129.89	129.36	129.02
11.6	130.40	131.56	130.16
12.9	132.66	133.48	133.08
14.0	125.97	125.31	125.78

Table 4.2 Initial conditions of specimens prior to the static compaction tests

Compaction water content (%)	Soil mass (g)	Initial condition			
		Bulk unit weight (kN/m^3)	Dry unit weight (kN/m^3)	Void ratio (-)	Degree of saturation (%)
7.5	122.84	8.074	7.510	2.461	8.07
8.6	127.57	8.388	7.723	2.366	9.63
9.6	128.23	8.427	7.689	2.381	10.68
10.5	129.02	8.482	7.68	2.39	11.66
11.6	130.16	8.554	7.665	2.392	12.85
12.9	133.08	8.751	7.751	2.354	14.52
14	125.78	8.270	7.254	2.584	14.36

4.3 Results and discussion

4.3.1 Static compaction tests

4.3.1.1 Load-displacement curves

The load versus displacement (i.e., compaction stroke) curves for all specimens are presented in Figure (4.1). Seeking clarity in presentation, compaction displacement and the corresponding load are plotted at each 1 mm intervals. The maximum load that can be applied was limited to the capacity of the loading machine used for the static compaction tests, which is 40 kN (see Section 3.5.2). Repeatability of the tests was checked for the specimen at 10.5% water content and indicated as error bars. For the repeated tests, the standard deviation of the errors increased from 0.001 to 0.4 with displacement during the compaction process.

At a constant water content, increasing the compaction load produced an increase in the displacement of specimens. It can also be noted in Figure (4.1) that both the peak load and the final thickness of specimens are not constant. The applied static compaction load on specimens generally varied from 10 to 40 kN caused the compaction displacement to be varied between 11 and 12 mm. The results indicated that higher the water content of specimens, lower compaction load required to attain a given displacement. This is primarily due to the surface tension and high frictional resistance of soil specimens with low water contents, which provides the soil with sufficient shear strength to resist the compaction forces. Derived pressure-displacement curves are given in Figure (4.2). The peak applied compaction pressure was about 5 MPa and corresponds to the maximum applied load of 40 kN.

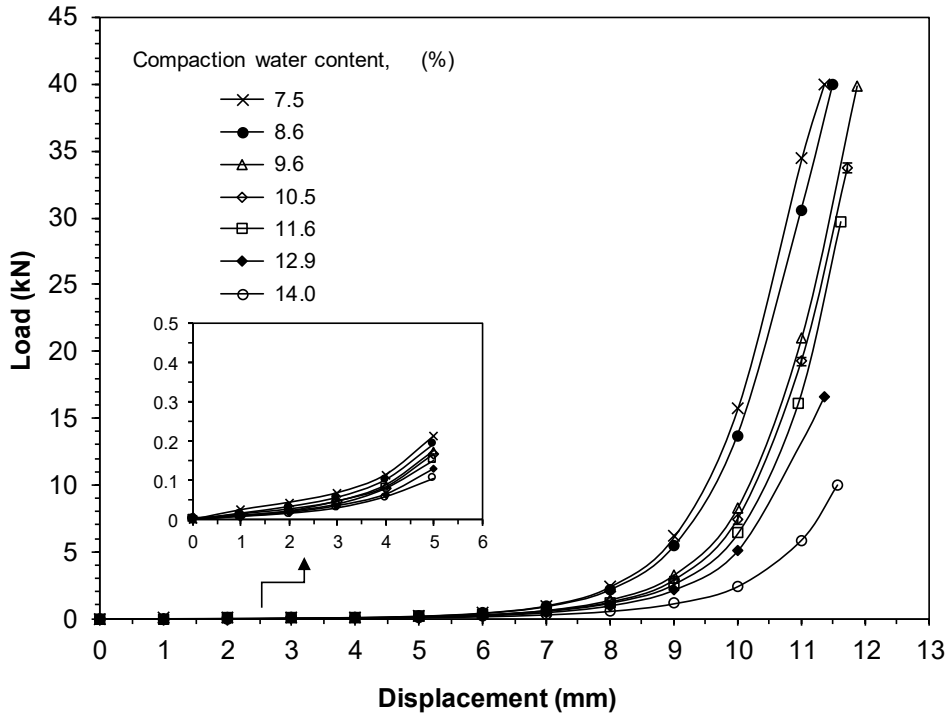

Figure 4.1 Static compaction tests result of the tested specimens

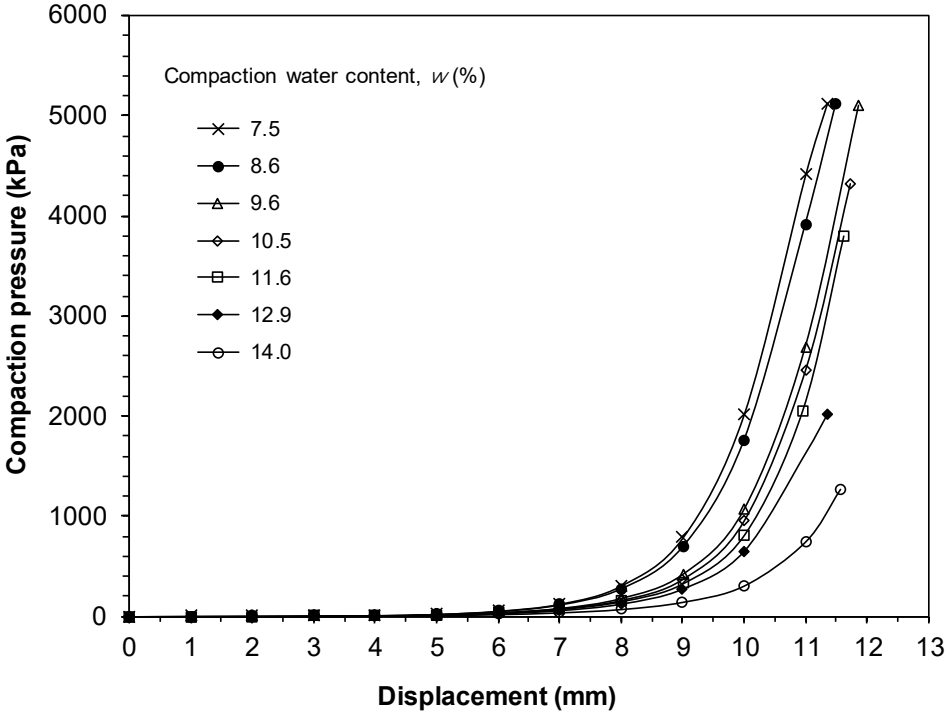

Figure 4.2 Applied compaction pressure versus displacement for specimens during the static compaction tests

4.3.1.2 Degree of saturation changes during the compaction process

Based on the initial height and mass of the specimens along with the recorded vertical displacement during the compaction process, the void ratio and hence the degree of saturation can be calculated at any stage of the tests. The water content remained constant since no drainage was provided during the static compaction tests.

The increase in the degree of saturation at a constant water content during the static compaction tests is plotted with displacement for all specimens in Figure (4.3). The results showed that specimens with higher water contents attained a greater degree of saturation of about 95%, whereas the final reached degree of saturation varied between 50 to 90% for low water content specimens.

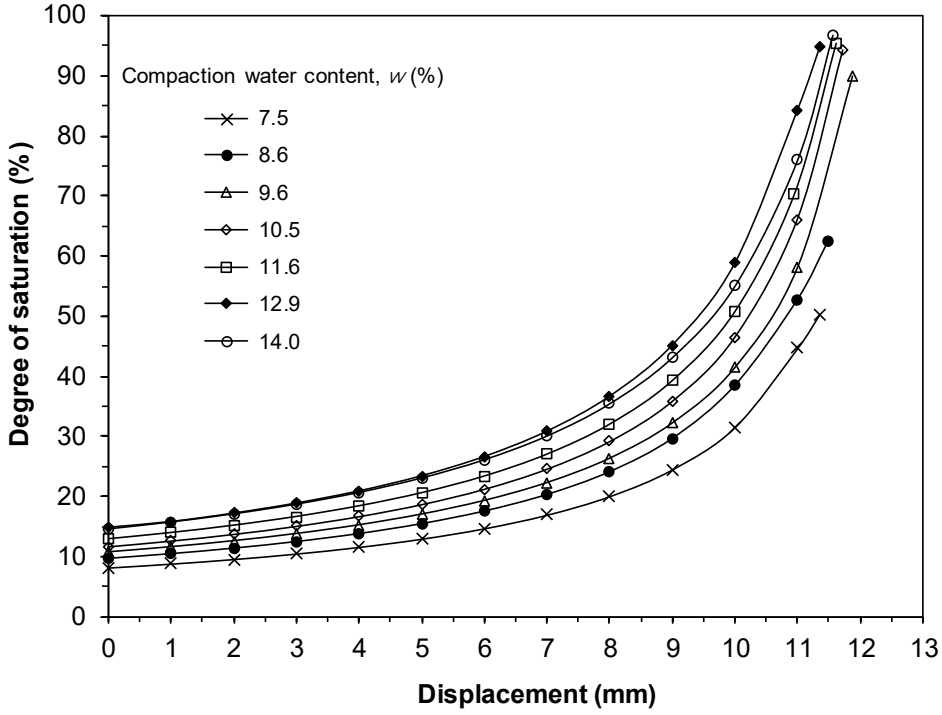

Figure 4.3 Degree of saturation changes during the static compaction tests of specimens

4.3.1.3 Dry unit weight changes during the compaction process

The variation of dry unit weight with the applied compaction pressure of specimens is shown in Figure (4.4). At a given dry unit weight, the applied compaction pressure was found to decrease with increasing the compaction water content. The final dry unit weight of specimens at various water contents was found to vary between 18.5 and 20.5 kN/m^3. For specimens with water contents greater than 10%, the applied static compaction pressure was ranged from 1000 to 4000 kPa, whereas the maximum compaction pressure of 5000 kPa was applied on specimens with lower water contents. It can also be seen in Figure (4.4) that the increase in the water content of specimens leads to achieving higher dry unit weights for a given applied pressure.

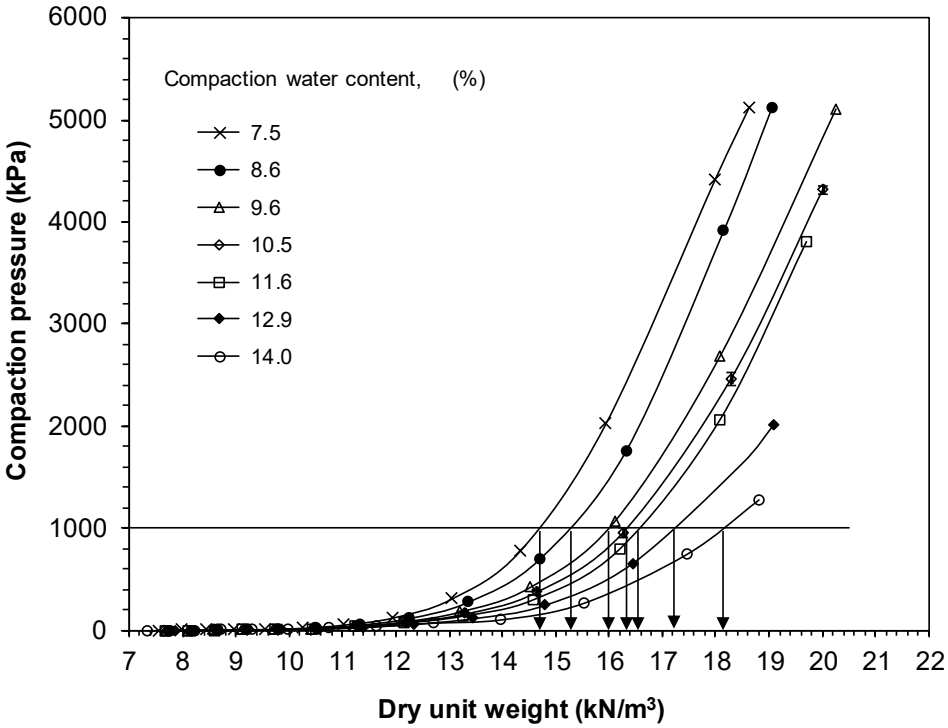

Figure 4.4 Applied compaction pressure versus dry unit weight of specimens during the static compaction tests

The load-displacement curves (Figure 4.1) enabled the subsequent determination of energy transmitted to the soil specimens. The compaction energy was calculated by integrating the area under the load-displacement curve. This area can be best evaluated by using a trapezoidal rule since the data are recorded each 0.002 mm ( ) of the displacement (i.e., displacement rate of 1.25 mm/min and data transmission rate of 10 readings/second) as given in Equation (4.1).

Area – – (4.1)

Figure (4.5) shows the relationship between the compaction energy per unit volume and dry unit weight for specimens at various water contents. The applied compaction effort at the end of the static compaction tests on the specimens at various water contents was found to be varied between 200 and 800 kJ/m^3. At given compaction energy the increase in water content of specimens produced higher dry unit weights.

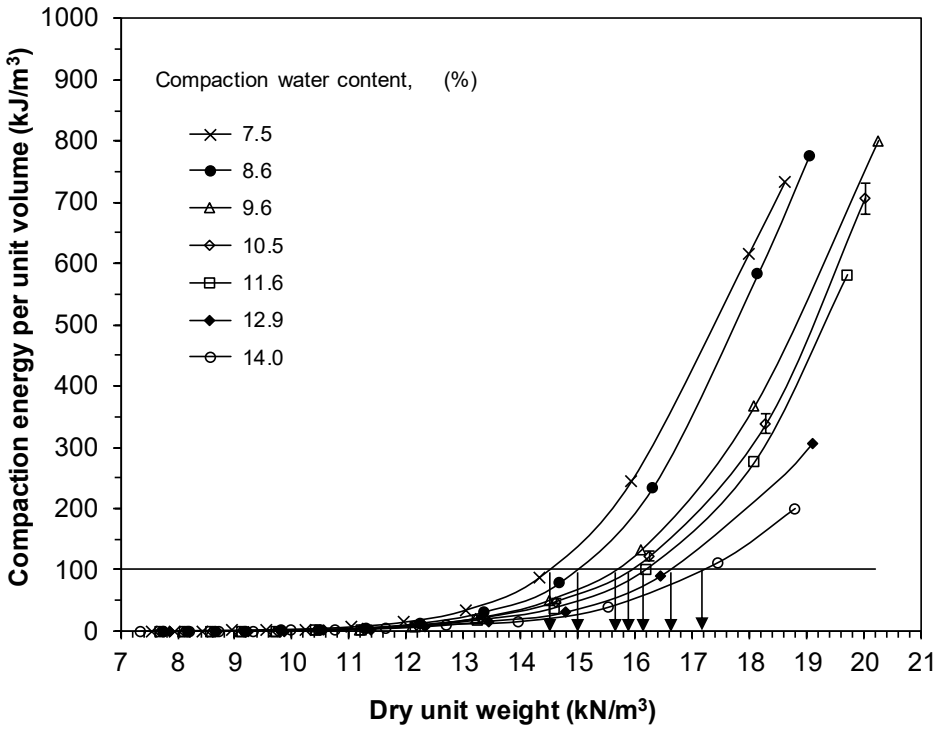

Figure 4.5 Compaction energy input per unit volume and dry unit weight relationship for all the tested specimens

4.3.1.4 Static compaction curves

Figure (4.6) shows the static compaction curves of the soil in terms of applied compaction pressures. These curves were established by drawing a horizontal line at any compaction pressure value in Figure (4.4) to read the target dry unit weight on the abscissa for various water contents as shown in the example provided in Figure (4.4) to establish the compaction curve of 1000 kPa. Similarly, by using data in Figure (4.5) the static compaction energy curves shown in Figure (4.7) were established. An example to establish the compaction curve of 100 kJ/m^3 is shown in Figure (4.5). The standard Proctor compaction curve is also included in Figures (4.6) and (4.7).

The water content-dry unit weight relationships obtained by the static compaction tests were almost increasing straight lines with no definable peak (Figures 4.6 and 4.7). Thus, the wet side of optimum was not present in the static compaction curves as in the Proctor curve since the nature and approach of these two compaction methods are fundamentally different (Yaghoubi et al. 2017). Other factors responsible of the differences in water content versus dry unit weight relationships included the amount of compaction effort, the maximum size of aggregates permitted and method of preparing the soil for testing (Lee and Suedkamp 1972).

The static compaction tests introduced in this study enabled establishing compaction curves at various compaction pressure ranged from 0.2 MPa to the highest pressure of about 5 MPa (Figure 4.6). Similarly, various compaction energy per unit volume curves ranged from 50 to 700 kJ/m^3 were also established by using the static compaction tests data (Figure 4.7). Whilst, most of the reported data on the static compaction tests were limited to either establishing static compaction curves in terms of compaction energy (Venkatarama-Reddy and Jagadish 1993) or in terms of

compaction pressure (Turnbull 1950; Olivier and Mesbah 1987; Romero et al. 1999; Tarantino et al. 2005).

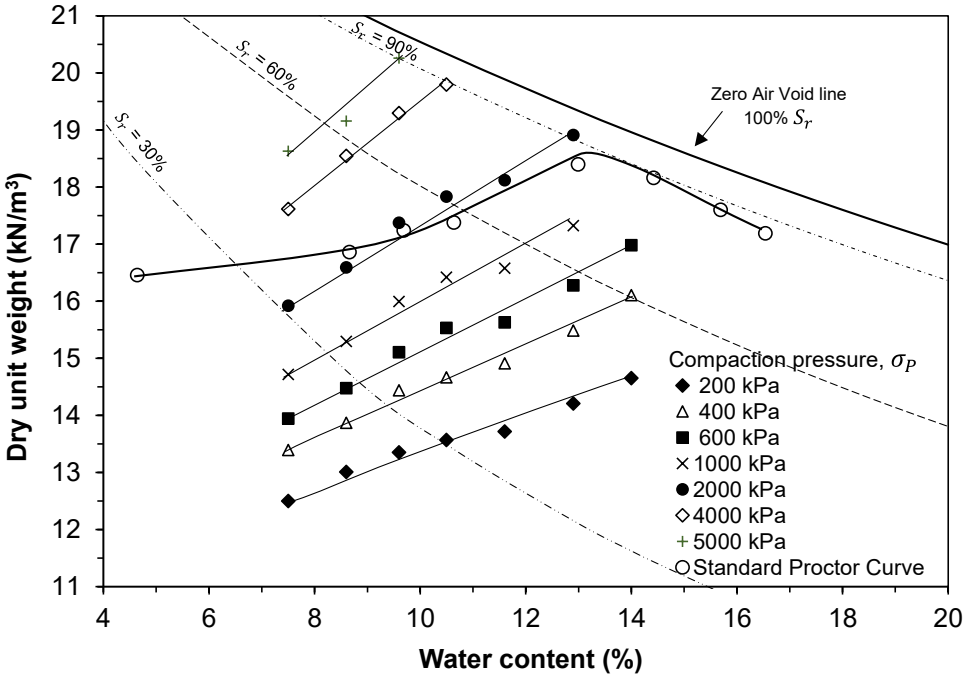

Figure 4.6 Static compaction curves at various applied compaction pressures

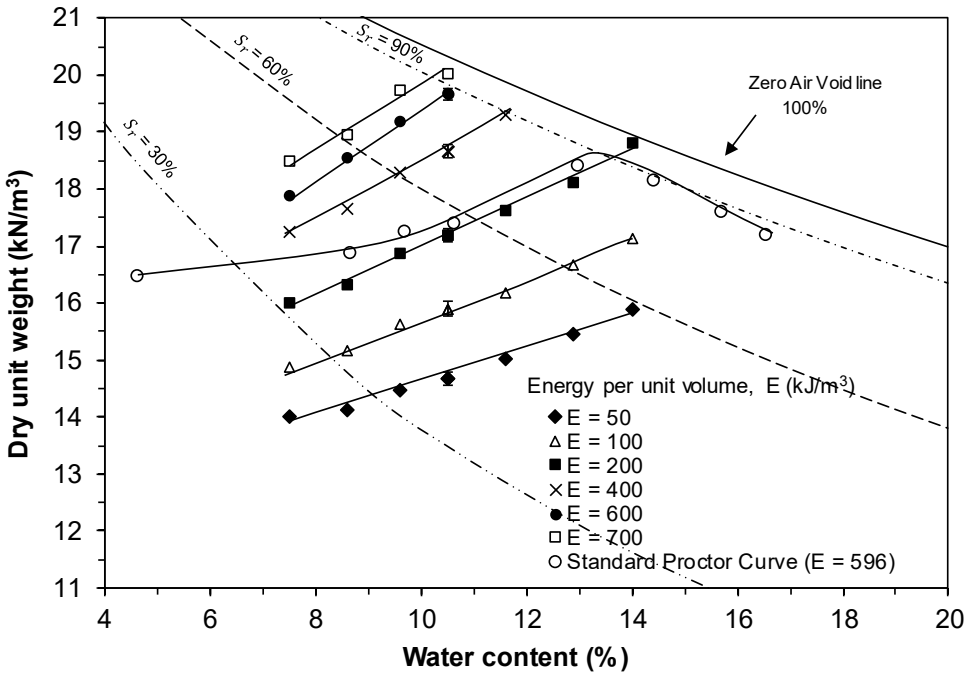

Figure 4.7 Static compaction curves at various applied compaction energies per unit volume

It can also be seen in Figure (4.7) that the static compaction at E = 600 kJ/m^3 (i.e., similar to the standard Proctor compaction effort) produced much higher dry unit weights than the dynamic compaction. Similar observation was also outlined by Venkatarama-Reddy and Jagadish (1993) and Hafez et al. (2010). The differences in the dry unit weights obtained by applying similar static and dynamic compaction effort caused by the possible energy losses during the dynamic compaction process due to the impact of the falling weight (Venkatarama-Reddy and Jagadish 1993).

The benefit of the adopted static compaction procedure is not only studying the static compaction behaviour of the soil used, but also the established static compaction curves can be used as a reference for choosing the initial condition of specimens (i.e., dry unit weight, water content and compaction effort) for the main testing programme. In this case, the initial condition of specimens is better defined and their resulting behaviour can be reasonably compared.

4.3.1.5 Static compaction energy and pressure relationship

Figure (4.8) shows the compaction pressure and compaction energy transmitted to the soil specimens during the static compaction tests. For each specimen (i.e., at any water content), the increase in the static compaction pressure produced a relatively linear increase in compaction energy. It can be observed in Figure (4.8) that the lines of compaction energy and compaction pressure relationship have different slopes with varying the water content of specimens.

Figure (4.9) shows the variation in compaction pressure with water contents of specimens along a constant compaction energy curve. At given compaction energy, an

increase in the water content of specimens leads to a linear decrease in the compaction pressure.

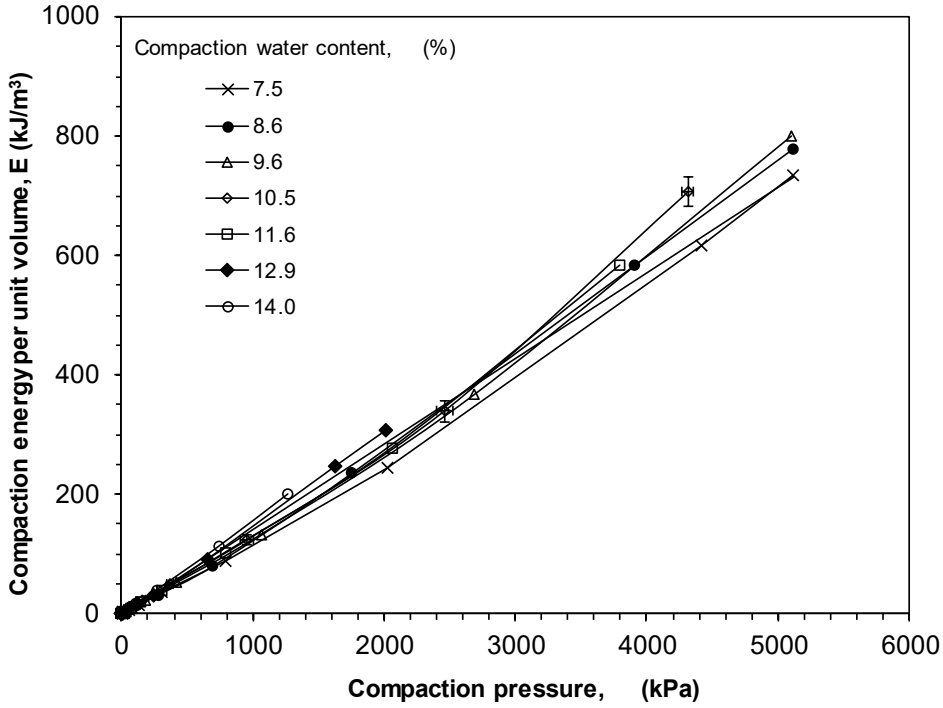

Figure 4.8 Compaction energy and compaction pressure transmitted to specimens during the static compaction tests

The compaction pressure decreased linearly with an increase in the water content of the specimens. In general, higher the compaction energy, greater the decrease in the compaction pressure. The resulting decrease in compaction pressure for specimens subjected to a constant compaction effort can be attributed to the reduction in the frictional resistance of soil particles to the rearrangement with the increase in the water contents.

Figure (4.10) shows the variation in compaction energy with water contents of specimens along a constant compaction pressure curve. At a constant compaction pressure, a linear increase in the static compaction energy was observed with increasing water content of specimens. Higher the compaction pressure, greater the increase in compaction energy with the increase in water content of specimens.

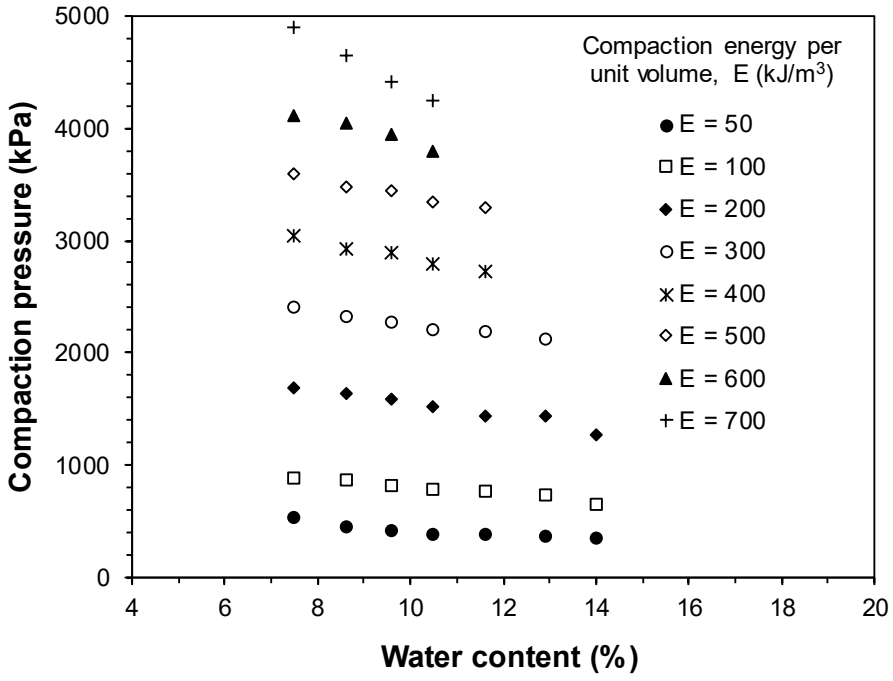

Figure 4.9 Variation of compaction pressure with water content of specimens along a constant compaction energy

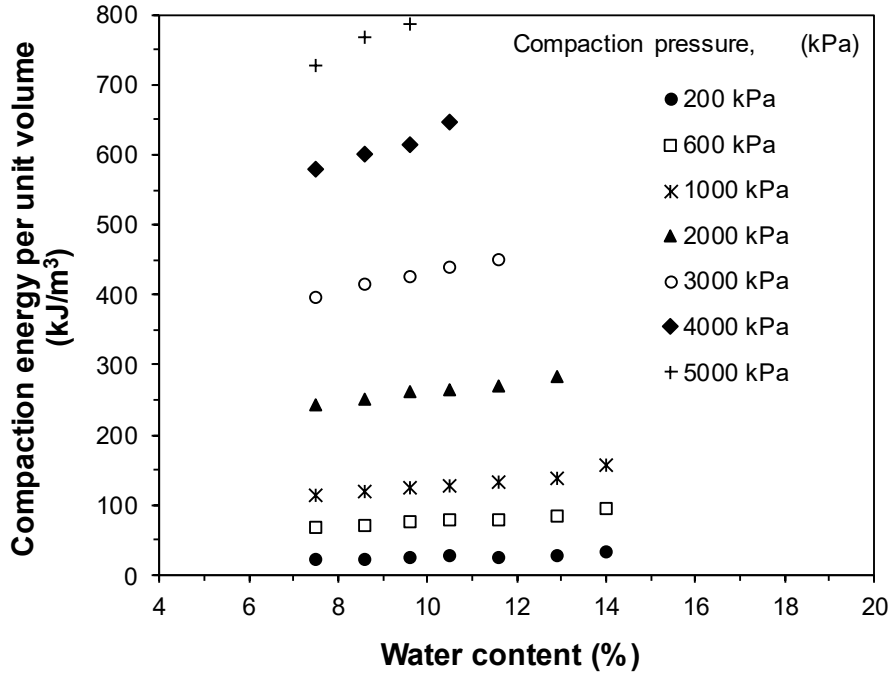

Figure 4.10 Variation of compaction energy with water content of specimens along a constant compaction pressure

4.3.2 Factors influencing the static compaction curves

Factors affect the static compaction test results are briefly discussed in this section. The explored factors included the effect of the initial soil mass, displacement rate, and compaction mould size. The study attempted to investigate the effects of these factors mainly for specimens on the dry side, as the entire study is about collapsible soils.

4.3.2.1 Effect of initial soil mass

The first stage of the static compaction test (i.e., specimen preparation) involved filling the compaction mould (100 mm in diameter and 19 mm in height) with moist soil (Section 3.5.1). However, the mass of moist soil required to fill the compaction mould can vary (see Table 4.1). One of the challenges in the testing procedure was to verify whether the test is repeatable under different initial soil masses.

Results of static compaction tests of specimens having various initial soil mass, but same compaction water content given in Table (4.1) were compared. The differences in the initial soil mass of the tested specimens at a constant water content were found to vary between 0.8 to 2.3 grams. Typical results of static compaction tests for constant water content specimens with different initial soil mass are presented in Figure (4.11). The tested specimens had a constant water content of 7.5% and a difference in the initial soil mass of about 2 grams. Figure (4.12) shows the effect of different initial soil mass of specimens on the static compaction curves. The difference in the achieved dry unit weights during the static compaction tests under a constant water content of specimens with different initial soil mass was found to be within 0.3 kN/m^3.

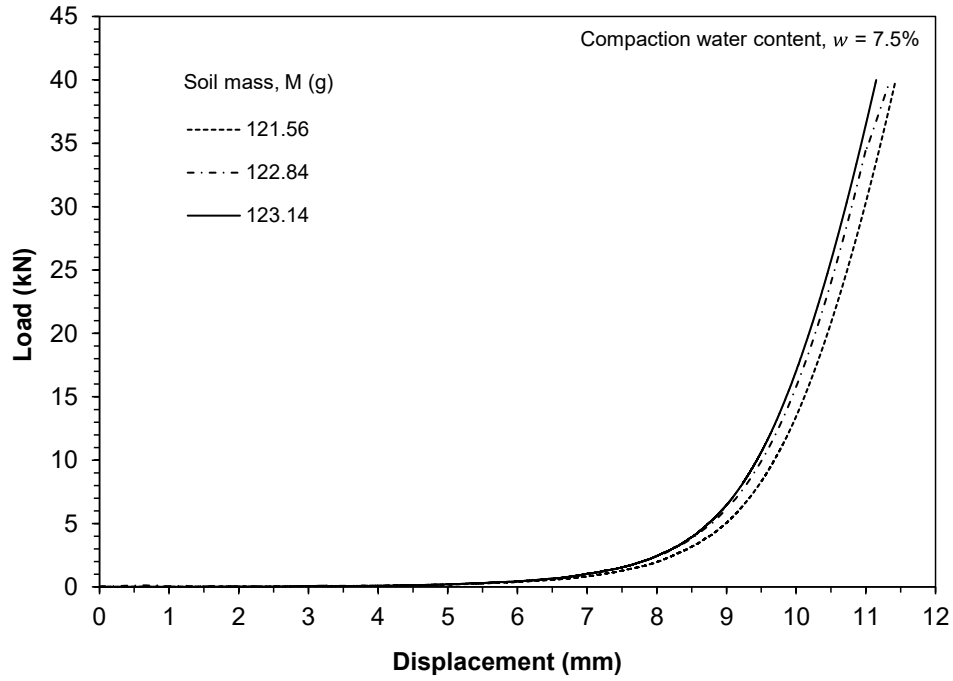

Figure 4.11 Static compaction tests result for specimens having different initial soil mass but constant water content

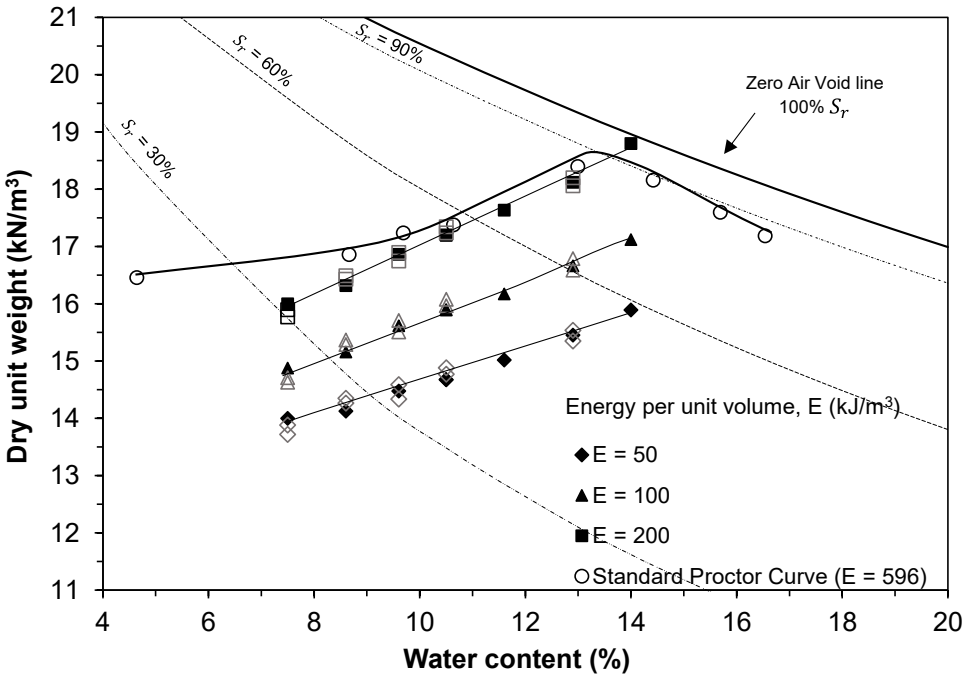

Figure 4.12 Effect of initial soil mass on the static compaction curves

4.3.2.2 Effect of displacement rate during the static compaction tests

Results of static compaction tests at a displacement rate of 0.5 mm/min of five specimens were compared to the original tests result conducted at 1.25 mm/min. Figure (4.13) shows the static compaction curves established by both tests.

By decreasing the compaction speed, a slight difference in the dry density of 0.015 kN/m^3 was observed for low water content specimens. Static compaction curves of the tests conducted at 0.5 mm/min remained below the compaction curves of tests at 1.25 mm/min for specimens with a water content greater than 9%. The dry unit weights were lower by about 0.1 to 0.5 kN/m^3. The reduction in the dry unit weights accompanied by decreasing the compaction speed could be due to the moisture-redistribution within the soil specimen, which may reduce the susceptibility to compaction and prevent particles from slipping over each other freely.

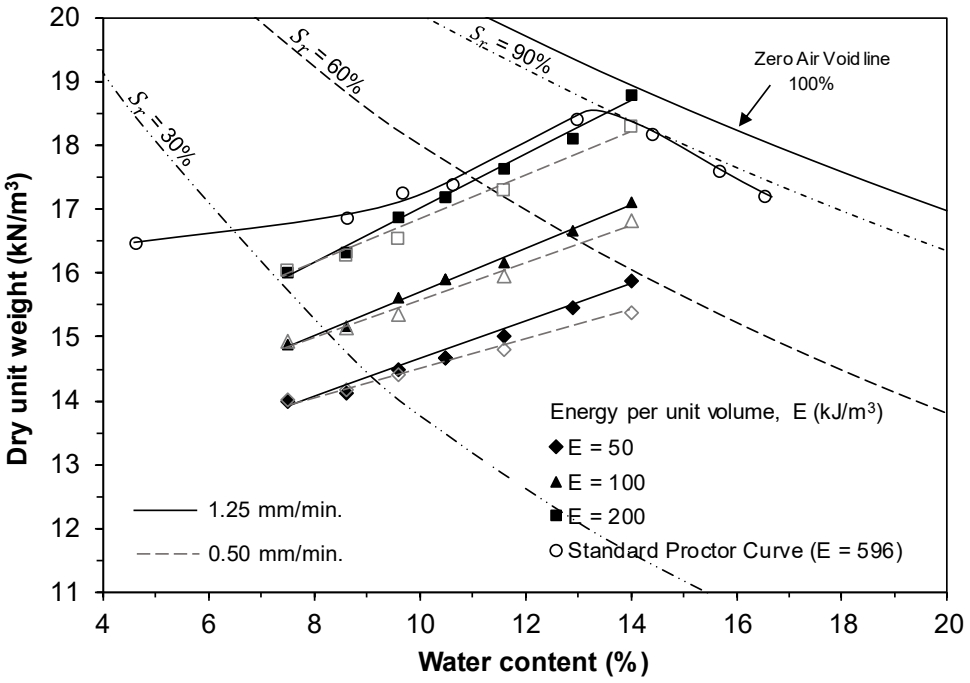

Figure 4.13 Effect of displacement rate on the static compaction curves

4.3.2.3 Effect of mould size

Results of static compaction tests using different compaction mould sizes were compared. In addition to the originally used compaction mould (dia. = 100 mm and height = 19 mm), three moulds of diameter varied from 45 to 105 mm and height ranged from 12 to 115.5 mm were utilised. Figure (4.14) shows the changes in the attained dry unit weights of specimens at a constant water content in response to using different compaction moulds.

Generally, due to reducing the mould size there was a decrease in the dry unit weight of about 0.3 to 0.7 kN/m^3 for specimens at a constant water content. Such that, the smallest specimen (mould 4) yielded the lowest dry unit weights. This observation has been interpreted by the higher boundary friction effects of smaller moulds due to the highest ratio of surface area to volume (Lawton et al. 1989; Venkatarama-Reddy and Jagadish 1993).

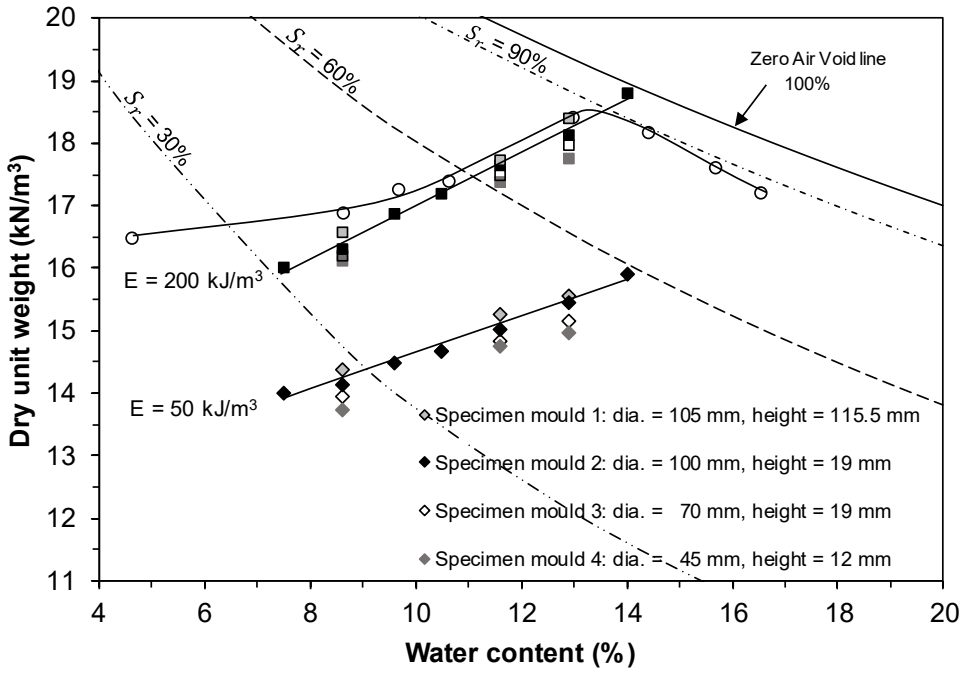

Figure 4.14 Effect of mould size on the static compaction curves

4.3.3 Suction measurements

4.3.3.1 Suction measurements of compacted specimens

The suction of compacted specimens along the static compaction curves was measured using the WP4C dew point potentiameter. The measured suctions were plotted on the plane of compaction curves in terms of pressure and energy as shown in Figures (4.15) and (4.16), respectively. Also presented in Figures (4.15) and (4.16) are contours of equal suction and contours of equal degree of saturation. The suction contours were obtained from a bilinear interpolation of adjacent suction data along a given compaction curve. An example of the calculation is included in Figure (4.15). Using bilinear interpolation, suction was assumed to change linearly both with water content and dry unit weight. Such an assumption for establishing suction contours was also adopted by several researchers (e.g., Tombolato et al. 2005; Tarantino and De Col 2008).

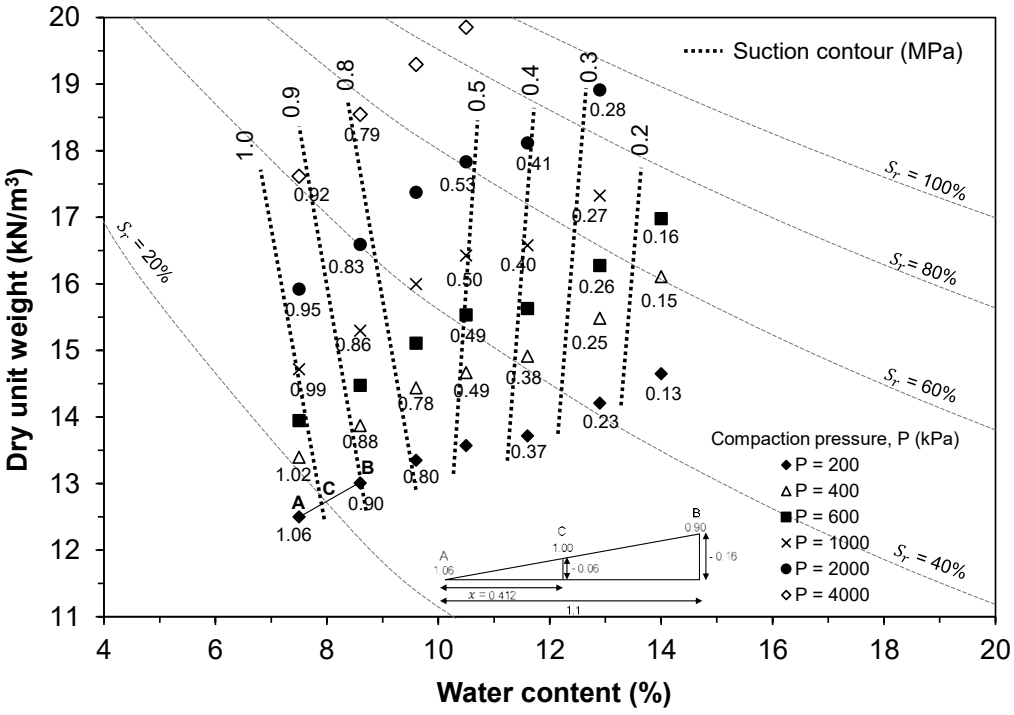

Figure 4.15 Suction contours along static compaction pressure curves

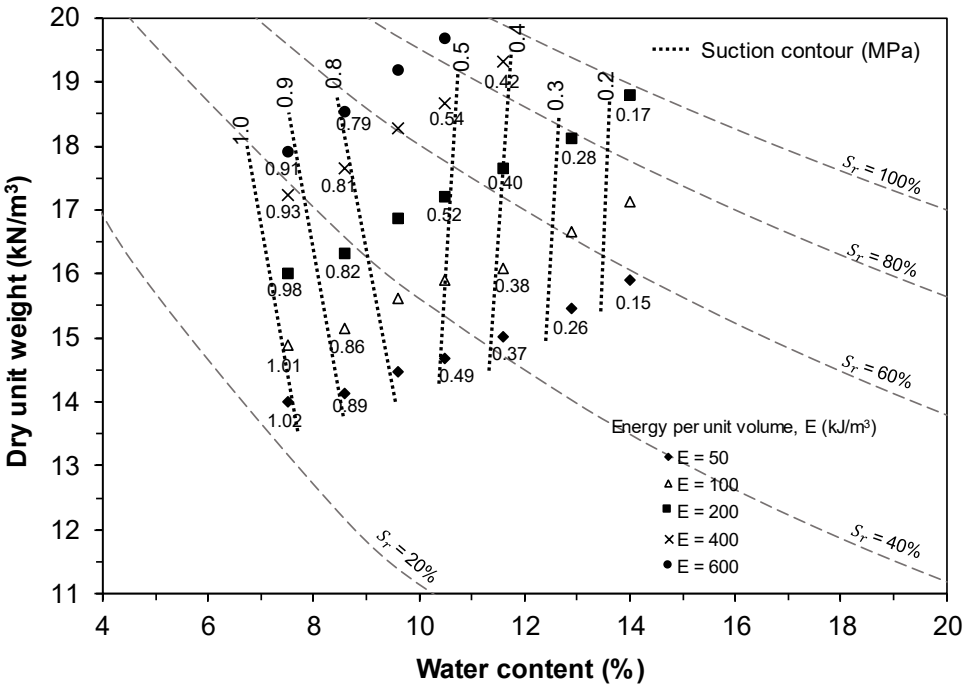

Figure 4.16 Suction contours along static compaction energy curves

The results presented in Figures (4.15) and (4.16) revealed that suction decreased by about 0.1 MPa with increasing dry unit weight from about 14 to 19 kN/m^3 for specimens with water content less than 10%. In contrast, suction increased by an average value of 40 kPa with the same increase in the dry density for specimens at water content greater than 10%. The trend of suction changes for specimens along the compaction plane can be clearly seen by the suction contours, in which two slopes of suction contour were identified. For suction contours of a negative slope, the decreasing in suction values can be explained by the increase in the degree of saturation of soil specimens during the compaction process. The positive slope of the suction contours was interpreted by the dependency of the main wetting retention curve on the void ratio (Tombolato et al. 2005). Soil subjected to compaction at constant water content experiences the main wetting. Subsequent unloading and loading at different stages of compaction would influence the degree of saturation and the wetting path leading suction to increase (see Figure 2.5).

4.3.3.2 Suction measurements of soil-water mixtures

The variation of matric suction with water content of specimens was studied by using a water potential sensor (MPS-6). The specimens were soil-water mixtures with no stress history, which allows assessing the impact of compaction process on suction changes and comparing the results of suction measurements with the chilled mirror potentiameter (WP4C) results.

Figure (4.17) shows the measured suction versus elapsed time plots for the tested soil specimens using the MPS-6 sensor. Suction equalisation was assumed to be reached when a variation of the measured suction remained within about ±2.0 kPa over a period of 6 h (Tripathy et al. 2016). The measured suctions decreased with the elapsed time prior to attaining equilibrium due to the water-exchange with the soil specimens. The results indicated that the suction equilibrium time generally varied between 6 to less than about 24 h for specimens at higher water content, whereas higher equilibrium times were noted for low water contents specimens.

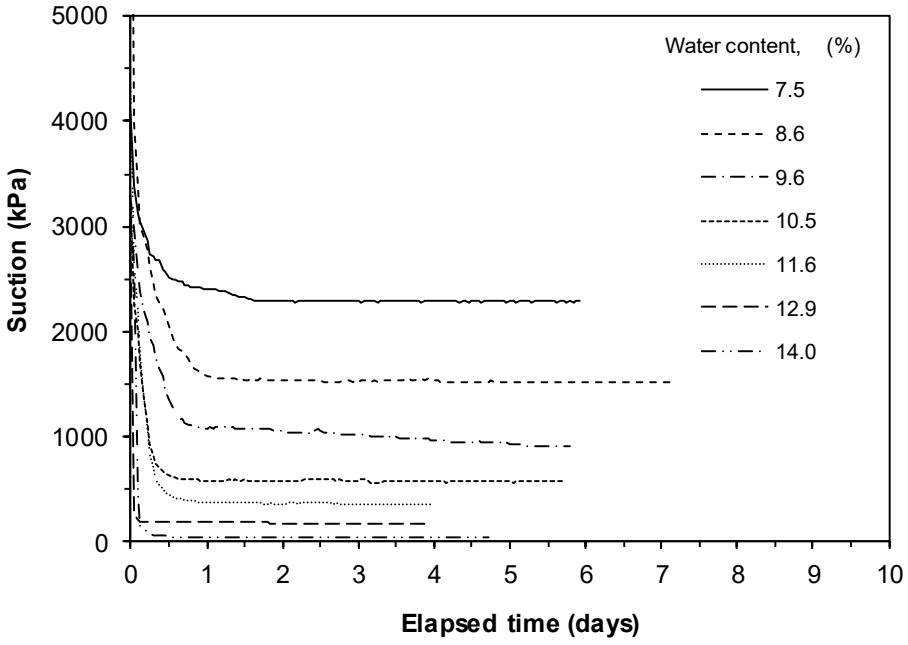

Figure 4.17 Suction equilibration plots of specimens at various water contents

4.3.3.3 Water potential sensor versus chilled mirror potentiameter device

The measured suction at equilibrium of specimens by the MPS-6 water potential sensors (see Figure 4.17) was superimposed on the compaction plane as shown in Figure (4.18). The dry unit weight of the tested specimens was found to remain between 9 and 10 kN/m^3. Noting that the water contents considered in Figure (4.18) are for the soil specimens after the suction measurements were completed. The originally established suction contours of compacted specimens based on results of the chilled mirror device (WP4C) were extended to the suction of specimens having no stress history measured by the MPS-6 sensor.

The results presented in Figure (4.18) emphasised the effect of the compaction process on changing suction of specimens at various water contents. The results also suggested that the measured suction of specimens would have different values if various devices were used.

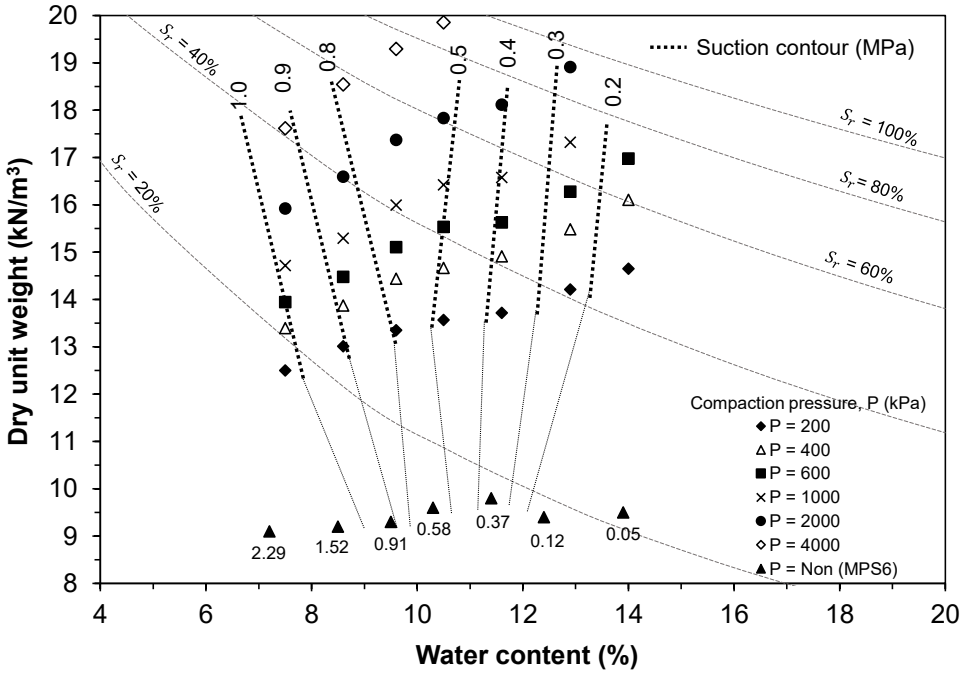

Figure 4.18 Extended suction contours along the compaction pressure curves

Figure (4.19) shows the water content versus suction plots based on the water potential sensor and chilled-mirror potentiameter tests for loose and compacted specimens, respectively. By decreasing the water content of specimens from 7% to 14%, the measured suction by the MPS-6 sensors decreased by about 2.2 MPa and a general decrease in suction of less than 1 MPa when using the WP4C dew point potentiameter.

The matric suction results from the water potential sensor remained above that of the total suction measured by the chilled-mirror dew-point device for the specimens with water content less than 9.5%. The values of suction recorded by the two methods were in agreement for the specimens at water contents between 9.5 and 11.6%. Whilst, at water content greater than 11.6%, suctions of loose specimens remained below that of the measured suctions of compacted specimens. The differences in the suction results from two devices are due to the effects of the initial condition of specimens (loose and compacted), the measured suction component (matric and total) and lacking hydraulic contact when using the sensor. Considerations of the accuracies of the both measuring devices suggest that the chilled-mirror dew-point device measures low suctions with an accuracy of ± 50 kPa.

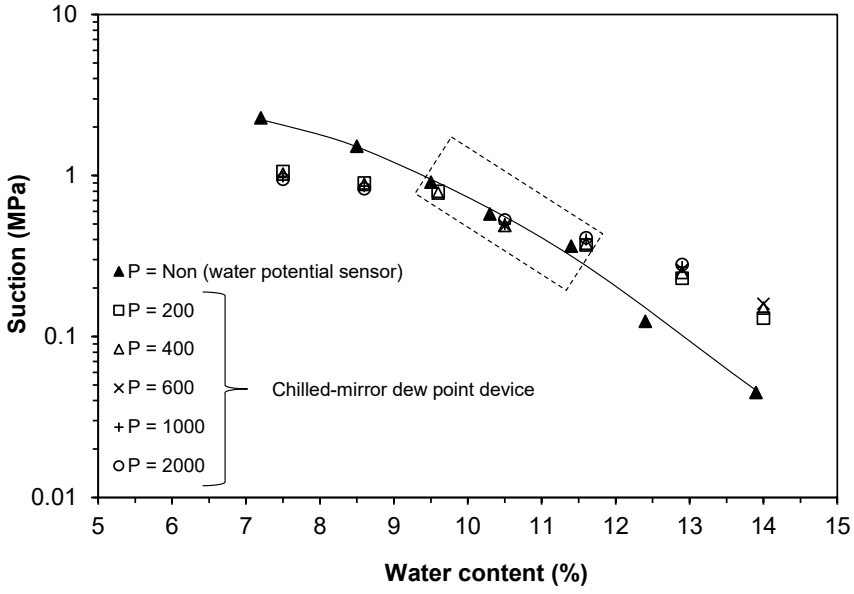

Figure 4.19 Variation of suction with water contents of loose and compacted specimens

4.4 Concluding remarks

This chapter presented the static compaction tests result. The influences of initial soil mass, displacement rate and compaction mould size were investigated. Contours of equal suction along the compaction curves were also established. The main findings from this chapter can be summarised as follows:

1. Static compaction curves both in terms of compaction pressure and compaction energy at various levels were successfully established following the detailed proposed procedure of static compaction tests provided in Section (3.5).
2. For a given static compaction energy curve, the compaction pressure was found to decrease linearly with increasing the water content of specimens. Whilst for a given static compaction pressure, the compaction energy was found to increase linearly with increasing the water content of specimens.
3. At given compaction water content, a small difference in the initial mass of specimens (less than 2.5 gram) apparently influenced the attained dry unit weights along the static compaction curves by a difference of about 0.3 kN/m^3.
4. The effect of reducing the displacement rate from 1.25 to 0.5 mm/min on the results of the static compaction tests was insignificant when specimens compacted at low water contents but was found to be more pronounced for specimens with high compaction water contents. This behaviour can be attributed to the moisture-redistribution within the soil specimen at higher water contents, which prevent particles from slipping over each other freely.
5. Considerations of compaction mould size showed that the smallest mould generated static compaction energy curves of less dry unit weights than the equivalent curves using the larger moulds. The results were agreed well with

those reported in the literature (Lawton et al. 1989; Venkatarama-Reddy and Jagadish 1993).

6. The established suction contours based on the results of the chilled-mirror dew point potentiameter were found to have two slopes. Negative slope indicated a decrease in suction with increasing dry unit weights for specimens with water contents less than 10% and positive slope for specimens with higher water contents referred to increasing suction with increasing dry unit weights. Such finding indicates the dependency of suction on the compaction efforts and this could be particularly important when assessing the hydro-mechanical behaviour of the soil.
7. Differences in the measured suction from the water potential sensor and chilled-mirror dew point potentiameter were attributed to the combined effects of the initial condition of specimens and hydraulic contact issue.
8. The findings of this chapter suggested that the proposed static compaction tests were easier and more efficient than the Proctor test. This is because of providing detailed and straight forward steps of the static compaction tests as well as identifying energy losses between the input energy of the Proctor tests and output energy of the static compaction tests.

Chapter 5

Collapse behaviour along the static compaction curves

5.1 Introduction

Upon wetting, unsaturated compacted soils can collapse or swell based on the type of soil, compaction conditions and the level of vertical stress at wetting (Alonso et al. 1987; Houston et al. 2001; Sivakumar et al. 2015). Soils compacted at the dry side of optimum water content and at a low dry density tend to exhibit collapse during wetting (Barden et al. 1973; Pereira and Fredlund 2000). The reported results about wetting-induced collapse behaviour in soils suggested that the initial water content, dry density and vertical stress are the main factors in controlling the amount of collapse potential (Basma and Tuncer 1992; Delage et al. 2005; Sharma and Singhal 2006; Jiang et al. 2012). Most of these studies were focused on a given initial state of a compacted soil by exploring the effect of the initial water content at a constant dry density and/or the effect of the initial dry density at a constant water content under varied compaction effort. Therefore, investigating the collapse behaviour of specimens along the compaction curves subjected to a constant compaction effort is needed. The outcomes of such studies encompass a wide range of compaction conditions and provide a wider perspective on soil collapsibility. Additionally, knowledge of the collapse behaviour along compaction curves is important for choosing the compaction condition to be used in field for construction quality control and foundations design.

The objectives of this chapter are to explore the impacts of applied (*i*) compaction energy and (*ii*) compaction pressure during specimen preparation on wetting-induced collapse behaviour at various applied vertical stresses.

This chapter is divided into several sections which include the experimental programme, presentation and discussion of the results of wetting-induced collapse tests. The main findings are summarised towards the end of the chapter.

5.2 Experimental programme

Under Test series II (Section 3.7), compacted specimens were prepared following the procedure specified in Section (3.7.1). Single and double oedometer tests were conducted on the prepared compacted specimens as detailed in Section (3.7.2). A few tests were repeated at least twice. The selection criteria of the initial conditions of the specimens were divided into two categories:

1. The specimens follow a constant compaction energy per unit volume curve (E, kJ/m^3) to better define the initial conditions, to enable a reasonable comparison of the collapse behaviour.
2. The specimens follow a constant compaction pressure curve (P, kPa) to explore the difference in the collapse response compared to specimens that were prepared by applying the constant compaction energy.

The pre-established static compaction energy curve of 50 kJ/m^3 and compaction pressure curve of 200 kPa (in Chapter 4) were chosen since specimens had low densities and were at the dry side of optimum, therefore were expected to exhibit collapse upon wetting. The initial condition of the specimens is given in Figure (5.1) and Table (5.1).

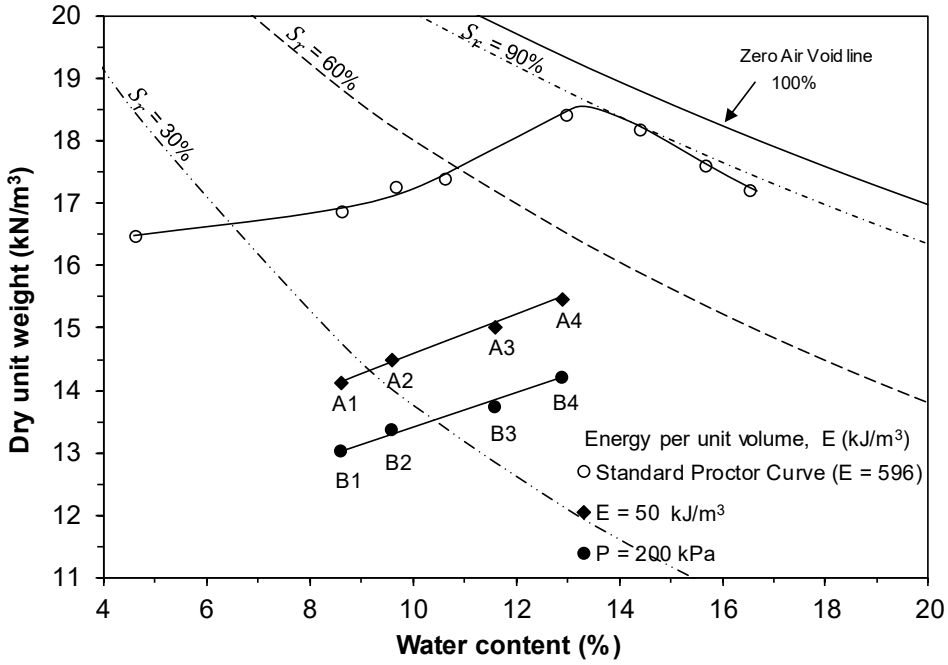

Figure 5.1 Specimens condition along compaction curves

Table 5.1 Compaction condition of specimens for wetting-induced collapse tests

Specimen no.	Compaction water content (%)	Dry unit weight (kN/m^3)	Initial degree of saturation (%)	Compaction pressure (kPa)	Compaction energy per unit volume (kJ/m^3)
Compaction energy per unit volume curve					
A1	8.6	14.12	27.1	450	50
A2	9.6	14.48	32.0	410	50
A3	11.6	15.02	42.1	380	50
A4	12.9	15.45	50.1	365	50
Compaction pressure curve					
B1	8.6	13.01	22.8	200	22
B2	9.6	13.35	26.9	200	23
B3	11.6	13.72	34.3	200	25
B4	12.9	14.21	41.2	200	26

5.3 Results and discussion

5.3.1 Collapse behaviour along the compaction energy curve of 50 kJ/m^3

Four specimens along the static compaction energy per unit volume curve of 50 kJ/m^3 were tested for their potential to collapse. Although the transmitted compaction energy during the specimens preparation was constant, the applied static compaction pressure was different (see Figure 4.9). The pressure applied in the specimens during the compaction process decreased from 450 to 365 kPa when increasing the water content of specimens at the constant compaction energy (see Table 5.1).

5.3.1.1 Single and double oedometer tests

Figures 5.2 (a-d) show the changes in the void ratio of specimens along the compaction energy of 50 kJ/m^3 subjected to wetting at various levels of vertical stress during the single oedometer tests. The initial condition highlighted in the relevant figures represents the average initial void ratio and the applied compaction pressure of the multiple specimens at the beginning of the tests.

Figure (5.3) shows the compression curves (i.e., void ratio changes with the applied vertical stress) of unsaturated and saturated specimens during the double oedometer tests. Both results from Figures (5.2) and (5.3) indicated that the yielding point of the unsaturated compression curves was close to the applied compaction pressure during the specimen preparation. Therefore, a greater reduction in the void ratio was observed when the specimen was subjected to higher vertical stress than the compaction pressure.

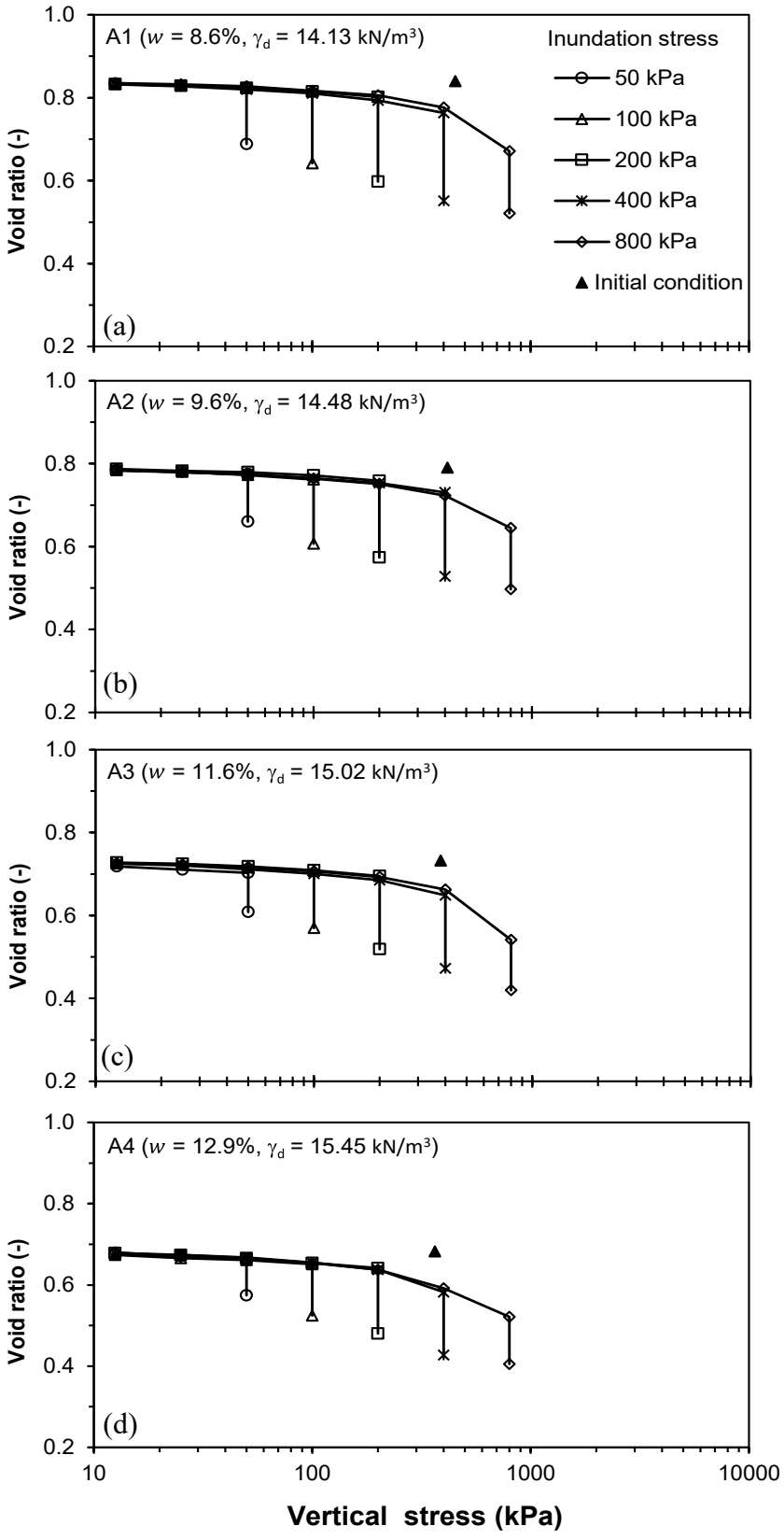

Figure 5.2 Results of the single oedometer collapse test for specimens along E = 50 kJ/m^3 (a) A1, (b) A2, (c) A3 and (d) A4

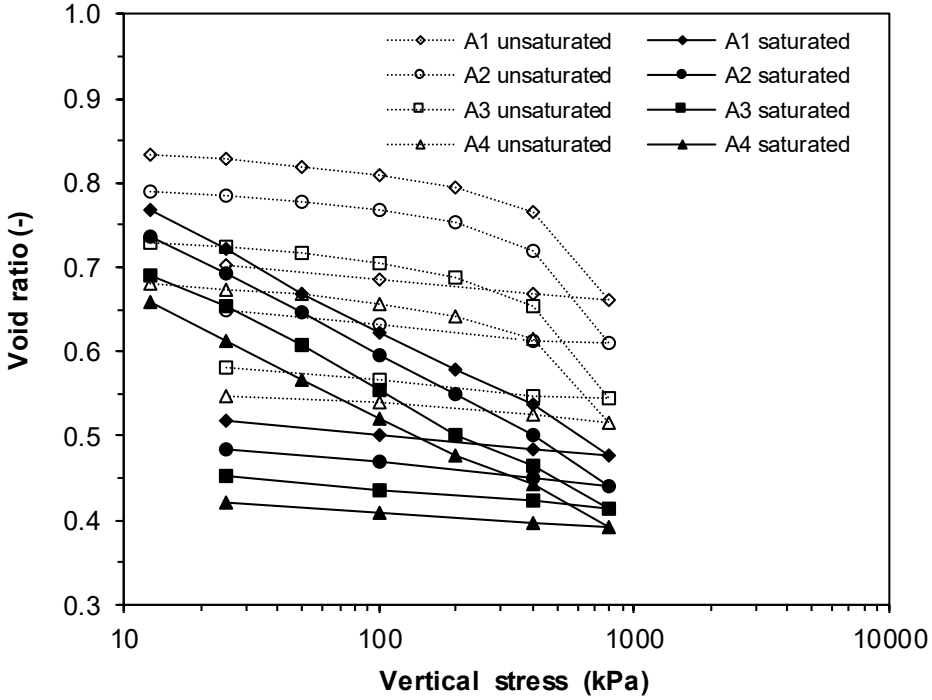

Figure 5.3 Results of the double oedometer tests for specimens along E = 50 kJ/m^3

5.3.1.2 Changes in collapse strain with the applied vertical stress at wetting

The collapse strain under a wide range of vertical stress for each specimen condition along the compaction energy curve of E = 50 kJ/m^3 is shown in Figures 5.4 (a-d) based on the results of the single and double oedometer tests. A comparison of collapse strain obtained from both tests (Figures 5.2 and 5.3) revealed that the mean value of collapse strains obtained by the double per single oedometer tests was 1.08 ± 0.03, which indicates good agreement. It can be seen in Figures 5.4 (a-d) that the amount of collapse strain was stress level dependent. In general, the collapse strain of the tested specimens varied between 1 and 13% when the applied vertical stress ranged from 12.5 to 800 kPa. However, the collapse strain increased approximately linearly with increasing the vertical stress (in a log scale) up to a particular stress level and decreased at vertical stress higher than this value.

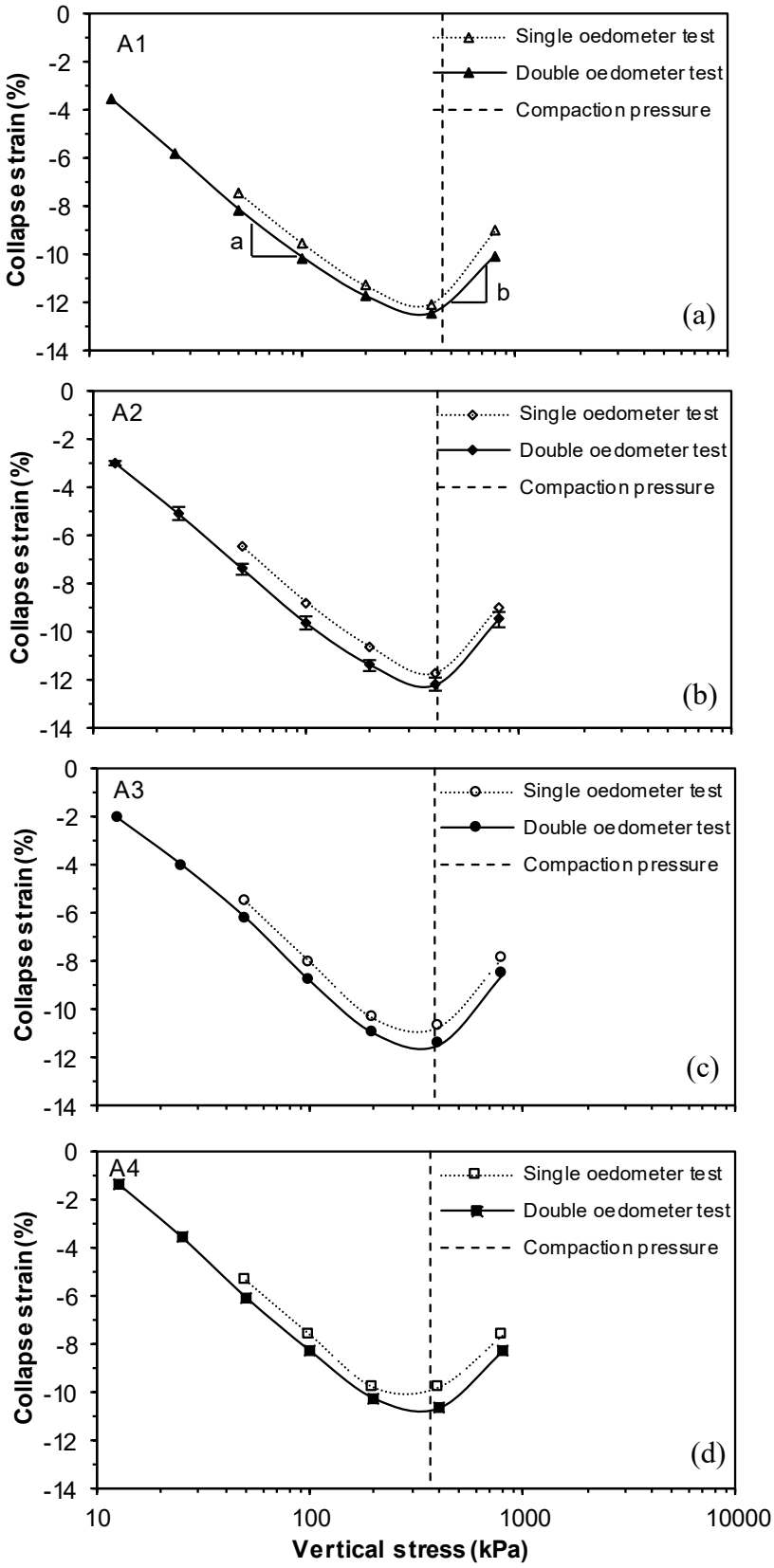

Figure 5.4 Collapse strain as affected by the vertical stress for specimens along E = 50 kJ/m^3 (a) A1, (b) A2, (c) A3 and (d) A4

5.3.1.3 Maximum collapse strain and the applied compaction pressure

The stress level at which the collapse behaviour changes with the applied vertical stress was noticed to be close to the compaction pressure applied during the static compaction process. For a given specimen condition subjected to increasing vertical stress (in log scale), when the applied stress was less than the compaction pressure the collapse strain increased broadly linearly by a general slope of 3.1 denoted as (a). Whilst when the applied stress was exceeded the compaction pressure the slope of collapse reduction line was about 3.8 indicated as (b) (Figure 5.4a).

For the tested specimens along the compaction curve of 50 kJ/m^3, the maximum collapse strain varied between 10 and 13%. The vertical stress leading to the maximum collapse was found to be equal to the applied compaction pressure (Figures 5.4a-d). The occurrence of the maximum collapse strain at a vertical stress equal to the compaction pressure applied for a given specimen condition is attributable to the dry density, and degree of saturation at wetting. At vertical stress levels lower than the induced compaction pressure, insignificant volume change had taken place and the dry density and degree of saturation are almost similar. Therefore, the wetting-induced collapse increased with increasing the vertical stress. However, for vertical stress level greater than the compaction pressure, reduction in the collapse strain is caused by the densification and increasing degree of saturation of the soil specimen. These observations agreed well with the general knowledge of collapse strain increases with increasing the vertical stress up to a certain level of stress and decreases thereafter (Sharma and Singhal 2006; Muñoz-Castelblanco et al. 2011; Okonta 2012; Rabbi et al. 2014; Singhal et al. 2015).

5.3.1.4 Changes in collapse strain with the applied static compaction pressure

Figures (5.5a and b) show the exhibited collapse strain at various vertical stresses of all the tested specimens that were prepared by applying a 50 kJ/m^3 compaction energy per unit volume obtained by the single and double oedometer tests, respectively.

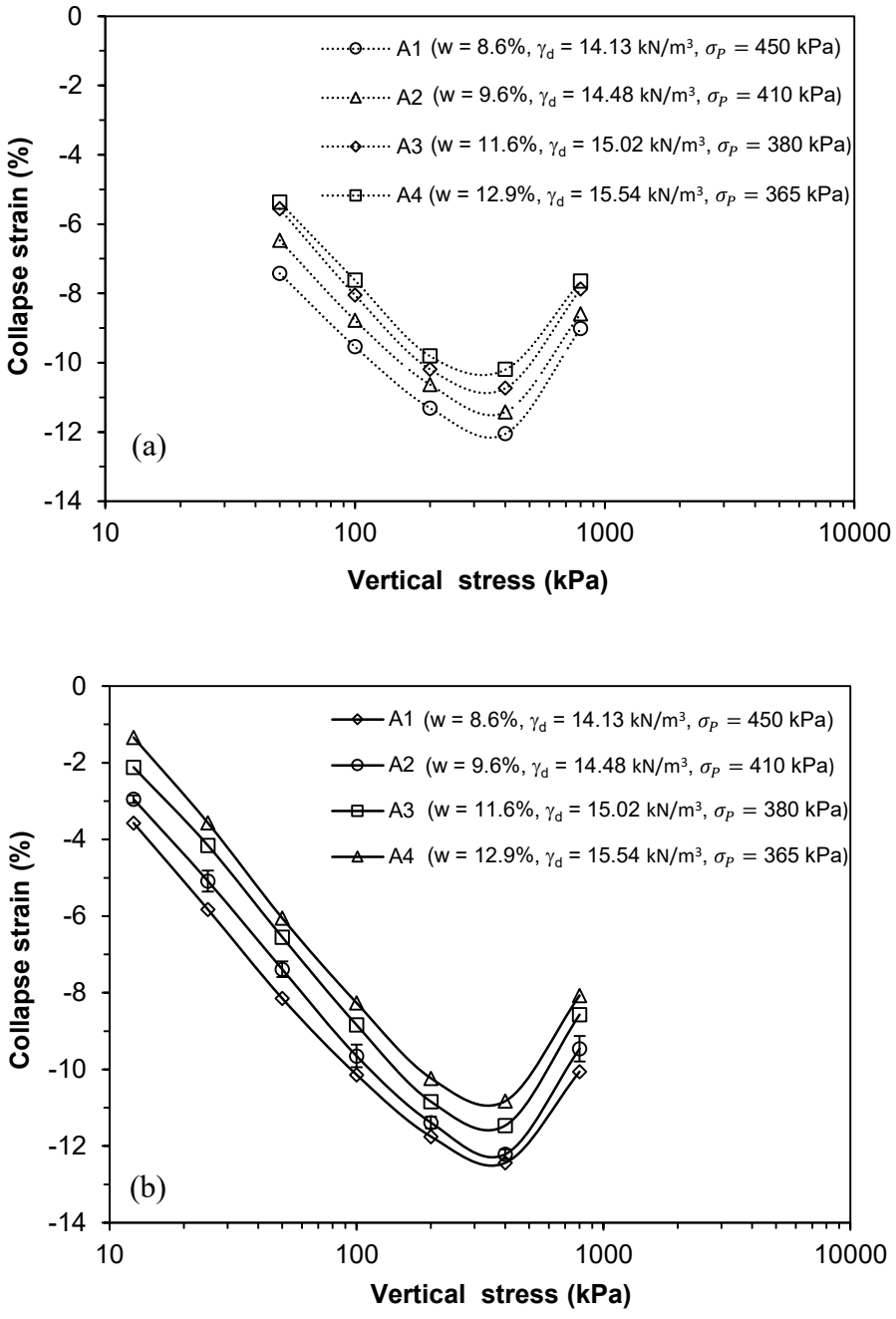

Figure 5.5 Collapse strain variation with vertical stress for specimens along the compaction curve of 50 kJ/m^3: (a) single oedometer tests, (b) double oedometer tests

Since specimens along the compaction energy curve of 50 kJ/m^3 have increasing water content and dry density, the combined effect of these parameters on the collapse behaviour will be discussed based on the applied compaction pressure to transmit constant compaction energy during the specimen preparation.

Results presented in Figures (5.5a and b) are replotted in Figures (5.6a and b) in terms of the variation of collapse strain with the compaction pressure of specimens along the compaction energy of 50 kJ/m^3 at different vertical stresses obtained by the single and double oedometer tests, respectively. Noting that the compaction pressure was plotted in reverse to represent its decrease along the compaction energy curve. The results revealed that the decrease in the applied compaction pressure on the specimens along the compaction energy curve produced a reduction in the collapse strain at all levels of the vertical stress.

For a given applied vertical stress at wetting, the decrease in collapse along the compaction energy curve with reduced compaction pressure appeared to be relatively straight line with a general slope of 0.02. Therefore, applying constant compaction energy but decreasing compaction pressure on specimens with increased water content and dry density lead to reduce their potential to collapse. These results suggested that the collapse depend largely on the compaction pressure applied during specimen preparation. This behaviour is primarily attributed to the pre-defined relationship between the compaction pressure and the vertical stress at the maximum collapse strain. It is therefore expected that a soil specimen with smaller compaction pressure will exhibit a smaller maximum collapse strain.

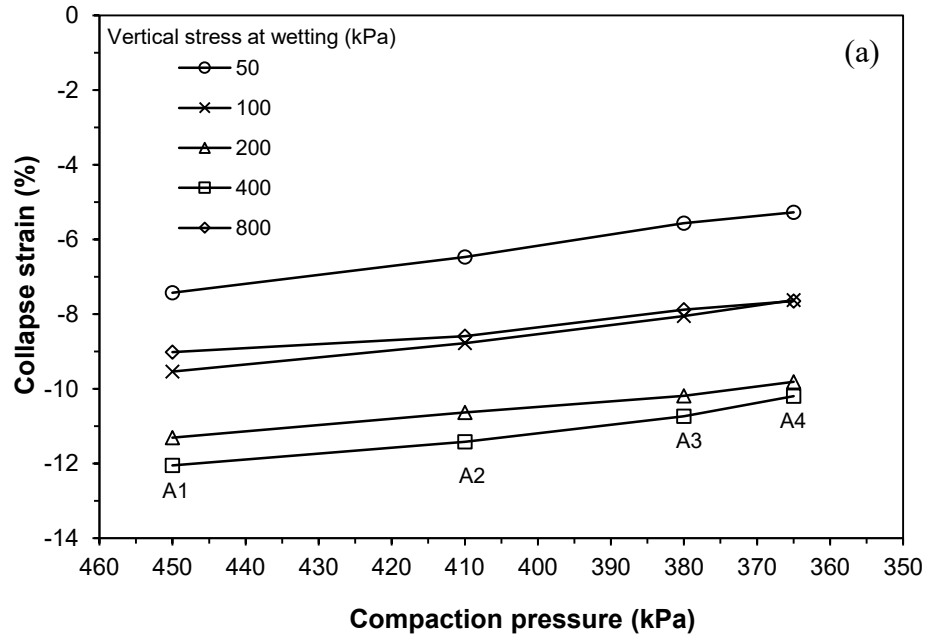

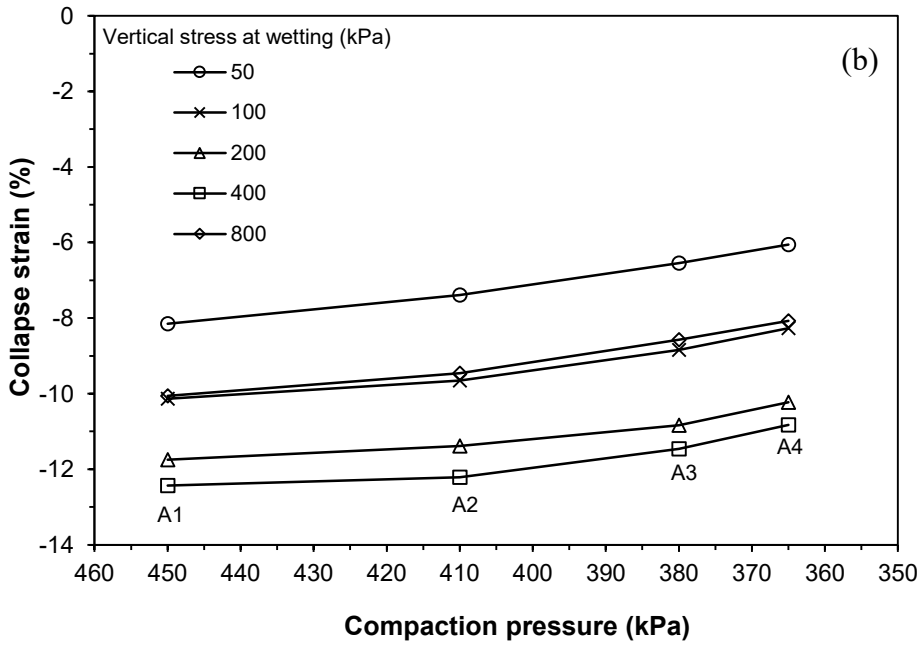

Figure 5.6 Collapse strain changes along the compaction energy curve of 50 kJ/m^3
(a) single oedometer tests, (b) double oedometer tests

5.3.2 Collapse behaviour along the compaction pressure curve of 200 kPa

Four samples along the static compaction curve of 200 kPa were tested for their potential to collapse. Noting that the static compaction of specimens with increasing water content to a given applied pressure resulted in transmitting different compaction energy (see Figure 4.10). The compaction energy increased from 22 to 26 kJ/m^3 for specimens along the 200 kPa compaction pressure curve (see Table 5.1).

5.3.2.1 Single and double oedometer tests

Figures 5.7 (a-d) and (5.8) show the void ratio changes in specimens along the compaction pressure curve of 200 kPa subjected to wetting at various levels of vertical stress during the single and double oedometer tests, respectively. In general, the higher the applied vertical stress the greater was the volume change of specimens. During the inundation, the collapse was taken place for all the specimens tested by conducting the single oedometer. The results of the double oedometer tests presented in Figure (5.8) also indicated a potential to collapse since the compression curves of saturated specimens remained below the corresponding unsaturated ones.

Both results from Figures (5.7) and (5.8) indicated that the unsaturated compacted specimens had a maximum curvature near the compaction pressure applied during preparation. There were insignificant changes in the void ratio (< 0.05) of specimens during the recompression process compared to void ratio reduction of about 0.32 during the virgin compression to 800 kPa. Therefore, the compaction pressure seems to have a similar effect as the pre-consolidation pressure since it represents the maximum pressure that specimens ever subjected to.

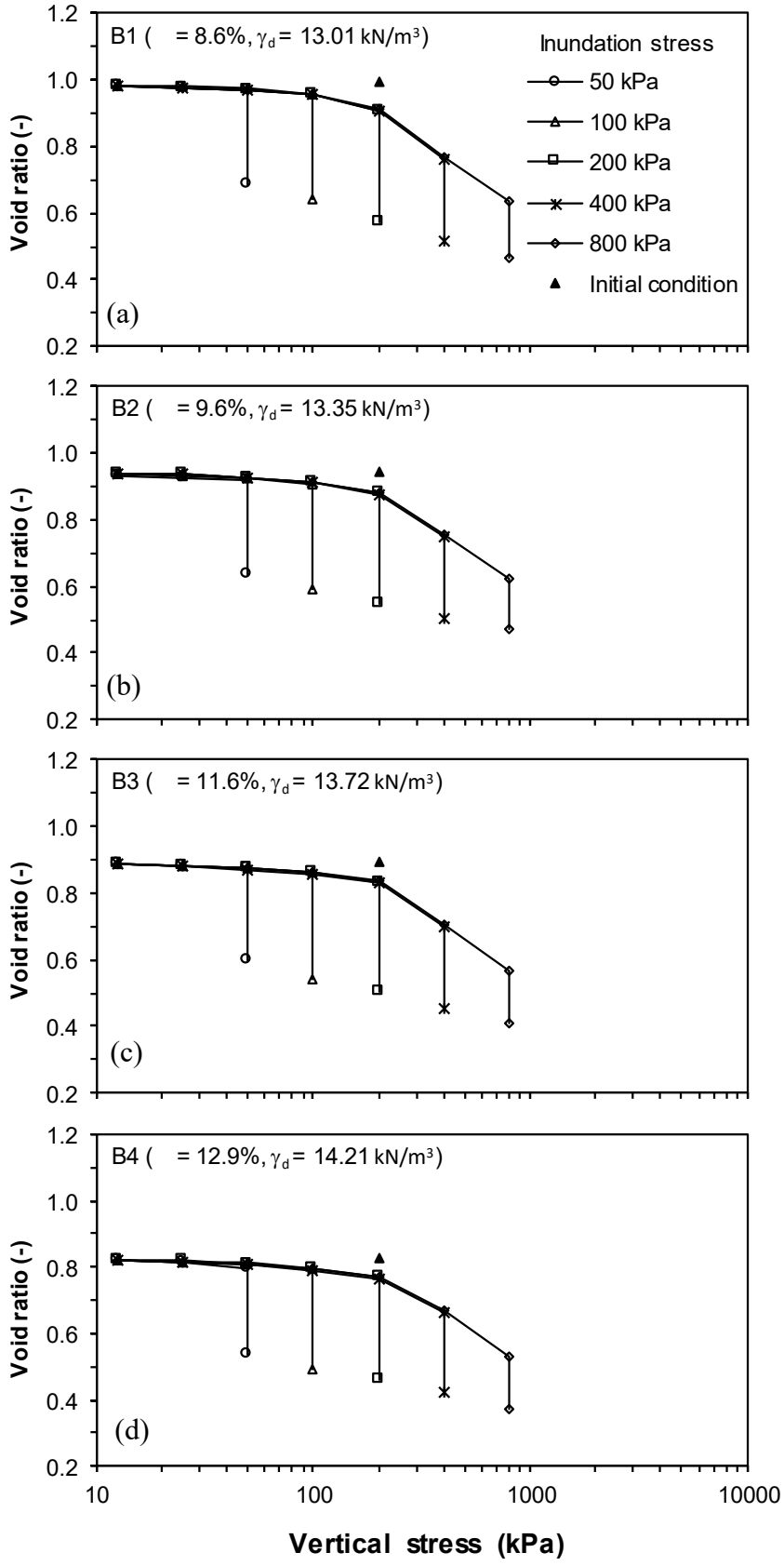

Figure 5.7 Results of the single oedometer tests for specimens along P = 200 kPa (a) B1, (b) B2, (c) B3 and (d) B4

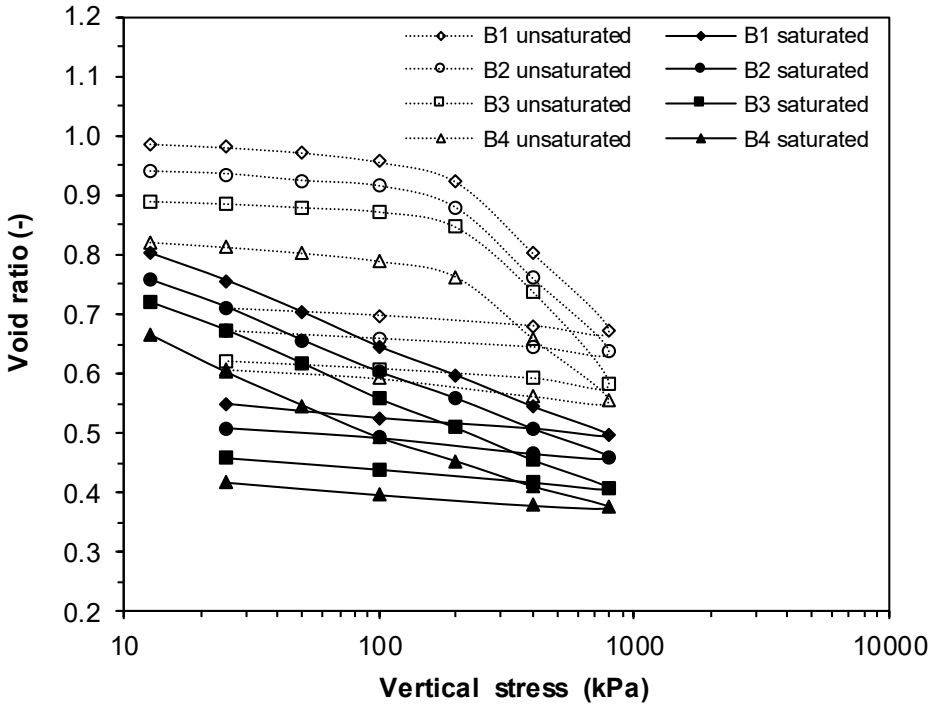

Figure 5.8 Results of the double oedometer tests for specimens along P = 200 kPa

5.3.2.2 Changes in collapse strain with the applied vertical stress at wetting

The exhibited collapse strain for each specimen condition along the compaction pressure curve of 200 kPa is plotted against various vertical stresses (in log scale) in Figures 5.9 (a-d) based on the results of the single and double oedometer tests. The results of both tests provide almost similar magnitudes of collapse strain at any applied vertical stress. This observation further supports the independence of collapse on the loading-wetting sequence (Jennings and Knight 1957; Lawton et al. 1989).

For the range of the applied vertical stress, the collapse strain of the tested specimens varied from 8 to 18% (Figures 5.9a-d). For a given specimen condition, the collapse strain increased approximately linearly with increasing the vertical stress up to a certain stress level and decreased thereafter.

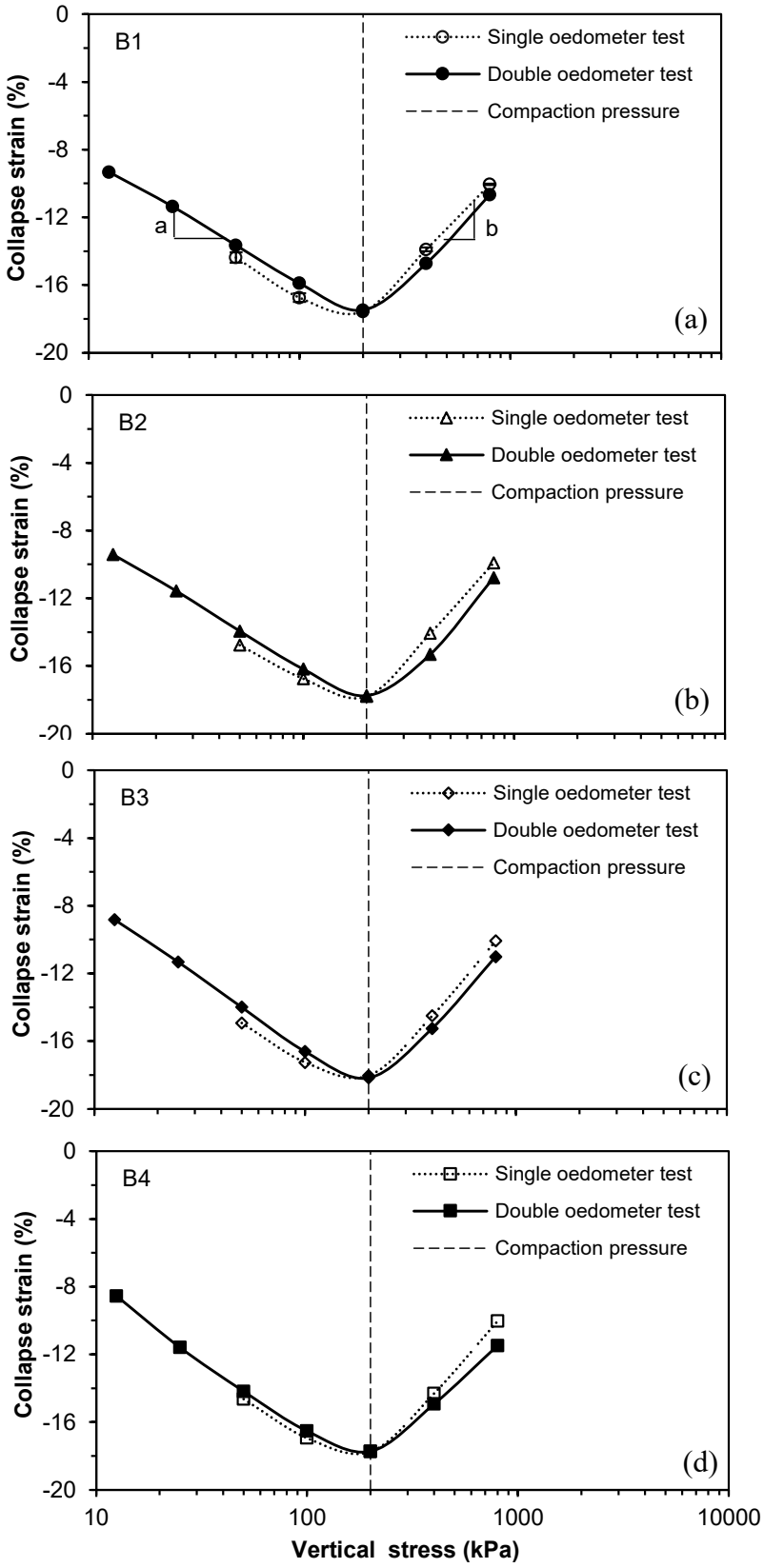

Figure 5.9 Collapse strain as affected by the vertical stress for specimens along P = 200 kPa (a) B1, (b) B2, (c) B3 and (d) B4

5.3.2.3 Maximum collapse strain and the applied compaction pressure

The maximum collapse strain was close to 18% for all the tested specimens under each condition along the compaction curve of 200 kPa. The maximum collapse strain reached when the applied vertical stress at wetting was equal to the applied compaction pressure (Figures 5.9a-d). Prior to the compaction pressure, the average slope line of increasing collapse strain was about 2.7 denoted as (a) with the logarithmic increase in the vertical stress. However, the collapse strain reduced linearly by an average slope of 5.9 denoted as (b) with a further increase in the vertical stress (log scale) beyond the compaction pressure (Figure 5.9a). These results suggested that if a compacted soil subjected to a pressure higher than applied compaction pressure, the potential wetting-induced collapse would minimise. This behaviour is consistent with the typical behaviour reported on the collapse potential of soils (e.g., Sun et al. 2004; Islam and Kodikara 2016).

5.3.2.4 Changes in collapse strain with the applied static compaction energy

Figures (5.10a and b) show the exhibited collapse strain at various vertical stresses of all the tested specimens that were prepared by applying 200 kPa compaction efforts obtained by the single and double oedometer tests, respectively. Since specimens along the compaction pressure curve of 200 kPa have increasing water content and dry density, the collapse behaviour will be discussed based on the transmitted compaction energy to apply a constant compaction pressure. Figures (5.11a and b) show the collapse strain changes with the compaction energy of specimens along the compaction pressure curve of 200 kPa under different vertical stresses obtained by the single and double oedometer tests, respectively. The results revealed that the slight

increase in the applied energy on specimens along the compaction pressure curve had a minor effect on changing the collapse strain within 1% at all levels of vertical stress.

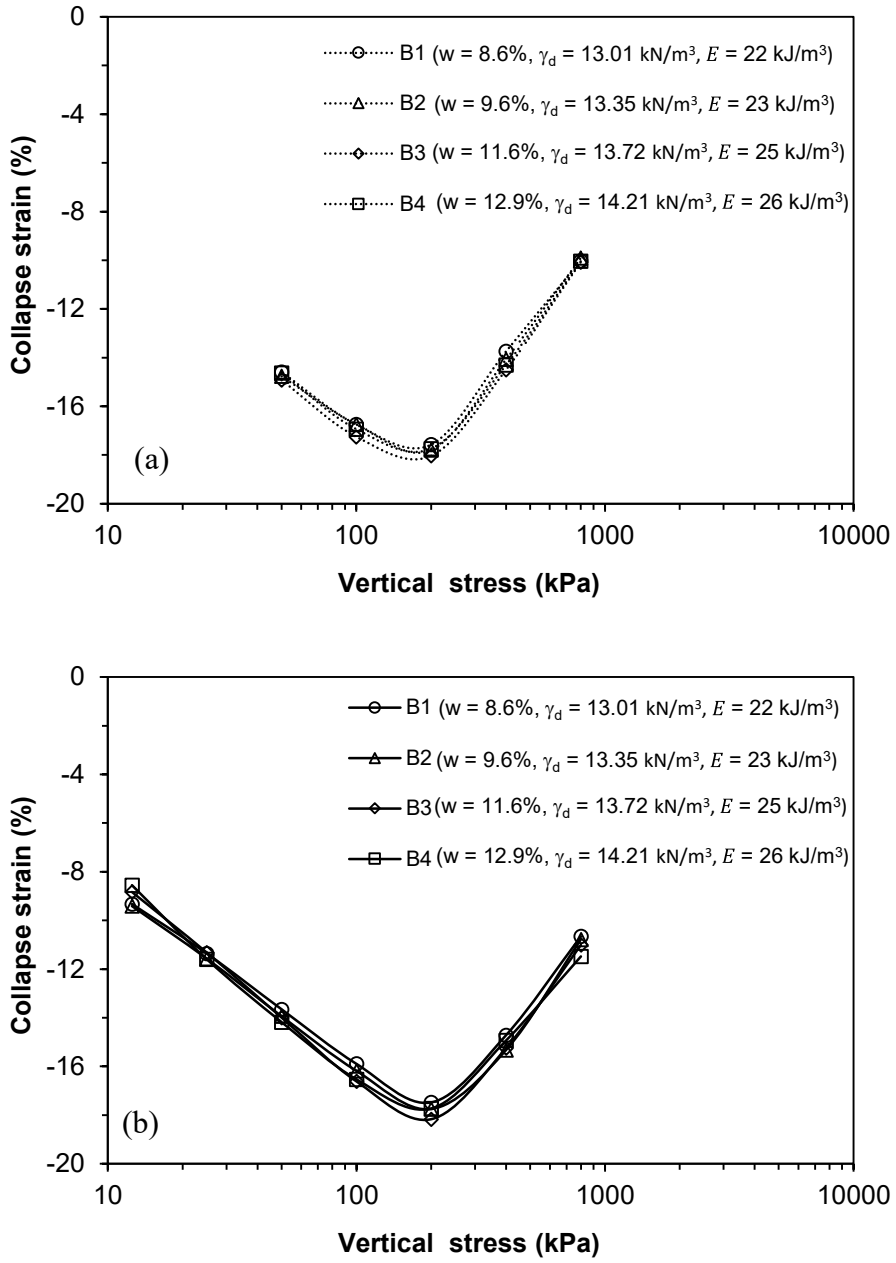

Figure 5.10 Collapse strain variation with vertical stress for specimens along the compaction curve of 50 kJ/m^3: (a) single oedometer tests, (b) double oedometer tests

For a given applied vertical stress, the collapse strain remained almost constant with the increasing compaction energy. This indicates that specimens having increased water content and dry unit weight that were prepared by applying constant compaction

pressure exhibited unchanged collapse strain under the applied stress. This behaviour again could be related to the compaction pressure and vertical stress relationship at the maximum collapse strain. Since the applied compaction pressure on the specimens was the same, their maximum collapse strains were also of the same value. Having recognised that the collapse strain was equal along the compaction pressure curve, the workable and easier compaction condition to be accomplished in the field can be used.

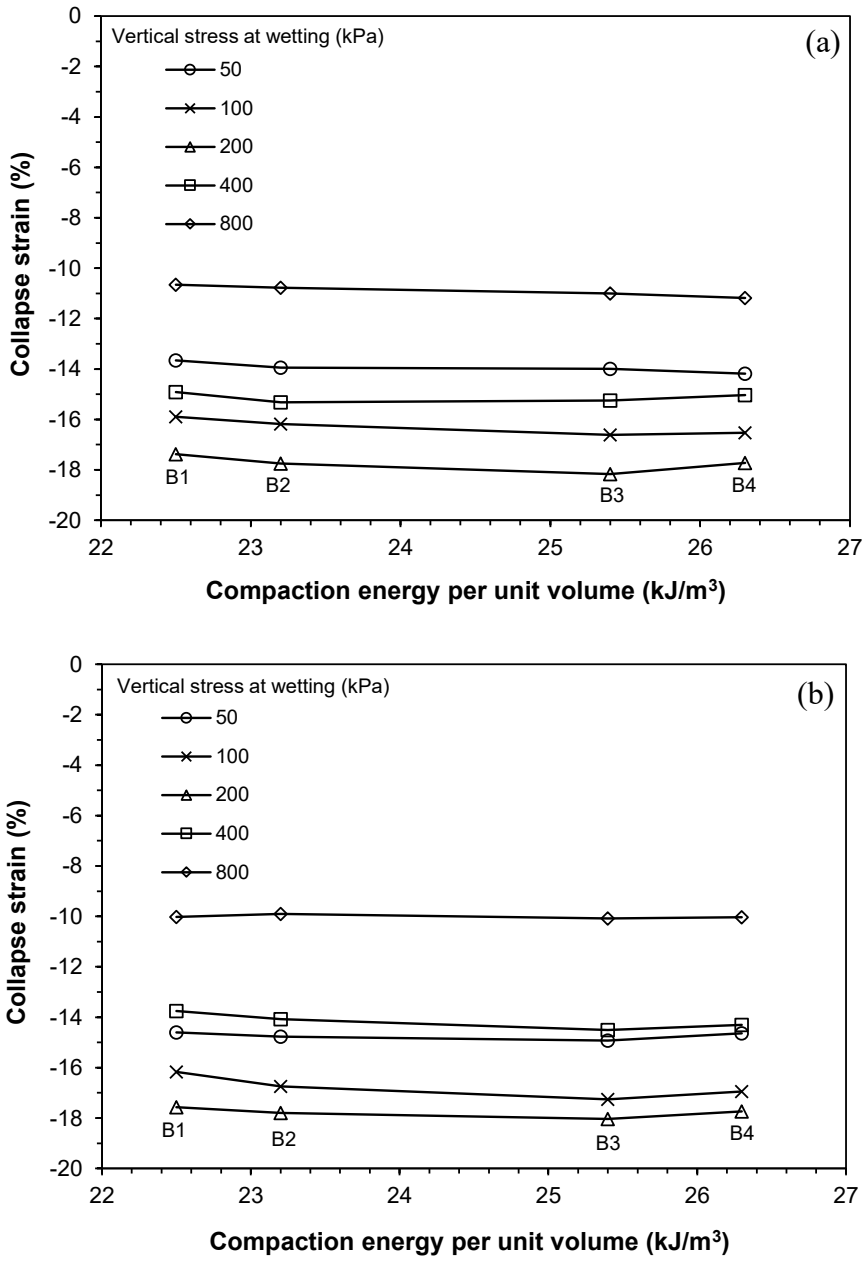

Figure 5.11 Collapse strain along the compaction pressure curve of 200 kPa (a) single oedometer tests, (b) double oedometer tests

5.4 Concluding remarks

One-dimensional wetting-induced collapse tests (i.e., single and double oedometer tests) were conducted on soil specimens along static compaction curves in terms of applied energy and applied pressure. The collapse response of the compacted specimens was investigated under a wide range of vertical stresses at wetting (12.5 to 800 kPa) using a conventional oedometer. The main findings from this chapter can be summarised as follows:

1. The collapse was independent of the loading-wetting sequence, and therefore, the collapse strains obtained from the single and double oedometer tests were found to be similar. The tests results agree well with the findings reported in the literature (Lawton et al. 1992; Leong et al. 2013).
2. Under increasing applied vertical stress at wetting (in log scale), the collapse strain of specimens that were prepared by applying constant compaction energy and constant compaction pressure increased linearly by slopes of 3.1 and 2.7, respectively and then decreased by slope lines of about 3.8 and 5.9, respectively.
3. For the range of the applied vertical stress, the maximum collapse strain of the statically compacted specimens was found to be reached when the applied vertical stress equals to the applied compaction pressure during specimen preparation. The maximum collapse strain varied between 10 and 13% for the tested specimen along the compaction energy curve of 50 kJ/m^3, whereas it remained around 18% for the tested specimen along the compaction pressure curve of 200 kPa.

4. Along the compaction energy curve of 50 kJ/m^3, reducing the applied compaction pressure from 450 to 365 kPa on specimens contributed to a linear reduction in their collapse strain of 0.02 at a given applied vertical stress. This behaviour is primarily attributed to the pre-defined relationship between the compaction pressure and the vertical stress at the maximum collapse strain. It is therefore expected that a soil specimen with smaller compaction pressure will exhibit a smaller maximum collapse strain.
5. Along the compaction pressure curve of 200 kPa, increasing the transmitted compaction energy from 22 to 26 kJ/m^3 on specimens produced constant collapse strain at a given applied vertical stress.
6. Among all other factors, the collapse behaviour of compacted specimens along the static compaction curves was found to be predominantly controlled by the applied compaction pressure during specimen preparation.

Chapter 6

Collapse behaviour due to suction reduction under various wetting tests

6.1 Introduction

The collapse behaviour of unsaturated soils has been extensively studied by conducting wetting tests under suction control (e.g., Pereira and Fredlund 2000; Sun et al. 2004; Jotisankasa et al. 2007; Muñoz-Castelblanco et al. 2011; Haeri et al. 2014; Karami et al. 2015; Liang et al. 2016). The most commonly used technique for controlling suction in these wetting tests is the axis translation technique. Both single and multiple specimens can be tested during the wetting process, however, the compatibility of these test results are not known.

Using single specimen for the entire stepwise wetting offers testing economy both in terms of the number of soil specimen required and testing time. However, the water contents corresponding to the reduced suction are calculated based on the measured volumetric inflow of water and final water contents. Several studies have acknowledged the dissimilarity between the measured and calculated final water contents (e.g., Perez-Garcia et al. 2008). The differences between calculated and measured water content are expected to be due to the challenges of utilizing the axis translation technique, such as air diffusion through the ceramic disk and soil water evaporation through the compressed air line, which are known to influence the obtained data (Bocking and Fredlund 1980; Marinho et al. 2008; Vanapalli et al. 2008).

On the other hand, testing multiple specimens may introduce possible errors on the test results associated with the specimens variability (Khalili and Zargarbashi 2010; Fredlund and Houston 2013). However, such testing procedure allowed for the equilibrium water content corresponding to each applied suction to be measured by using multiple specimens.

Since the work in the thesis deals with studying the impact of suction and net stress on the volumetric behaviour of collapsible soils, it is important to first explore the limitations and advantages of testing single and multiple specimens. Therefore, the objective of this chapter is to study the effect of various testing procedures during suction-controlled oedometer wetting tests on the collapse behaviour both in terms of deformation and water absorption characteristics.

In this chapter, results of the wetting-induced collapse tests under suction control are presented. The experimental programme is recalled in Section (6.2). The effects of various wetting tests using single and multiple specimens on the collapse and water absorption ability are explained in Section (6.3.2). The main findings from this chapter are summarised in Section (6.4).

6.2 Experimental programme

Under Test series III (Section 3.8), a total of 11 practically identical compacted specimens were prepared at a preselected compaction condition (i.e., 12.9% water content, 15.45 kN/m^3 dry unit weight, 365 kPa compaction pressure and 50 kJ/m^3 compaction energy) following the procedure specified in Section (3.7.1). The prepared specimens had an average initial dry unit weight of 15.45 kN/m^3 with a standard deviation of 0.05 kN/m^3 and an average water content of 12.9% with a standard deviation of 0.08%.

The suction-controlled oedometer tests were carried out using the test set up shown in Figure (3.13). The initial suction of the specimens was measured by the null-type axis translation technique as detailed in Section (3.8.3). The tests were performed on the statically compacted specimens as detailed in Section (3.8.4). after measuring the initial suction, all the specimens were incrementally loaded to a 365 kPa vertical net stress, which equals to the applied compaction pressure during specimen preparation. This stress level was chosen because the results presented in Chapter 5 revealed that the maximum collapse can be reached at that level. The testing programme involved reducing the initial suction of specimens at the constant applied vertical net stress (365 kPa) in three wetting tests as explained in the following subsections.

6.2.1 Test 1: Single specimen taken through stepwise wetting

Figure (6.1) shows the stress path followed using a single specimen for the entire test. The initial matric suction of the specimen was measured, and the specimen was incrementally loaded to 365 kPa. During the loading stage, the initially measured matric suction fluctuated within 1 kPa. Under the applied vertical net stress, the measured matric suction reduced to zero by six steps. The specimen was allowed to equilibrate at matric suctions equal to 70, 50, 30, 20, 10 and 0 kPa as summarised in Table (6.1).

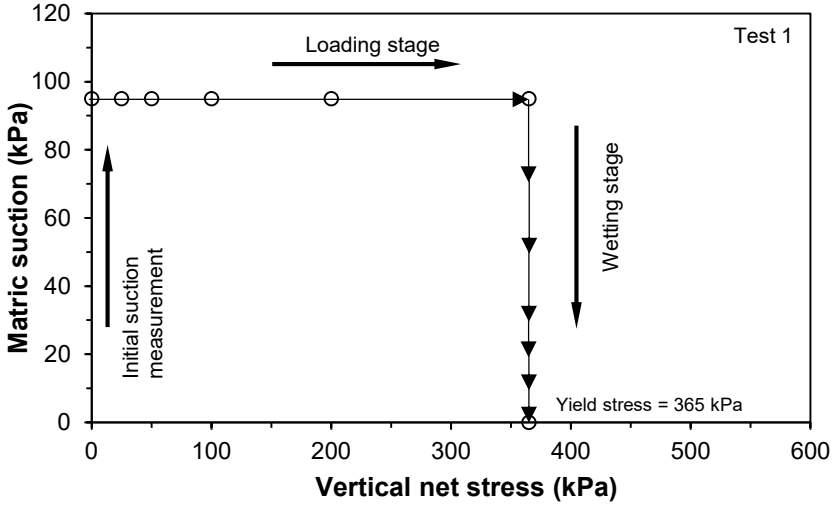

Figure 6.1 Stress paths followed during the wetting test 1

Table 6.1 Applied suctions for the specimen tested under wetting test 1

Specimen no.	Initial measured matric suction (kPa)	Targeted matric suction (kPa)	Suction reduction steps (kPa)
OS*	94.3	0	6 (70, 50, 30, 20, 10, 0)

* OS denotes the one specimen-stepwise wetting.

6.2.2 Test 2: Multiple specimens taken through stepwise wetting

Figure (6.2) shows the stress path followed using multiple specimens. The initial matric suction of the specimens was measured, and the specimens were incrementally loaded to 365 kPa. Under the applied vertical net stress, the initial suction was reduced stepwise. However, five specimens were used, and the tests were terminated at a pre-selected suction value for water content measurements as given in Table (6.2).

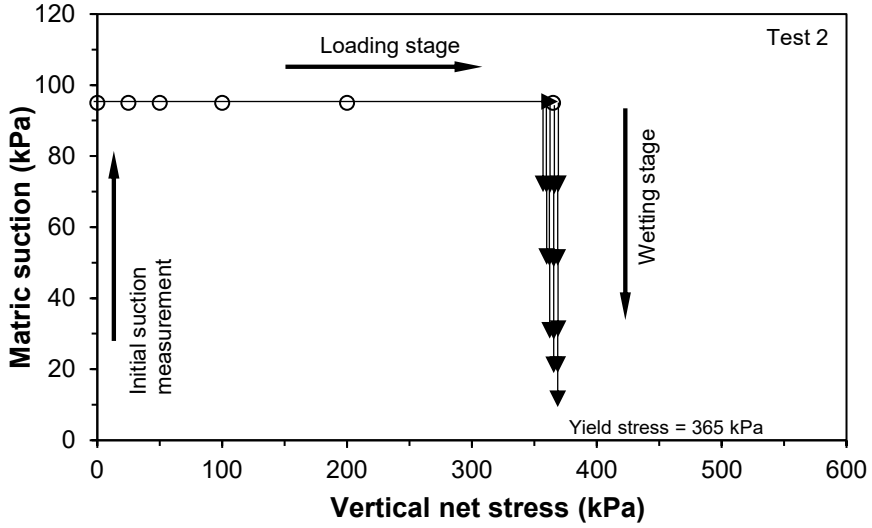

Figure 6.2 Stress paths followed during wetting test 2

Table 6.2 Applied suctions for specimens tested under wetting test 2

Specimen no.	Initial measured matric suction (kPa)	Targeted matric suction (kPa)	Suction reduction steps (kPa)
MS (70)*	93.2	70	1 (70)
MS (50)	95.4	50	2 (70, 50)
MS (30)	96.1	30	3 (70, 50, 30)
MS (20)	93.9	20	4 (70, 50, 30, 20)
MS (10)	95.2	10	5 (70, 50, 30, 20, 10)

* MS denotes the multiple specimens-stepwise wetting and the number between brackets is the targeted final suction value.

6.2.3 Test 3: Multiple specimens taken through one-step wetting

Figure (6.3) shows the stress path followed using multiple specimens. The initial matric suction of the specimens was measured, and the specimens were incrementally loaded to 365 kPa. Unlike test 1 and 2, the initial suction was reduced in one step to a targeted value for water content measurements and to reduce the time needed for testing multiple specimens as summarised in Table (6.3).

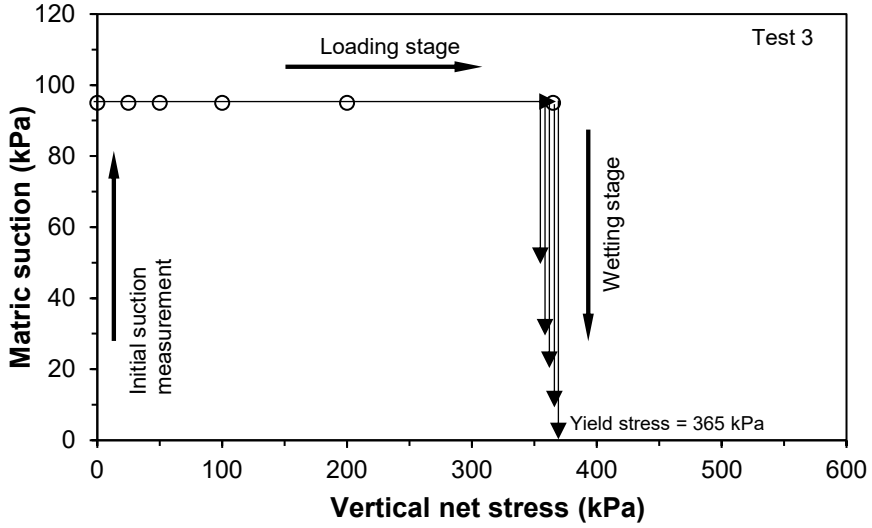

Figure 6.3 Stress paths followed during wetting test 3

Table 6.3 Applied suctions for specimens tested under wetting test 3

Specimen no.*	Initial measured matric suction (kPa)	Targeted matric suction (kPa)	Suction reduction steps (kPa)
MO (50)	96.6	50	1
MO (30)	92.4	30	1
MO (20)	94.4	20	1
MO (10)	95.3	10	1
MO (00)	94.5	00	1

* MO denotes the multiple specimens-one step wetting and the number between brackets is the targeted suction value.

6.3 Results and discussion

6.3.1 Initial suction measurement by null-type tests

Figures 6.4 (a-c) show the elapsed time versus measured suction plots of specimens during the test 1, 2 and 3, respectively. For all the tested specimens, the measured suctions increased with the elapsed time prior to attaining equilibrium. However, the suction equilibrium time of specimens was found to vary between 55 and 110 minutes. Despite the differences in the specimen response in terms of an increase in the air pressure required to maintain a zero-water pressure during the tests, the equilibrium matric suctions for all specimens remained nearly similar. The average measured matric suction at equilibrium of the eleven specimens was found to be 94.7 kPa with a standard deviation of 1.2 kPa. The variation in the suction equilibrium time of the tested specimens could be related to a lack of good contact between the ceramic disk and the specimens with a longer equilibrium time, and discontinued water phase within the soil specimen due to non-uniform distribution of water.

6.3.2 Suction-controlled oedometer wetting tests

Results of the suction-controlled oedometer tests of the three wetting tests are presented in the following sections. In these tests, the deformation and the water volume change (Δ) were all counted from the beginning of the test. A negative deformation refers to a reduction in the specimen volume and a negative Δ means that water inflow into the soil specimen.

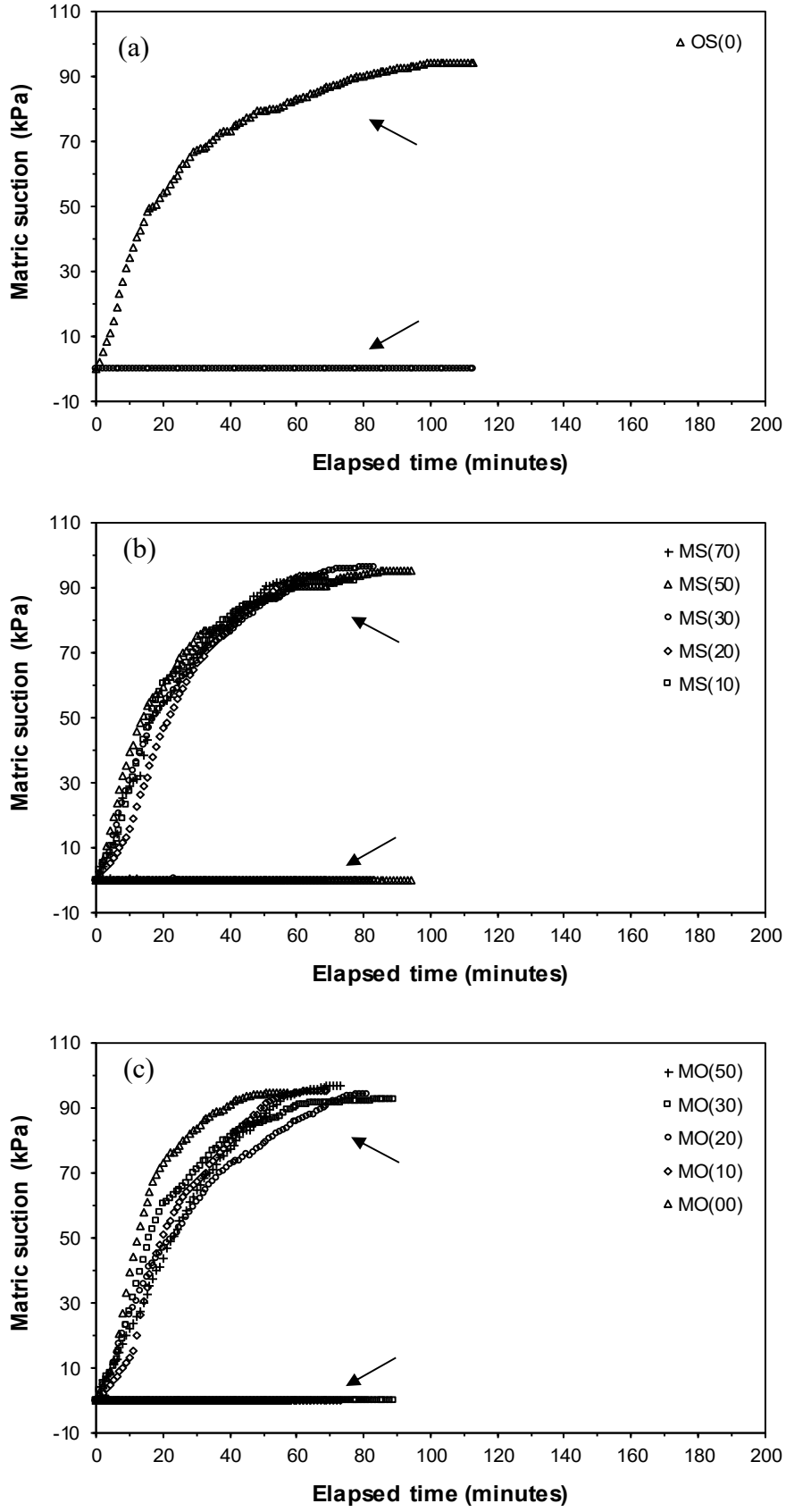

Figure 6.4 Matric suction measurement by the null-type tests of specimens tested under (a) test 1, (b) test 2 and (c) test 3

6.3.2.1 Single specimen taken through stepwise wetting (Test 1)

Figures (6.5a and b) show results of suction-controlled oedometer tests following wetting test 1. During the increment loading to 365 kPa, some water outflow occurred as indicated by positive water volume change (Figure 6.5b). A deformation of 1.07 mm resulted from the loading stage. For applying the six values of successive reduction in matric suction and to achieve water content equilibrium within the specimens, the wetting test 1 was found to last for about 14 days.

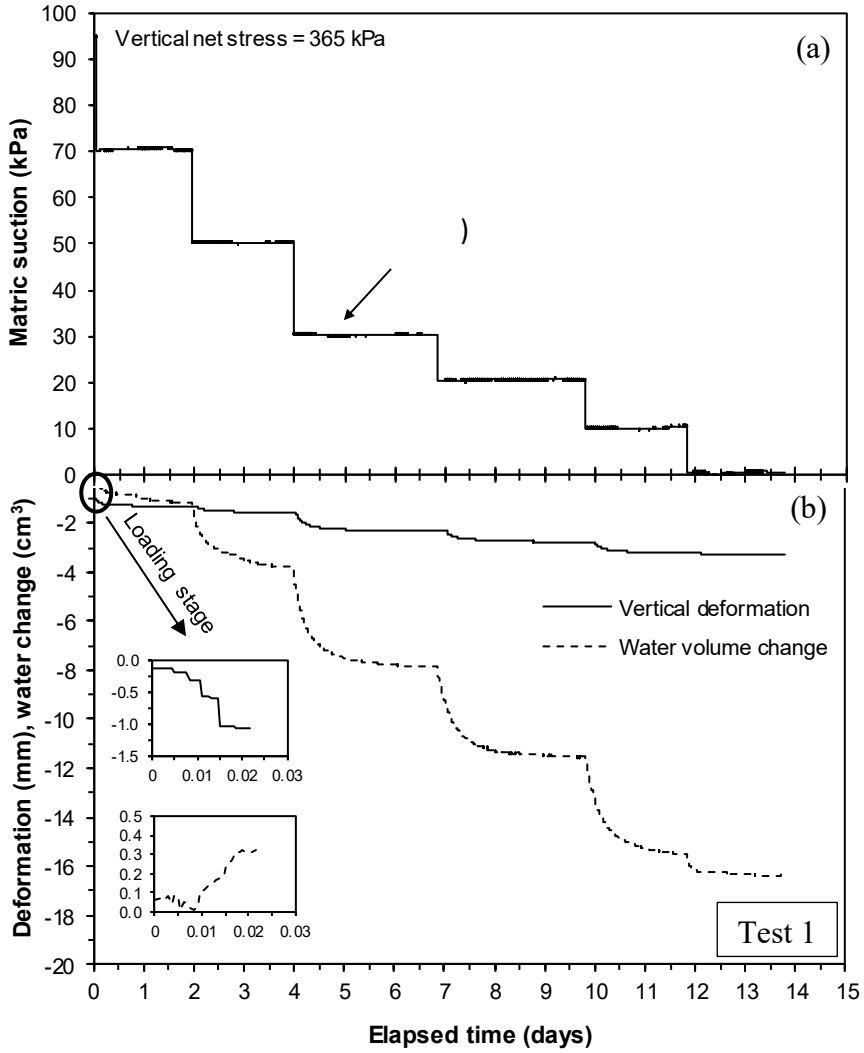

Figure 6.5 Results of suction-controlled oedometer tests conducted on specimen tested under test 1, (a) suction reduction steps and (b) deformation and water volume change

6.3.2.2 Multiple specimens taken through stepwise wetting (Test 2)

Figures (6.6a and b) show the induced suction reduction and the resulted deformation, respectively of the tested specimens under wetting test 2. The measured water content at the end of each test is also presented in Figure (6.6b). A slight variation in the compression characteristics of the multiple specimens was observed during both loading and wetting. The average deformation of the five specimens was about 1.04 ± 0.02 mm caused by applying the vertical stress of 365 kPa and varied within ±0.03 mm at any applied matric suction. A total duration of 32 days was required to test the five specimens and the duration would be 46 days for testing six specimens.

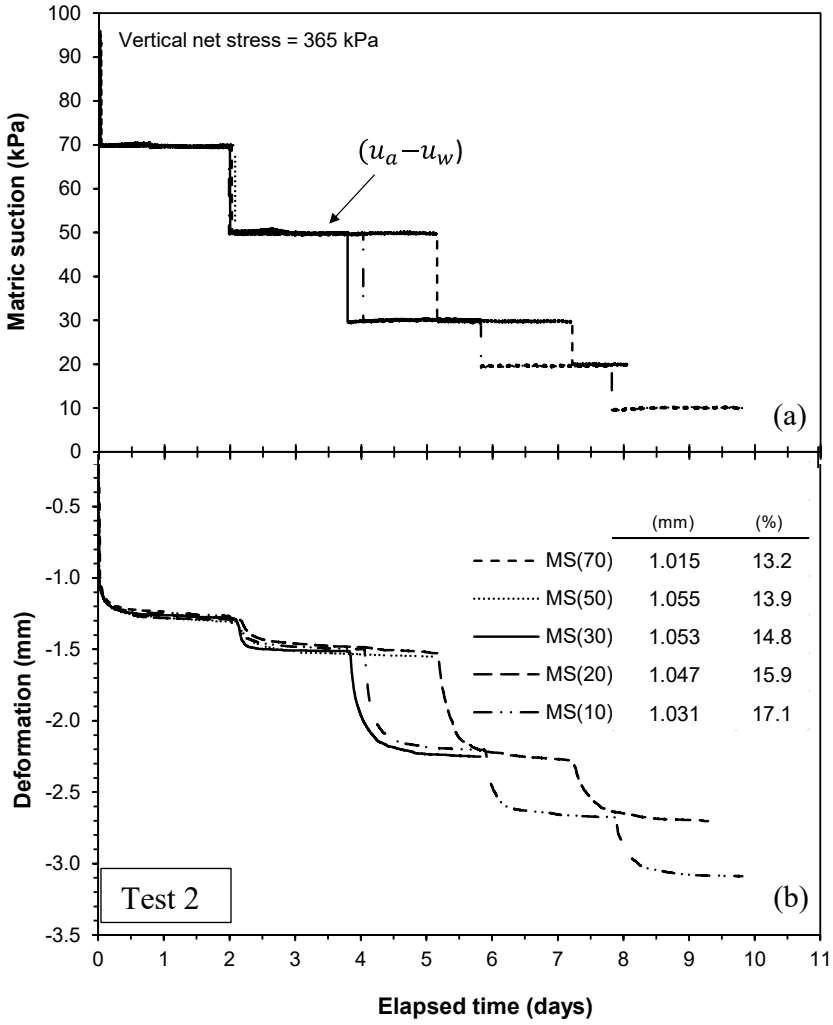

Figure 6.6 Results of suction-controlled oedometer tests conducted on specimens tested under test 2, (a) suction reduction steps and (b) deformation

6.3.2.3 Multiple specimens taken through one step wetting (Test 3)

Figures (6.7a and b) show the imposed suction reduction at a constant vertical stress and the resulted deformation, respectively of the tested specimens under test 3. The measured water content at the end of each test is also presented in Figure (6.7b). During the loading stage, the resulted average deformation of the five specimens was about 1.06 ± 0.06 mm (Figure 6.7b). In total, 16 days was the testing duration to applying the same range of suction as in the other tests.

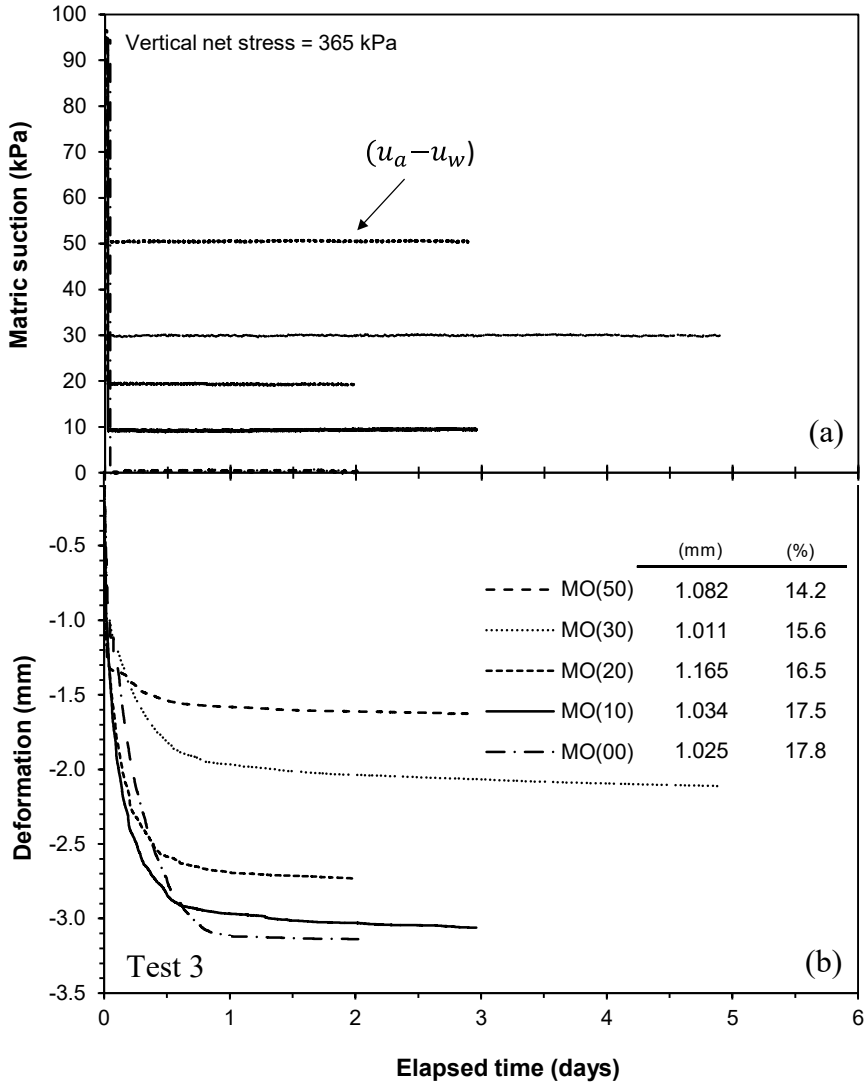

Figure 6.7 Results of suction-controlled oedometer tests conducted of specimens tested under test 3, (a) suction reduction steps and (b) deformation

6.3.3 Effect of testing procedures on collapse behaviour

6.3.3.1 Collapse strain

Figures 6.8 (a-c) show the collapse strain as a function of the applied matric suction for specimens that were tested under wetting tests 1, 2 and 3, respectively. As expected that after the application of a given stress path the magnitude of the exhibited collapse strain was dependent on the applied suction value. As such, the smaller the applied suction the greater the collapse strain.

Figure (6.9) shows a comparison of the collapse behaviour of specimens subjected to three procedures of wetting tests using the suction-controlled oedometer. A fairly good compatibility was observed between the collapse strains obtained from the three wetting tests. The exhibited collapse strain by testing single and multiple specimens were relatively similar at a given applied suction. It was found that the collapse strain obtained from various suction-controlled oedometer wetting tests increased with decreasing suction and reached about 9% at zero-suction. This value of collapse strain agreed well with the collapse strains obtained from the single and double oedometer tests of about 10%.

(a)

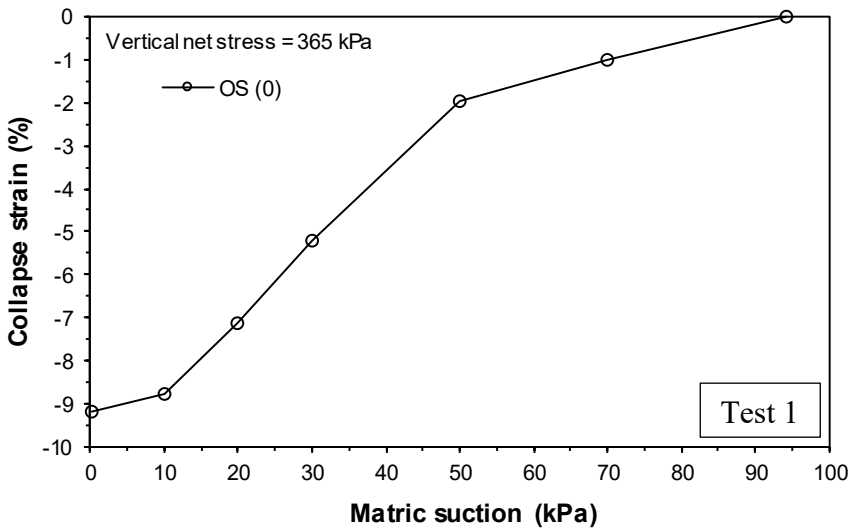

(b)

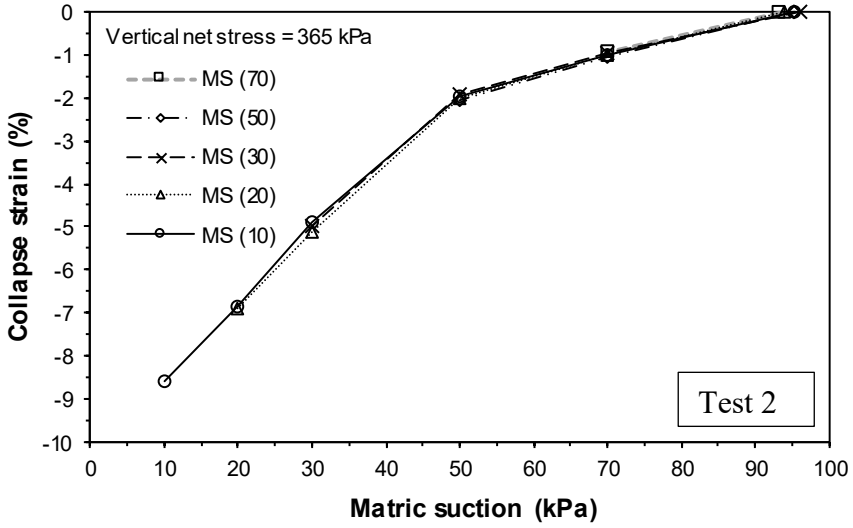

(c)

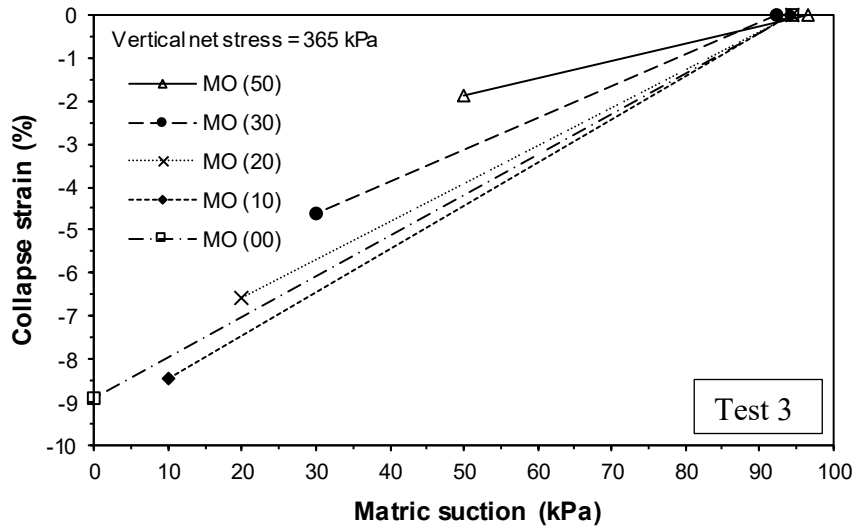

Figure 6.8 Collapse strain as influenced by the suction reduction for specimens tested under (a) test 1, (b) test 2 and (c) test 3

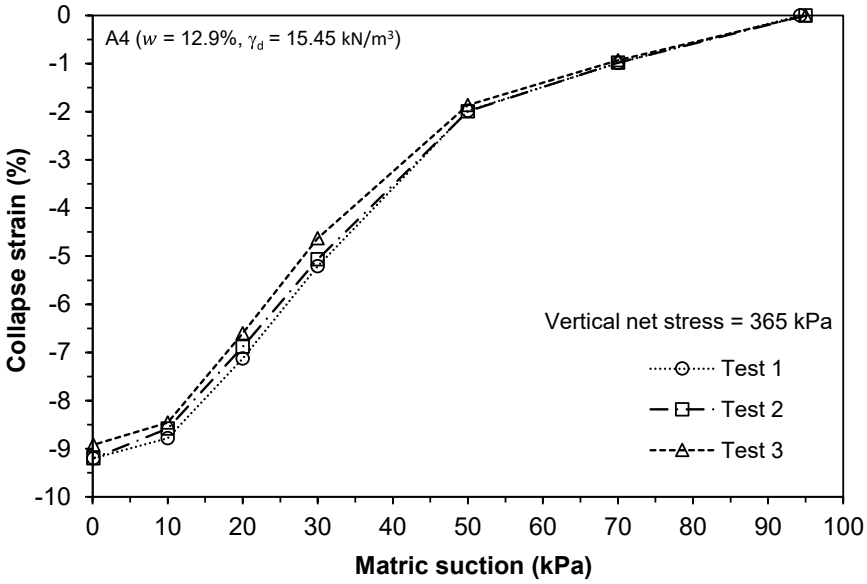

Figure 6.9 Collapse strain obtained from different wetting tests

6.3.3.2 Suction-water content SWCCs

Since a single specimen was used for the entire wetting process in the test 1, the water content at equilibrium under each suction reduction step was calculated. The calculation of the water content of the specimen tested under test 1 can be based on either the initial or final measured water contents along with the measurements of volumetric water inflow.

Figure (6.10) shows the changes in the water content with the decrease in suction during the stepwise wetting test of the tested specimen under test 1. Based on the measured final water content, the back-calculation of the equilibrium water content at each applied suction lead to a smaller water content than the initial measured one by about 0.6%. Similarly, the calculated water contents based on the initial measured water content yielded a higher final value than the measured one at the end of the test (Figure 6.10). Therefore, data adjustment was adopted similar to the one proposed by (Perez-Garcia et al. 2008) to correct the water content values using Equation (6.1).

– (6.1)

where is the correction factor at a specified level of matric suction, is the elapsed time up to equalisation at the specific level of matric suction; is the total equalisation time to run the test for all matric suction levels, and is the difference in water contents that calculated based on volumetric water inflow and directly measured at the end of the test by oven dry method.

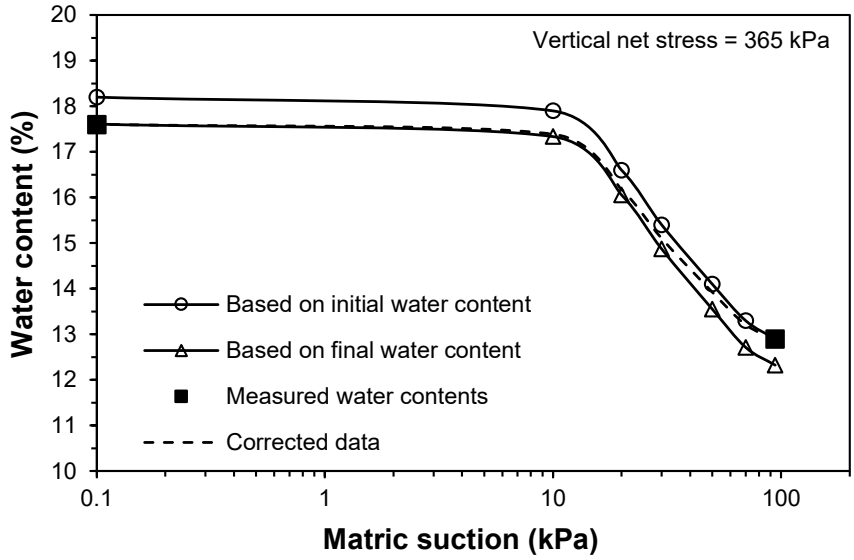

Figure 6.10 Changes in water content with reduced suction of the tested specimen under wetting test 1

Under wetting test 2 and for one test in which the suction reduction was also stepwise on a single specimen, the differences between measured and calculated water content were also noted. Figure (6.11) shows a comparison between the results of the wetting test 2 at a chosen specimen with the results of the wetting test 1. The calculated water contents from both tests were very similar, confirming the repeatability of the stepwise wetting tests. The final measured water contents from both tests were also slightly dissimilar to the calculated ones at a given suction, supporting the possible differences between measured and calculated water contents in the stepwise wetting tests.

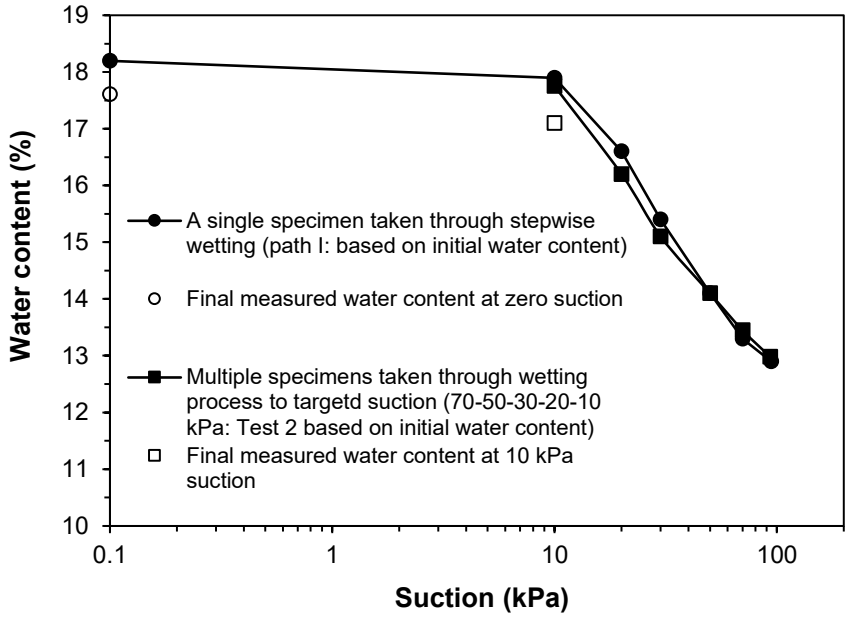

Figure 6.11 Final measured and calculated water contents during stepwise wetting

Under wetting test 2 and 3, however, the water content corresponding to the applied suction was measured by oven drying (Figures 6.6b and 6.7b). Figure (6.12) shows the wetting SWCCs plotted in terms of the water content for the tested specimens under the three wetting tests. It can be seen in Figure (6.12) that the water content of specimens increased from 12.9% to about 17.5% by decreasing the matric suction to a zero-value.

The comparison of the SWCCs obtained from the three suction-controlled oedometer wetting tests (Figure 6.12) showed that the variation in the water contents at a given matric suction was generally less than 0.4%, whereas higher differences were only observed at suction values of 50 and 30 kPa.

It can also be seen in Figure (6.12) that the water content versus suction results of the stepwise wetting test 1 and other tests was fairly similar, suggesting that the adopted correction to the calculated water content in the test 1 provided reliable data.

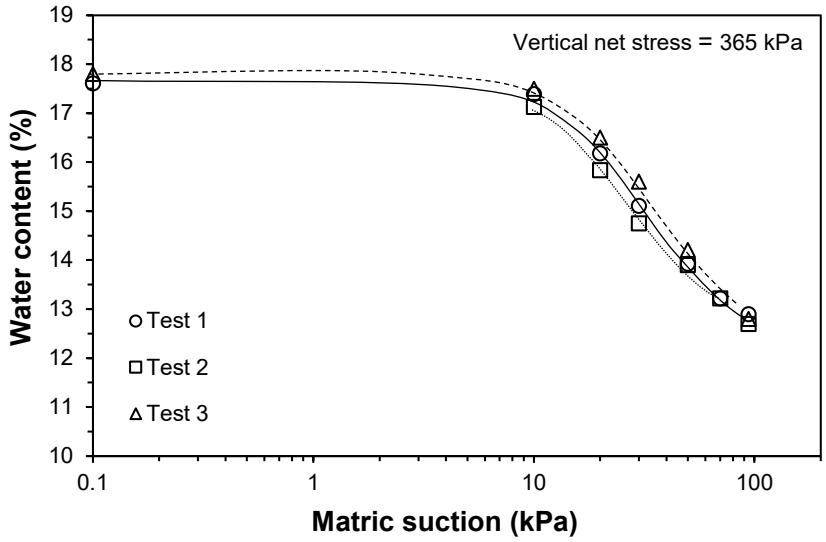

Figure 6.12 Water content SWCCs of specimens at different wetting tests

6.3.3.3 Suction-degree of saturation SWCCs

For deformable soils, it is recommended to interpret the SWCCs based on either degree of saturation or volumetric water content for consideration of soil volume changes (Fredlund and Houston 2013). Therefore, the SWCCs data is plotted in Figure (6.13) in terms of the degree of saturation versus suction for all the three wetting tests. The wetting SWCCs measured by using single and multiple specimens were similar, which revealed the independence of the SWCCs on the adopted wetting tests.

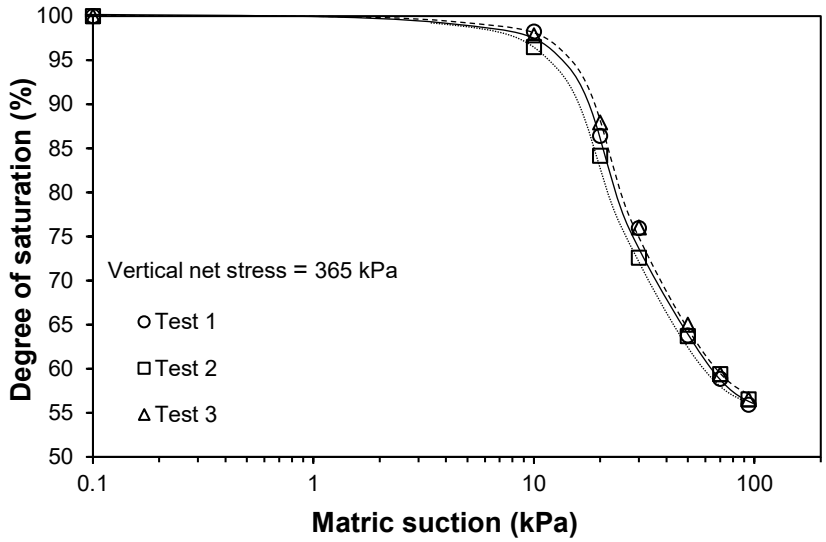

Figure 6.13 Degree of saturation SWCCs of specimens at different wetting tests

6.4 Concluding remarks

In this chapter, wetting-induced collapse tests under suction control were performed on practically identical compacted specimens at a constant vertical net stress of 365 kPa using a suction-controlled oedometer. The tests involved measurements of the initial suction of specimens by the null-type axis translation technique. Three different wetting tests were successfully adopted and the rationale behind each followed test was also highlighted. The results of the three testing procedures were compared. The following main findings can be drawn from this chapter:

1. The initial suction of practically identical specimens measured by the null-type tests was found to be similar (i.e., 94.7 ± 1.2 kPa), but the suction equilibrium time was different (i.e., varied between 55 and 110 minutes). The similarity in the measured suction is due to the dependence of suction on the initial water content of specimens, which is rather constant (i.e., 12.9 ± 0.08%). Whilst the dissimilarity in the measurement equilibrium time is assumed to be due to water phase discontinuity within the soil specimens and between the specimens and the ceramic disk and the measuring system.
2. Comparisons of suction-controlled oedometer tests under different wetting tests showed that the results were compatible both in terms of collapse strain and SWCCs (particularly in the degree of saturation plot). This finding provides flexibility in choosing the preferred and practical testing procedure based on the testing duration and the number of specimens required.

Since different testing procedures provided compatible results, the single specimen taken through the stepwise wetting test (1) was adopted for the remaining tests presented in the subsequent chapter.

Chapter 7

Collapse behaviour along the static compaction curve due to suction reduction

7.1 Introduction

Compacted soils are invariably unsaturated and tend to collapse upon wetting under certain conditions (Lawton et al. 1992; Pereira et al. 2005). These conditions are intrinsically related to stress state variables and the compaction variables. Several laboratory research works have been aimed at understanding the effect of matric suction on the collapse behaviour (Kato and Kawai 2000; Futai and Almeida 2005; Zhou and Sheng 2009; Muñoz-Castelblanco et al. 2011; Garakani et al. 2015). Similarly, various studies have explored the effect of the applied net stress on the subsequent hydro-mechanical behaviour of collapsible soils (Dudley 1970; Wheeler and Sivakumar 1995; Pereira and Fredlund 2000; Sun et al. 2007; Vilar and Rodrigues 2011; Haeri et al. 2016; Liang et al. 2016).

Contradictory results, however, have been reported about the variation of collapse potential with the applied net stress and uniqueness of the wetting SWCCs under different applied net stresses. In addition, very limited works considered the effect of initial compaction conditions on collapse behaviour during controlled-suction wetting tests because of the technical difficulties and time-consuming nature of such tests (Sun et al. 2007). Collapsible soils in practice span a wide range of compaction conditions and it may be rare to find study investigated the collapse behaviour along the

compaction curve. Not only such studies will link the deformation and hydraulic characteristics of collapsible soils to the compaction state, but also it can be used to establish and validate constitutive models. Therefore, the objective of this chapter is to provide comprehensive study about the effects of all these factors (i.e., matric suction, net stress and compaction conditions) on the volume change and water retention behaviour of collapsible soils.

7.2 Experimental programme

Under test series IV (Section 3.8), statically compacted samples were prepared at preselected compaction conditions following the procedure specified in Section (3.7.1). The initial conditions of the soil samples were chosen to be along the compaction energy curve of 50 kJ/m^3 (see Figure 5.1). These sample conditions at a low compaction energy (low dry density) are more susceptible to collapse upon wetting (Barden et al. 1973; Pereira and Fredlund 2000). The testing programme was divided into four groups of tests. Each group represents a sample condition laid on the compaction energy curve and for each condition, three specimens were tested. The suction-controlled oedometer wetting tests were carried out using the test set up shown in Figure (3.13). The tests were performed on the compacted specimens as explained in Section (3.8.5). The stress path applied in each test involved measuring the initial suction of the specimen by the null-type axis translation technique immediately after preparation (Section 3.8.3), then incrementally loading the specimen to a pre-selected stress level and taken it through the stepwise wetting test 1 (see Section 6.2.1) as summarised in Table (7.1). An example of the loading-wetting path followed is sketched in Figure (7.1).

Table 7.1 Applied state of stress of all the tested specimens

Specimen no.	Vertical net stress (kPa)	Initial measured matric suction (kPa)	Suction reduction steps (kPa)
group A1 (= 8.6 %, 14.12 kN/m^3, 450 kPa)			
A1L	200	281.3	7 (250, 150, 100, 50, 25, 10, 0)
A1E	450	274.4	7 (250, 150, 100, 50, 25, 10, 0)
A1G	600	277.6	7 (250, 150, 100, 50, 25, 10, 0)
group A2 (= 9.6 %, 14.48 kN/m^3, 410 kPa)			
A2L	200	233.6	7 (200, 150, 100, 50, 25, 10, 0)
A2E	410	231.3	7 (200, 150, 100, 50, 25, 10, 0)
A2G	600	234.9	7 (200, 150, 100, 50, 25, 10, 0)
group A3 (= 11.6 %, 15.02 kN/m^3, 380 kPa)			
A3L	200	147.6	5 (100, 50, 25, 10, 0)
A3E	380	153.5	5 (100, 50, 25, 10, 0)
A3G	600	149.8	5 (100, 50, 25, 10, 0)
group A4 (= 12.9 %, 15.45 kN/m^3, 365 kPa)			
A4L	200	97.1	7 (70, 50, 30, 20, 10, 5, 0)
A4E	365	94.3	6 (70, 50, 30, 20, 10, 0)
A4G	600	95.0	6 (70, 50, 30, 20, 10, 0)

* The letters L, E and G refer to specimens subjected to load less than, equal to and greater than the applied compaction pressure during specimen preparation ( ).

During the loading stage, the three specimens at each compaction condition were incrementally loaded to different applied net stresses. The applied vertical net stress was varied between 200 and 600 kPa. These values were less than, equal to and greater than the applied compaction pressure during the specimen preparation to cover a wide range of collapse responses.

During the wetting stage, the measured suction of the specimens was reduced in a stepwise manner up to saturation in seven steps for most tests. However, fewer steps were considered in some tests due to anticipated problems for such prolonged tests and owing to essential electrical power and gas line maintenance in the university buildings.

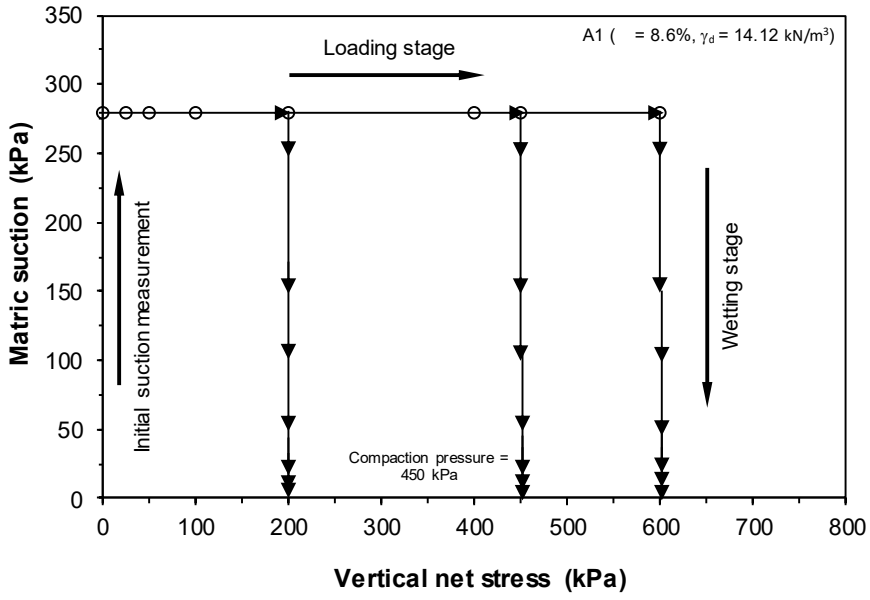

Figure 7.1 Stress path followed for specimens in series A1

7.3 Results and discussion

7.3.1 Initial matric suction by the null-type tests

Figures 7.2 (a-d) show the elapsed time versus measured suction plots of specimens in groups A1, A2, A3 and A4, respectively using the suction-controlled oedometer. For all the tested specimens, the suction was measured immediately after specimen preparation and before applying the vertical stress. The measured suctions of the compacted specimens increased with the elapsed time prior to attaining equilibrium. The average suction equilibrium time for lower water content specimens in groups A1 and A2 were found to be 155 and 125 minutes respectively, whereas lower equilibrium time of about 90 minutes was noted for specimens with higher water contents in groups A3 and A4.

The average measured matric suction by the null-type axis translation technique of the three identical specimens in groups A1, A2, A3 and A4 were found to be 277.8, 233.3, 150.9 and 95.5 kPa, respectively. As expected, the drier the specimen the higher the suction level and the longer the equilibrium time.

7.3.2 Suction-controlled oedometer tests

Figures 7.3 (a-c) to 7.6 (a-c) show the results of suction-controlled oedometer wetting tests of specimens tested in groups A1, A2, A3 and A4, respectively. During the tests, the pore water pressure was observed to fluctuate within about ± 1 kPa. A total duration of about 40 to 50 days was required for testing three specimens in each group. The results were analysed in terms of collapse strain and soil-water absorption ability as discussed in the subsequent sections.

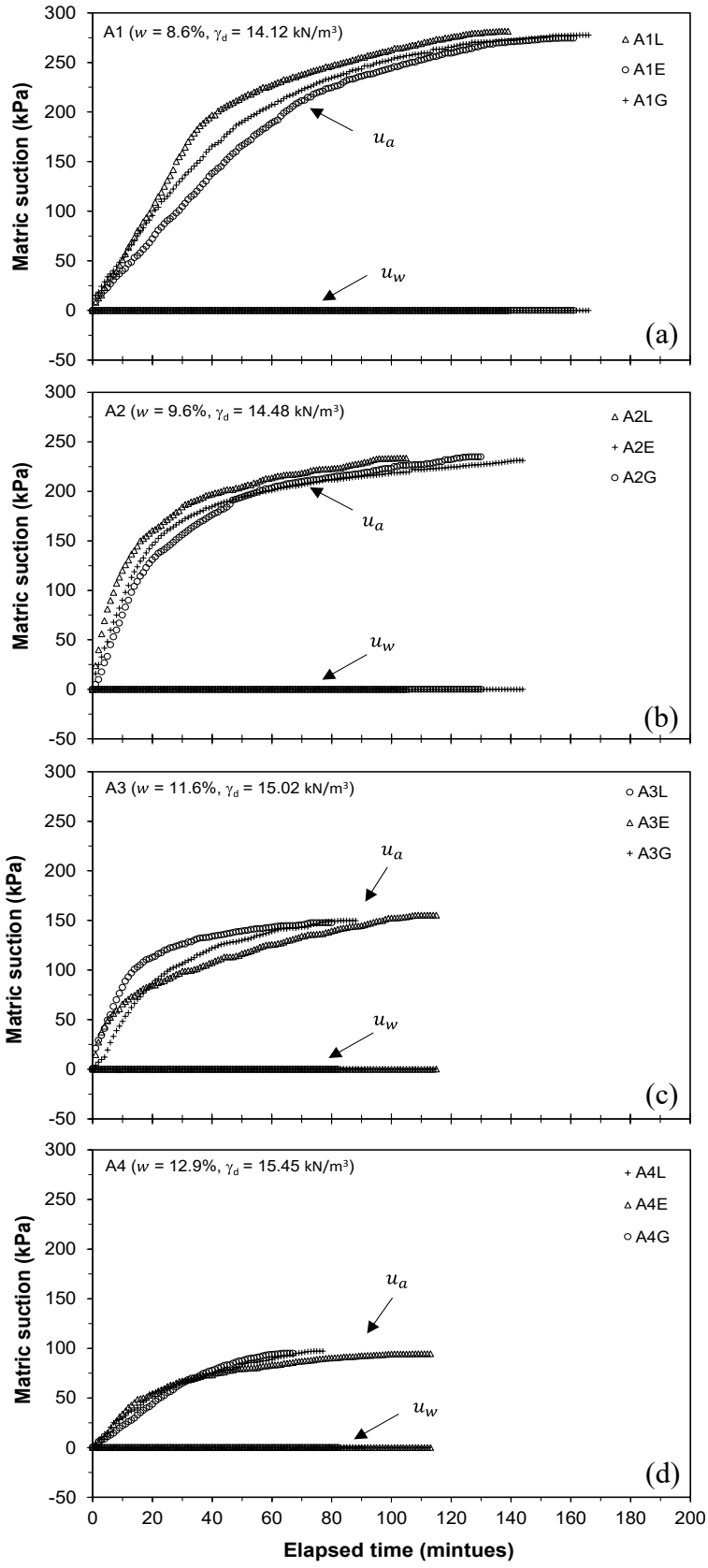

Figure 7.2 Initial suction measurement of specimens in groups (a) A1, (b) A2, (c) A3 and (d) A4 by the null-type tests

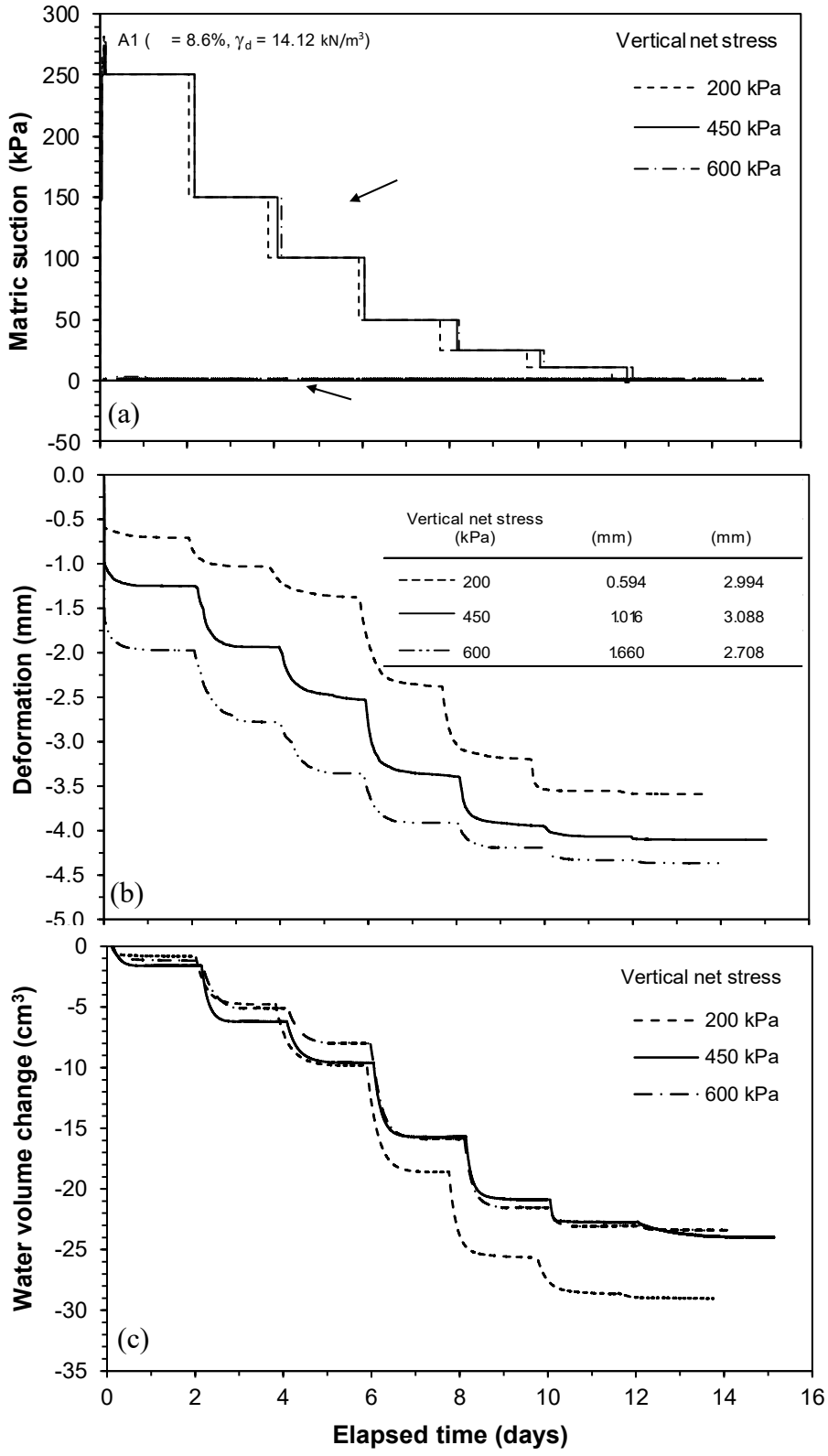

Figure 7.3 Results of suction-controlled oedometer wetting tests conducted at different vertical net stresses for specimens in groups A1, (a) applied suction reduction steps, (b) deformation and (c) water volume change

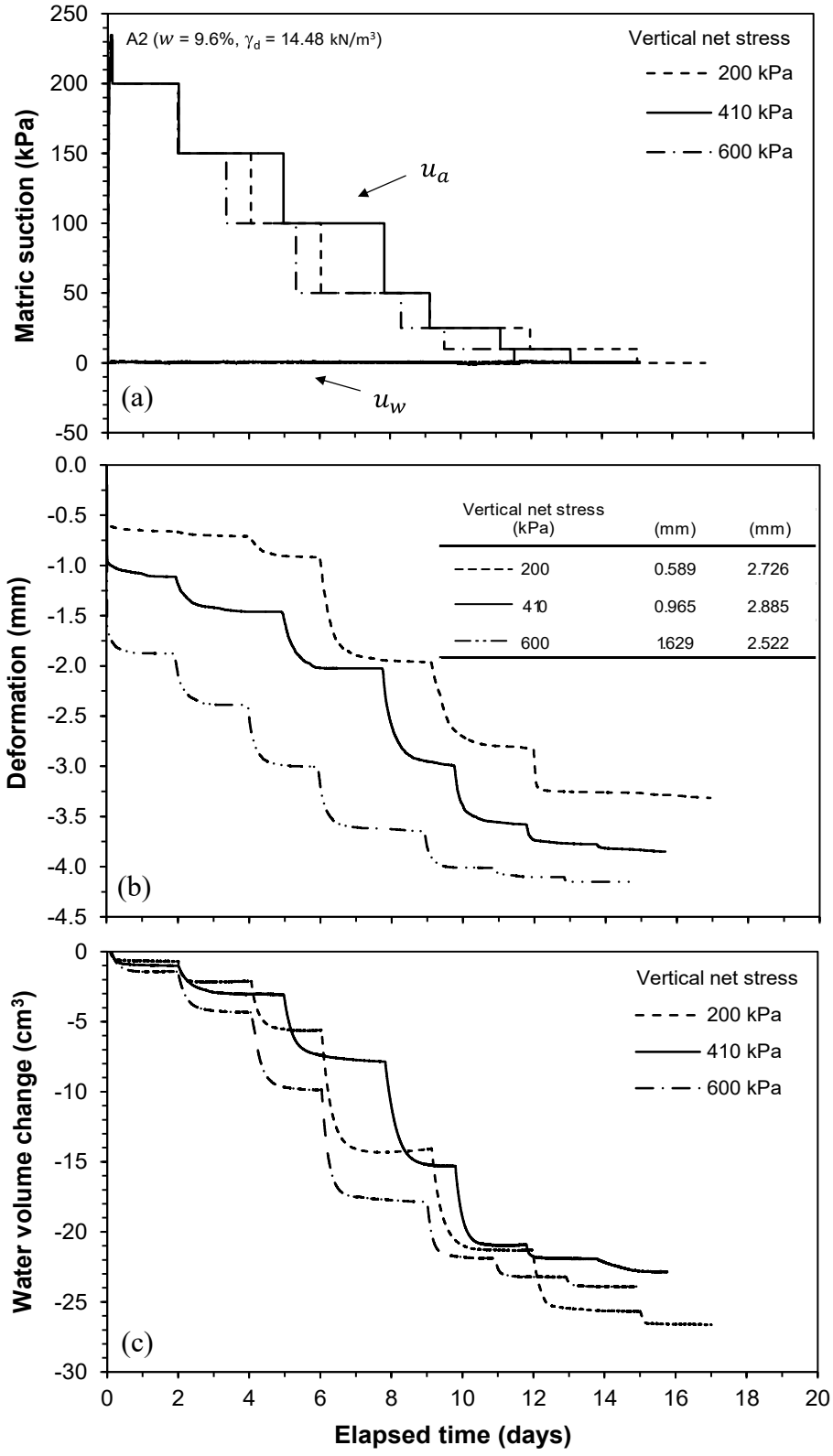

Figure 7.4 Results of suction-controlled oedometer test conducted at different vertical net stresses for specimens in groups A2, (a) applied suction reduction, (b) deformation and (c) water volume change

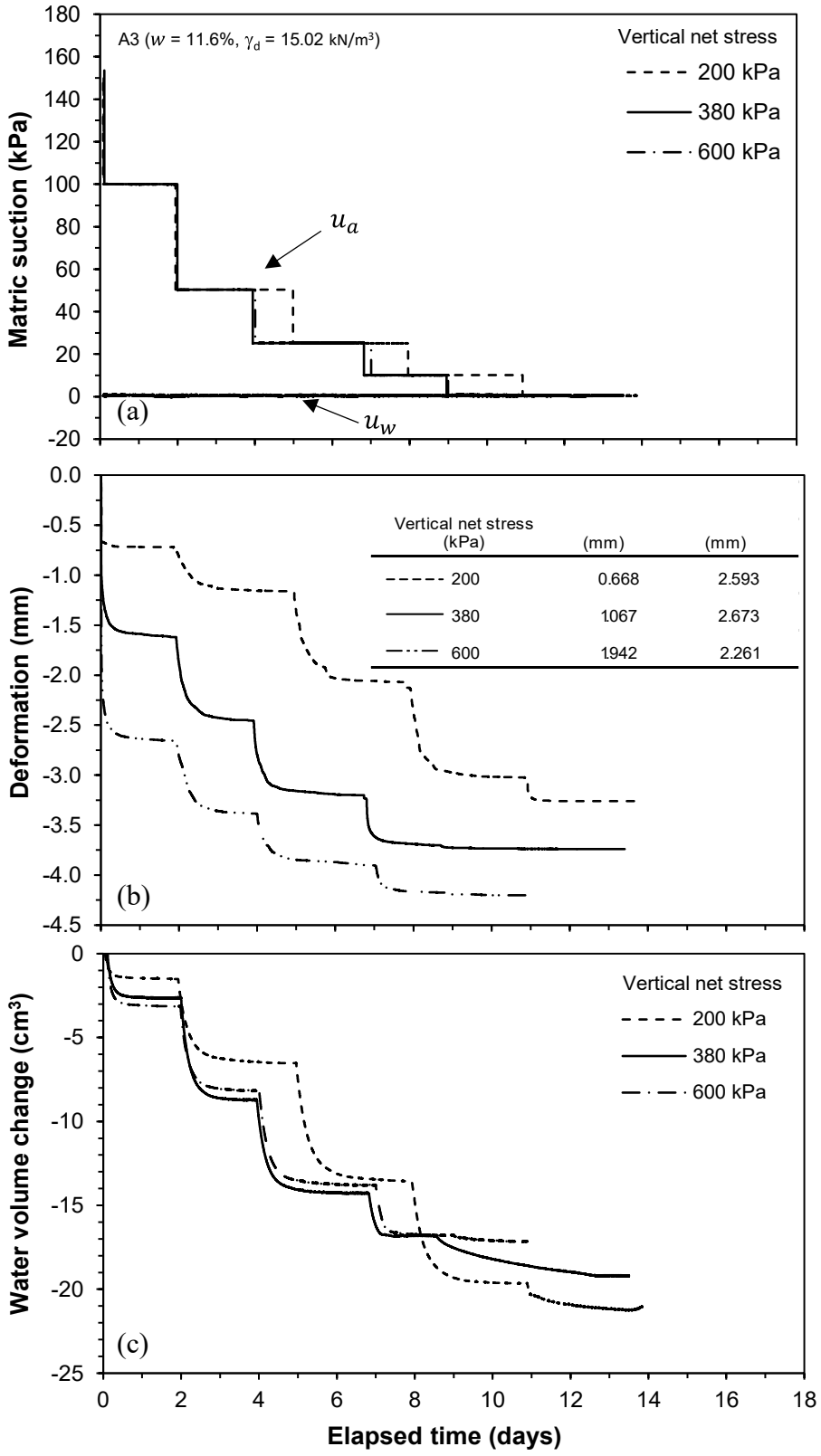

Figure 7.5 Results of suction-controlled oedometer wetting tests conducted at different vertical net stresses for specimens in groups A3, (a) applied suction reduction steps, (b) deformation and (c) water volume change

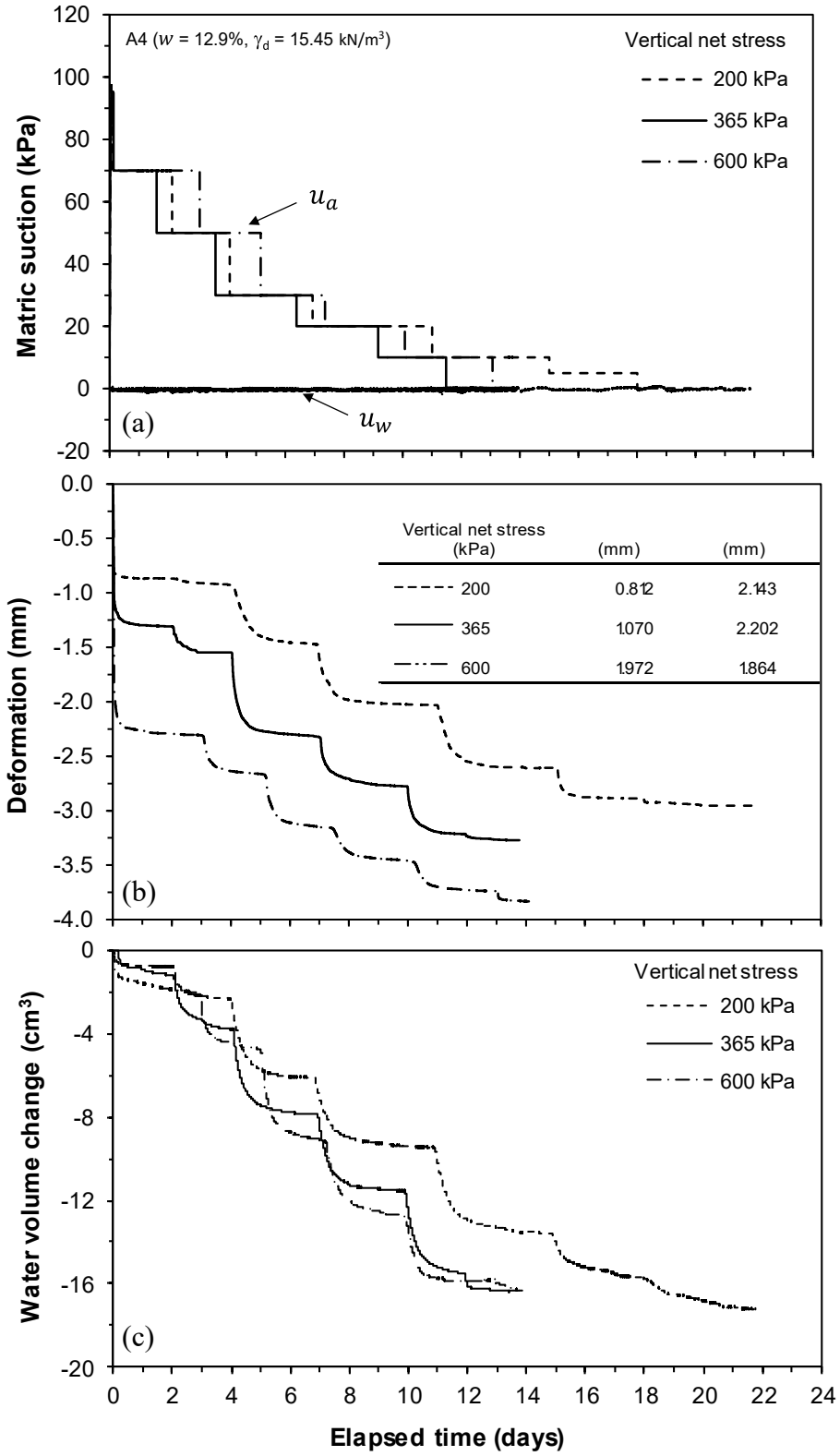

Figure 7.6 Results of controlled-suction wetting tests conducted at different vertical net stresses for specimens in groups A4, (a) imposed suction reduction, (b) deformation and (c) water volume change

7.3.2.1 Changes in collapse strain with matric suction and vertical net stress

The variation of collapse strain with matric suction at different vertical net stresses of specimens in groups A1, A2, A3 and A4 are shown in Figures 7.10 (a-d) respectively. For a given specimen at a constant vertical net stress subjected to suction reduction, considerable collapse (7.5% - 12.8%) was observed as the suction was reduced from the initial value to 10 kPa (nearly saturation), whereas in response to further decreases in suction to zero-value the exhibited collapse strain was found to be insignificant (< 1%).

For a given specimen under different vertical net stresses (200 to 600 kPa), the combined effect of loading and wetting resulted in two distinct trends of collapse. In the early steps of wetting as the suction was reduced from the initial value, the higher the applied vertical net stress, the greater the collapse strain, whereas towards saturation at low suction values this trend changed to note a maximum collapse strain when the vertical net stress equals to the applied compaction pressure. It can also be noticed that for the highest vertical net stress (i.e., 600 kPa), the specimens tend to have a relatively linear collapse strain response with decreasing the matric suction.

In literature, however, only the increasing trend of collapse with the net stress was noted by Pereira and Fredlund (2000), whereas only the occurrence of maximum collapse at the yielding stress was reported by Sun et al. (2004). The controlling factor of such observations is the range of the applied net stress. As such, when the range of the applied stress is less than the yield stress of the unsaturated soil the increasing trend of the collapsibility would be observed. Whist, for the applied stresses greater than the yield stress, a decrease in collapse strain has been observed (see Section 2.6.1.1 and Section 2.6.2.1).

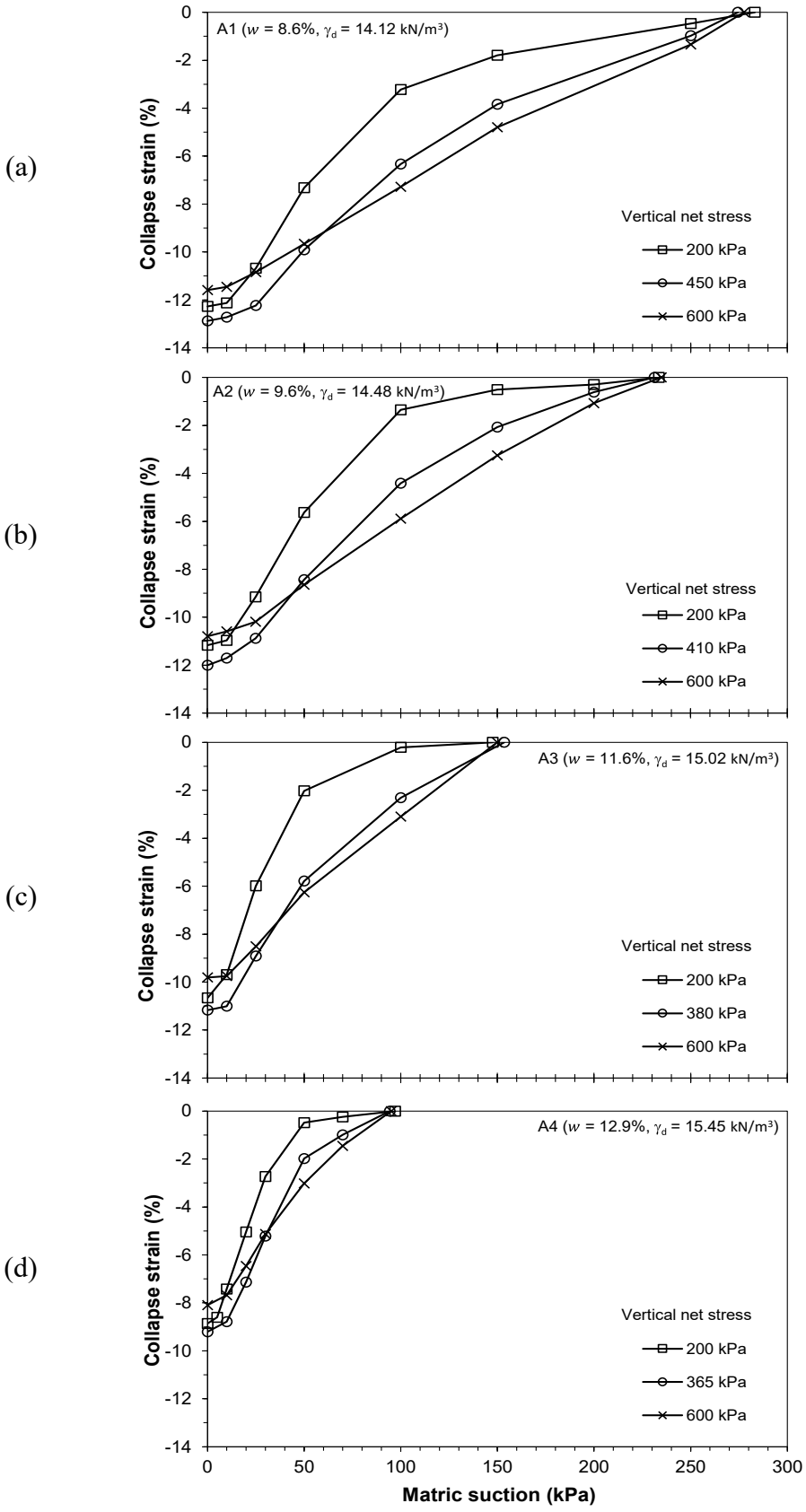

Figure 7.7 Collapse strain changes with suction reduction of specimens in groups (a) A1, (b) A2, (c) A3 and (d) A4

7.3.2.2 Changes in collapse strain with the compaction state of specimens

Although the tested samples have different initial water contents and dry unit weights, the samples were subjected to the same static compaction energy of 50 kJ/m^3 during preparation. As discussed in Chapter 4, along the static compaction curve increased water content and dry density was obtained at smaller compaction pressure. The applied compaction pressure decreased from 450 to 365 kPa (see Table 5.1). The discussion on the effect of compaction conditions, therefore, will be based on the applied static compaction pressure.

Figures 7.8 (a-c) show the changes in the collapse strain of samples along the compaction energy curve for the three applied vertical stresses. At a particular energy of compaction, the applied compaction pressure during specimen preparation affects the collapse strain. At a given vertical net stress, the smaller the applied compaction pressure, the lower the exhibited collapse strain at all levels of matric suction. These results complement the earlier finding in Chapter 5, which can be explained by the corresponding relationship between the compaction pressure and water content, which dominates the resulting dry density and the volume change behaviour.

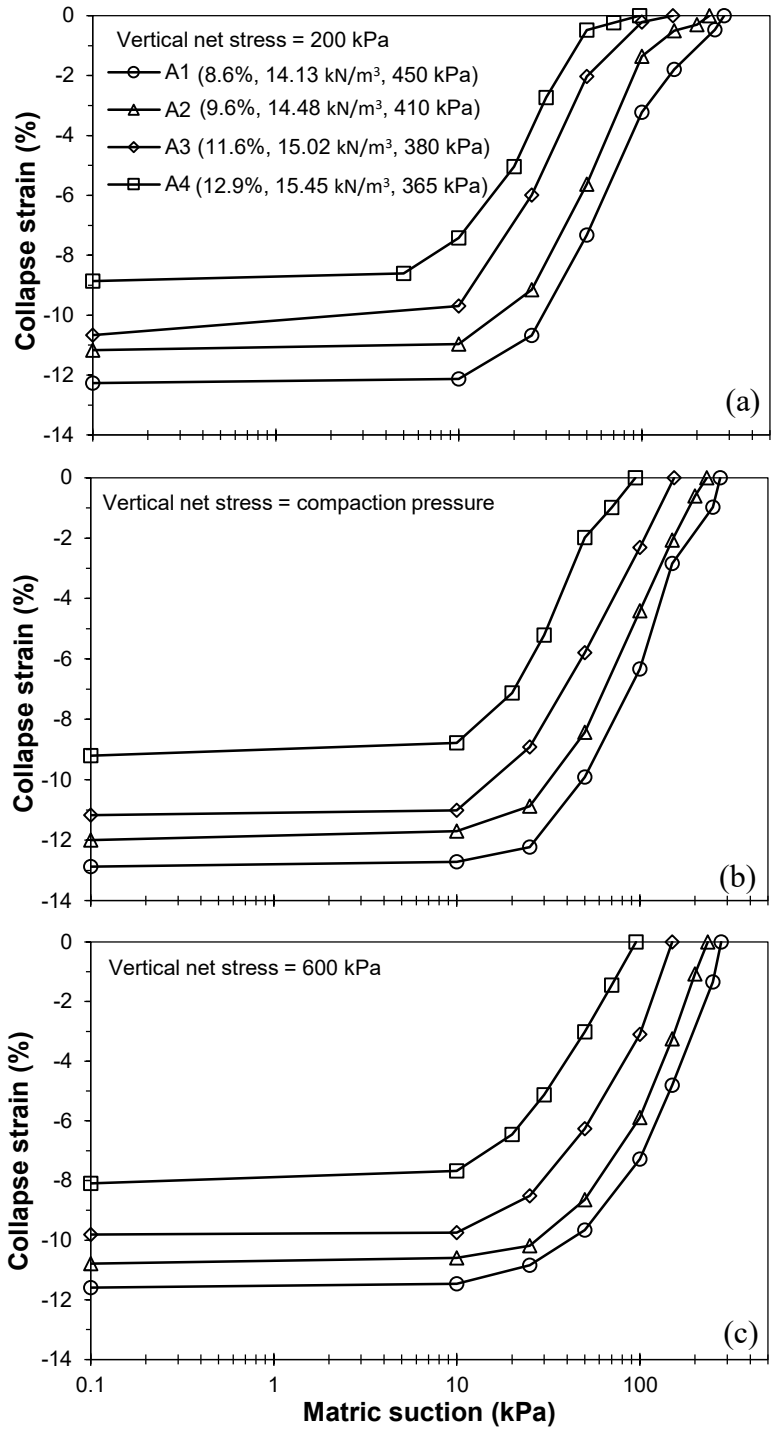

Figure 7.8 Collapse behaviour at different compaction conditions during controlled-suction oedometer tests at constant vertical net stresses of (a) 200 kPa (b) compaction pressure and (c) 600 kPa

7.3.2.3 Suction-water content SWCCs

Figures 7.9 (a-d) show the soil-water characteristic curves in terms of water content of the specimens at different vertical net stresses that tested under groups A1, A2, A3 and A4, respectively. The differences between the final measured water contents and the calculated ones based on the volumetric water measurements varied from 0.2% to 1.5% and therefore the correction was applied as discussed in Section (6.3.3.2).

For a given specimen condition under different vertical net stresses, the water contents increased almost similarly during collapse when the matric suction reduced from the initial value to 10 kPa. However, the influence of collapse was only noticeable at low suctions as the specimen approached saturation and the SWCCs became sensitive to the variation of vertical net stress. The saturated water content was found to be smaller at high vertical net stress. The decrease in the saturated water content at zero-suction is attributed to the smaller void ratio corresponding to the higher applied pressure.

Figures 7.10 (a-c) show the changes in water content during the collapse of specimens having different compaction conditions (i.e., along the compaction energy curve) under the three applied vertical stresses. At a given compaction energy, the compaction pressure affects the SWCCs, particularly at low suction values. As observed in earlier chapters that the higher the initial water content of specimens the smaller the compaction pressure. At low suctions, specimens with smaller compaction pressure approached slightly higher water content within about 2%. Prior to saturation at relatively high suction, SWCCs with different initial water contents and dry densities were less affected by the compaction pressure.

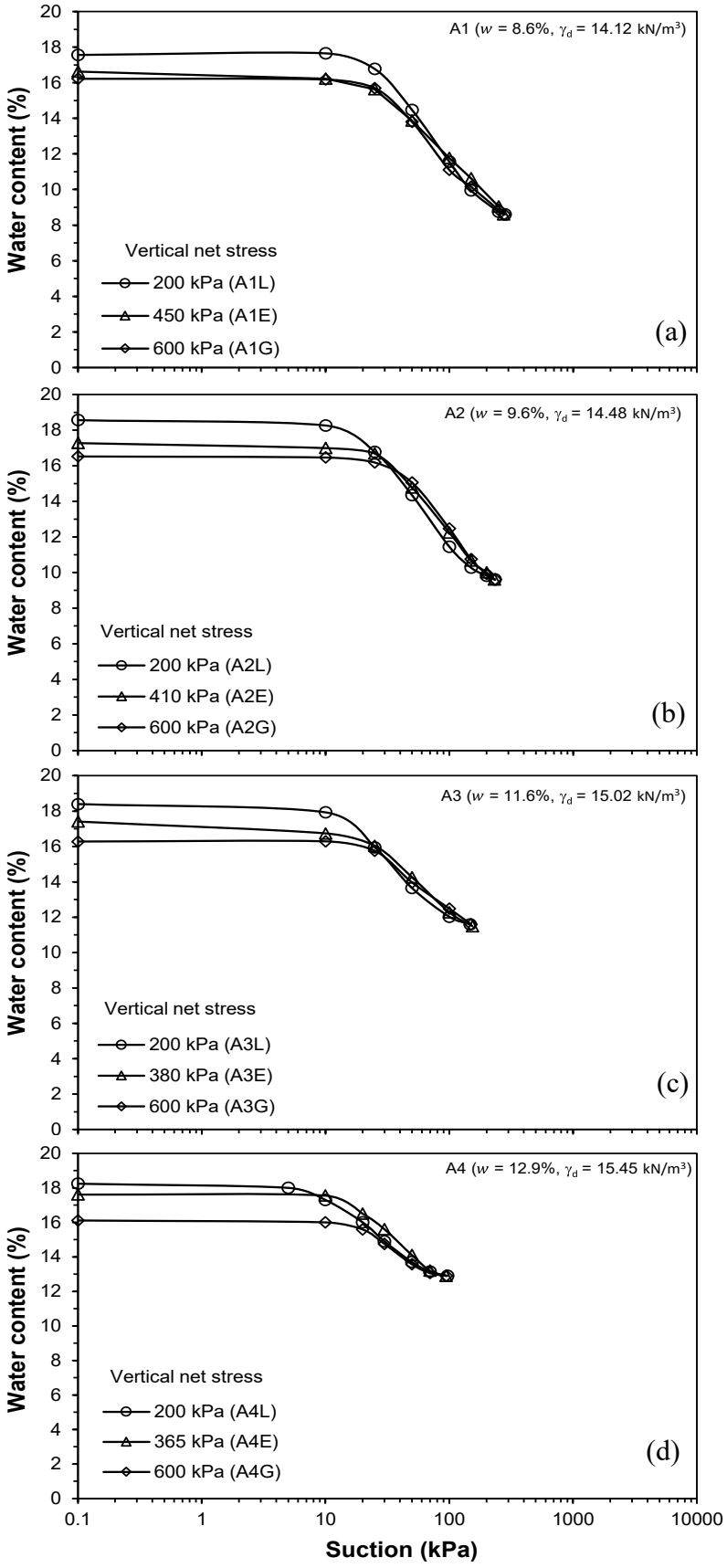

Figure 7.9 Changes in water content with suction reduction of specimens in groups (a) A1, (b) A2, (c) A3 and (d) A4

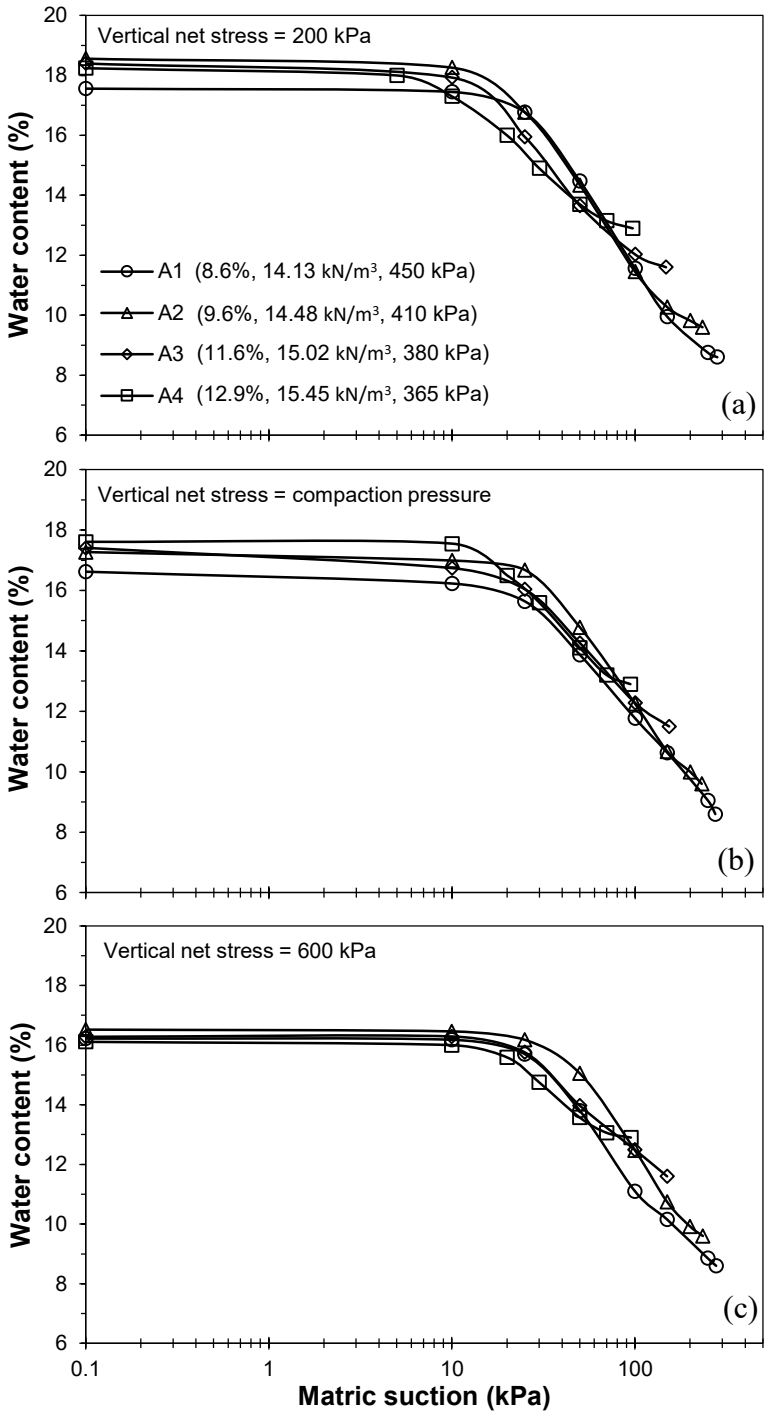

Figure 7.10 Soil-water absorption behaviour at different compaction conditions during suction-controlled oedometer tests at constant vertical net stresses of (a) 200 kPa (b) compaction pressure and (c) 600 kPa

NB: the values between brackets are the water content, dry unit weight and the applied compaction pressure of specimens

7.3.2.4 Suction-degree of saturation SWCCs

The degree of saturation changes during wetting under different applied net stresses is plotted in Figures 7.11 (a-d) for specimens in groups A1, A2, A3 and A4, respectively. For a given specimen at different vertical net stresses, a higher degree of saturation was observed for specimens subjected to higher pressures at a given suction. The SWCC curves shifted to the right at high vertical net stress. The right-shifting in the SWCCs with increasing vertical stress is due to the presence of a lower void ratio of smaller average pore sizes for specimens under a higher net stress, which resulted in higher matric suction at a given degree of saturation (Gallipoli et al. 2003; Tarantino 2009). Although the observed non-unique SWCCs at various net stresses differ from some published studies by Pereira and Fredlund (2000) and Garakani et al. (2015), they are consistent with those by Sun et al. (2007) and Haeri et al. (2016). This is due to the effect of the soil structure (e.g., undisturbed and reconstituted specimens), type of the tests (e.g., constant stress with varying suction test or constant suction with varying stress test) and the loading condition (e.g., K_o and triaxial).

Figures 7.12 (a-c) show the changes in the degree of saturation during the collapse of specimens along the compaction energy curve for the three applied vertical stresses. The wetting SWCCs at a given vertical stress of specimens at a given compaction energy affected by the compaction pressure notably near saturation. At low suctions, the smaller the pressure of compaction the higher is the degree of saturation of the SWCC, whereas the SWCCs of all specimens become practically unique at high suctions. This behaviour is attributed mainly to the soil structure. The entrapped air by the ink-bottle effect is a prominent feature in loosely compacted specimens, whereas it can be readily displaced from small pores of the denser specimen at the applied suction as air can flow rapidly through the narrow pores (Sun et al. 2007).

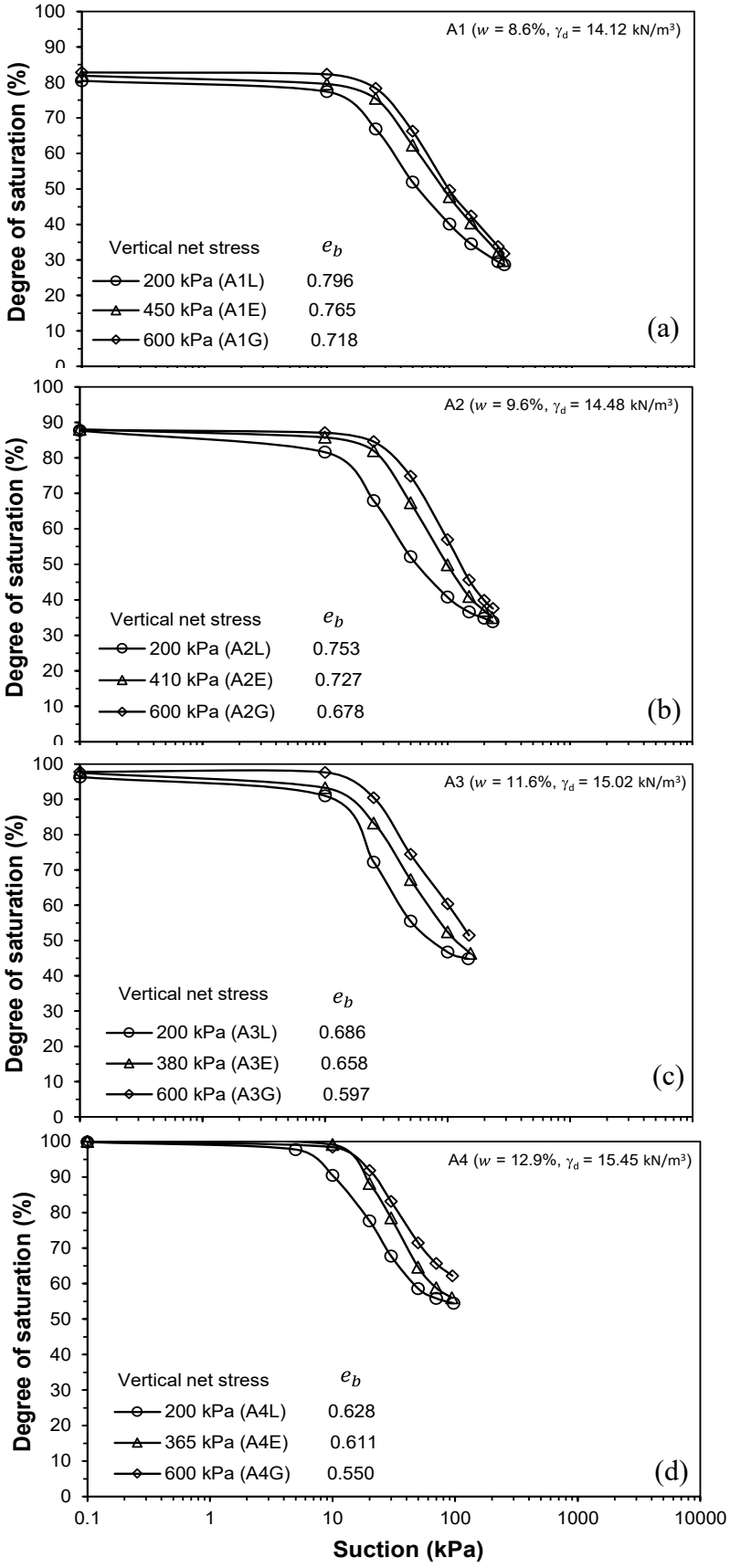

Figure 7.11 Changes in degree of saturation during wetting of specimens in group (a) A1, (b) A2, (c) A3 and (d) A4. is the void ratio of specimens just before wetting

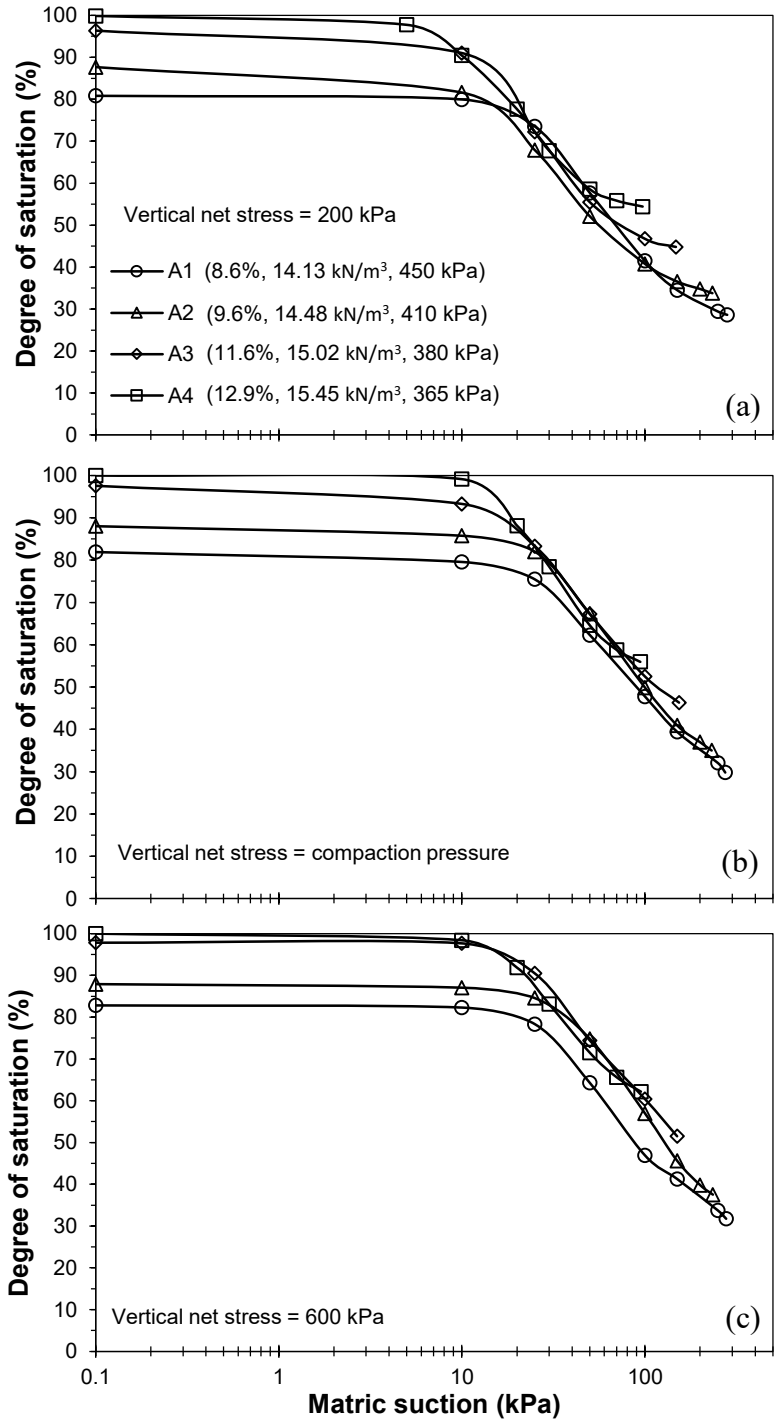

Figure 7.12 Degree of saturation SWCCs at different compaction conditions during suction-controlled oedometer tests at constant vertical net stresses of (a) 200 kPa (b) compaction pressure and (c) 600 kPa

7.4 Concluding remarks

Suction-controlled oedometer tests during wetting-induced collapse were conducted on statically compacted specimens along the static compaction curve of 50 kJ/m^3. The compacted specimens were subjected to various vertical net stresses. The main findings from this chapter can be summarised as follows:

1. For a given compacted specimen, the collapse behaviour and water absorption characteristics were found to be strongly influenced by the combined effect of the applied matric suction and vertical net stress. At relatively high matric suction, higher the applied net stress, greater was the collapse strain, similar was the increase in water contents and greater was the increase in degrees of saturation. Towards saturation (at low matric suction values), maximum collapse reached when the applied stress equals the compaction pressure. Higher the applied vertical net stress less was the increase in water contents and similar was the increase in degrees of saturation near saturation. This behaviour is consistent with the general findings reported on collapsible soils (e.g., Pereira and Fredlund 2000; Sun et al. 2004).
2. For specimens along the static compaction energy curve at a given applied net stress, the collapse strain was found to decrease with the decrease in the applied compaction pressure. The SWCCs in terms of both water content and degree of saturation were found to be independent of the applied compaction pressure at high suctions, whereas the SWCCs were strongly influenced by the compaction pressure at the low suctions. The results indicated that the SWCC of the specimen with smaller compaction pressure was above those with larger compaction pressure.

Chapter 8

Collapse behaviour based on effective stress in unsaturated soils

8.1 Introduction

The effective stress concept, established by Terzaghi (1936) for saturated soils and extended by Bishop (1959) for unsaturated soils, plays a key role in interpreting, predicting and constitutive modelling of the mechanical behaviour (Loret and Khalili 2000; Gallipoli et al. 2003; Wheeler et al. 2003; Sheng et al. 2004; Lu and Likos 2006; Khalili et al. 2008; Nuth and Laloui 2008; Lu et al. 2010; Alonso et al. 2010). Since compacted soils with a tendency to collapse are initially unsaturated soils, the effective stress in unsaturated soils is more applicable for describing their behaviour (Fredlund and Rahardjo 1993).

Bishop (1959) introduced the effective stress parameter ( ) to represent the contribution of matric suction to the effective stress. The effective stress parameter was considered to vary between zero and unity as a function of the degree of saturation ( ) (Bishop 1959; Bishop and Blight 1963). The inequality between and and failure to capture the collapse behaviour have been major obstacles for the wide acceptance of Bishop effective stress (Bishop and Donald 1961; Jennings and Burland 1962). Therefore, different proposals have been introduced to determine the Bishop's parameter χ both experimentally and theoretically (see Table 2.4). A unique relationship has been successfully obtained between the effective stress parameter and

the suction ratio for most soils by (Khalili and Khabbaz 1998; Khalili et al. 2004). However, little is known about the variation of the effective stress parameter along the wetting path (Khalili and Zargarbashi 2010).

Similar to Bishop effective stress, the suction stress characteristic curve (SSCC) has been introduced to represent the state of stress in unsaturated soil (Lu and Likos 2006; Lu et al. 2010). Unlike Bishop effective stress, the suction stress approach eliminates the need to determine the effective stress parameter by presenting a micromechanically based concept. The SSCCs can be experimentally determined from tensile strength tests, shear strength tests and can be predicted based on the soil-water characteristic curve. Based on the SWCCs, the curve fitting parameters are needed to establish the SSCCs (see Section 8.2.2). It has been verified that the suction stress concept could adequately describe the unsaturated shear strength behaviour (Alsherif and McCartney 2014; Oh and Lu 2014; Pourzargar et al. 2014). However, knowledge concerning its applicability in capturing the collapse behaviour of unsaturated soils is still scarce.

The objectives of this chapter are to (*i*) investigate changes in the effective stress parameter and suction stress with suction, applied load and compaction condition of specimens along the static compaction curve and (*ii*) examine the applicability of using the single effective and suction stress approaches in describing the collapse behaviour.

In this chapter, the results of suction-controlled oedometer wetting tests of compacted specimens that presented in Chapter 7 are theoretically analysed based on the single effective stress by Khalili and Khabbaz (1998) and suction stress approaches by Lu et al. (2010) . The main findings are summarised towards the end of the chapter.

8.2 Effective stress approaches in unsaturated soils

8.2.1 The single effective stress approach by Khalili and Khabbaz (1998)

The general form of the effective stress in unsaturated soils is proposed by (Bishop 1959) as given in Equation (8.1).

(8.1)

where is the effective stress, is the total stress, is the pore air pressure, is the pore water pressure, is the matric suction, and is the effective stress parameter that represents the contribution of matric suction to the effective stress.

Based on shear strength data of various soils, Khalili and Khabbaz (1998) proposed a formula for quantifying the effective stress parameter (χ) by using Equation (8.2), which was also verified by volume change data (Khalili et al. 2004).

(8.2)

where, is the matric suction and is suction value marking the transition between saturated and unsaturated states. For wetting process, is equal to the air expulsion value, and — is the suction ratio.

The air expulsion value ( ) required for quantifying the effective stress parameter in equation (8.2) can be found by using the curve best-fit models of the SWCC. Khalili et al (2008) used the Brooks and Corey (BC) (1964) model given in Equation (8.3) to represent the SWCC as a sharp air expulsion suction can be represented by the BC model.

(8.3)

where, is the effective degree of saturation described in Equation (8.4), is the air expulsion suction and is pore size distribution index.

The fitting parameters can be readily visualized from the SWCC data in terms of the effective degree of saturation. To determine the effective saturation, the residual degree of saturation should be known. An optimization routine was used to fit the parametric models to the measured SWCCs data with the error being minimized by an iterative approach using Slover subroutine included in Microsoft Excel.

8.2.2 Suction stress approach

The suction stress characteristic curve (SSCC) (Lu and Likos 2004; 2006) can be established based on the measured SWCC of unsaturated soils (Lu et al. 2010) by employing the effective saturation as the effective stress parameter. This permits the integration of the van Genuchten (1980) SWCC into the definition of the suction stress. The set of equations used for the calculation of suction stress are as follows:

(8.4)

(8.5)

(8.6)

(8.7)

where is the effective degree of saturation, is the degree of saturation, is the residual degree of saturation, is the degree of saturation at zero suction, is usually equal to 1, but in some cases soils may not reach fully saturated condition especially under the wetting process (Sun et al. 2007) and therefore, can be less than one (Zhou et al. 2012), and are fitting parameters, and is the suction stress. The VG model was used by Lu et al. (2010) due to its ability to facilitate closed form analytical solutions for suction stress profiles, with a minimum number of parameters.

The following procedure was adopted for establishing the SSCCs:

1. The suction-degree of saturation SWCCs were used to derive the effective degree of saturation values using Equation (8.4) which enabled determining the suction-effective saturation SWCCs.
2. The suction-effective degree of saturation SWCCs were fitted to van Genuchten model (VG) described by Equation (8.5) using Solver to obtain the fitting parameters (and). An optimization routine was used to fit the parametric models (Equation 8.5) to the measured data (Equation 8.4) using an iterative approach until the sum of the squared residuals (SSR) differences between the predicted and measured data becomes minimal.
3. The fitting parameters (and) were then used to calculate the suction stress as a function of effective saturation using Equation (8.6) and as a function of suction using Equation (8.7), the closed-form equations by Lu et al. (2010).

The effective stress under the suction stress concept can be calculated from Equation (8.8).

(8.8)

8.3 Results and discussion

8.3.1 Residual degree of saturation

To identify the part of effective stress resulting from matric suction changes in both the pre-described effective stress approaches, the SWCC with an identified residual degree of saturation is needed. The measured SWCCs presented in Chapter 7 were limited to matric suction less than 300 kPa and the residual degree of saturation ( ) was not identified (see Figures 7.11a-d).

The SWCCs were therefore established at the higher suction range to determine the residual degree of saturation of specimens. The chilled mirror dew point device (WP4C) was used for suction measurements of specimens. Soil specimens were prepared by statically compacting soil-water mixtures as explained in Section (3.6.1.1). The targeted compaction dry densities and water contents of the statically compacted specimens were corresponding to the specimen conditions tested in groups A1, A2, A3 and A4 presented in Chapter 7. Four different testing procedures were adopted on the specimens to enable a comparison between the SWCCs established by each testing method, in which the effect of wetting and dying paths, and the applied stress are considered. In addition, a proposed procedure that considers the stress history of the specimen is introduced as a type of the SWCCs. The testing methods for SWCCs measurements at high suction are as follows:

Method (a): SWCC at high suctions was established by measuring suction of specimens with varying water contents but equal dry unit weight. Under this method, most of the data were obtained from the suction contours along compaction curves

(Figure 4.11) by drawing a horizontal line at the desired dry unit weight for reading suction values and the corresponding water content.

Method (b): wetting SWCC at high suctions was established by measuring suction of a single specimen at varying water contents. Wetting was performed by carefully dropping small amounts of water over a filter paper in contact with the upper face of the specimen to ensure homogeneous wetting. The specimen was allowed to equilibrate for uniform distribution of water within the soil.

Method (c): drying SWCC at high suctions was established by measuring suction of a single specimen at varying water contents. Drying was achieved by allowing evaporation of the specimen-water under laboratory conditions for various drying period.

Method (d): stress-dependent drying SWCC was established by measuring suction of specimens with varying water contents and dry unit weight. Initially identical specimens were loaded to a pre-selected pressure using the conventional oedometer and allowed to dry out for various drying period. The specimens were allowed to attain water content equilibration and were extruded for suction measurement.

Method (e): suction-history SWCC was established by measuring suction of a specimen at different stages of the static compaction process until the specimen reached the desired compaction condition.

After establishing the entire SWCC, the residual degree of saturation can be then experimentally defined by the intersection point between a line from the point of inflection on the straight-line portion of the SWCC, and a line from the point at 10^6 kPa, tangent to the original curve (Vanapalli et al. 1999).

A combination of the original SWCCs measured using the suction-controlled oedometer and the established SWCCs at high suctions by adopting the five different testing procedures discussed in earlier paragraphs using the chilled-mirror potentiameter is shown in Figure (8.1). A comparison between the testing methods (a, b, c and d) adopted to establish the SWCCs at suction varied from 0.3 to 150 MPa indicated comparable results. Testing method e that considered the stress history of the statically compacted specimen enabled tracing SWCCs of relatively different slopes. By using the graphical method as illustrated in Figure (8.1), the residual degrees of saturation were found to be 6% for the tested specimens in group A4.

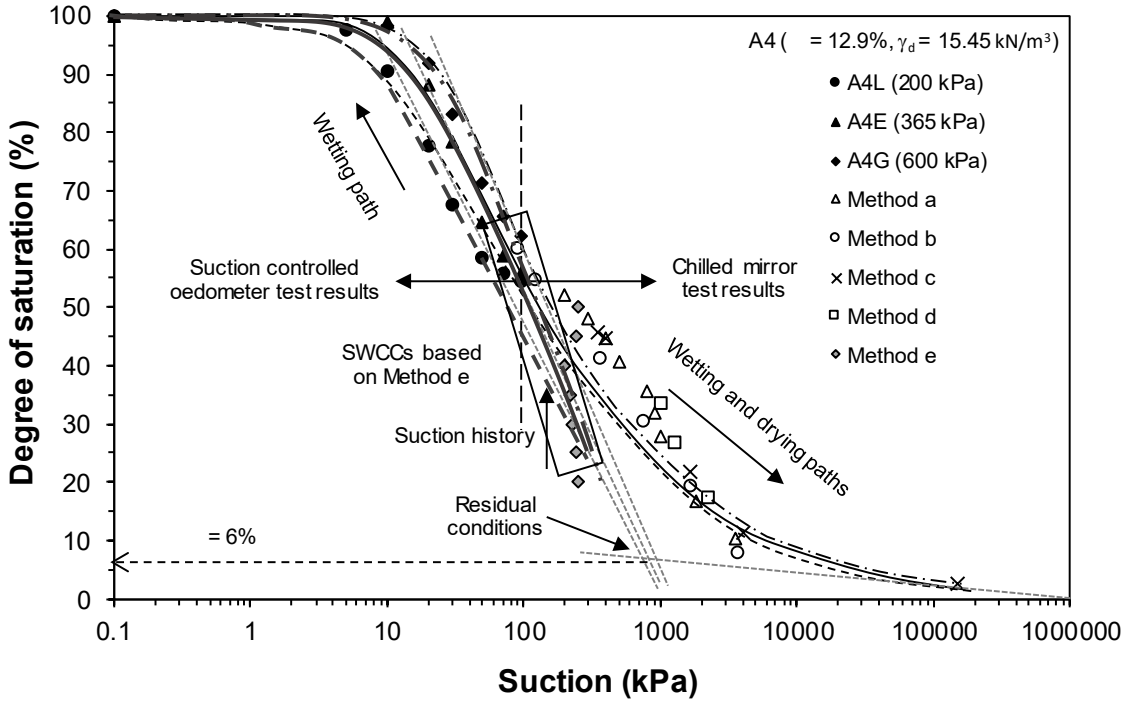

Figure 8.1 SWCCs of specimens in groups A4 extended to a high suction range

Since the adopted methods (a, b, c and d) yielded similar SWCC, for the remaining samples (A1, A2 and A3) the SWCCs at high suctions was only obtained by following Method (a), and the results are shown in Figures 8.2 (a-d), respectively. The residual degrees of saturation were experimentally determined to be about 6% for all the tested specimens as shown in the relevant figures.

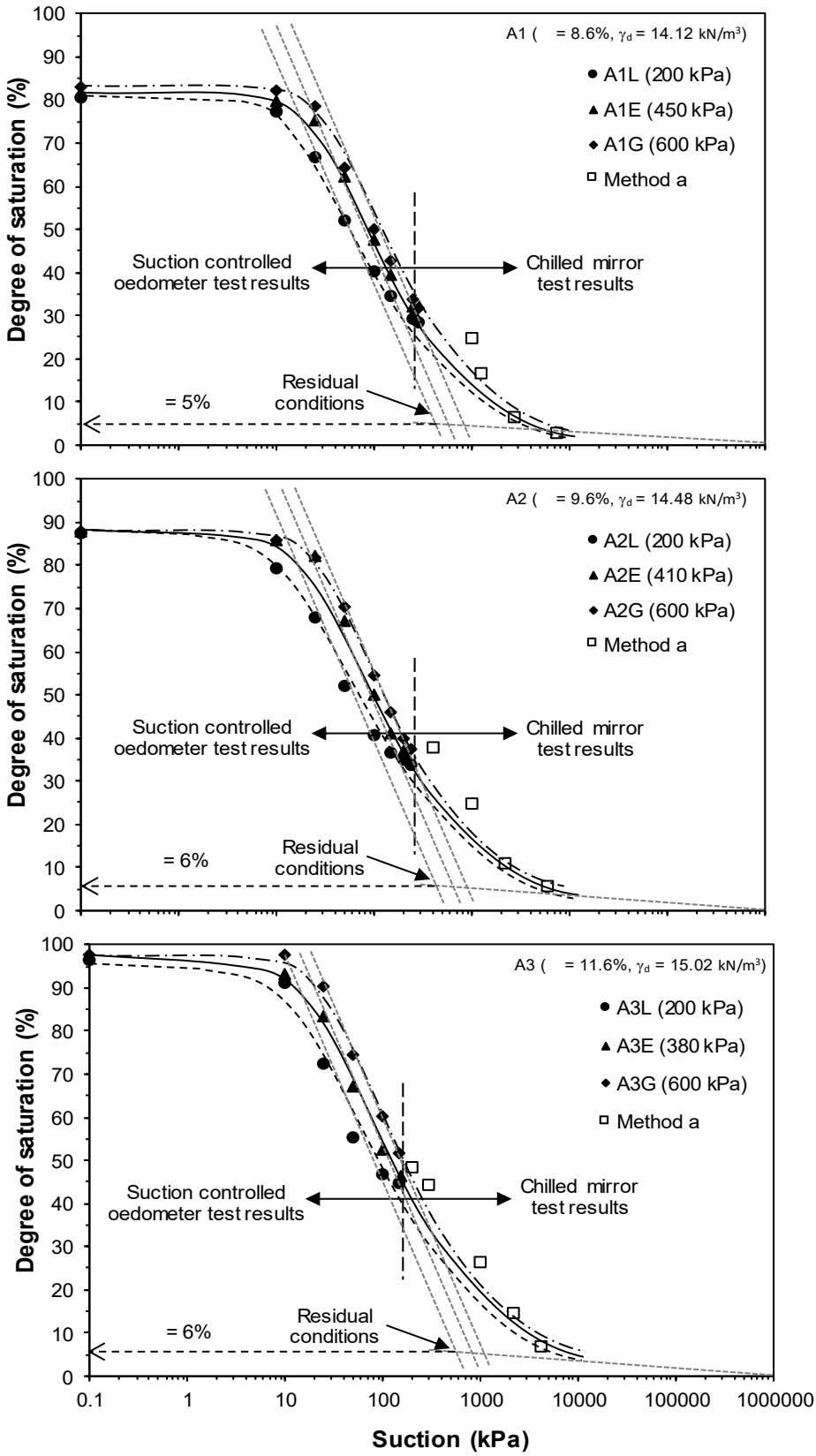

Figure 8.2 SWCCs of specimens in groups (a) A1, (b) A2 and (c) A3 extended to high suctions

8.3.2 Effective stress parameters

Based on the single effective stress approach, the effective stress parameters suggested by Khalili and Khabbaz (1998) were evaluated by first determining the air expulsion values of each specimen. Figures 8.3 (a-d) show the entire SWCCs in terms of the effective degree of saturation fitted to the Brooks and Corey (BC) model of specimens in groups A1, A2, A3 and A4, respectively. As can be seen in Figures 8.3 (a-d) that the BC model fitted well the SWCCs by recognition the air expulsion values as sharp points.

Table (8.1) summarises the fitting parameters (i.e., air expulsion suctions and pore size distribution index) that were derived from the SWCCs at different net vertical stresses. For a given specimen subjected to increasing vertical net stress, the pore size distribution index was found to vary in a narrow range, while there was a linear trend between the air expulsion suction values ( ) and the vertical net stress. As the vertical net stress increased, the air expulsion suction also increased linearly.

Table (8.1) also shows that the resulting fitting parameters (and) are influenced by the initial conditions of the specimens along the compaction curve. The compaction pressure seems to affect the level of air expulsion suction. At a given applied net stress, specimens with smaller compaction pressure (i.e., higher initial water content and dry density) had smaller .

Figures 8.4 (a-d) show the variation in the effective stress parameter (χ) with matric suction for specimens tested in groups A1, A2, A3 and A4, respectively. The variation in the air expulsion values with the applied stress and specimen condition obviously resulted in different values of the effective stress parameters at a given matric suction.

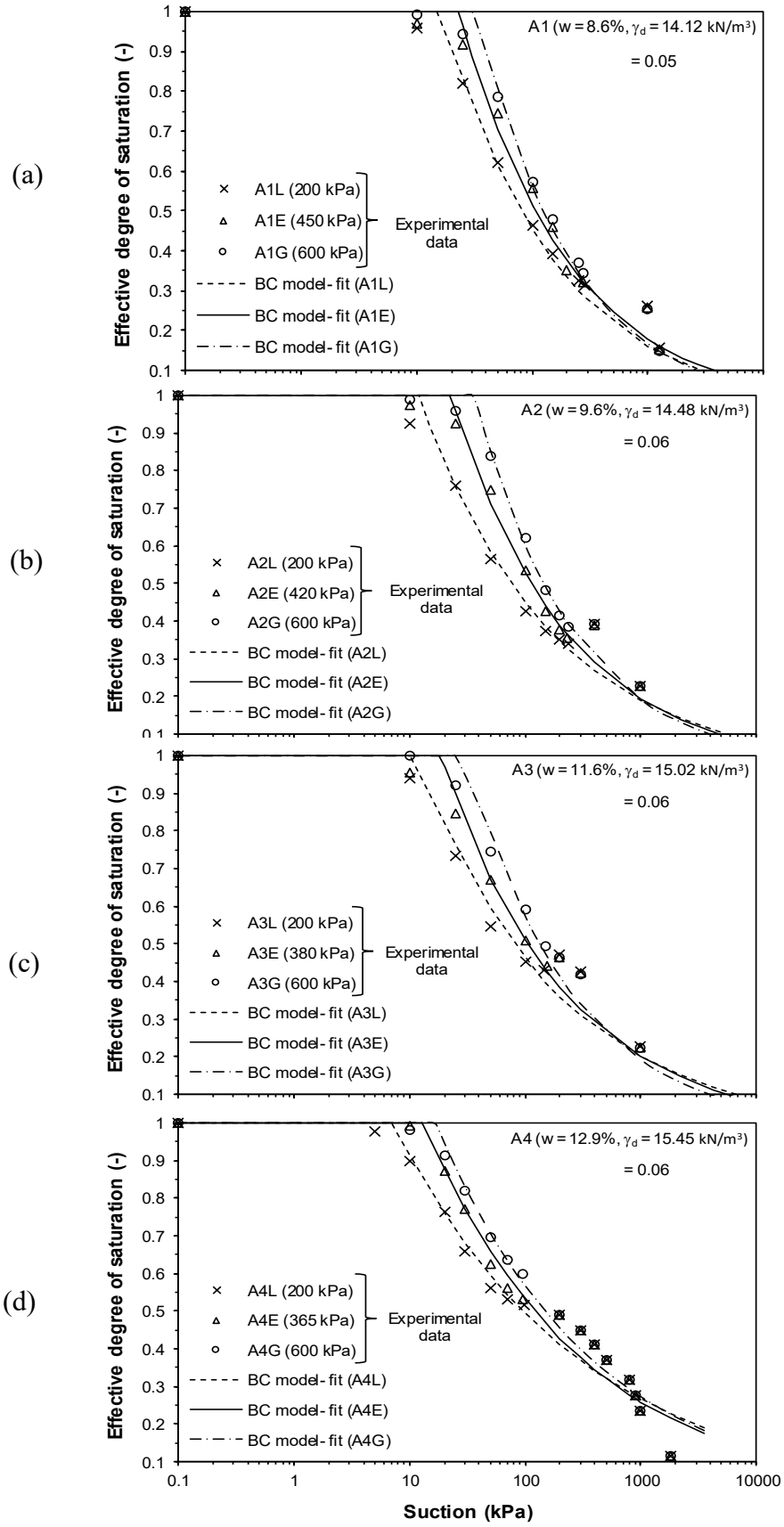

Figure 8.3 Suction-effective saturation SWCCs fitted to BC model of specimens in groups (a) A1, (b) A2, (c) A3 and (d) A4

Table 8.1 Brooks and Corey model fitting parameters for all specimens

Specimen no.	Vertical net stress, (kPa)	Fitting parameters		R^2
			(kPa)	
A1L	200	0.45	16.7	0.9975
A1E	450	0.46	23.2	0.9972
A1G	600	0.53	33.5	0.9978
A2L	200	0.38	12.0	0.9966
A2E	410	0.43	22.7	0.9975
A2G	600	0.50	36.7	0.9980
A3L	200	0.36	11.9	0.9942
A3E	380	0.40	18.6	0.9957
A3G	600	0.47	31.3	0.9964
A4L	200	0.27	07.1	0.9965
A4E	365	0.31	13.1	0.9970
A4G	600	0.32	16.9	0.9974

It can be observed in Figures 8.4 (a-d) that χ increased gradually during wetting as suction was decreased until it reached a value equal to 1 when suction reduced beyond the air-expulsion value. This behaviour agreed well with the general observation reported by Zargarbashi and Khalili (2011) and Brink and Heymann (2014).

At a given matric suction, specimens subjected to higher applied stress was found to have higher χ values (Figures 8.4a-d). Similarly, χ values as a representing of the suction contribution to the effective stress also affected by the specimen conditions. The study brings out the observation that for a given soil the compaction conditions and the applied vertical stress had a notable influence on the resulted effective stress parameters.

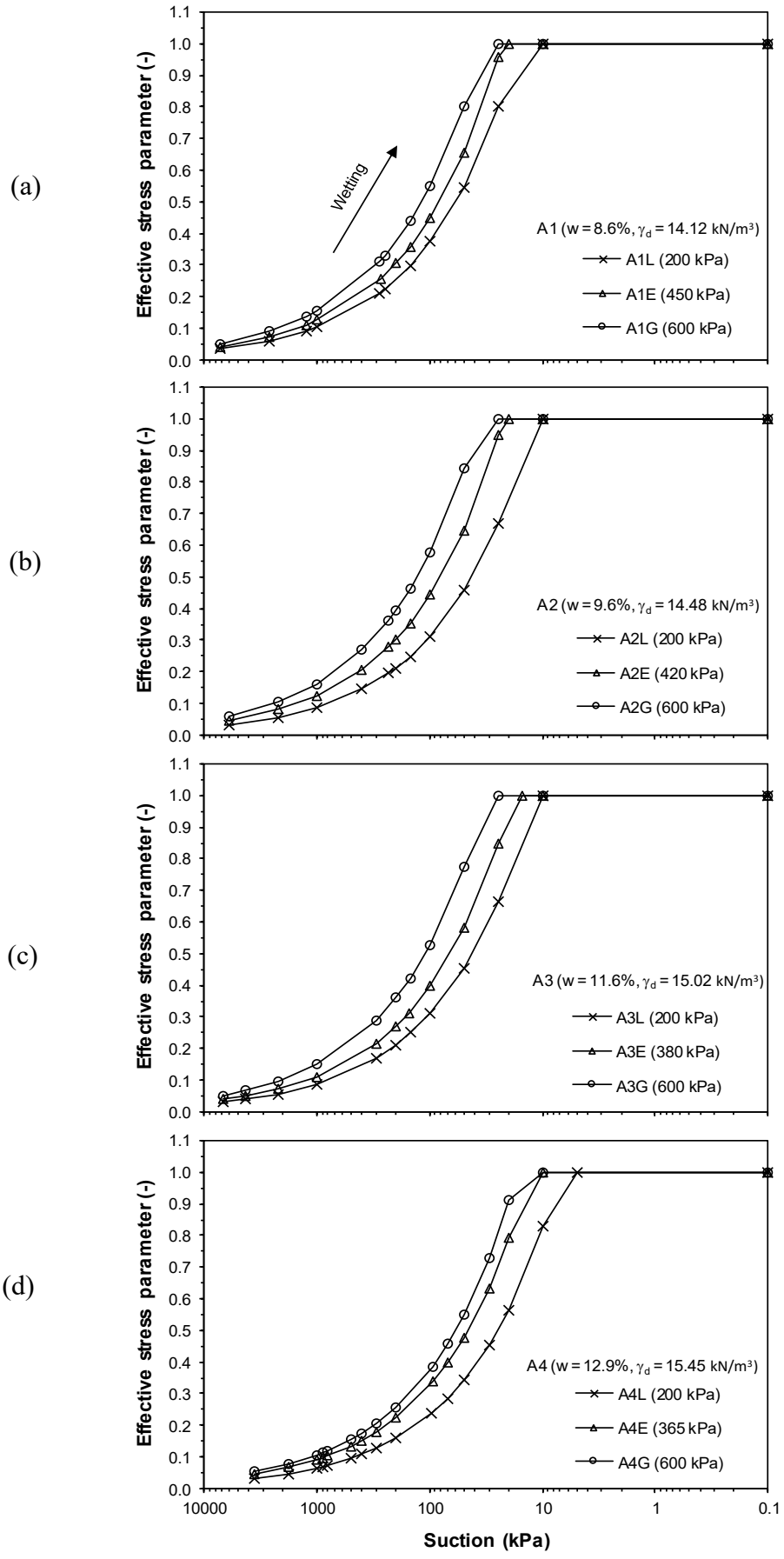

Figure 8.4 Effective stress parameter of specimens (a) A1, (b) A2, (c) A3 and (d) A4

8.3.3 Suction Stress Characteristic Curve (SSCC)

By following the aforementioned steps in Section (8.2.2), the SSCCs of the compacted specimens in groups A1, A2, A3 and A4 were established as shown in Figures 8.5 (a-c) to 8.8 (a-c), respectively.

Based on the entire SWCCs in terms of the effective saturation provided in Figures (8.5a to 8.8a), the fitting parameters were derived and summarised in Table (8.2). For a given specimen, the indicator of the pore size distribution ( ) was found to increase, whereas α (inverse of air expulsion pressure) decreased with the increase in the applied vertical pressure. Similarly, and α values were also different for various specimen conditions.

It can be seen in Figures (8.5b and c to 8.8 b and c) that the suction stress increased gradually (i.e., became less negative) with increasing effective saturation and decreasing matric suction until it reached zero at saturation. The SSCCs were also found to be affected by the applied net vertical stress. At the same matric suction, higher the applied net stress smaller was the suction stress, indicating upward shifting in the SSCCs. The dependence of the SSCCs on the applied vertical net stress obtained in this study is dissimilar to the reported results in the literature for soils having unique SWCCs and consequently unique SSCCs under different applied load (Oh and Lu 2014; Haeri et al. 2016). This behaviour is related to the dependence of the SWCCs of the tested soil specimens on the void ratio (see Figures 7.9a-d).

(a)

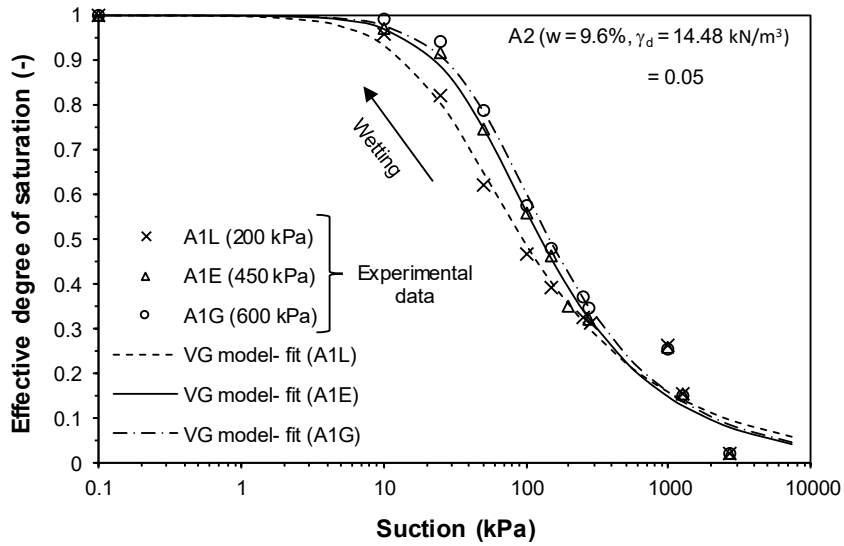

(b)

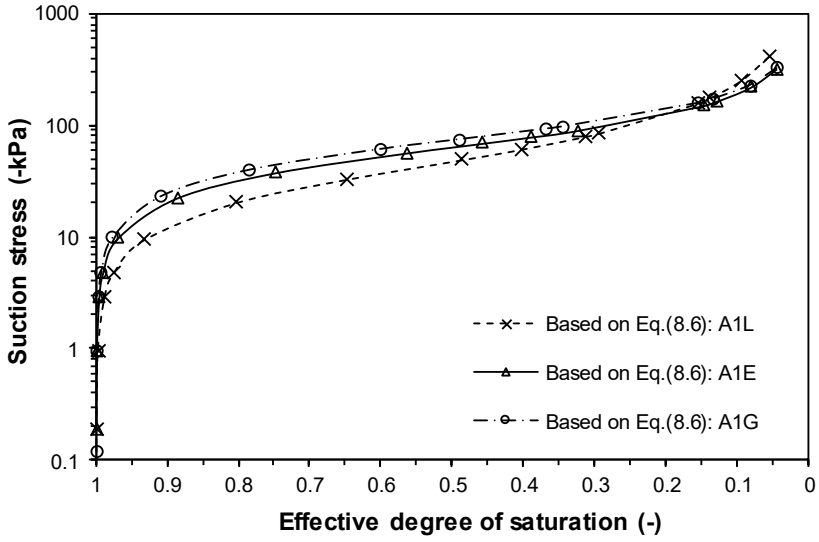

(c)

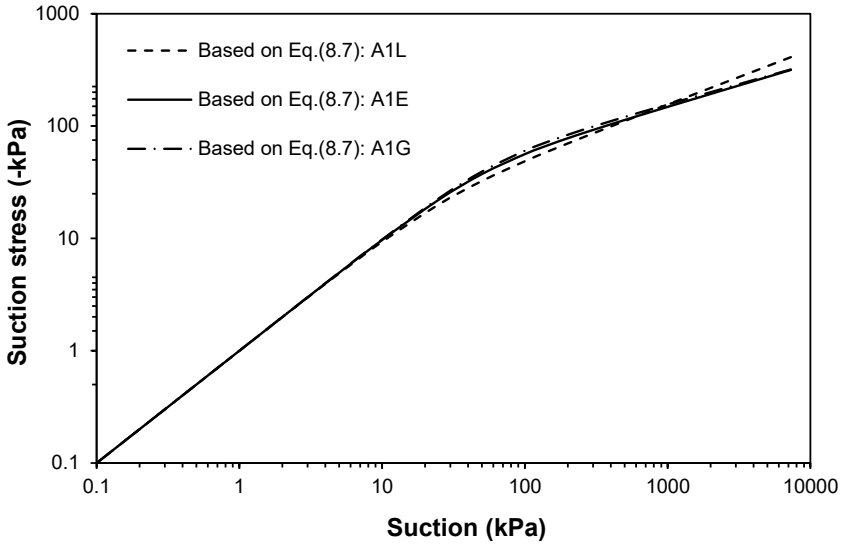

Figure 8.5 SWCCs in terms of effective saturation and SSCCs in terms of (b) effective saturation and (c) suction of specimens in groups A1

(a)

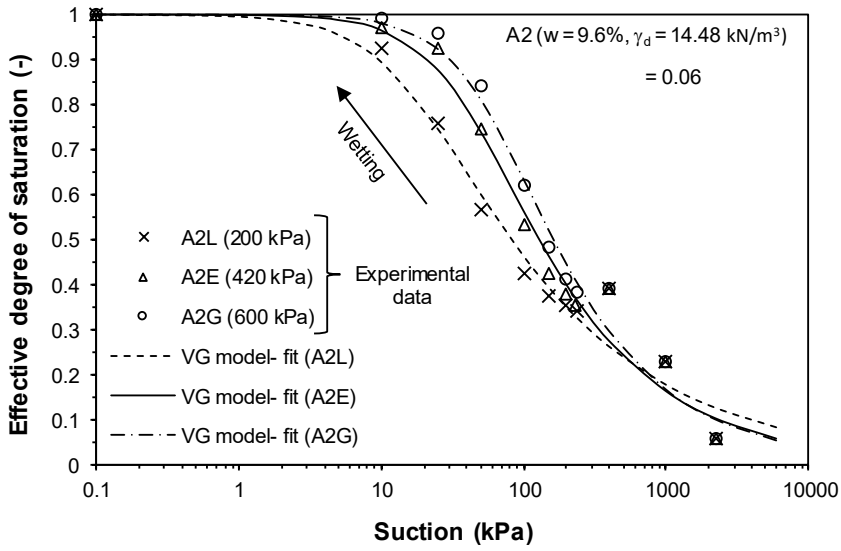

(b)

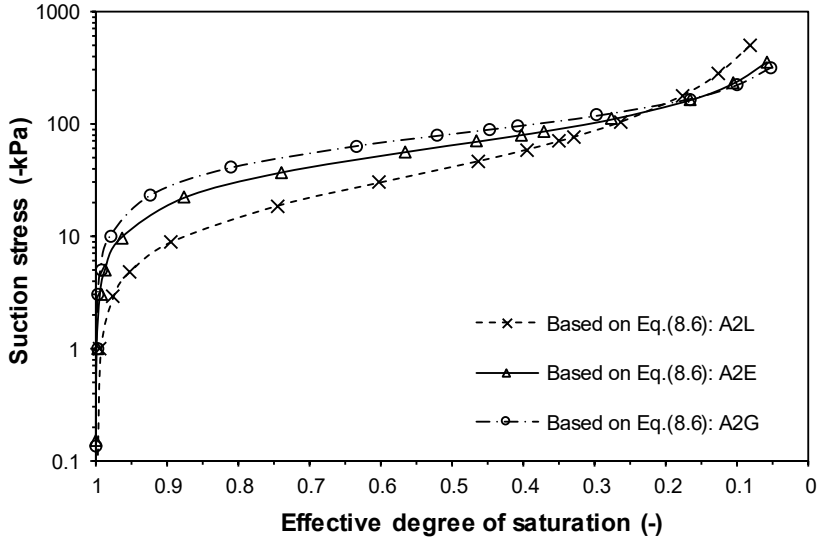

(c)

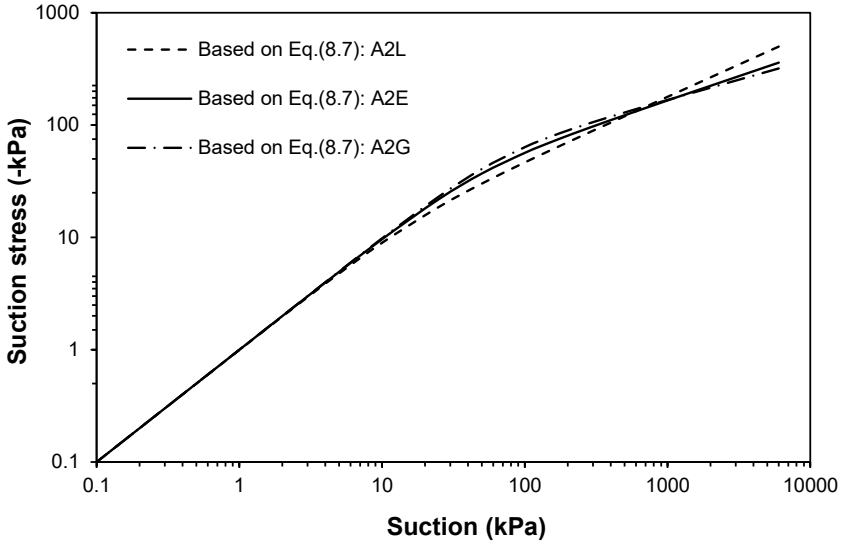

Figure 8.6 SWCCs in terms of effective saturation and SSCCs in terms of (b) effective saturation and (c) suction of specimens in groups A2

(a)

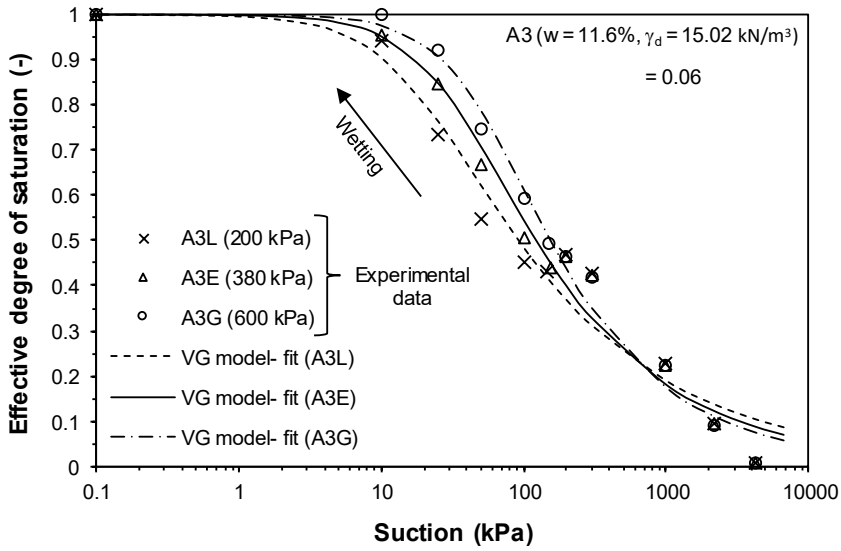

(b)

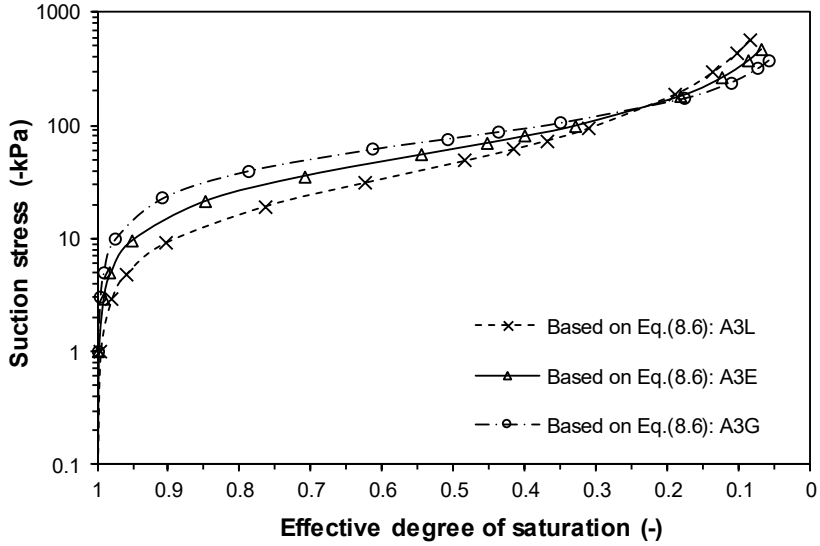

(c)

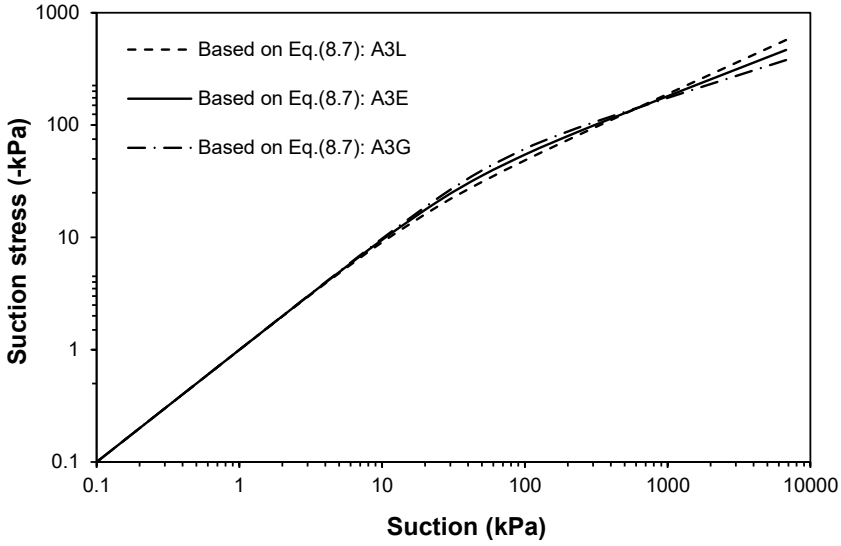

Figure 8.7 SWCCs in terms of effective saturation and SSCCs in terms of (b) effective saturation and (c) suction of specimens in groups A3

(a)

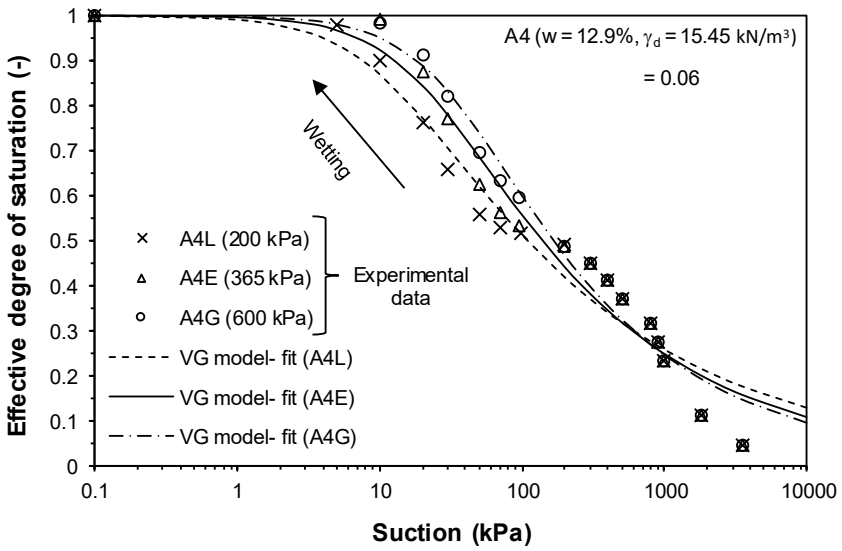

(b)

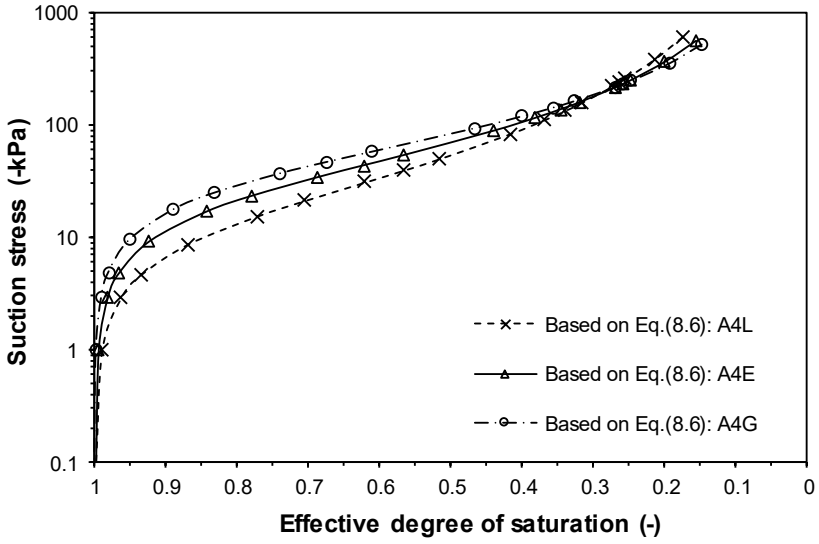

(c)

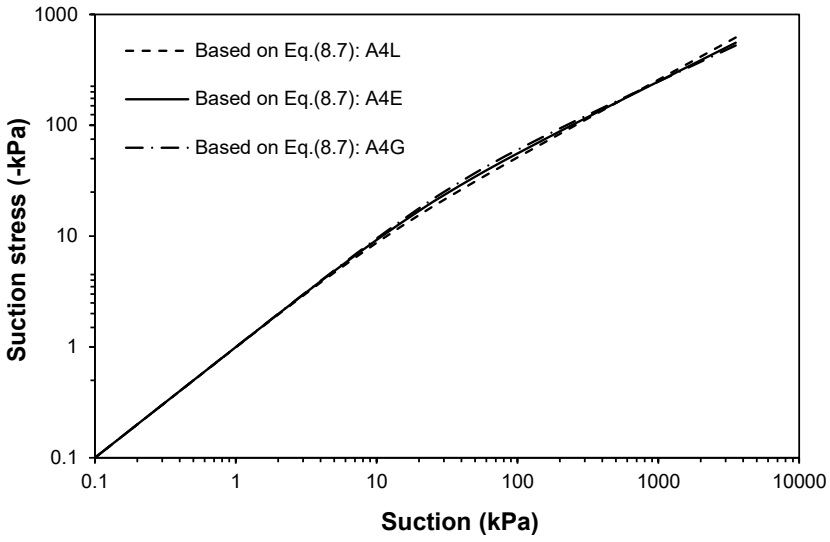

Figure 8.8 SWCCs in terms of effective saturation and SSCCs in terms of (b) effective saturation and (c) suction of specimens in groups A4

Table 8.2 van Genuchten model fitting parameters for all specimens

Specimen no.	Vertical net stress, (kPa)	Fitting parameters			R^2
			(kPa^{-1})	(kPa)	
A1L	200	1.513	0.038	26.3	0.9978
A1E	450	1.620	0.022	45.5	0.9980
A1G	600	1.640	0.018	55.6	0.9982
A2L	200	1.426	0.057	17.5	0.9970
A2E	410	1.569	0.023	43.5	0.9976
A2G	600	1.642	0.016	62.5	0.9981
A3L	200	1.420	0.053	18.9	0.9949
A3E	380	1.505	0.029	34.5	0.9969
A3G	600	1.596	0.019	52.6	09979
A4L	200	1.305	0.085	11.8	0.9965
A4E	365	1.364	0.046	21.7	0.9968
A4G	600	1.408	0.030	33.3	0.9980

Together the results presented in Figures (8.5 to 8.8) and Table (8.2) revealed that for soil specimens having different SWCCs as influenced by the applied stress and compaction conditions, different values of fitting parameters were obtained and therefore the predicted suction stress was varied.

8.3.4 Collapse behaviour based on effective stress

At a constant applied vertical net stress, changes in the effective stress of unsaturated soils are mainly related to changes in the matric suction. The effective stress parameters (Figures 8.4a-d) and the SSCCs (Figures 8.5b to 8.8b) enabled determination of effective stress changes during the wetting process at a constant applied vertical stress by using Equations (8.1) and (8.8), respectively.

Figures 8.9 (a-d) show the effective stress-collapse strain results of specimens in groups A1, A2, A3 and A4 under the three applied vertical net stresses. Based on both approaches (single effective stress and suction stress) and at a given applied net stress, the effective stress decreased with the increase in the collapse strain until it reduced to the applied vertical net stress by the end of the wetting.

For a given specimen and at a constant vertical net stress, the part of effective stress resulted from suction changes during wetting was found to be higher in the suction stress approach than that calculated by the single effective stress as can be seen clearly in Figures 8.9 (a-d). The reason could be that the suction stress based on the SWCCs compared to the measured one was over-predicted as has been reported by Pourzargar et al. (2014); Alsherif and McCartney (2014).

Although the reduction of effective stress during wetting would indicate swelling, the collapse behaviour has been considered to be compatible with the effective stress concept. Collapse has been interpreted to occur due to (i) local shear failure between soil particles (Barden et al. 1973), (ii) multi-directional failure at the grain level (Lu 2011), and (iii) suction decrease which produced higher volume decrease than the amount of volume increase (expand, dilation or elastic rebound) resulted from the decrease in the effective stress (Garakani et al. 2015). The post-failure behaviour of collapsible soils was completely described under the effective stress framework with a proper plasticity model (Khalili et al. 2004).

The interpretation of collapse behaviour based on the effective stress concept in unsaturated soils was compared to the interpretation provided by the total stress. Figure (8.10) shows a typical collapse result obtained by the suction-controlled oedometer test that was analysed based on the effective stress and the collapse result obtained by the single oedometer test that was analysed based on the total stress.

(a)

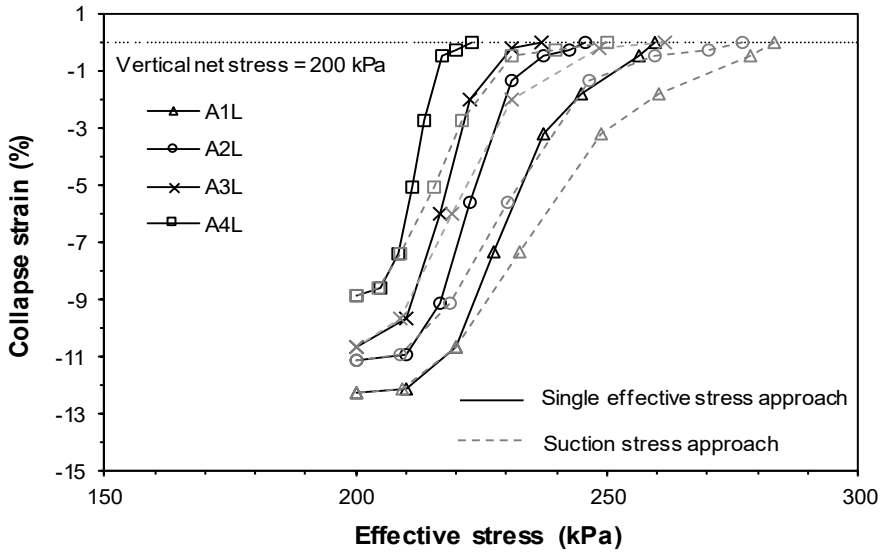

(b)

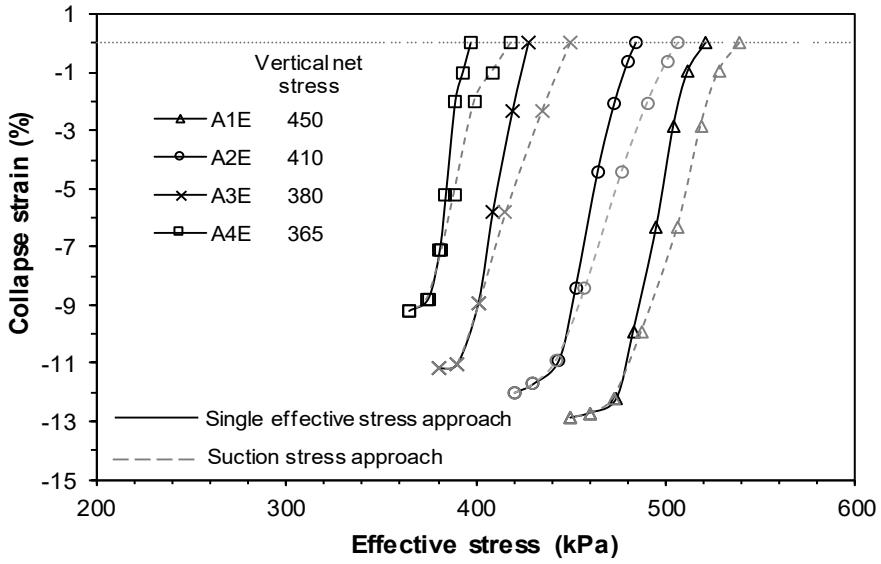

(c)

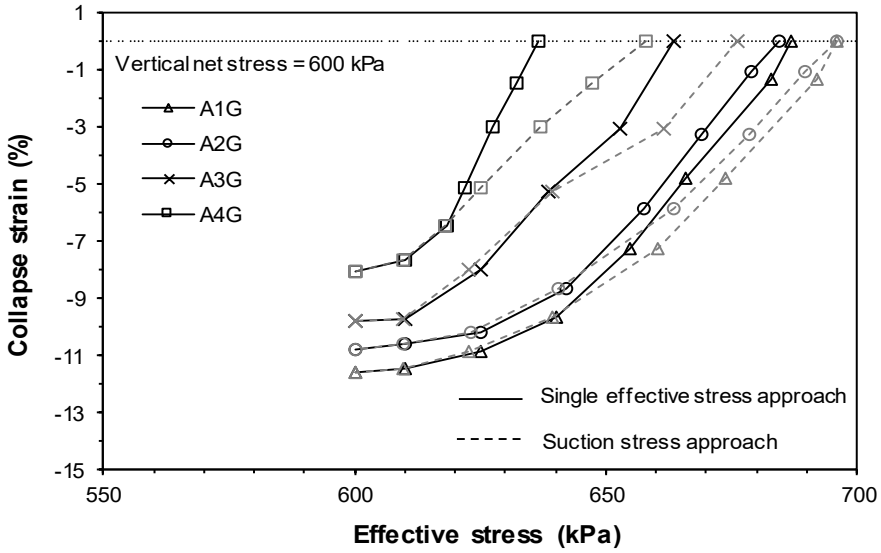

Figure 8.9 Effective stress changes with soil collapse of all specimens at the vertical net stress of (a) 200 kPa, (b) compaction pressure and (c) 600 kPa

The example presented in Figure (8.10) is for the specimen in group A1 subjected to the vertical stress of 200 kPa tested by using both conventional oedometer and suction-controlled oedometer showing changes in the void ratio during loading and wetting.

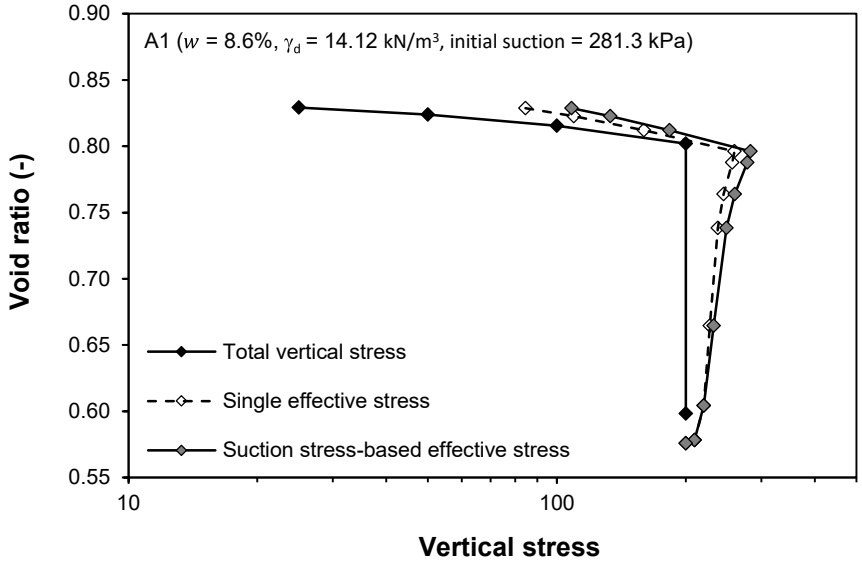

Figure 8.10 Collapse behaviour in two interpretations, total and effective stress

After the static compaction of the specimen A1, the initially measured matric suction was 281.3 kPa and the air expulsion suction was 16.7 kPa, which translates into the effective stress of 59.6 kPa based on the single effective stress and into 83.3 kPa based on the suction stress approach (Figure 8.9a). During loading at a constant water content, the initial matric suction remained almost constant, while the change in effective stress corresponded to the applied vertical stress. During wetting, the decrease in suction produced a reduction in the effective stress.

It can also be seen in Figure (8.10) that the final void ratio reached at the end of the wetting was relatively greater in the single step wetting by the conventional oedometer than the ones reached during the stepwise wetting by the suction-controlled oedometer.

8.4 Concluding remarks

In this chapter, the experimental results of suction-controlled oedometer tests presented in Chapter 7 were re-analysed based on the effective stress in unsaturated soils expressed as the sum of two components: the net stress and a scaled value of suction. Two effective stress approaches (i.e., single effective stress and suction stress) were chosen for the analysis. The main findings obtained from this chapter can be summarised as follows:

1. Based on the single effective stress by Khalili and Khabbaz (1998), the effective stress parameter (χ) increased gradually with the suction reduction until it reached 1 at the air expulsion suction. This observation agreed well with the findings of (Zargarbashi and Khalili 2011). The results also showed that χ values varied with the applied stress and specimen compaction conditions. The χ of a specimen subjected to higher applied stress was found to be higher at a given matric suction. At a given applied net stress, specimens with smaller compaction pressure have smaller values of χ.
2. Based on suction stress approach by Lu et al (2010), the suction stress increased with decreasing matric suction until it reached zero at saturation. The established SSCCs were significantly affected by the change of vertical net stress. The suction stress at higher applied vertical net stress was found to be smaller at a given applied matric suction. The SSCCs were also found to be non-unique at different compaction conditions of the same soil as indicated by the different values of the fitting parameters (and α). Therefore, it can be concluded that the applied stress and compaction conditions were the controlling factors of the SSCCs for the same soil.

3. Based on both the single effective stress and suction stress approaches, the increase in the effective stress parameter and suction stress resulted from the reduction of matric suction was found to cause a decrease in the effective stress during the soil collapse. A similar observation has been reported in the literature (Lu 2011; Brink et al 2014; Garakani et al. 2015). A comparison of the two approaches revealed that the proportion of suction contribution to the effective stress was higher in the suction stress approach than the single effective stress at a given vertical net stress.

Chapter 9

Conclusions and recommendations

9.1 Introduction

Unsaturated compacted soils are used in many civil engineering applications, such as earth dams, embankments, foundations, roadways and canals. Compacted soils tend to collapse upon wetting under certain conditions. The wetting-induced collapse of unsaturated soils is controlled by several factors including soil suction, applied stress and the initial compaction conditions. The aim of this thesis was to study the one-dimensional volume change behaviour and SWCCs of compacted collapsible soils when subjected to various loading, wetting and compaction conditions.

The material used in this investigation was a mixture of 40% silt, 40% sand and 20% Speswhite kaolin. Selection of the material was based on the reported composition of collapsible soils in the literature and on the results of preliminarily single oedometer tests (Section 3.2). The physical and compaction properties of the material used was determined following the standard laboratory procedures. As per the British Standard, the prepared soil was classified as sandy clay with low plasticity (CLS). Compacted specimens were prepared by statically compacting the soil-water mixtures at several dry densities and water contents. Specimens were subjected to either constant static compaction pressure or constant static compaction energy during preparation.

Four series of tests were carried out on the material used. In Test series I, static compaction behaviour and suction measurements were investigated (Chapter 4). A detailed procedure of static compaction tests was introduced that enables establishing static compaction curves both in terms of compaction pressure and compaction energy at various levels. The established static compaction curves were used to define the initial conditions of soil specimens for the main testing programme. The proposed static compaction tests were evaluated by identifying the factors influencing the results and studying suction changes induced by compaction. In Test series II, collapse behaviour of compacted specimens along the established static compaction curves was studied (Chapter 5). The impact of applying constant compaction energy or pressure during specimen preparation on the collapse behaviour during single and double oedometer tests was evaluated over a wide range of applied vertical stress. In Test series III, limitations and advantages of testing single and multiple specimens during wetting tests using a suction-controlled oedometer were investigated (Chapter 6). Identical compacted specimens were taken through wetting process under a constant applied stress by adopting various testing procedures. Compatibility of the test results obtained from different wetting paths was explored, and accordingly, the convenient testing procedure was chosen for the remaining work of this thesis. In Test series IV (Chapter 7), collapse behaviour both in terms of volume change and water-retention characteristics was studied by conducting suction-controlled oedometer wetting tests. The effects of different applied net stresses and compaction conditions were explored. The results presented in Chapter 7 were replotted in terms of the effective stress in unsaturated soils using the single effective stress and suction stress approaches (Chapter 8).

9.2 Conclusions

Based on the findings reported in this thesis, the following conclusions were drawn. Some of these conclusions (3, 4 and 11) are in consistency with the findings reported in the literature and the others represent the key findings of this study.

Static compaction and suction

1. The static compaction pressure was found to decrease linearly with increasing the water content of specimens at a given compaction energy, whereas the transmitted compaction energy to apply a constant compaction pressure was found to increase linearly with increasing the water content of specimens.
2. The established static compaction curves were found to be influenced by the size of the compaction mould used, the displacement rate applied during the compaction process and less by the amount of initial soil mass of specimens used for compaction.
3. The measured suction of specimens with increased dry density by compaction was found to decrease at initially low-water contents, whereas it increased for specimens with relatively high-water contents as indicated by the two different slopes of the established suction contours on the compaction plane.

Collapse at different loading and static compaction efforts

4. For a given specimen condition, the exhibited collapse strain was found to be influenced by the applied vertical stress at wetting. The collapse strain increased linearly with the logarithmic increase in the applied vertical stress and decreased thereafter. The maximum collapse strain of the statically

compacted specimens was found to be reached when the applied vertical stress equals to the applied compaction pressure during specimen preparation.

5. For specimens along the static compaction energy curve, the decrease in the applied compaction pressure contributed to a linear reduction in their collapse strain at a given applied vertical stress. In contrast, increasing the transmitted compaction energy for specimens along the static compaction pressure curve produced constant collapse strain at a given applied vertical stress. Therefore, the collapse behaviour was found to be predominantly controlled by the applied static compaction pressure during specimen preparation. This behaviour is attributed to the corresponding relationship of the applied compaction pressure and the applied vertical stress at the maximum collapse strain.

Collapse and SWCCs at various wetting tests

6. The initial suction of practically identical compacted specimens measured by the null-type tests using the suction-controlled oedometer was found to be similar, but the suction equilibrium time was different. The behaviour is due to the dependence of the suction value on the initial water content of specimens and the dependence of suction equilibrium time on the water phase continuity between the specimen, ceramic disk and the water compartment.
7. Compatible results were obtained by testing single and multiple specimens under constant applied net stress but various testing procedures during the suction-controlled oedometer wetting tests. Therefore, collapse strain and SWCCs of identical compacted specimens were found to be independent of the adopted procedure of the suction-controlled oedometer wetting tests.

Collapse and SWCCs at various vertical stress and compaction conditions

8. For a given compacted specimen, the combined effect of the applied vertical net stress and matric suction resulted in two distinct trends of collapse and water-absorption behaviour. The collapse was found to be greater at higher applied net stress and high suctions, whereas maximum collapse reached when the applied stress equals to the compaction pressure at low matric suctions. The water content- SWCCs were identical at high suctions, while smaller water content was observed at higher applied net stress and low suctions. The degree of saturation-SWCCs shifted upward at higher applied net stress and high suctions, whereas at low suctions the SWCCs were independent of the applied stress.
9. For specimens along the static compaction energy curve, the applied compaction pressure during specimen preparation was found to affect both the collapse and water absorption behaviour. The collapse strain decreased with decreasing the applied static compaction pressure at a given applied net stress. The SWCCs in terms of both water content and degree of saturation were found to be independent of the initial compaction conditions at the early steps of wetting, while at low suction range, the SWCC of the specimen with smaller compaction pressure was notably upper those with larger compaction pressure.

Collapse based on effective stress in unsaturated soils

10. The fitting parameters of the wetting SWCCs required for the calculation of the effective stress both by the single effective and suction stress approaches were found to be significantly affected by the applied stress and the compaction conditions for the same soil.

11. Based on the single effective stress and suction stress approaches, the effective stress was found to decrease during the collapse for all the tested samples, indicating a decrease in the shear strength at the inter particle level and suggesting the validity of the investigated effective stress approaches in decreasing the collapse behaviour.

9.3 Recommendations for future research

Although this study has provided insights into the general behaviour of unsaturated compacted soil subjected to a variety of loading, wetting and compaction conditions, several areas of the work presented in this thesis have been identified as requiring further research including:

1. Investigating the collapse behaviour of compacted soils with different conditions to those considered in this research, such as dynamically compacted specimens, different soil mixtures and different loading conditions.
2. Developing elasto-plastic models of the collapse behaviour along the compaction curves. This would enable the prediction of the collapse strain at various compaction conditions and applied stresses.
3. Future experimental work should also include investigating the microstructure of the compacted soils by Environmental Scanning Electron Microscopy and MIP tests. Such tests would enhance the interpretation of the collapse behaviour.
4. Studying the effect of wetting/drying cycles at a wide range of vertical net stress, suction and compaction conditions on the collapse behaviour is

recommended. Such study would simulate the field conditions when the climate is changing.

5. It would be advisable to investigate the collapse strain induced by increasing the vertical net stress at a constant suction for a collapsible soil at different compaction conditions. Such study would simulate the construction of a new structure on the collapsible soil and could give a clearer picture of the collapse behaviour.

References

Agus, S.S. and Schanz, T. 2005. Comparison of four methods for measuring total suction. *Vadose Zone Journal* 4(4), pp. 1087–1095.

Airò Farulla, C., Ferrari, A. and Romero, E. 2010. Volume change behaviour of a compacted scaly clay during cyclic suction changes. *Canadian Geotechnical Journal* 47(6), pp. 688–703.

Airò Farulla, C. and Ferrari, A. 2005. Controlled suction oedometric tests: analysis of some experimental aspects. *In: Proceedings of an International Symposium on Advanced Experimental Unsaturated Soil Mechanics*. Trento, Italy, 27–29 June. pp. 43–48.

Al-Janabi, A. 2014. *Hydro-mechanical analysis of unsaturated collapsible soils and their stabilization*. PhD Thesis. Kiel University.

Al-Obaidi, Q.A.J. 2014. *Hydro-mechanical behaviour of collapsible soils*. PhD Thesis, Ruhr University.

Al-Saoudi, N., Al-Khafaji, A.N. and Al-Mosawi, M. 2013. Challenging problems of gypseous soils in Iraq. *In: Proceedings of the 18th International Conference on Soil Mechanics and Geotechnical Engineering*. Paris, pp. 479–482.

Alonso, E.E., Gens, A. and Hight, D.W. 1987. Special problem soils. General report. *In: Proceedings of the 9th European Conference on Soil Mechanics and Foundation Engineering*. Dublin. pp. 1087–1146.

Alonso, E.E., Gens, A. and Josa, A. 1990. A constitutive model for partially saturated soils. *Géotechnique* 40(3), pp. 405–430.

Alonso, E.E., Gens, A. and Lloret, A. 1993. The landslide of Cortes de Pallas, Spain. *Géotechnique* 43(4), pp. 507–521.

Alonso, E.E., Vaunat, J., Pereira, J.-M. and Olivella, S. 2010. A microstructurally based effective stress for unsaturated soils. *Géotechnique* 60(12), pp. 913–925.

Alonso, E.E., Pinyol, N.M. and Gens, A. 2013. Compacted soil behaviour: initial state, structure and constitutive modelling. *Géotechnique* 63(6), pp. 463–478.

Alsherif, N.A. and McCartney, J.S. 2014. Effective stress in unsaturated silt at low degrees of saturation. *Vadose Zone Journal* 13(5), pp. 1–41.

Asmani, M.Y.D., Hafez, M.A. and Shakri, M.S. 2013. Comparison between static and dynamic compaction for California Bearing Ratio (CBR). *Electronic Journal of Geotechnical Engineering* 18, pp. 5857–5869.

Assallay, A.M., Rogers, C.D.F. and Smalley, I.J. 1997. Formation and collapse of metastable particle packings and open structures in loess deposits. *Engineering Geology* 48(1), pp. 101–115.

ASTM D1557-07 2007. Standard test methods for laboratory compaction characteristics of soil using modified effort (56,000 ft-lbf/ft^3 (2,700 kN-m/m^3). ASTM Standards.

ASTM D4546-14 2014. Standard test methods for one-dimensional swell or collapse of soils. ASTM Standards, pp. 1–10.

ASTM D4943-10 2010. Standard test method for shrinkage factors of soils by the wax method. ASTM Standards, pp. 1–5.

ASTM D5333-03 2003. Standard test method for measurement of collapse potential of soils. ASTM Standards, pp. 1–4.

ASTM D698-00 2000. Standard test methods for laboratory compaction characteristics of soil using standard effort (12 400 ft-lbf/ft^3 (600 kN-m/m^3). Method A (Standard Proctor).

Aversa, S. and Nicotera, M.V. 2002. A triaxial and oedometer apparatus for testing unsaturated soils. *ASTM Geotechnical Testing Journal* 25(1), pp. 3–15.

Ayadat, T. and Hanna, A. 2007. Prediction of collapse behaviour in soil. *Revue Européenne de Génie Civil* 11(5), pp. 603–619.

Aziz, A.A., Ali, F.H., Heng, C.F., Mohammed, T.A. and Huat, B.B.K. 2006. Collapsibility and volume change behavior of unsaturated Residual soils. *American Journal of Environmental Sciences* 2(4), pp. 161–166.

Baille, W., Tripathy, S. and Schanz, T. 2014. Effective stress in clays of various mineralogy. *Vadose Zone Journal* 13(5), pp. 1–10.

Baille, W., Lang, L., Tripathy, S. and Schanz, T. 2016. Influence of effective stress on swelling pressure of expansive soils. *In: E3S Web of Conferences 9*. EDP Sciences, pp. 3–7.

Barden, L., McGown, A. and Collins, K. 1973. The collapse mechanism in partly saturated soil. *Engineering Geology* 7(1), pp. 49–60.

Basma, A.A. and Tuncer, E.R. 1992. Evaluation and control of collapsible soils. *Journal of Geotechnical Engineering* 118(10), pp. 1491–1504.

Beer, F.P. and Johnston, E.R. 1990. *Vector Mechanics for Engineers-Dynamic*. McGraw-Hill Book Company, Singapore.

Bell, F.G. and Culshaw, M.G. 2001. Problem soils: a review from a British perspective. *In: Proceeding of Problematic Soils Conference*. Nottingham, 8 November, pp. 1–37.

Bishop, A.W. 1959. The effective stress principle. *Teknisk Ukeblad* 39, pp. 859–863.

Bishop, A.W. and Blight, G.E. 1963. Some aspects of effective stress in saturated and partly saturated soils. *Géotechnique* 13(3), pp. 177–197.

Bishop, A.W. and Donald, I.B. 1961. The experimental study of partly saturated soil in the triaxial apparatus. I*n: Proceedings of the 5th International Conference on Soil Mechanics and Foundation Engineering*. Paris. pp. 13–21.

Blatz, J.A., Cui, Y.-J. and Oldecop, L. 2008. Vapour Equilibrium and Osmotic Technique for Suction Control. *Geotechnical and Geological Engineering* 26(6), pp. 661–673.

Bocking, K. and Fredlund, D.G. 1980. Limitations of the axis translation technique. *In: Proceedings of the 4th International Conference on Expansive Soils*. Denver, Colorado, June 16–18, pp. 117–135.

Booth, A.R. 1977. *Collapse settlement in compacted soils*. CSIR Research Report 324, NITRR Bulletin13, Council for Scientific and Industrial Research, Pretoria, South Africa, pp. 1–34.

Brink, G. and Heymann, G. 2014. Soil collapse from an effective stress perspective. *Journal of the South African Institution of Civil Engineering* 56(3), pp. 30–33.

Brooks, R.H. and Corey, A.T. 1964. Hydraulic properties of porous media. *Colorado State University, Hydrology Paper*. 3(3), pp. 1–27.

BS 1377-2 1990. Methods of test for soils for civil engineering purposes: Part 2: Classification tests. British Standard Institution.

BS 1377-4 1990. Methods of test for soils for civil engineering purposes: Part 4: Compaction-related tests. British Standard Institution.

BS 1377-5 1990. Methods of test for soils for civil engineering purposes: Part 5: Compressibility, permeability and durability tests. British Standard Institution.

Bulut, R. and Leong, E.C. 2008. Indirect measurement of suction. *Geotechnical and Geological Engineering* 26(6), pp. 633–644.

Burger, C.A. and Shackelford, C.D. 2001. Soil-water characteristic curves and dual porosity of sand–diatomaceous earth mixtures. *Journal of Geotechnical and Geoenvironmental Engineering* 127(9), pp. 790–800.

Burland, J.B. 1965. Some aspects of the mechanical behaviour of partly saturated soils. *In: Moisture Equilibria and Moisture Changes in Soils Beneath Covered Areas, A Symposium in Print*. Butterworth, Sidney, Australia. pp. 270–278.

Campbell, G.S., Smith, D.M. and Teare, B.L. 2007. Application of a dew point method to obtain the soil water characteristic. In: Schanz, T. ed. *Experimental Unsaturated Soil Mechanics*. Springer, Berlin, Heidelberg, pp. 71–77.

Cardoso, R., Romero, E., Lima, A. and Ferrari, A. 2007. A Comparative study of soil suction measurement using two different high-range psychrometers. *In: Schanz, T. ed. Experimental Unsaturated Soil Mechanics*. Springer, Berlin, Heidelberg., pp. 79–93.

Casagrande, A. 1936. The determination of the pre-consolidation load and its practical significance. *In: Proceedings of the International Conference on Soil Mechanics and Foundation Engineering*. Harvard University Cambridge, pp. 60–64.

Cetin, H., Fener, M., Söylemez, M. and Günaydin, O. 2007. Soil structure changes during compaction of a cohesive soil. *Engineering Geology* 92(1–2), pp. 38–48.

Chae, J., Kim, B., Park, S. wan and Kato, S. 2010. Effect of suction on unconfined compressive strength in partly saturated soils. *KSCE Journal of Civil Engineering* 14(3), pp. 281–290.

Chen, C., Gao, P. and Hu, Z. 2006. Moistening deformation characteristic of loess and its relation to structure. *Chinese Journal of Rock Mechanics and Engineering* 25(7), pp. 1352–1360.

Chen, Z.H., Fredlund, D.G. and Gan, J.K. 1999. Overall volume change, water volume change, and yield associated with an unsaturated compacted loess. *Canadian Geotechnical Journal* 36(2), pp. 321–329.

Coleman, J.D. 1962. Stress-strain relations for partly saturated soil. *Géotechnique* 12(4), pp. 348–350.

Crispim, F.A., de Lima, D.C., Schaefer, C.E.G.R., de Carvalho Silva, C.H., de Carvalho, C.A.B., de Almeida Barbosa, P.S., et al. 2011. The influence of laboratory compaction methods on soil structure: Mechanical and micromorphological analyses. *Soils and Rocks* 34(1), pp. 91–98.

Croney, D. and Coleman, J.D. 1961. Pore pressure and suction in soil. *In: Proceedings of the Conference on Pore Pressure and Suction in Soils*. Butterworths, London, pp. 31–37.

Decagon Devices. 2007. Commercial publications, operator's manual for models WP4 and WP4-T. Pullman www.decagon.com.

Decagon Devices. 2010. Commercial publications, operator's manual for WP4C Dew Point PotentiaMeter. Pullman www.decagon.com.

Decagon Devices. 2014. Commercial publications, operator's manual for MPS-2 & MPS-6 dielectric water potential sensors. Pullman www.decagon.com.

Delage, P., Audiguier, M., Cui, Y.-J. and Howat, M.D. 1996. Microstructure of a compacted silt. *Canadian Geotechnical Journal* 33(1), pp. 150–158.

Delage, P., Cui, Y.-J. and Antoine, P. 2005. Geotechnical problems related with loess deposits in Northern France. *In: Proceedings of International Conference on Problematic Soils*. pp. 517–540.

Delage, P., Romero, E. and Tarantino, A. 2008. Recent developments in the techniques of controlling and measuring suction in unsaturated soils. *In: Keynote Lecture, Proceedings of the 1st European Conference on Unsaturated Soils. Durham*. CRC Press, pp. 33–52.

Delage, P. and Lefebvre, G. 1984. Study of the structure of a sensitive Champlain clay and of its evolution during consolidation. *Canadian Geotechnical Journal* 21(1), pp. 21–35.

Della Vecchia, G., Dieudonné, A.C., Jommi, C. and Charlier, R., 2015. Accounting for evolving pore size distribution in water retention models for compacted clays. *International Journal for Numerical and Analytical Methods in Geomechanics*, 39(7), pp.702-723.

Dineen, K., Colmenares, J.E., Ridley, A.M. and Burland, J.B. 1999. Suction and volume changes of a bentonite-enriched sand. *Proceedings of the Institution of Civil Engineers-Geotechnical Engineering* 137(4), pp. 197–201.

Dudley, J.H. 1970. Review of collapsing soils. *Journal of Soil Mechanics and Foundations Division, ASCE* 96(3), pp. 925–947.

Elgabu, H.M. 2013. *Critical evaluation of some suction measurement techniques*. PhD Thesis, Cardiff University.

Estabragh, A.R., Javadi, A.A. and Boot, J.C. 2004. Effect of compaction pressure on consolidation behaviour of unsaturated silty soil. *Canadian Geotechnical Journal* 41(3), pp. 540–550.

Evans, R.D., Jefferson, I., Northmore, K.J. and Jackson, P. 2004. In-situ investigation of problematical soils. In: *Advances in Geotechnical Engineering*: The Skempton Conference on 29–31 March. London, UK: Thomas Telford Publishing, pp. 1269–1279.

Fattah, M.Y. and Dawood, B.A. 2016. Collapse potential determination of gypseous soils. *Global Journal of Engineering Science and Research Management* 3(12), pp. 1–12.

Feda, J. 1995. Mechanisms of collapse of soil structure. In: Derbyshire, E. et al. eds. *Genesis and Properties of Collapsible Soils*. Netherlands: Kluwer Academic Publishers, pp. 149–172.

Fookes, P.G. and Best, R. 1969. Consolidation characteristics of some late Pleistocene periglacial metastable soils of East Kent. *Quarterly Journal of Engineering Geology and Hydrogeology* 2(2), pp. 103–128.

Fredlund, D.G. 1975. A diffused air volume indicator for unsaturated soils. *Canadian Geotechnical Journal* 12(4), pp. 533–539.

Fredlund, D.G. 1979. Second Canadian Geotechnical Colloquium: Appropriate concepts and technology for unsaturated soils. *Canadian Geotechnical Journal* 16(1), pp. 121–139.

Fredlund, D.G. 1991. How negative can pore-water pressures get. *Geotechnical News* 9(3), pp. 44–46.

Fredlund, D.G. 2000. The 1999 R.M. Hardy Lecture: The implementation of unsaturated soil mechanics into geotechnical engineering. *Canadian Geotechnical Journal* 37(5), pp. 963–986.

Fredlund, D.G. 2002. Use of soil-water characteristic curves in the implementation of unsaturated soil mechanics. *Proceedings of the 3rd International Conference on Unsaturated Soils*. Recife, Brazil, pp. 20–23.

Fredlund, D.G. 2006. Unsaturated soil mechanics in engineering practice. *Journal of Geotechnical and Geoenvironmental Engineering* 132(3), pp. 286–321.

Fredlund, D.G., Rahardjo, H. and Fredlund, M.D. 2012. *Unsaturated soil mechanics in engineering practice*. John Wiley & Sons, Hoboken, NJ.

Fredlund, D.G. and Gan, J.K.M. 1995. The collapse mechanism of a soil subjected to one-dimensional loading and wetting. In: Derbyshire, E. et al. eds. *Genesis and Properties of Collapsible Soils*. Netherlands: Kluwer Academic Publishers, pp. 173–205.

Fredlund, D.G. and Houston, S.L. 2013. Interpretation of soil-water characteristic curves when volume change occurs as soil suction is changed. In: Caicedo, B. ed. *Advances in Unsaturated Soils*. London: Taylor & Francis Group, pp. 15–31.

Fredlund, D.G. and Morgenstern, N.R. 1977. Stress state variables for unsaturated soils. *Journal of the Geotechnical Engineering Division, ASCE* 103(GT5), pp. 447–466.

Fredlund, D.G. and Rahardjo, H. 1993. *Soil mechanics for unsaturated soils*. John Wiley & Sons, Inc. New York.

Fredlund, D.G. and Xing, A. 1994. Equations for the soil-water characteristic curve. *Canadian Geotechnical Journal* 31(4), pp. 521–532.

Futai, M.M. and Almeida, M.S.S. 2005. An experimental investigation of the mechanical behaviour of an unsaturated gneiss residual soil. *Géotechnique* 55(3), pp. 201–213.

Gallage, C.P.K. and Uchimura, T. 2010. Effects of dry density and grain size distribution on soil-water characteristic curves of sandy soils. *Soils and Foundations* 50(1), pp. 161–172.

Gallipoli, D., Wheeler, S.J. and Karstunen, M. 2003. Modelling the variation of degree of saturation in a deformable unsaturated soil.*Géotechnique*.53(1), pp.105–12.

Gan, J.K.M., Fredlund, D.G. and Rahardjo, H. 1988. Determination of the shear strength parameters of an unsaturated soil using the direct shear test. *Canadian Geotechnical Journal* 25(3), pp. 500–510.

Gao, Y. and Sun, D. 2017. Soil-water retention behavior of compacted soil with different densities over a wide suction range and its prediction. *Computers and Geotechnics* 91, pp. 17–26.

Garakani, A.A., Haeri, S.M., Khosravi, A. and Habibagahi, G. 2015. Hydro-mechanical behavior of undisturbed collapsible loessial soils under different stress state conditions. *Engineering Geology* 195, pp. 28–41.

Garcia-Bengochea, I. 1979. Pore distribution and permeability of silty clays. *Journal of Geotechnical Engineering Division* 105, pp. 839–856.

van Genuchten, M.T. 1980. A closed-form equation for predicting the hydraulic conductivity of unsaturated soils. *Soil Science Society of America Journal* 44(5), pp. 892–898.

van Genuchten, M.T., Leij, F.J. and Yates, S.R. 1991. The RETC code for quantifying the hydraulic functions of unsaturated soils. Ada, Okla: US Environmental Protection Agency.

Goldsmith, W. 1960. Impact: *The theory and physical behavior of colliding solids*. London: Edward Arnold Ltd.

Gonzalez, N.A. and Colmenares, J.E. 2006. Influence of matric suction on the volume change behavior of a compacted clayey soil. *Geotechnical Special Publication* 147(1), pp. 825–836.

Habibagahi, G. and Mokhberi, M. 1998. A hyperbolic model for volume change behavior of collapsible soils. *Canadian Geotechnical Journal* 35(2), pp. 264–272.

Haeri, S.M., Khorshidi, M., Akbari Garakani, A. and Garakani, A.A. 2012. Variation of the volume change and water content of undisturbed loessial samples in controlled matric suction odometer tests. *In: 4th International Conference on Problematic Soils*. Wuhan, China. pp. 1–8.

Haeri, S.M., Garakani, A.A., Khosravi, A. and Meehan, C.L. 2014. Assessing the hydro-mechanical behavior of collapsible soils using a modified triaxial test device. *Geotechnical Testing Journal* 37(2).

Haeri, S.M., Khosravi, A., Garakani, A.A. and Ghazizadeh, S. 2016. Effect of soil structure and disturbance on hydromechanical behavior of collapsible loessial soils. *International Journal of Geomechanics* 17(1), pp. 1–15.

Haeri, S.M., Beigi, M., Saberi, S. and Garakani, A.A. 2016. Study on the stress path dependency of collapse behavior of Gorgan loess implementing unsaturated oedometer devices. *In: E3S Web of Conferences, EDP Sciences*, pp. 1–6.

Hafez, M.A., Doris Asmani, M. and Nurbaya, S. 2010. Comparison between static and dynamic laboratory compaction methods. *Electronic Journal of Geotechnical Engineering* 15(1), pp. 1641–1650.

Head, H.H. 1980. *Manual of soil laboratory testing, volume I: Soil classification and compaction testing*. 1st editio. London: Pentech Press.

Hilf, J.W. 1956. *An investigation of pore water pressure in compacted cohesive soils.* Technical Memo No. 654, US Bureau of Reclamation, Denver, CO.

Houston, S.L., Houston, W.N. and Spadola, D.J. 1988. Prediction of field collapse of soils due to wetting. *Journal of Geotechnical Engineering* 114(1), pp. 40–58.

Houston, S.L., Mahmoud, H.H.H. and Houston, W.N. 1995. Down-hole collapse test system. *Journal of Geotechnical Engineering* 121(4), pp. 341–349.

Houston, S.L., Houston, W.N., Zapata, C.E. and Lawrence, C. 2001. Geotechnical engineering practice for collapsible soils. *Geotechnical and Geological Engineering* 19(3), pp. 333–355.

Houston, S.L. and Houston, W.N. 1997. Collapsible soils engineering. *In: Unsaturated Soil Engineering Practice. ASCE*, pp. 199–232.

Islam, T. and Kodikara, J. 2016. Interpretation of the loading – wetting behaviour of compacted soils within the "MPK" framework. Part I: Static compaction. *Canadian Geotechnical Journal* 53(5), pp. 783–805.

Jennings, J.E. and Knight, K. 1957. The additional settlement of foundations due to a collapse of structure of sandy subsoils on wetting. *In: Proceedings of 4th International Conference on Soil Mechanics and Foundation Engineering*. Butterworths, London, pp. 316–319.

Jennings, J.E.B. and Burland, J.B. 1962. Limitations to the use of effective stresses in partly saturated soils. *Géotechnique* 12(2), pp. 125–144.

Jiang, M., Hu, H. and Liu, F. 2012. Summary of collapsible behaviour of artificially structured loess in oedometer and triaxial wetting tests. *Canadian Geotechnical Journal* 49(10), pp. 1147–1157.

Jotisankasa, A., Ridley, A. and Coop, M. 2007. Collapse behavior of compacted silty clay in suction-monitored oedometer apparatus. *Journal of Geotechnical and Geoenvironmental Engineering* 133(7), pp. 867–877.

Karami, Q., Maleki, M., Makarchian, M. and Karijani, M.S. 2015. Factors affecting mechanical behavior of unsaturated silty sand on wetting path. *Journal of GeoEngineering* 10(2), pp. 45–51.

Kato, S. and Kawai, K. 2000. Deformation characteristics of a compacted clay in collapse under isotropic and triaxial stress state. *Soils and Foundations* 40(5), pp. 75–90.

Khalili, N., Geiser, F. and Blight, G.E. 2004. Effective Stress in Unsaturated Soils: Review with New Evidence. *International Journal of Geomechanics* 4(2), pp. 115–126.

Khalili, N., Habte, M.A. and Zargarbashi, S. 2008. A fully coupled flow deformation model for cyclic analysis of unsaturated soils including hydraulic and mechanical hystereses. *Computers and Geotechnics* 35(6), pp. 872–889.

Khalili, N. and Khabbaz, M.H. 1998. A unique relationship for chi for the determination of the shear strength of unsaturated soils. *Géotechnique* 48(2), pp. 681–687.

Khalili, N. and Zargarbashi, S. 2010. Influence of hydraulic hysteresis on effective stress in unsaturated soils. *Géotechnique* 60(9), pp. 729–734.

Kodikara, J. 2012. New framework for volumetric constitutive behaviour of compacted unsaturated soils. *Canadian Geotechnical Journal* 49(11), pp. 1227–1243.

Krahn, J. and Fredlund, D.G. 1972. On total, matric and osmotic suction. *Soil Science* 114(5), pp. 339–348.

Kurucuk, N., Kodikara, J. and Fredlund, D.G. 2009. Evolution of the compaction process: Experimental study-preliminary results. In: Buzzi, O. et al. eds. *Unsaturated Soils–Theoretical and Numerical Advances in Unsaturated Soil Mechanics*. CRC Press, pp. 887–893.

Lambe, T.W. 1958. The engineering behaviour of compacted clay. *Journal of Soil Mechanics and Foundations Division* 84(2), pp. 1–35.

Lambe, T.W. and Whitman, R. V. 1969. *Soil Mechanics*. John Wiley and Sons, New York.

Lawton, E.C., Fragaszy, R.J. and Hardcastle, J.H. 1989. Collapse of compacted clayey sand. *Journal of Geotechnical Engineering* 115(9), pp. 1252–1267.

Lawton, E.C., Fragaszy, R.J. and Hetherington, M.D. 1992. Review of wetting-induced collapse in compacted soil. *Journal of Geotechnical Engineering* 118(9), pp. 1376–1394.

Lee, H.C. and Wray, W.K. 1995. Techniques to evaluate soil suction-a vital unsaturated soil water variable. In: Alonso, A. A. and Delage, P. E. E. eds. *Unsaturated Soils: Proceedings of the 1st International Conference on Unsaturated Soils*. Paris, 6–8 September: Balkema, Rotterdam, The Netherlands, pp. 615–622.

Lee, I.M., Sung, S.G. and Cho, G.C. 2005. Effect of stress state on the unsaturated shear strength of a weathered granite. *Canadian Geotechnical Journal* 42(2), pp. 624–631.

Lee, P.Y. and Suedkamp, R.J. 1972. Characteristics of irregularly shaped compaction curves of soils. *Highway Research Record* 381, pp. 1–9.

Leong, E.C., Tripathy, S. and Rahardjo, H. 2003. Total suction measurement of unsaturated soils with a device using the chilled-mirror dew-point technique. *Géotechnique* 53(2), pp. 173–182.

Leong, E.C., Tripathy, S. and Rahardjo, H. 2004. A modified pressure plate apparatus. *Geotechnical Testing Journal* 27(3), pp. 322–331.

Leong, E.C., Lee, C.C. and Low, K.S. 2009. An active control system for matric suction measurement. *Soils and Foundations* 49(5), pp. 807–811.

Leong, E.C., Widiastuti, S. and Rahardjo, H. 2013. Estimating wetting-induced settlement of compacted soils using oedometer test. *Geotechnical Engineering* 44(1), pp. 26–33.

Leong, E.C. and Rahardjo, H. 1997. Review of soil-water characteristic curve equations. *Journal of Geotechnical and Geoenvironmental Engineering* 123(12), pp. 1106–1117.

Li, P., Vanapalli, S. and Li, T. 2016. Review of collapse triggering mechanism of collapsible soils due to wetting. *Journal of Rock Mechanics and Geotechnical Engineering* 8(2), pp. 256–274.

Li, X. and Zhang, L.M. 2009. Characterization of dual-structure pore-size distribution of soil. *Canadian Geotechnical Journal* 46(2), pp. 129–141.

Liang, C., Cao, C. and Wu, S. 2016. Hydraulic-mechanical properties of loess and its behavior when subjected to infiltration-induced wetting. *Bulletin of Engineering Geology and the Environment*, pp. 1–13.

Lim, Y.Y. and Miller, G. a. 2004. Wetting-Induced Compression of Compacted Oklahoma Soils. *Journal of Geotechnical and Geoenvironmental Engineering* 130(10), pp. 1014–1023.

Lloret, A., Villar, M. V., Sanchez, M., Gens, A., Pintado, X. and Alonso, E.E. 2003. Mechanical behaviour of heavily compacted bentonite under high suction changes. *Geotechnique* 53(1), pp. 27–40.

Loret, B. and Khalili, N. 2000. A three phase model for unsaturated soils. *International Journal for Numerical and Analytical Methods in Geomechanics* 24(11), pp. 893–927.

Lu, N., Godt, J.W. and Wu, D.T. 2010. A closed-form equation for effective stress in unsaturated soil. *Water Resources Research* 46(5), pp. 1–14.

Lu, N. 2011. Interpreting the “collapsing” behavior of unsaturated soil by effective stress principle. In: Borja, R. I. ed. *Multiscale and multiphysics processes in geomechanics*. Springer, Berlin, Heidelberg, pp. 81–84.

Lu, N., Kaya, M. and Godt, J.W. 2014. Interrelations among the soil-water retention, hydraulic conductivity, and suction-stress characteristic curves. *Journal of Geotechnical and Geoenvironmental Engineering* 140(5), pp. 1–10.

Lu, N. and Likos, W.J. 2004. *Unsaturated soil mechanics*. John Wiley, New York.

Lu, N. and Likos, W.J. 2006. Suction stress characteristic curve for unsaturated soil. *Journal of Geotechnical and Geoenvironmental Engineering* 132(2), pp. 131–142.

Lu, N., Ristow, G.H. and Likos, W.J., 2000. The accuracy of hydrometer analysis for fine-grained clay particles. *Geotechnical Testing Journal* 23(4), pp.487-495.

Malaya, C. and Sreedeep, S. 2012. Critical Review on the Parameters Influencing Soil-Water Characteristic Curve. *Journal of Irrigation and Drainage Engineering* 138(1), pp. 55–63.

Marinho, F.A.M., Take, W.A. and Tarantino, A. 2008. Measurement of matric suction using tensiometric and axis translation techniques. *Geotechnical and Geological Engineering* 26(6), pp. 615–631.

Marinho, F.A.M. and Stuermer, M.M. 2000. The influence of the compaction energy on the SWCC of a residual soil. In: *Advances in Unsaturated Geotechnics*. pp. 125–141.

Matyas, E.L. and Radhakrishna, H.S. 1968. Volume change characteristics of partially saturated soils. *Géotechnique* 18(4), pp. 432–448.

Medero, G.M., Schnaid, F. and Gehling, W.Y.Y. 2009. Oedometer behavior of an artificial cemented highly collapsible soil. *Journal of Geotechnical and Geoenvironmental Engineering* 135(6), pp. 840–843.

Miller, G. a., Khoury, C.N., Muraleetharan, K.K., Liu, C. and Kibbey, T.C.G. 2008. Effects of soil skeleton deformations on hysteretic soil water characteristic curves: Experiments and simulations. *Water Resources Research* 44(5), pp. 1–10.

Miller, H., Djerbib, Y., Jefferson, I.F. and Smalley, I.J. 1998. Modelling the collapse of metastable loess soils. *In: Proceedings of the 3rd International Conference on GeoComputation, University of Bristol.* United Kingdom. Nottingham Trent University, pp. 17–19.

Mitchell, J.K. 2005. *Fundamentals of soil behavior*. 2nd Editio. John Wiley and Sons ed. Inc., New York.

Monroy, R., Zdravkovic, L. and Ridley, A. 2010. Evolution of microstructure in compacted London Clay during wetting and loading. *Géotechnique* 60(2), pp. 105–119.

Mou, C.H. and Chu, T.Y. 1981. Soil-suction approach for evaluation of swelling potential. *Transportation Research Record* 790, pp. 54–60.

Munoz-Castelblanco, J.A., Pereira, J.M., Delage, P. and Cui, Y.J. 2012. The water retention properties of a natural unsaturated loess from northern France. *Géotechnique* 62(2), pp. 95–106.

Muñoz-Castelblanco, J.A., Delage, P., Pereira, J.M. and Cui, Y.J. 2011. An experimental study on the compression and collapse behaviour of a natural loess from Northern France. *In: Proceedings of the 21st European Young Geotechnical Engineers' Conference*. Rotterdam.

Muñoz-Castelblanco, J.A., Pereira, J.M., Delage, P. and Cui, Y.J. 2011. Some aspects of the compression and collapse behaviour of an unsaturated natural loess. *Géotechnique Letters* 1, pp. 17–22.

Murray, E.J. and Sivakumar, V. 2010. *Unsaturated soils: a fundamental interpretation of soil behaviour*. John Wiley & Sons.

Ng, C.W.W. and Menzies, B. 2007. *Advanced unsaturated soil mechanics and engineering*. Taylor and Francis, Abingdon, UK.

Ng, C.W.W. and Pang, Y.W. 2000. Influence of stress state on soil-water characteristics and slope stability. *Journal of Geotechnical and Geoenvironmental Engineering* 126(2), pp. 157–166.

Nolz, R. and Kammerer, G. 2017. Evaluating a sensor setup with respect to near-surface soil water monitoring and determination of in-situ water retention functions. *Journal of Hydrology* 549, pp. 301–312.

Northmore, K.J., Jefferson, I., Jackson, P.D., Entwisle, D.C., Milodowski, A.E., Raines, M.R., et al. 2008. On-site characterisation of loessic deposits in Kent, UK. *Proceedings of the ICE-Geotechnical Engineering* 161(1), pp. 3–17.

Nouaouria, M.S., Guenfoud, M. and Lafifi, B. 2008. Engineering properties of loess in Algeria. *Engineering Geology* 99(1), pp. 85–90.

Nowamooz, H. and Masrouri, F. 2008. Hydromechanical behaviour of an expansive bentonite/silt mixture in cyclic suction-controlled drying and wetting tests. *Engineering Geology* 101(3–4), pp. 154–164.

Nuth, M. and Laloui, L. 2008. Effective stress concept in unsaturated soils: Clarification and validation of a unified framework. *International Journal for Numerical and Analytical Methods in Geomechanics* 32(7), pp. 771–801.

Oh, S., Lu, N., Kim, Y.K., Lee, S.J. and Lee, S.R. 2012. Relationship between the soil-water characteristic curve and the suction stress characteristic curve: Experimental evidence from residual soils. *Journal of Geotechnical and Geoenvironmental Engineering* 138(1), pp. 47–57.

Oh, S. and Lu, N. 2014. Uniqueness of the suction stress characteristic curve under different confining stress conditions. *Vadose Zone Journal* 13(5), pp. 1–10.

Okonta, F.T. 2012. Collapse settlement behaviour of remoulded and undisturbed weathered quartzite. *International Journal of the Physical Sciences* 7(32), pp. 5239–5247.

Oliveira, O.M. and Fernando, F.A.M. 2006. Study of equilibration time in the pressure plate. In: Miller GA, Zapata CE, Houston SL, F. D. ed. *Proceedings of 4th International Conference on Unsaturated Soils*. Carefree, Arizona: ASCE, GSP, pp. 1864–1874.

Oliveira, O.M. and Marinho, F.A.M. 2008. Suction equilibration time for a high capacity tensiometer. *Geotechnical Testing Journal* 31(1), pp. 101–105.

Olivier, M. and Mesbah, A. 1987. Influence of different parameters on the resistance of earth, used as a building material. *In: International Conference on Mud Architecture*. Trivandrum, India.

Olson, R.E. and Langfelder, L.J. 1965. Pore water pressures in unsaturated soils. *Journal of Soil Mechanics and Foundations Division* 91(4), pp. 127–150.

Othmer, H., DiekkrÜger, B. and Kutilek, M. 1991. Bimodal porosity and unsaturated hydraulic conductivity. *Soil Science* 152(3), pp. 139–150.

Padilla, J.M., Perera, Y.Y., Houston, W.N., Perez, N. and Fredlund, D.G. 2006. Quantification of air diffusion through high air-entry ceramic disks. *Proceedings of the 4th International Conference on Unsaturated Soils 2*, pp. 1852–1863.

Pereira, J.H., Fredlund, D.G., Cardão Neto, M.P. and Gitirana, G. de F. 2005. Hydraulic behavior of collapsible compacted gneiss soil. *Journal of Geotechnical and Geoenvironmental Engineering* 131(10), pp. 1264–1273.

Pereira, J.H.F. and Fredlund, D.G. 2000. Volume change behavior of collapsible compacted gneiss soil. *Journal of Geotechnical and Geoenvironmental Engineering* 126(10), pp. 907–916.

Perez-Garcia, N., Houston, S.L., Houston, W.N. and Padilla, J.M. 2008. An oedometer pressure plate SWCC apparatus. *Geotechnical Testing Journal* 31(2), pp. 115–123.

Petry, T.M. and Jiang, C.-P. 2007. Round-robin testing of a dewpoint potentiameter versus filter paper to determine total suction. *In: Proceedings of GeoDenver, Advances in Measurement and Modeling of Soil Behavior*. Denver, Colorado, USA: GSP 173, pp. 1–10.

Pourzargar, A., König, D., Heibrock, G., Datcheva, M. and Schanz, T. 2014. Comparison of measured and predicted suction stress in partially saturated compacted mixtures of sand and clay. *Vadose Zone Journal* 13(5), pp. 1–10.

Power, K.C. and Vanapalli, S.K. 2010. Modified null pressure plate apparatus for measurement of matric suction. *Geotechnical Testing Journal* 33(4), pp. 335–341.

Prakash, K., Sridharan, A. and Prasanna, H.S. 2014. Compaction induced yield stress. *Geotechnical and Geological Engineering* 32(2), pp. 311–319.

Proctor, R.R. 1933. Fundamental principles of soil compaction. *Engineering News Record* 111(9), pp. 245–248.

Rabbi, A., Cameron, D.A., Rahman, M.M., Environments, B., Lecturer, S., Rabbi, A., et al. 2014. Effect of initial partial saturation on collapse behavior of glacial sand with fines. *GeoCongress* 2014, pp. 103–112.

Rahardjo, H., Aung, K.K., Leong, E.C. and Rezaur, R.B. 2004. Characteristics of residual soils in Singapore as formed by weathering. *Engineering Geology* 73(1–2), pp. 157–169.

Rahardjo, H. and Leong, E.C. 2006. Suction measurements. In: *Unsaturated Soils* 2006. pp. 81–104.

Rao, S.M. and Revanasiddappa, K. 2000. Role of matric suction in collapse of compacted clay soil. *Journal of Geotechnical and Geoenvironmental Engineering* 126(1), pp. 85–90.

Richards, B.G. 1974. Behavior of unsaturated soils. In: Lee, I. K. ed. *Soil Mechanics-New Horizons*. American Elsevier, New York, pp. 112–157.

Ridley, A.M. and Wray, W.K. 1996. Suction measurement—theory and practice. A state of the art review. In: Alonso, E. E. and Delage, P. eds. *Proceeding of 1st International Conference on Unsaturated Soils*. Paris, pp. 1293–1322.

Rogers, C.D.F. 1995. Types and distribution of collapsible soils. In: *Genesis and Properties of Collapsible Soils*. Springer, pp. 1–17.

Romero, E., Gens, A., Lloret, A. and Romero Gens, A., Lloret, A., E. 1999. Water permeability, water retention and microstructure of unsaturated compacted Boom clay. *Engineering Geology* 54(1), pp. 117–127.

Romero, E. 2001. Controlled-suction techniques. In: Gehling, W. Y. Y. and Schnaid, F. eds. *4th National Brazilian Symposium on Unsaturated Soils*. Porto Alegre, Brasil, pp. 535–542.

Romero, E., Gens, a. and Lloret, a. 2003. Suction effects on a compacted clay under non-isothermal conditions. *Géotechnique* 53(1), pp. 65–81.

Romero, M.E. 1999. *Characterisation and thermo-hydro-mechanical behaviour of unsaturated Boom clay: An experimental study*. PhD Thesis. Polytechnic University of Catalonia.

Rorke, L., Tripathy, S., Otter, L., Clayton, C.R.I. and Powrie, W. 2015. Use of a chilled-mirror dew-point potentiometer to determine suction in a railway formation material. *In: Proceedings of the First Southern African Geotechnical Conference*. CRC Press London, p. 229.

Seki, K. 2007. SWRC fit-a nonlinear fitting program with a water retention curve for soils having unimodal and bimodal pore structure. *Hydrology and Earth System Sciences Discussions* 4(1), pp. 407–437.

Sharma, R.S. and Singhal, S. 2006. Preliminary observation on volumetric behavior of unsaturated collapsible loess. *Geotechnical Special Publication* 147(1), pp. 1017–1024.

Sheng, D., Sloan, S.W. and Gens, A. 2004. A constitutive model for unsaturated soils: thermomechanical and computational aspects. *Computational Mechanics* 33(6), pp. 453–465.

Sillers, W.S., Fredlund, D.G. and Zakerzaheh, N. 2001. Mathematical attributes of some soil–water characteristic curve models. *Geotechnical and Geological Engineering* 3(19), pp. 243–283.

Singhal, S., Sharma, R.S. and Phanikumar, B.R. 2015. A laboratory study of collapse behaviour of remoulded loess under controlled wetting and flooding. *Geomechanics and Geoengineering* 11(2), pp. 159–163.

Sivakumar, V. 1993. *A critical state framework for unsaturated soil*. PhD Thesis, University of Sheffield.

Sivakumar, V. 2014. The influence of high air entry filter on the testing of unsaturated soils using the axis translation technique. *Environmental Geotechnics* 3(2), pp. 90–98.

Sivakumar, V., Zaini, J., Gallipoli, D., Solan, B., Clay, L., Clay, B., et al. 2015. Wetting of compacted clays under laterally restrained conditions: initial state, overburden pressure and mineralogy. *Géotechnique* 65(2), pp. 111–125.

Sivakumar, V. and Wheeler, S.J. 2000. Influence of compaction procedure on the mechanical behaviour of an unsaturated compacted clay. Part 1: Wetting and isotropic compression. *Géotechnique* 50(4), pp. 359–368.

Song, Y.S., Hwang, W.K., Jung, S.J. and Kim, T.H. 2012. A comparative study of suction stress between sand and silt under unsaturated conditions. *Engineering Geology* 124(1), pp. 90–97.

Sridharan, A., Altschaeffl, A.G. and Diamond, S. 1971. Pore size distribution studies. *Journal of Soil Mechanics and Foundations Division* 97(5), pp. 771–787.

Sridharan, A. and Sivapullaiah, P.V. 2005. Mini compaction test apparatus for fine grained soils. *Geotechnical Testing Journal* 28(3), pp. 240–246.

Sun, D., Sheng, D. and Xu, Y. 2007. Collapse behaviour of unsaturated compacted soil with different initial densities. *Canadian Geotechnical Journal* 44(6), pp. 673–686.

Sun, D.A., Matsuoka, H. and Xu, Y.F. 2004. Collapse Behavior of Compacted Clays in Suction-Controlled Triaxial Tests. *Geotechnical Testing Journal* 27(4), pp. 1–9.

Sun, J.Z. 1957. Collapsibility of loess and the relationship with moisture. *Hydrogeology and Engineering Geology* 11, pp. 18–21.

Sun, P.P., Zhang, M.S. and Zhu, L.F. 2013. Typical case study of loess collapse and discussion on related problems. *Geological Bulletin of China* 32(6), pp. 847–851.

Tadepalli, R., Rahardjo, H. and Fredlund, D.G. 1992. Measurements of matric suction and volume changes during inundation of collapsible soil. *Geotechnical Testing Journal* 15(2), pp. 115–122.

Tadepalli, R. and Fredlund, D.G. 1991. The collapse behavior of a compacted soil during inundation. *Canadian Geotechnical Journal* 28(4), pp. 477–488.

Tarantino, A., Tombolato, S., Tarantino, A., Tombolato, S. and Tarantino, A. 2005. Coupling of hydraulic and mechanical behaviour in unsaturated compacted clay. *Géotechnique* 55(4), pp. 307–317.

Tarantino, A. 2009. A water retention model for deformable soils. Géotechnique 59(9), pp. 751–762.

Tarantino, A., Gallipoli, D., Augarde, C.E., De Gennaro, V., Gomez, R., Laloui, L., et al. 2011. Benchmark of experimental techniques for measuring and controlling suction. *Géotechnique* 61(4), pp. 303–312.

Tarantino, A. and De Col, E. 2008. Compaction behaviour of clay. *Géotechnique* 58(3), pp. 199–213.

Terzaghi, K. von 1936. The shearing resistance of saturated soils and the angle between the planes of shear. *In: Proceedings of the 1st international conference on soil mechanics and foundation engineering.* Harvard University Press Cambridge, MA, pp. 54–56.

Thom, R., Sivakumar, V., Sivakumar, R., Urray, E.J. and Mackinnon, P. 2007. Pore size distribution of unsaturated compacted kaolin: the initial states and final states following saturation. *Géotechnique* 57(5), pp. 469–474.

Tombolato, S., Tarantino, A. and Mongiovì, L. 2005. Suction induced by static compaction. In: Schanz, T. ed. *Unsaturated soils: Experimental studies*. Berlin: Springer-Verlag, pp. 101–110.

Tripathy, S., Leong, E.C. and Rahardjo, H. 2005. Suction of compacted residual soils. In: *Unsaturated Soils: Experimental Studies*: Proceedings of the International Conference" From Experimental Evidence towards Numerical Modeling of Unsaturated Soils", Weimar, Germany, September 18-19. Springer Science & Business Media, pp. 111–122.

Tripathy, S., Elgabu, H. and Thomas, H.R. 2011. Matric suction measurement of unsaturated soils with null-type axis-translation technique. *Geotechnical Testing Journal* 35(1), pp. 1–12.

Tripathy, S., Hesham, E. and Thomas, H.R. 2014. Soil-water characteristic curves from various laboratory techniques. In: Khalili, N. and Al., E. eds. *Unsaturated Soils: Research & Applications*. CRC Press London, pp. 1701–1707.

Tripathy, S., Al-Khyat, S., Cleall, P.J.P.J., Baille, W. and Schanz, T. 2016. Soil suction measurement of unsaturated soils with a sensor using fixed-matrix porous ceramic discs. *Indian Geotechnical Journal* 46(3), pp. 252–260.

Turnbull, W.J. 1950. Compaction and strength tests on soils. In: Lambe, T. W. and Whitman, R. V. eds. *Soil Mechanics*. John Wiley and Sons, New York.

Uchaipichat, A. 2011. Effective stress parameter of unsaturated granular soils. *In: International Conference on Mechanical, Automobile and Robotics Engineering*. pp. 231–234.

Vanapalli, S.K., Fredlund, D.G., Pufahl, D.E. and Clifton, A.W. 1996. Model for the prediction of shear strength with respect to soil suction. *Canadian Geotechnical Journal* 33(3), pp. 379–392.

Vanapalli, S.K., Fredlund, D.G. and Pufahl, D.E. 1996. The relationship between the soil-water characteristic curve and the unsaturated shear strength of a compacted glacial till. *ASTM Geotechnical Testing Journal* 19(3), pp. 259–268.

Vanapalli, S.K., Sillers, W.S. and Fredlund, M.D. 1998. The meaning and relevance of residual state to unsaturated soils. *In: Proceedings of the 51st Canadian Geotechnical Conference*. Edmonton, Alta. pp. 4–7.

Vanapalli, S.K., Fredlund, D.G. and Pufahl, D.E. 1999. The influence of soil structure and stress history on the soil-water characteristics of a compacted till. *Géotechnique* 49(2), pp. 143–159.

Vanapalli, S.K., Nicotera, M. V. and Sharma, R.S. 2008. Axis translation and negative water column techniques for suction control. *Laboratory and Field Testing of Unsaturated Soils* 26(6), pp. 33–48.

Vanapalli, S.K. 2009. Shear strength of unsaturated soils and its applications in geotechnical engineering practice. *In: Keynote Address. Proc. 4th Asia-Pacific Conf. on Unsaturated Soils*. Newcastle, Australia. pp. 579–598.

Vanapalli, S.K. and Fredlund, D.G. 2000. Comparison of different procedures to predict unsaturated soil shear strength. *In: Advances in Unsaturated Geotechnics*. pp. 195–209.

Venkatarama-Reddy, B. V and Jagadish, K.S. 1993. The static compaction. *Géotechnique* 43(2), pp. 337–341.

Venkatarama Reddy, B.V. and Jagadish, K.S.S. 1995. Discussion: The static compaction of soils. *Géotechnique* 45(2), pp. 363–367.

Vilar, O.M. and Rodrigues, R.A. 2011. Collapse behavior of soil in a Brazilian region affected by a rising water table. *Canadian Geotechnical Journal* 48(2), pp. 226–233.

Wheeler, S.J., Sharma, R.S. and Buisson, M.S.R. 2003. Coupling of hydraulic hysteresis and stress–strain behaviour in unsaturated soils. *Géotechnique* 53(1), pp. 41–54.

Wheeler, S.J. and Sivakumar, V. 1995. An elasto-plastic critical state framework for unsaturated soil. *Géotechnique* 45(1), pp. 35–53.

Xanthakos, P.P., Abramson, L.W. and Bruce, D.A. 1994. *Ground control and improvement*. John Wiley & Sons Inc., New York.

Xie, W.L., Li, P., Vanapalli, S.K. and Wang, J.D. 2018. Prediction of the wetting-induced collapse behaviour using the soil-water characteristic curve. *Journal of Asian Earth Sciences* 151(6), pp. 259–268.

Yaghoubi, E., Disfani, M.M., Arulrajah, A. and Kodikara, J. 2017. Impact of compaction method on mechanical characteristics of unbound granular recycled materials. *Road Materials and Pavement Design* 19(4), pp. 912–934.

Yahia, H. 1971. Soils and soil conditions in sediments of the Ramadi Province (Iraq). Amestrdam: Publicaties van het Fysisch-Geografisch en Bodemkundig Laboratorium, van de Universiteit van Amestrdam.

Yang, H., Rahardjo, H., Leong, E.-C. and Fredlund, D.G. 2004. Factors affecting drying and wetting soil-water characteristic curves of sandy soils. *Canadian Geotechnical Journal* 41(5), pp. 908–920.

Yang, S.R., Lin, H.D. and Huang, W.H. 2012. Variation of initial soil suction with compaction conditions for clayey soils. *Journal of Mechanics* 28(03), pp. 431–437.

Yang, Y.L. 1988. Study on collapsible mechanism of loess soils. *Science in China: Series B 7*, pp. 756–766.

Zargarbashi, S. and Khalili, N. 2011. Effective stress in unsaturated soils under wetting and drying. *Unsaturated Soils: Theory and Practice* 2011, pp. 307–311.

Zhemchuzhnikov, A., Ghavami, K. and dal Toé Casagrande, M. 2016. Static compaction of soils with varying clay content. *Key Engineering Materials* 668, pp. 238–246.

Zhou, A. and Sheng, D. 2009. Yield stress, volume change, and shear strength behaviour of unsaturated soils: validation of the SFG model. *Canadian Geotechnical Journal* 46(9), pp. 1034–1045.

Zhou, A.N., Sheng, D., Sloan, S.W. and Gens, A. 2012. Interpretation of unsaturated soil behaviour in the stress - Saturation space, I: Volume change and water retention behaviour. *Computers and Geotechnics* 43(9), pp. 178–187.

Zhou, J. and Yu, J.L. 2005. Influences affecting the soil-water characteristic curve. *Journal of Zhejiang University-Science A* 6(8), pp. 797–804.

Zorlu, K. and Kasapoglu, K.E. 2009. Determination of geomechanical properties and collapse potential of a caliche by in situ and laboratory tests. *Environmental Geology* 56(7), pp. 1449–1459.